Computational Fluid Dynamic Analysis of Scaled Hypersonic Re-Entry Vehicles

A project presented to
The Faculty of the Department of Aerospace Engineering
San Jose State University

In partial fulfillment of the requirements for the degree
Master of Science in Aerospace Engineering

by

Simon H.B. Sorensen

March 2019

approved by

Dr. Periklis Papadopoulous
Faculty Advisor

ABSTRACT

With the advancement of technology in space, reusable re-entry space planes have become a focus point with their ability to save materials and utilize existing flight data. Their ability to not only supply materials to space stations or deploy satellites, but also in atmosphere flight makes them versatile in their deployment and recovery. The existing design of vehicles such as the Space Shuttle Orbiter and X-37 Orbital Test Vehicle can be used to observe the effects of scaling existing vehicle geometry and how it would operate in identical conditions to the full-size vehicle. These scaled vehicles, if viable, would provide additional options depending on mission parameters without losing the advantages of reusable re-entry space planes.

Table of Contents

Nomenclature

CFD = Computational Fluid Dynamics
SSO = Space Shuttle Orbiter
OTV = Orbital Test Vehicle
t = Time
T= Temperature
ρ = Density
P = Pressure
τ = Stress
Et = Total Energy
q = Heat Flux
Re = Reynolds Number
Pr = Prandtl Number
M = Mach
L = Lift
D = Drag
C_L = Coefficient of Lift
C_D = Coefficient of Drag
S = Area
V = Velocity

1. Introduction

In 1969, the Space Task Group concluded its study of the future of space with the recommendation that the United States emphasize specific program objectives in future projects. One program objective was to "develop new systems and technology for space operations with emphasis upon the critical factors of: (1) commonality, (2) reusability, and (3) economy, through a program directed initially toward development of a new space transportation capability and space station modules which utilize this new capability." (Space Task Group, 1969) This recommendation by the Space Task Group was the backbone for the development of the program that would become the Space Shuttle Program. The Space Shuttle Program became iconic through its use of reusable orbiters that were launched with crew and cargo into space on various missions, and the gliding capabilities of the orbiters that allowed them to land on an airfield like a traditional aircraft. The ability of the Space Shuttle Orbiters to be reusable was a major advantage of the vehicle as it prevented the manufacture of a new vehicle for every mission.

In 2011, the shuttle Atlantis completed the final flight by a Space Shuttle Orbiter, the 135th mission, 30 years after the maiden voyage of the shuttle Columbia. However, the concept of a reusable space transportation vehicle that would be able to land at an airstrip was already in the works in both the public and private sectors before the termination of the Space Shuttle Program. Through NASA's involvement in the X-planes program, the X-33, X-37, and X-38 were all experimental designs that took the concept of a reusable space plane, with the X-37 and X-38 being constructed and flown. Private industry vehicles, such as the Sierra Nevada Corporation (SNC) Dream Chaser, are also being developed and produced with the same program objective in mind that drove the Space Shuttle Program.

These vehicles are all varying sizes, and apart from the X-37, they are all designed to be manned vehicles. But with the push for automation in flight as with the X-37, vehicles can be designed without the need to accommodate an onboard human pilot and instead can be designed solely for the mission. By reducing the size of these vehicles to meet a specification for a mission with a small payload, the cost per launch can be reduced and these reusable unmanned vehicles can open an avenue to affordable satellite deployment, maintenance, and retrieval.

The purpose of this project is to compare the hypersonic re-entry profile of the previously listed Space Transportation Vehicles (STV) to those of their corresponding scale models. This comparison will help establish a link in scaling of reusable re-entry vehicles.

2. Literature Review

The primary space transportation vehicles that will be reviewed, modeled, and tested in this report are the Space Shuttle Orbiter Vehicle (SSO) and the X-37 Orbital Test Vehicle (OTV).

2.1 Space Shuttle Orbiter

The Space Shuttle Orbiter Vehicle was developed as part of the Space Shuttle Program in 1972. The Orbiter was designed to be a reusable glider that acted as the primary vehicle of the Space Transportation System (STS) alongside two reusable solid rocket boosters and an external fuel tank. The SSO is the only component of the STS that makes it to orbit, as the other components are jettisoned shortly after launch. The STS Orbiter was the first reusable manned spacecraft to operate and had 135 flights and almost 21,000 orbits of the earth between the five SSOs that were produced. (NASA)The SSO was designed to operate as an unpowered glider upon re-entry as there is no fuel in the main engines. Although most gliders are designed with a lift-to-drag ratio of around 70 to allow for a long flight time, the SSO was designed with a lift-to-drag ratio of about 1 due to the rapid deceleration from 17,300mph to 250mph over the course of its glide. (Space Shuttle as a Glider) The Angle of Attack of the Space Shuttle Orbiter has a direct effect on the lift-to-drag ratio, with the lift-to-drag ratio of 1 correlating with the Angle of Attack of approximately 40 degrees. There is slight variance based on other factors, however this provides a starting point to achieve that lift-to-drag ratio.(Stone.D, 1970)

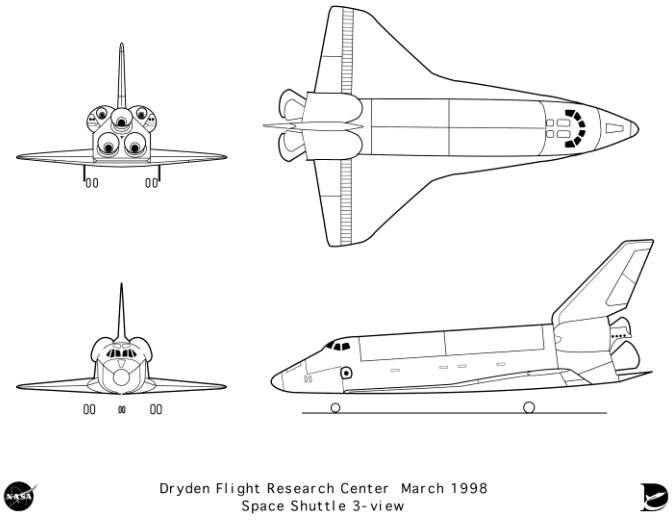

Figure 1 - 4-view of the Space Shuttle Orbiter
(Reprinted from NASA.). Retrieved May 1, 2018, from https://www.dfrc.nasa.gov/Gallery/Graphics/STS/index.html)

Table 2.1 Space Shuttle Orbiter dimensions

Space Shuttle Orbiter	
Length	122 ft
Wingspan	78 ft
Payload Bay Dimentions	66ftX15feet
Re-entry L/D ratio	~1

2.2 X-37 Orbital Test Vehicle

Developed by Boeing, the X-37 Orbital Text Vehicle (OTV) was designed to be a reusable unmanned spacecraft. The launch profile is almost identical to the SSO, as the OTV is boosted into space by a launch vehicle before re-entering and gliding as a spaceplane. The OTV was developed to test technologies within a space environment. The OTV can operate at speeds as fast as Mach 25. Being unmanned, the OTV provides a base for research in unmanned re-entry vehicles which can help in lowering the costs and risks of sending both payloads and passengers into space. Based on the USAF's X-40, the X-37 is a 120% scale derivative of the same geometry while utilizing advanced propulsion, thermal protection, and payload bay that the X-40 lacks.(Dunbar.B, 2003) Although the mission profile of the X-37 OTV is similar to the SSO, the X-37 OTV is capable of staying in orbit for a time of longer than 270 day, far exceeding that of the SSO. This allows for a lot more options in how the vehicle can assist in its launches as well as variability on re-entry planning. (X-37B Orbital Test Vehicle, 2015)

Table 2.2 X-37 Orbital Test Vehicle dimensions

X-37 OTV	
Length	27.5ft
Wingspan	15ft
Payload Bay Dimensions	7ft long, 4ft diameter

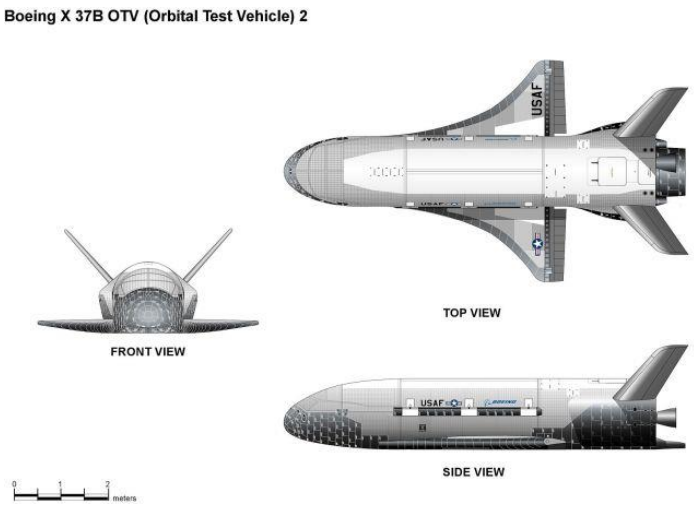

Figure 2 Orthographic projection of X-37 OTV
(reprinted from Seemangal, R ,SpaceX to Launch Secretive Robotic Spaceplane for US Air Force, from https://observer.com/2017/06/spacex-to-launch-secretive-robotic-spaceplane-for-u-s-air-force/)

3. Assumptions and Equations

3.1 Assumptions

There are several assumptions that need to be made with regards to the experiments to reduce the number of variables in the results of the tests. These models are assumed to be re-entering in viscous, turbulent air. The airflow will be assumed to be turbulent because the airflow will be hypersonic.

An addition assumption is that there is no ablation of material during this decent. In actual flight conditions at hypersonic speeds, there would be some mass loss that may result in subtle changes in the body of the re-entry vehicle, however for this report, the assumption is made that the bodies of the vehicles undergo no change in their form other than what is done through scaling. This allows for the flow over an ideal model be analyzed rather than include uncertainty of what differences a slightly altered aerodynamic body may generate.

3.2 Equations to Solve

Due to the format of this experiment, the analysis of the models will be done by observing the characteristics of the flow around the models with regards to velocity, temperature, and pressure. To analyze these characteristics, the Navier-Stokes equations for three dimensions will be solved through to use of the CFD program. The Navier-Stokes Equations for three-dimensional unsteady flow are as follows:

$$Continuity: \frac{\partial \rho}{\partial t} + \frac{\partial (\rho u)}{\partial x} + \frac{\partial (\rho v)}{\partial y} + \frac{\partial (\rho w)}{\partial z} = 0 \quad (3.1)$$

$$X_{momentum} = \frac{\partial (\rho u)}{\partial t} + \frac{\partial (\rho u^2)}{\partial x} + \frac{\partial (\rho uv)}{\partial y} + \frac{\partial (\rho uw)}{\partial z} = -\frac{\partial p}{\partial x} + \frac{1}{Re_r}\left[\frac{\partial \tau_{xx}}{\partial x} + \frac{\partial \tau_{xy}}{\partial y} + \frac{\partial \tau_{xz}}{\partial z}\right] \quad (3.2)$$

$$Y_{momentum} = \frac{\partial (\rho v)}{\partial t} + \frac{\partial (\rho uv)}{\partial x} + \frac{\partial (\rho v^2)}{\partial y} + \frac{\partial (\rho vw)}{\partial z} = -\frac{\partial p}{\partial y} + \frac{1}{Re_r}\left[\frac{\partial \tau_{xy}}{\partial x} + \frac{\partial \tau_{yy}}{\partial y} + \frac{\partial \tau_{yz}}{\partial z}\right] \quad (3.3)$$

$$Z_{momentum} = \frac{\partial (\rho w)}{\partial t} + \frac{\partial (\rho uw)}{\partial x} + \frac{\partial (\rho vw)}{\partial y} + \frac{\partial (\rho w^2)}{\partial z} = -\frac{\partial p}{\partial z} + \frac{1}{Re_r}\left[\frac{\partial \tau_{xz}}{\partial x} + \frac{\partial \tau_{yz}}{\partial y} + \frac{\partial \tau_{zz}}{\partial z}\right] \quad (3.4)$$

$$Energy = \frac{\partial (E_T)}{\partial t} + \frac{\partial (uE_T)}{\partial x} + \frac{\partial (vE_T)}{\partial y} + \frac{\partial (wE_T)}{\partial z} = -\frac{\partial (up)}{\partial x} - \frac{\partial (vp)}{\partial y} - \frac{\partial (wp)}{\partial z} - \frac{1}{Re_r Pr_r}\left[\frac{\partial q_x}{\partial x} + \frac{\partial q_y}{\partial y} + \frac{\partial q_z}{\partial z}\right] + \frac{1}{Re_r}\left[\frac{\partial}{\partial x}\left(u\tau_{xx} + v\tau_{xy} + w\tau_{xz}\right) + \frac{\partial}{\partial y}\left(u\tau_{xy} + v\tau_{yy} + w\tau_{yz}\right) + \frac{\partial}{\partial z}\left(u\tau_{xz} + v\tau_{yz} + w\tau_{zz}\right)\right] \quad (3.5)$$

The Navier-Stokes Equations can be defined as a time-dependent continuity equation for the conservation of mass, A time-dependent conservation of momentum equation for each dimension, and a time-dependent conservation of energy equation. The four independent variables across all the equations are x, y,and z for the coordinates, and t for the point in time. (Anderson J, 2017) These equations govern regardless of the velocity of the air, as they work in both subsonic, supersonic, and hypersonic situations. It should be noted that for large hypersonic Mach numbers, the pressure (p) cannot be assumed to be constant in the normal direction in a boundary layer in the boundary layer equations derived from the standard Naiver-Stokes equations. (Anderson J, 2006) However, this shouldn't have a large effect given the restriction on freestream velocity in this report. These equations will be solved within the CFD simulations and will be the governing set of equations that the simulation will be subject to.

The Equation for calculating the lift-to-drag ratio will also be utilized in order to compare the information that comes out of the CFD runs. The Equations for calculating the lift-to-drag ratio are as follows:

$$\text{lift-to-drag ratio} = \frac{F_{Lift}}{F_{Drag}} \quad (3.6)$$

$$F_{Lift} = C_L * S * V^2 * q_\infty * \frac{1}{2} \quad (3.7)$$

$$F_{Drag} = C_D * S * V^2 * q_\infty * \frac{1}{2} \quad (3.8)$$

Because these vehicles are all utilizing the same initial conditions of Mach 6 flow along the X-positive axis, the Density can be assumed to be uniform across each test. Because of the identical geometry and variable scale, there is a set relationship between the Area depending on which models are being compared. The Equation to compare the Area relationship is as follows:

$$Area(A): Area(B) = Scale(A): \left(\frac{Scale(B)}{Scale(A)}\right)^2 \quad (3.9)$$

This equation can be used by comparing the Area of Model A to the Area of Model B by utilizing the scale of the respective models. This can be used only when comparing the areas of models with identical geometry and only variable scale.

4. Methodology

The Purpose of the project will be achieved using Computational Fluid Dynamic (CFD) Software as well as Computer Assisted Design (CAD) models of the vehicles to create a simulated environment from which data will be collected. The geometries of the listed STVs will be modeled and simulated in specific conditions to mimic a realistic re-entry profile. The same process will be done with the scale models, and the CFD results between the models of the same style will be compared to see what effects sizing has on the flow characteristics

Due to the limited availability of in depth designs for any of the vehicles being used in this report, the models will all be constructed based on available information and pictures publicly available. Once constructed, the base sized vehicle model will be sized to the levels of 100%, 75% and 50% of the size of the original vehicles. These vehicles will all be tested at a uniform Mach number of 6.

5. Base Sized Vehicles

5.1 Space Shuttle Orbiter

Initial attempts at obtaining a model for the Space Shuttle were ultimately unsuccessful as the CAD models provided by NASA's public facing website were in the file type .3DS. This file was able to be opened on certain programs but was unable to be effectively converted into a SolidWorks part or Parasolid file for STAR-CCM+. Due to this setback, the NASA sourced files were used as reference along with orthographic projections such as the ones in Figure 3 and Figure 4. The resulting SolidWorks part was saved with variations at the appropriate scales and converted to Parasolid for the CFD testing. Rendered images of the CAD SSO are displayed in Figures 5 through 8.

The SSO base sized model was built in Solidworks through the provided sizing of the length and wingspan of the SSO and the orthographic projection of the SSO seen in Figures 3 and 4.

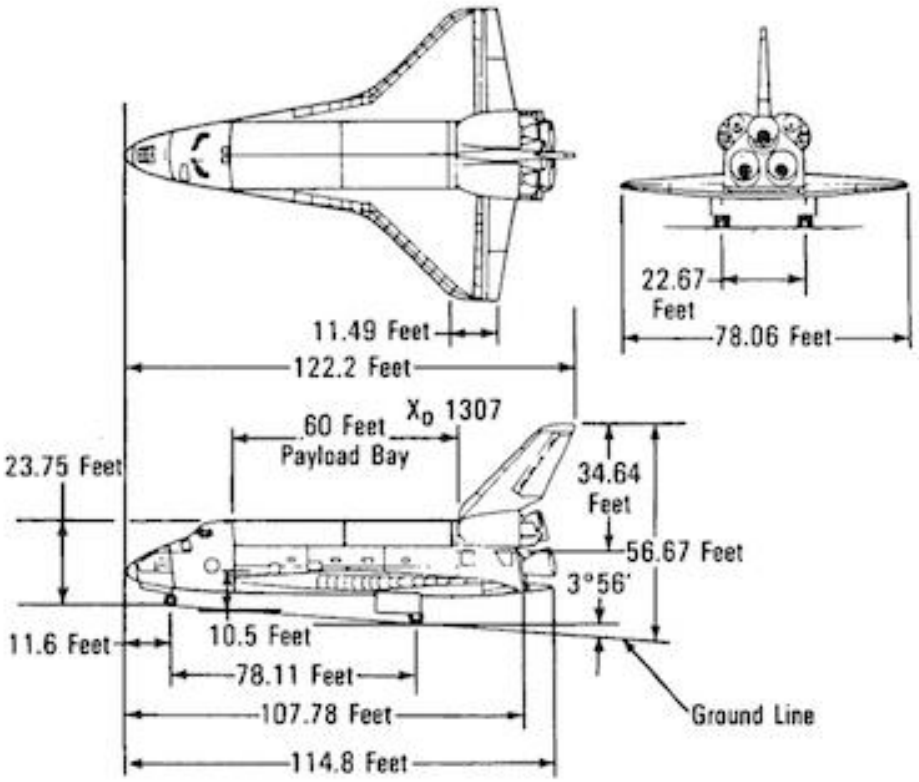

Figure 3 Orthographic projection of SSO with limited measurements
(Reprinted from Baker, D. (2017, June 03). Book Excerpt: Space Shuttle Owners' Workshop Manual. https://www.wired.com/2011/04/shuttle-manual-excerpt/)

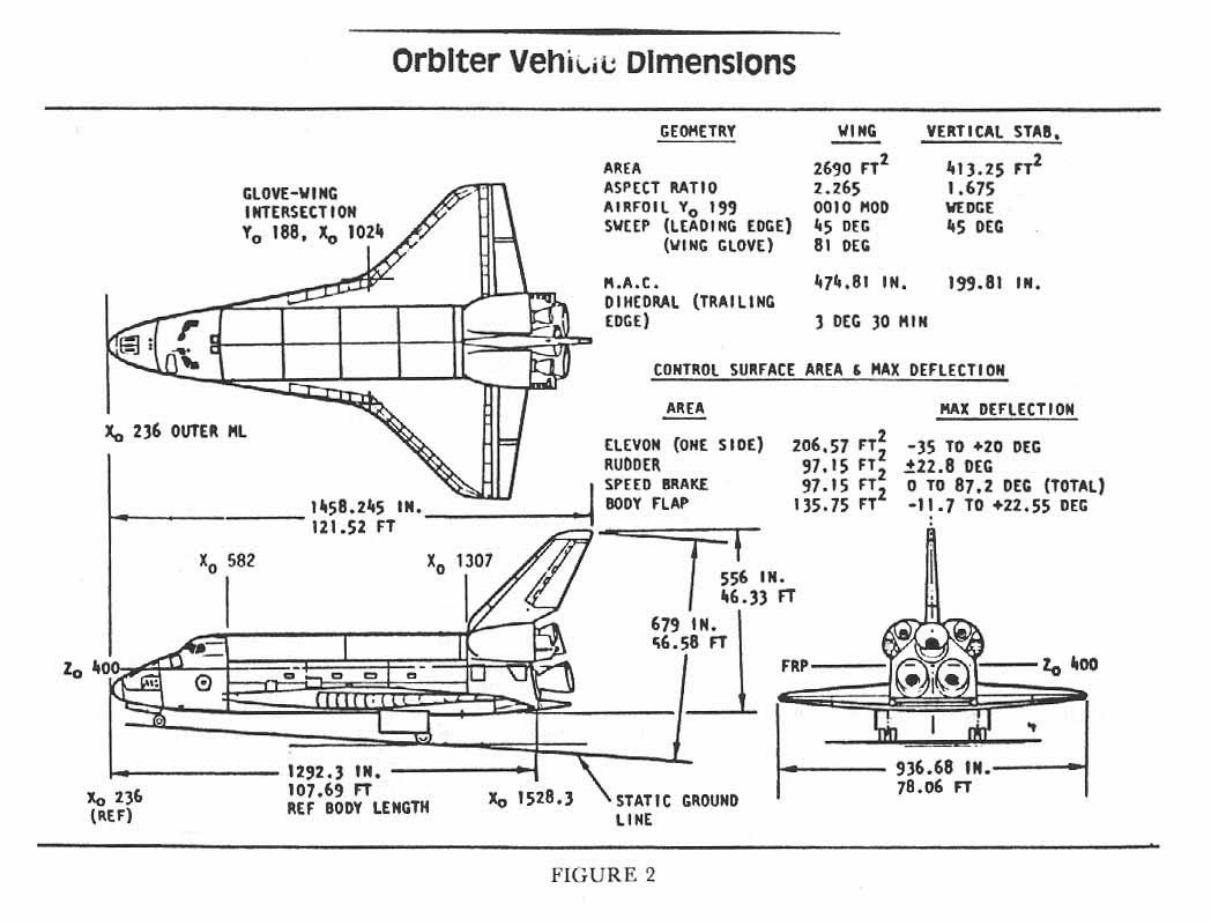

Figure 4 Orthographic projection of SSO with additional geometric information
(Reprinted from Orbiter Vehicle Dimensions. [Report of the PRESIDENTIAL COMMISSION on the Space Shuttle Challenger Accident]. (n.d), https://history.nasa.gov/rogersrep/v3o378b.htm)

These drawings were used to determine the angles and necessary lengths of components during the construction of the CAD models of the SSO in Solidworks.

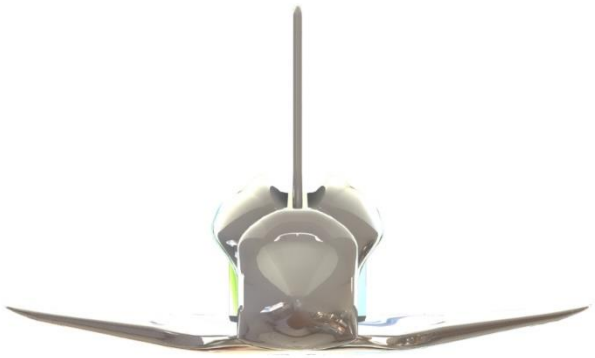

Figure 5 SolidWorks CAD of Space Shuttle Orbiter front

Figure 6 SolidWorks CAD of Space Shuttle Orbiter right side

Figure 7 SolidWorks CAD of Space Shuttle Orbiter top

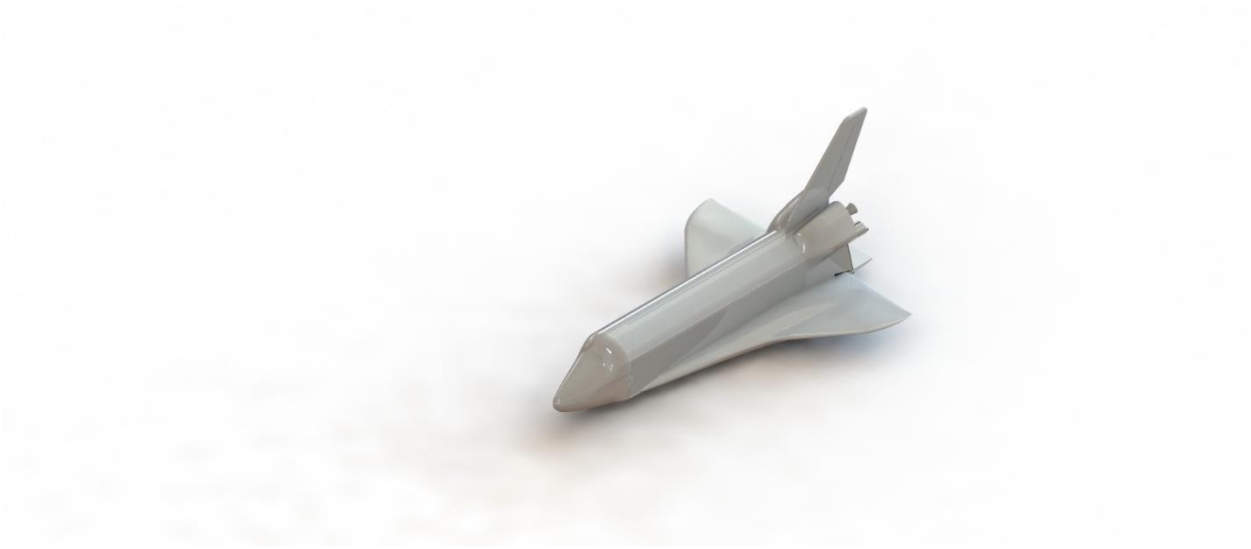

Figure 8 Isometric view of base sized Space Shuttle Orbiter

5.2 X-37

Due to the nature of the X-37's operation, attempts to find design documentation on the vehicle proved to be difficult and limited. Because to this, the design of the X-37 within this project cannot be considered perfect and may be displayed in the results that the model generates.

Similar to the SSO, the CAD for the X-37 was designed through the use of a generated orthographic projection as well as the dimensions listed above. The resulting model was then copied at the appropriate scales and converted to a Parasolid within the SolidWorks program for CFD testing. The renders of the model designed are displayed in Figures 9 through 12

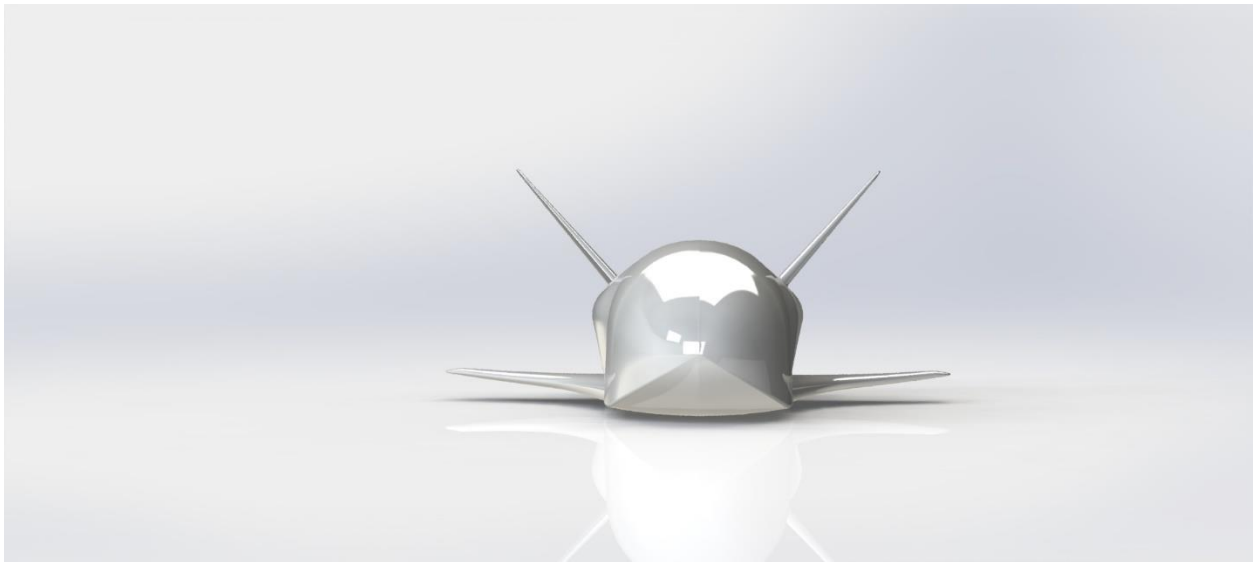

Figure 9 Front view of X-37

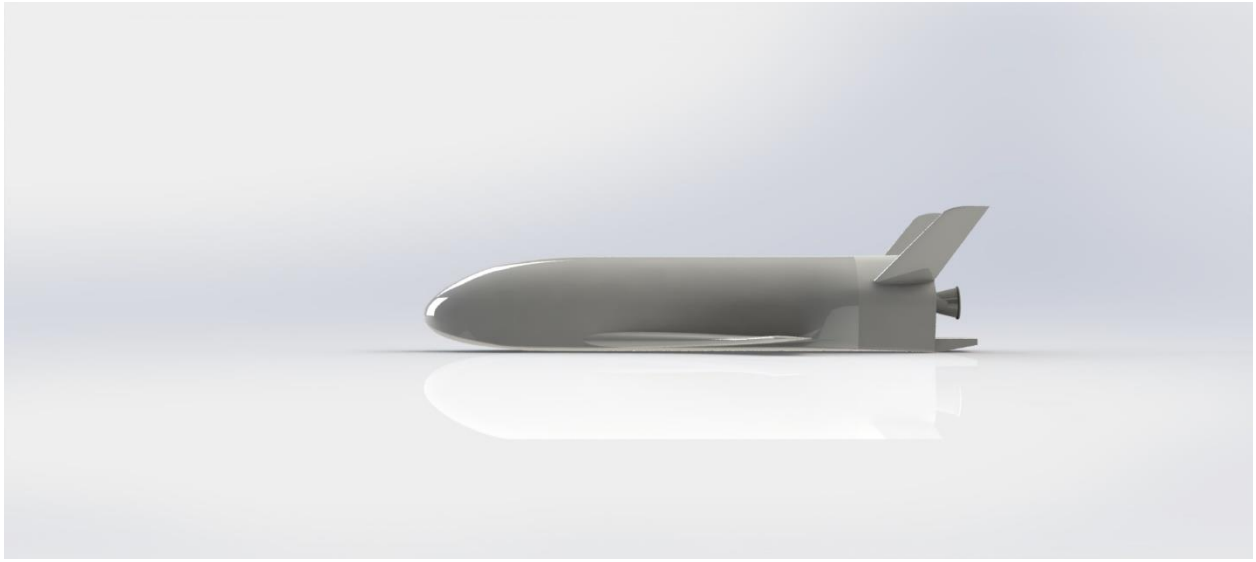

Figure 10 Right side view of X-37

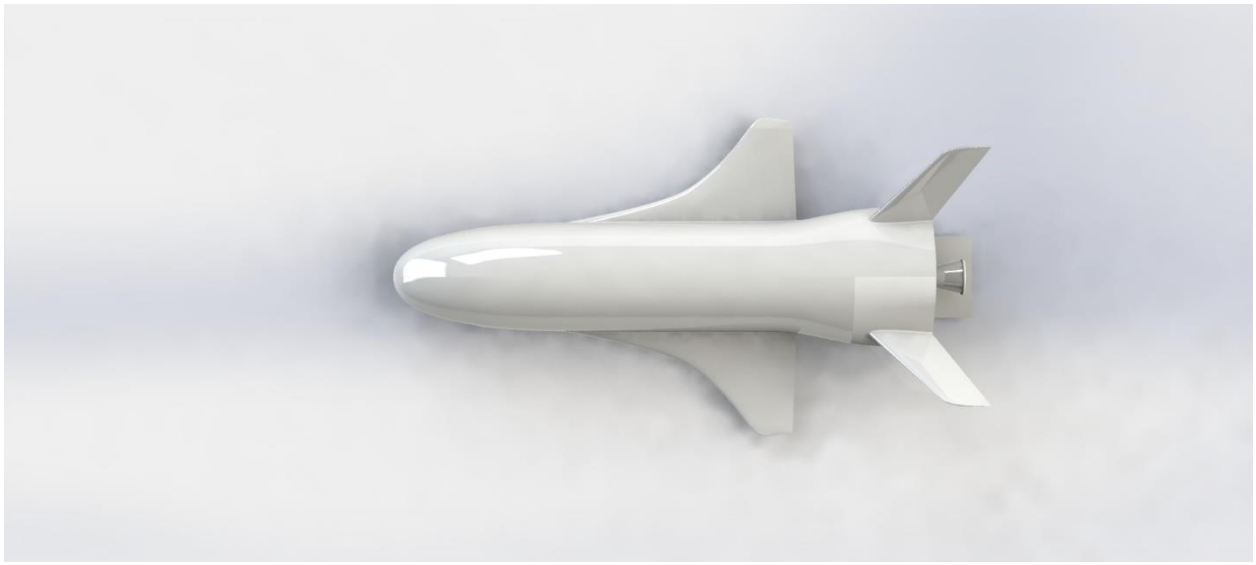

Figure 11 Top view of X-37

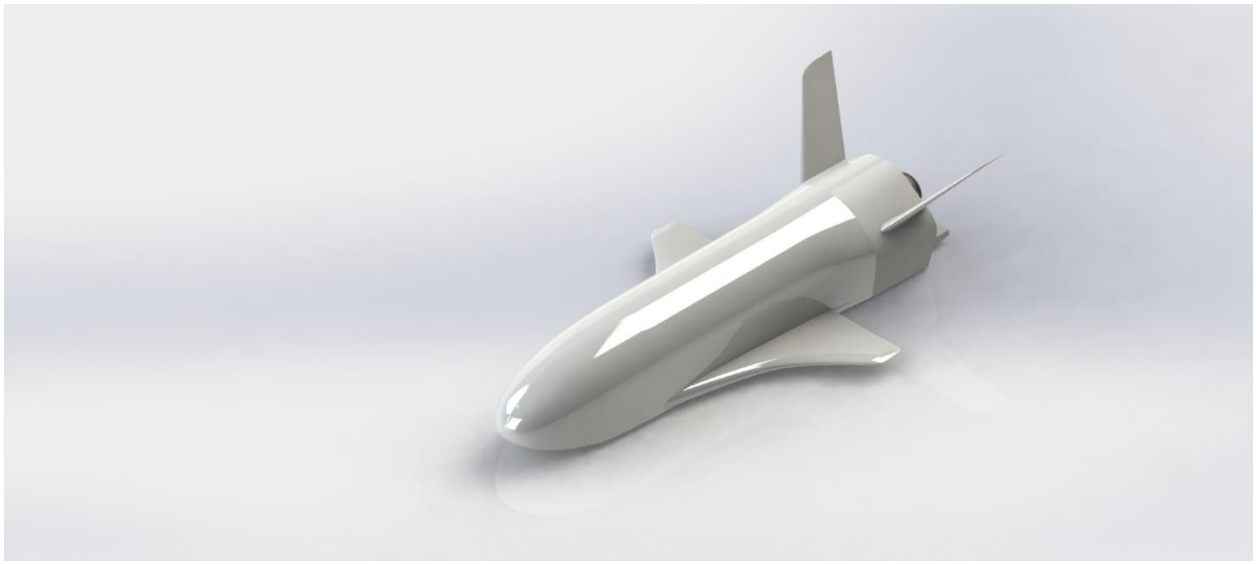

Figure 12 Isometric view of X-37

6. Scaled Vehicles

Scaled versions of both the SSO and the X-37 were developed for the purposes of this report. The scale the models are 50% and 25% of the 100%. The test areas designed for these vehicles had an origin designated so they would scale to the edge of the test area rather than the mid-point of the test area. This was done so that the test areas could be easily imported into STAR-CCM+ without excess time attempting to correctly position the test area relative to model's body. The test areas for both vehicles were also sized at 50% and 25% of their 100% scale model. Through this method, any imperfections or design flaws that were created in the CAD of either the SSO or X-37 would be carried trough the scale models, allowing the scale models to be compared with the errors accounted for.

7. Simulations

Simulations for these models was performed through the use of the programs STAR-CCM+ and SolidWorks 2017. SolidWorks was used to CAD the designs of the vehicles, which were then imported into the STAR-CCM+ Geometry tool. From there a control volume, as well as a refinement area, were defined and the simulations set up. The mesh was constructed utilizing the Automesh feature in STAR-CCM+ and allowed for various variables to be changed to affect the density of cells across a defined volume.

All Simulations were performed by modeling and setting up a mesh on half of the vehicle, splitting from nose to tail, and mirroring the results. This was done as it was assumed that there would be symmetrical results so long as the body was symmetrical on either side of the vehicle. For that reason, all figures will display a two-dimensional image of the CFD results at the plane that split the vehicle. This choice was made to reduce the computational time of the simulations by eliminating half the volume that a complete vehicle body simulation would generate.

7.1 Initial Conditions

The program STAR-CCM+ allows users to define the physics models for the simulation as well as reference values and initial conditions. This section will define the models, values, and conditions that these simulations were set with unless otherwise specified for specific runs.

The physics models used in the simulation are listed below:

- Coupled Energy
- Coupled Flow
- Equilibrium Air
- Exact Wall Distance
- Gas (equilibrium air)
- Gradients
- Linear Pressure Strain Two-Layer
- Real Gas
- Reynolds Stress Turbulence
- Reynolds-Averaged Navier-Stokes
- Steady
- Three Dimensional
- Turbulent
- Two-Layer All y+ Wall Treatment

The Reference Values and their values are listed below in Table 7.1

Table 7.1 Reference values for CFD

Reference Pressure	5000.0 Pa
Maximum Allowable Temperature	5000.0 K
Minimum Allowable Temperature	100.0 K
Minimum Allowable Wall Distance	1.0E-6 m

Initial Conditions and their associated settings and values are listed below in Table 7.2

Table 7.2 Initial conditions of CFD tests

Pressure	0.0 Pa
Static Temperature	300.0 K
Turbulence Intensity	0.01
Turbulence Specification	Intensity + Viscosity Ratio
Turbulent Velocity Scale	1 m/s
Turbulent Viscosity Ratio	10
Velocity	300 m/s

The Initial condition for Velocity was set at 300 m/s because the inlet's velocity is so high, it would cause errors in the program to assume for static initial air. The Pressure is set at 0 Pa for initial because it is in reference to the Reference Pressure which was already 5000.0 Pa.

All simulations are run with an inlet and outlet to simulate airflow. The inlet velocity was set with a Mach Number of 6, and a Pressure of 0 Pa (5000.0 Pa when adding reference pressure). The Temperature of the inlet air was set to 253.15 K and the Turbulence Intensity and Turbulence Viscosity Ratio were set to mimic those in the Initial Conditions.

7.2 Initial Testing Utilizing X-37

7.2.1 Initial Run

The first CFD simulation were initially set up utilizing the X-37, where the control volume was a cylinder of length 300m with a radius of 50m. The left side opening of the cylinder was designated as inlet, with the opposite side of the cylinder designated as outlet. The walls of the cylinder were defined as freestream, this was done to eliminate the possibility of viscous dynamics due to a wall. The model of a 75% scale X-37 was placed with the nose 100m from the inlet and set at a 30% angle of attack based on the SSO's re-entry angle of attack during part of its re-entry. (Dunbar B, 2017)

The Automated Mesh tool in STAR-CCM+ was used to generate the mesh for the simulation, utilizing the following meshers:

- Surface Remesher
- Automatic Surface Repair
- Trimmed Cell Mesher
- Prism Layer Mesher

The Surface Remesher performed both Curvature Refinement and Proximity Refinement. The Automatic Surface Repair assisted in remaking portions of the mesh as it relates to the surfaces within the simulation. The Trimmed Cell Mesher worked to cut a template mesh with the surface geometry and extrapolate it into a volume mesh. The Prism Layer Mesher generated Prismatic cell layers next to the surface of the vehicle in the simulation. The number of layers for this first test was limited to 6 as this first run was to see the flow of the body and to estimate where the shockwaves would be generated.

A refinement area was designated around the body of the vehicle so that cells within that area could be varied in size and density compared to cells outside the area. This allowed cells outside of this refinement area to be large and coarse so they would reduce computational time, while allowing for there to be a refined area directly around the

vehicle that would take longer to compute but produces more defined results. This cone was initially situated at the same 30 degree incline the vehicle was, but with one circle of the cone forward of the nose, and the second cone aft of the tail.

The purpose of this first initial test was to observe how STAR-CCM+ handled the simulation and to work out the set conditions so that the simulation would run without error. The first simulation ran to 9986 iterations before being stopped and observed. There following Figures 13-18, are all taken from this first test at iteration 9986.

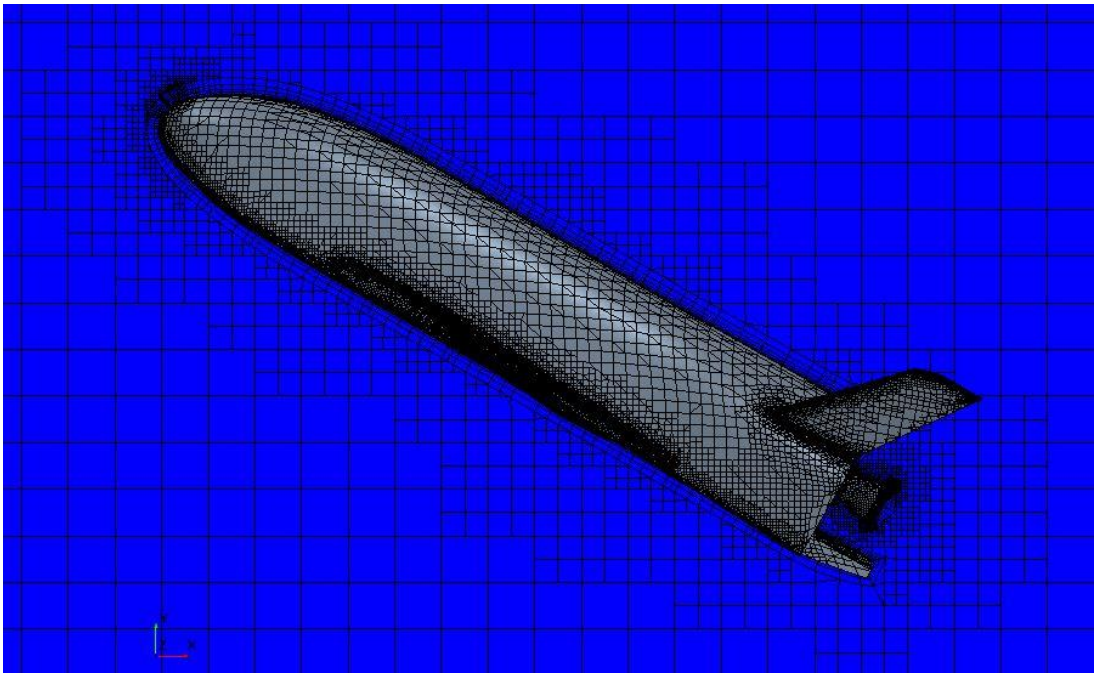

Figure 13 Mesh around body of X-37

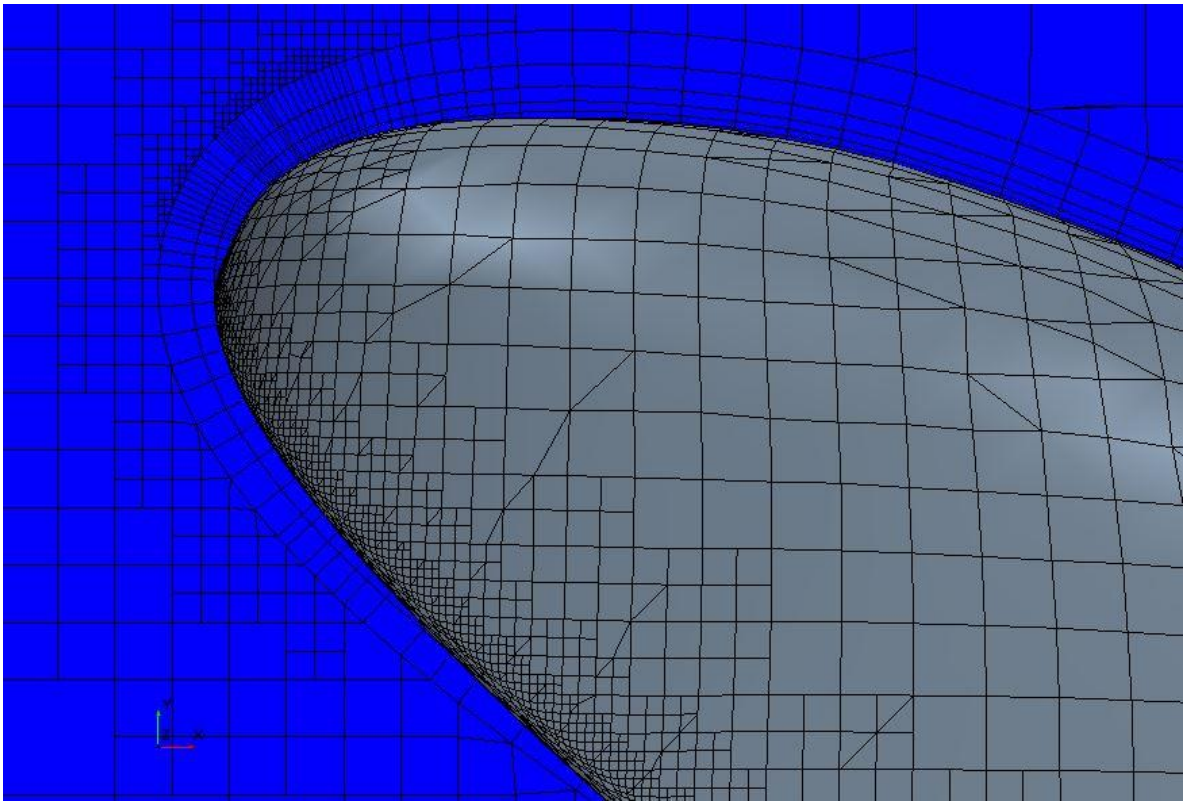

Figure 14 Mesh around nose of X-37

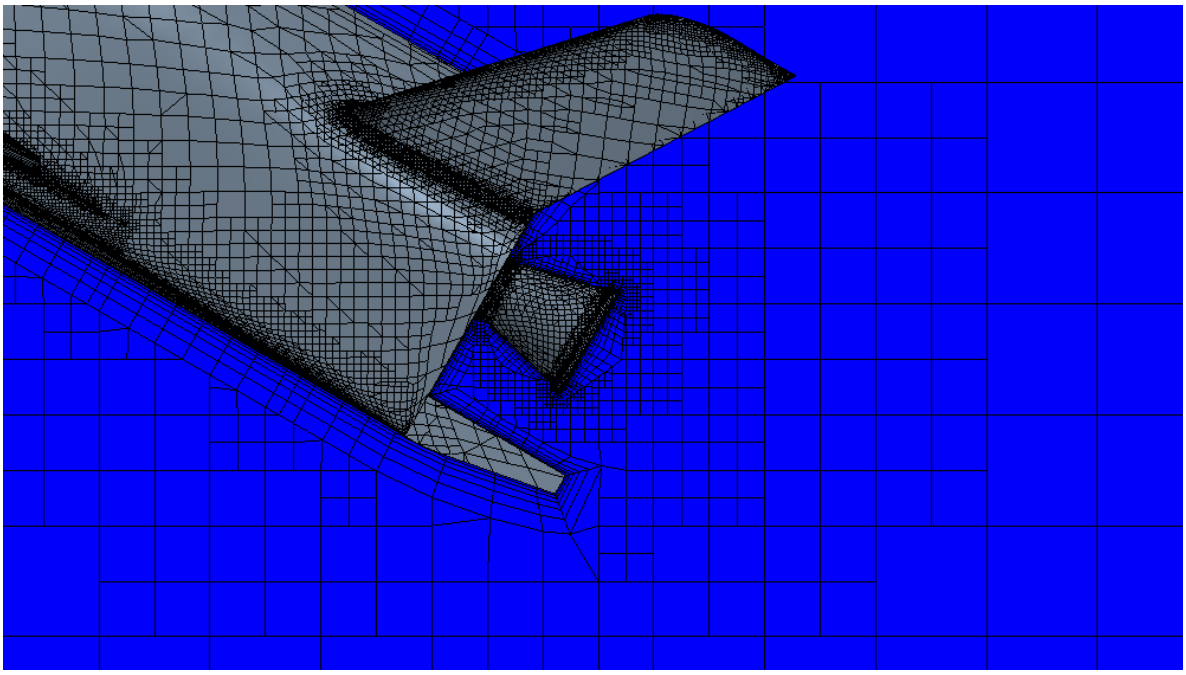

Figure 15 Mesh around tail section of X-37

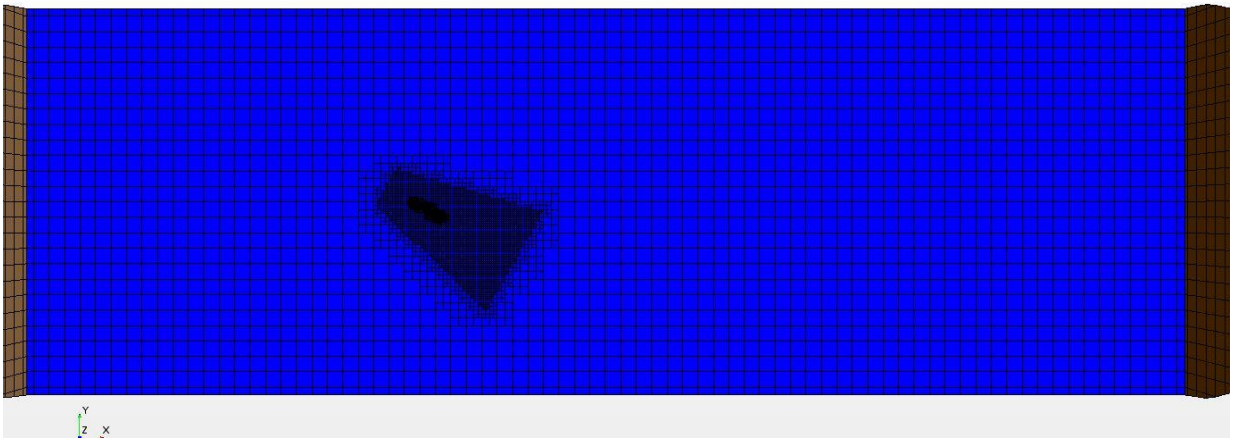

Figure 16 Mesh refinement area within test area

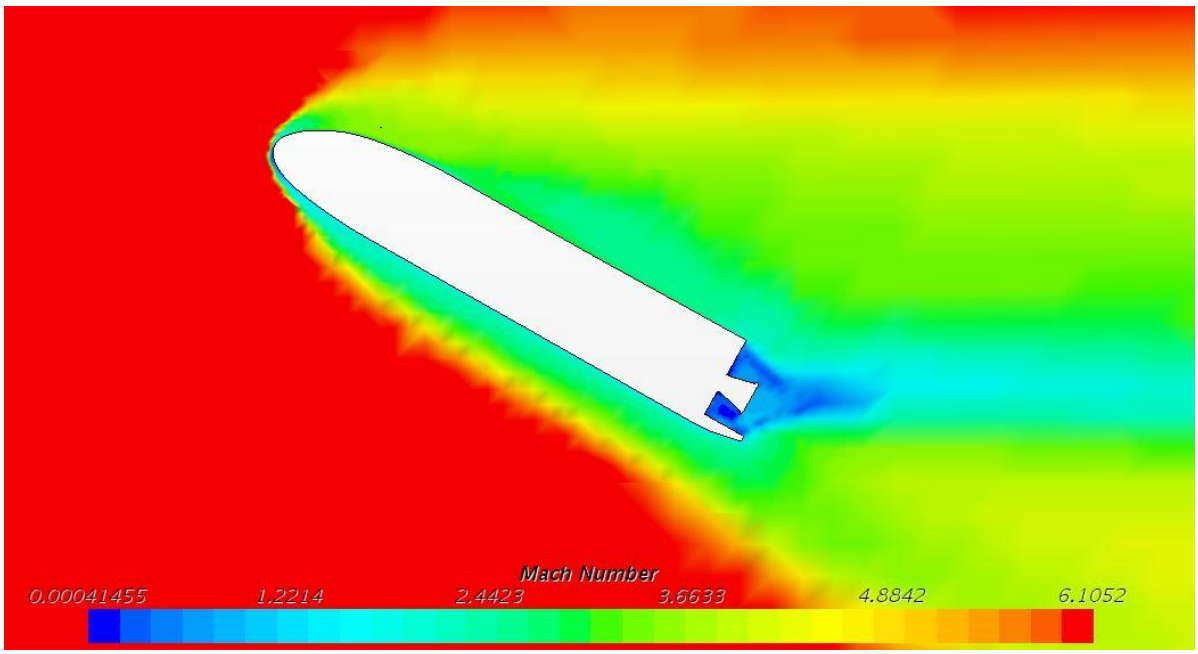

Figure 17 Mach number around body of X-37

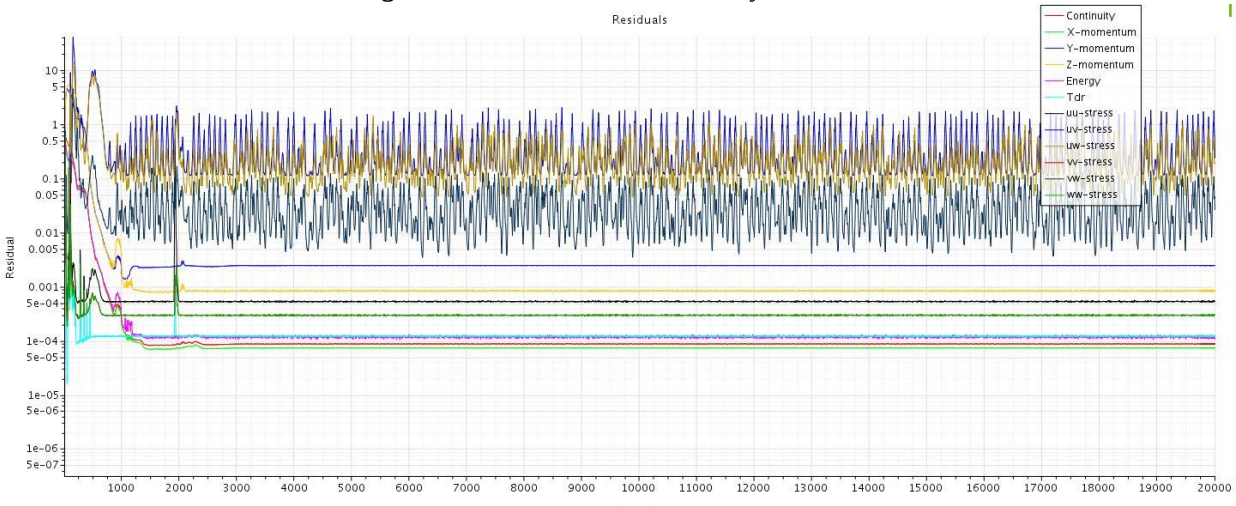

Figure 18 Residuals from Initial X-37 run

As can be seen in Figure 18, the residuals seem to oscillate after iteration 1000, remaining consistent except for a temporary spike around iteration 2000. This seems to be the result of the coarseness of the mesh, combined with the inability of the test area to capture the disturbances that the model created in the free flow of air. These residuals may be oscillating, but they are neither diverging nor converging so the simulation did not crash nor resolve itself, however with the large number of iterations, it can be assumed that given additional time, the results would not change.

The Figures 13 through 15 all show the initial mesh around the model of the X-37 in STAR-CCM+. This mesh was coarse and as such, was able to run quickly while producing low resolution results. The shape in Figure 16 was the bisection of the refinement area cone.

7.2.2 Initial 500K Cell Run

The Initial Run provided a lot of information for further iterations of the simulation. Through the initial run, the locations of the shockwaves for the X-37 were located and allowed for the creation of a test area that had less cells that could be ignored. This is because the initial run allowed for a lot of cells ahead and behind the model that had no effect on the wave and wasted time in calculations. The result was a test area that was much smaller and was focused around the model of the X-37, along with a refinement area that was focused on the resulting shockwaves. Once the simulation was set up, the base size of the mesh was reduced to 0.8 meters. The cell size of the far field refinement area was set to be 300 percent of base size, or 2.4 meters. The cell size of the cells within the shock refinement area was set to 20 percent of base size, or 0.16 meters. The size of the cells on the surface of the vehicle body was set to a target of 10 percent of base, or 0.08meters. The minimum surface size allowable was set to 5 percent of base or 0.04 meters. These settings allowed for the creation of a mesh with 544,872 cells. The mesh can be seen in 19

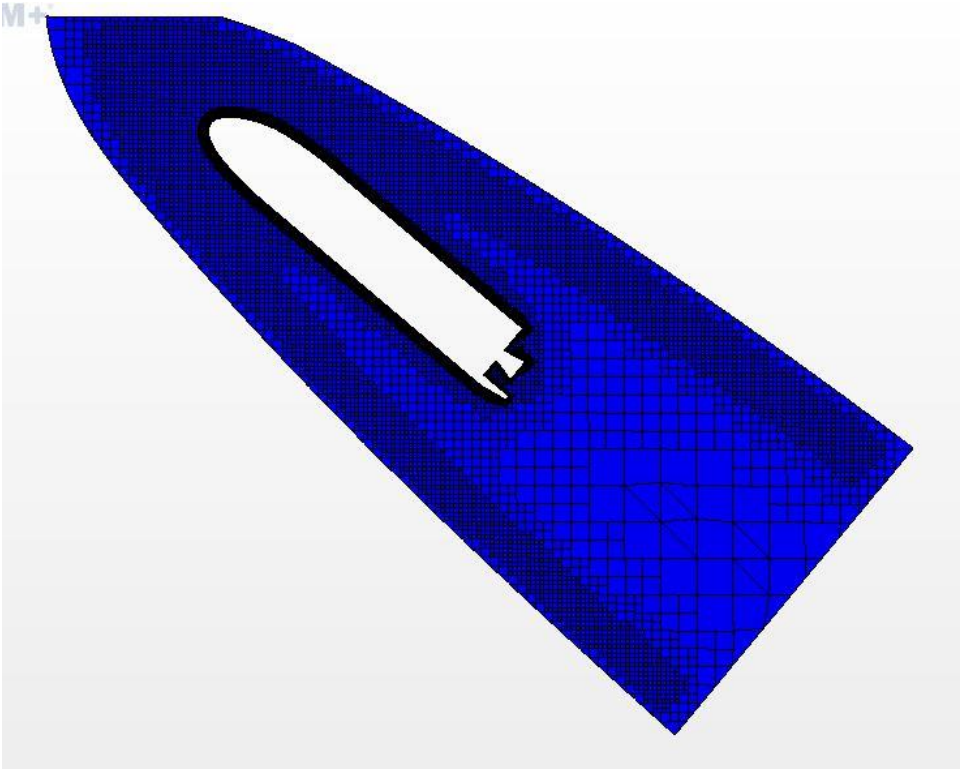

Figure 19 Full area mesh for Initial X-37 500K cell run

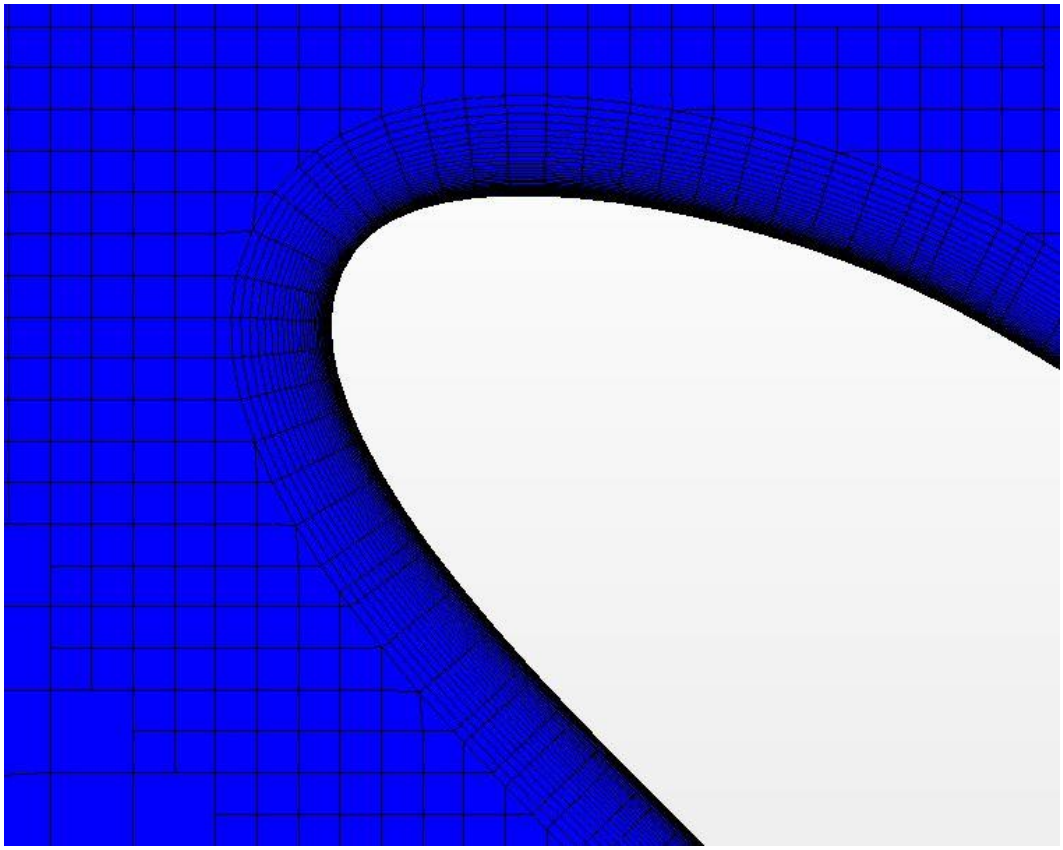

Figure 20 Nose mesh for the Initial X-37 500K run.

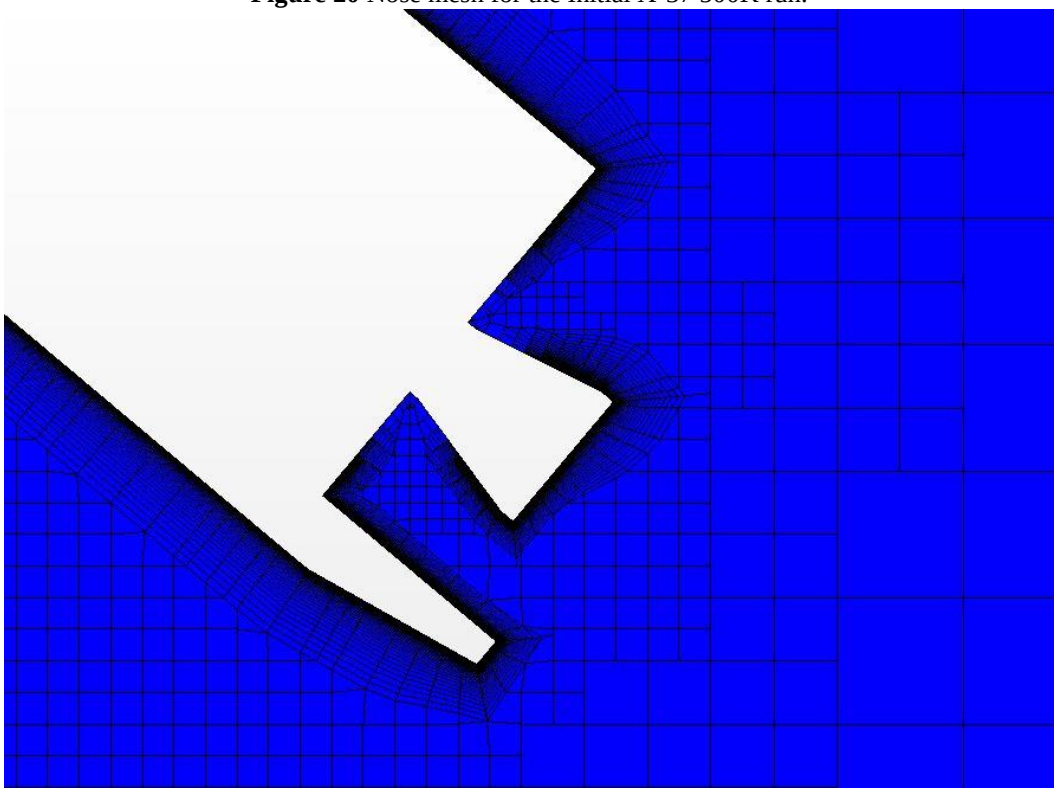

Figure 21 Tail mesh for the Initial X-37 500K run.

The boundary around the body of the vehicle was set to have 30 layers of prism cells around it with an increase of 10 percent for each cell as they separated from the body of the vehicle. The area extended to a third of a meter from the body of the vehicle.

The Mach number of the simulation can be seen in Figure 22. The area around the vehicle is noticeably smaller when compared with the previous iterations of the simulation, as unnecessary space was removed from the simulation. It can be seen however, that there is still space that can be removed in an effort to waste no processing power on those cells. There are two areas of low Mach number visible in Figure 22, the nose and the aft near the nozzle. The Shock waves of the vehicle can be clearly seen above and below the vehicle, however there is still adjustments needed to the shockwave refinement area so that it can entirely capture the shockwave.

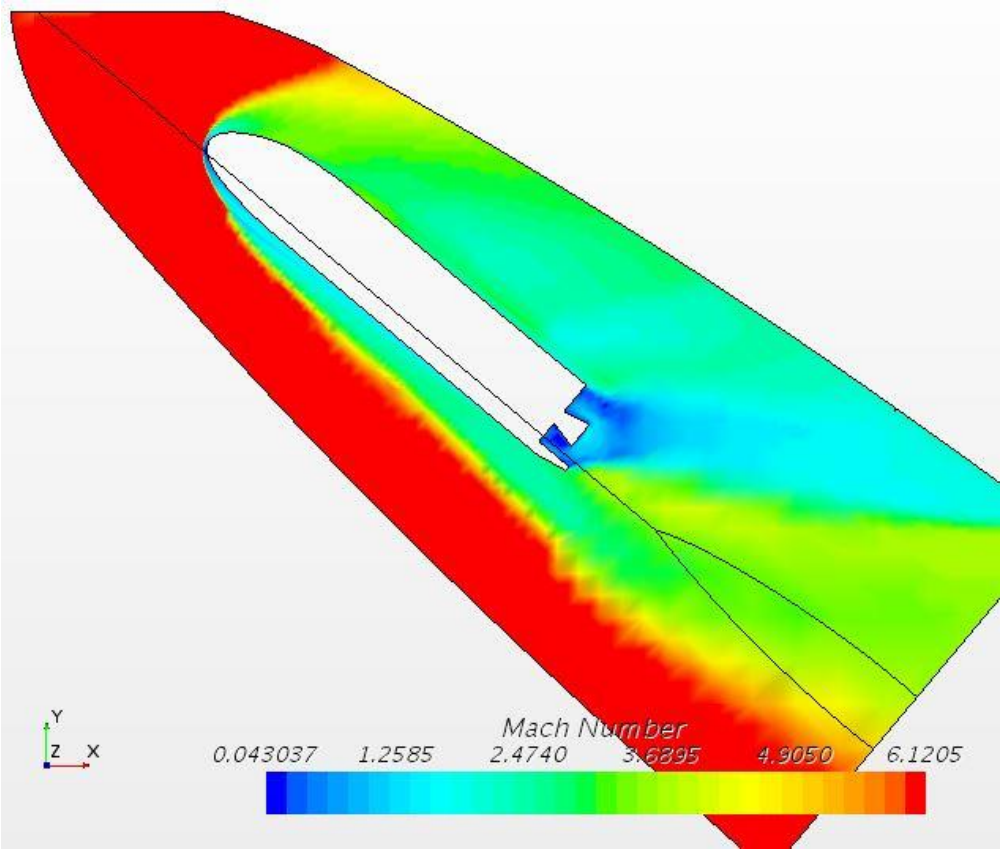

Figure 22 Mach number scene for Initial X-37 500K cell run

The areas where the air seems to stagnate around the nose and nozzle are also the areas where there seems to be some of the greatest heat. Figure 7.B.7 displays the temperature of the vehicle in the simulation and seems to correlate the absence of movement with the increase in temperature. This applies to the shockwaves as well, as there is an increase in temperature at the wave and behind it.

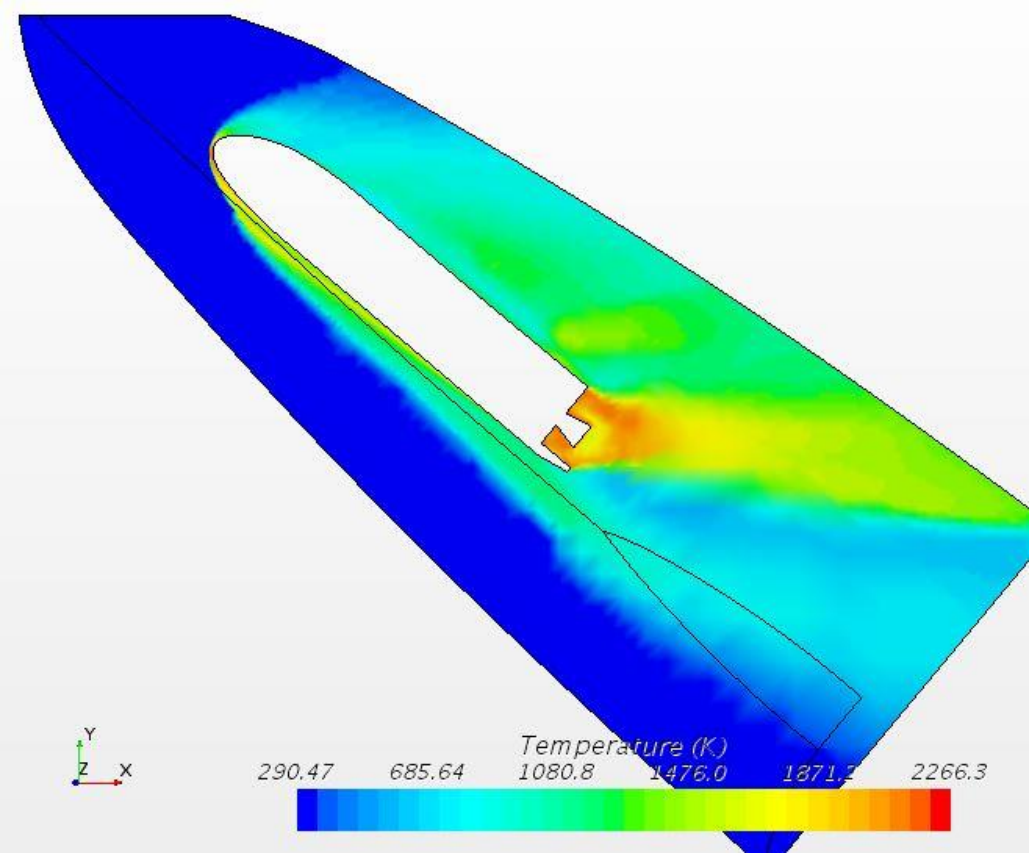

Figure 23 Temperature of the Initial X-37 500K cell run

For this simulation, there were force plots designated to show the force in Newtons in both the positive X direction and positive Y direction, denoting both the forces of drag and lift respectively. Figure 24 is the table showing the monitor plot for the force of lift of the vehicle, while Figure 25 is the table showing the monitor plot for the force of Drag.

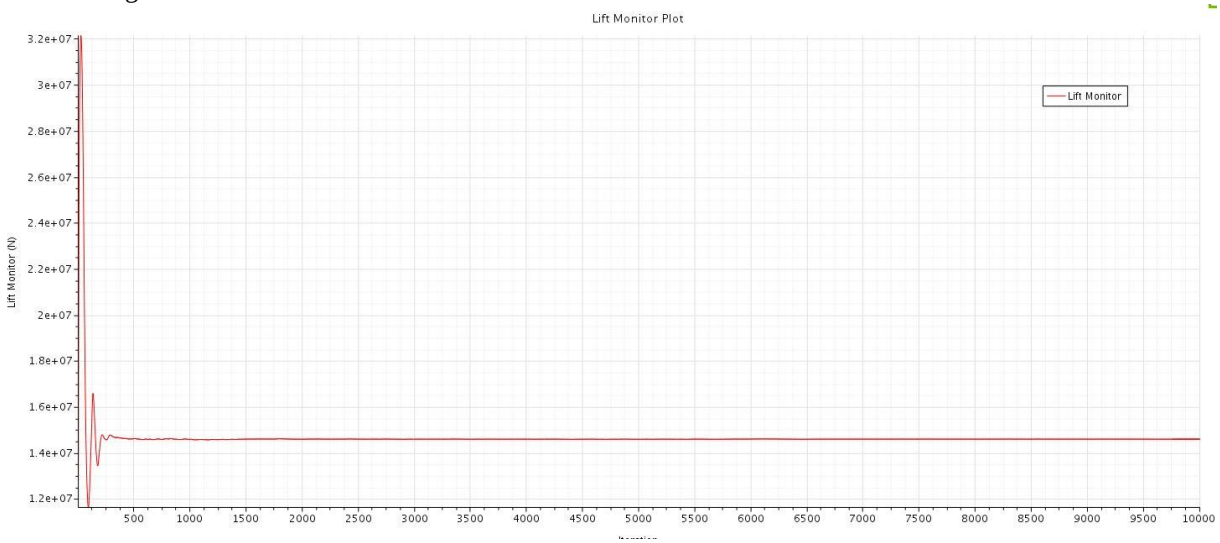

Figure 24 Lift plot for Initial X-37 500K run

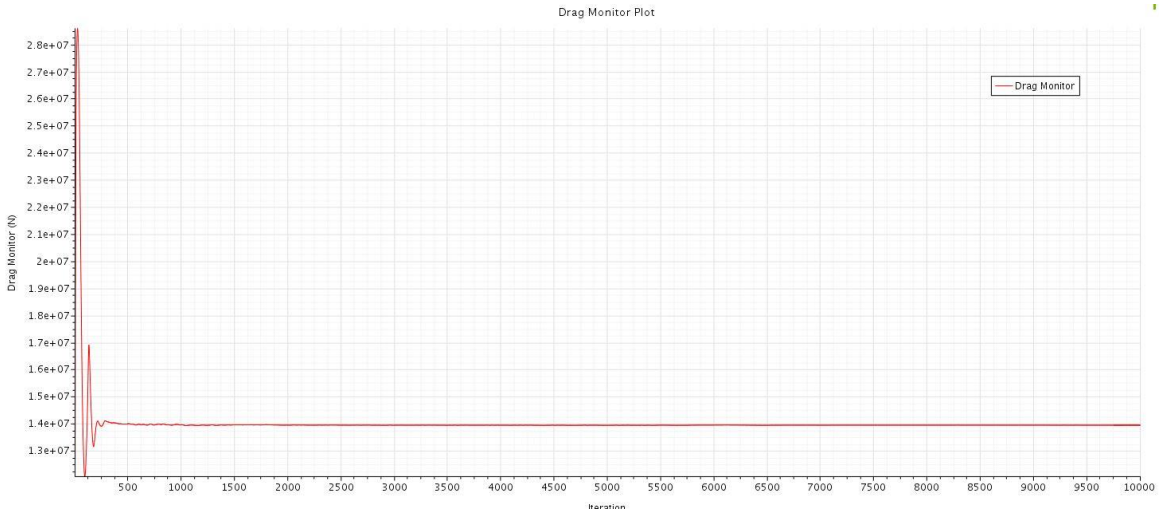

Figure 25 Drag plot for Initial X-37 500K run

This simulation was still course compared to what is needed for the confines of this report, however it provided insight into the reduction of the testing area as well as better definition as to where the shock waves are located in relation to the body. The future iterations will take this into account and adjust the shockwave refinement area so that the shockwaves are fully encapsulated in them. The simulation ran for a total of 8000 iterations, which is greater than the previously defined number of iterations before this simulation should converge. Due to this, the results for this run can be said to be accurate and unlikely to change with additional iterations.

7.3 X-37 OTV

There are a total of 5 final CFD runs with the X-37 OTV. There are 3 runs with the 100% scale model at 500 Thousand, 1 Million, and 2 Million Cells respectively. The final two runs utilize the 50% scale model at 1 million cells, and the 25% scale model at 500 Thousand cells. The CFD run of the 25% scale model was originally designed to be run at 1 Million cells, however repeated attempts resulted in Floating Point Errors and failed to converge. Due to time constraints, the 25% scale X-37 was run at 500 Thousand Cells. All the models for the X-37 OTV were set at an angle of attack of 40 degrees for these final tests to attempt to achieve a lift-to-drag ratio of 1. (Stone D, 1970)

7.3.1 100% X-37 at 500 Thousand Cells

A 100% scale model of the X-37 is tested at 572517 Cells. Figure 29 displays the mesh generated with Figure 30 and Figure 31 providing focus on the mesh near the nose and tail of the vehicle. The CFD simulation ran for a total of 10,000 iterations and seemed to converge towards a stable solution as seen in Figure 26. The Base cell size for the mesh was designated at 0.8 meters. The cone area behind the tail as well as the refinement area around the vehicle body were set to 20% of the base size (0.16m). The Far-field area outside of the refinement area was set to 300% of the base size (2.4m). The mesh was generated with 30 prism layers stretching at a rate of 1.1 the size of the previous layer, from the surface of the vehicle. The absolute thickness of these prism layers was 30% of the base size (0.24m). The target cell size on the surface of the vehicle was 10% of base size (0.08m) and the minimum surface cell size was set to 5% of the base size (0.04m). The lift force of the vehicle was 14,594,747N, and the drag force of the vehicle was 13,934,500N. Using these values for lift force and drag force and equation 3.6, the lift-to-drag ratio can be calculated to be 1.047.

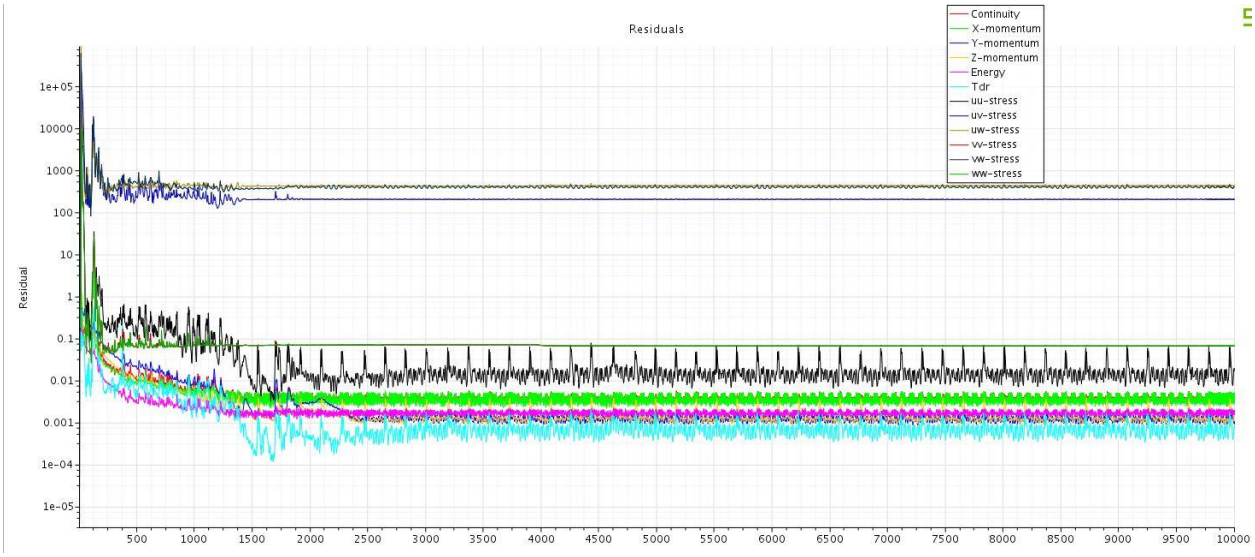

Figure 26 - 500K cells 100% scale X-37 Residual Plot

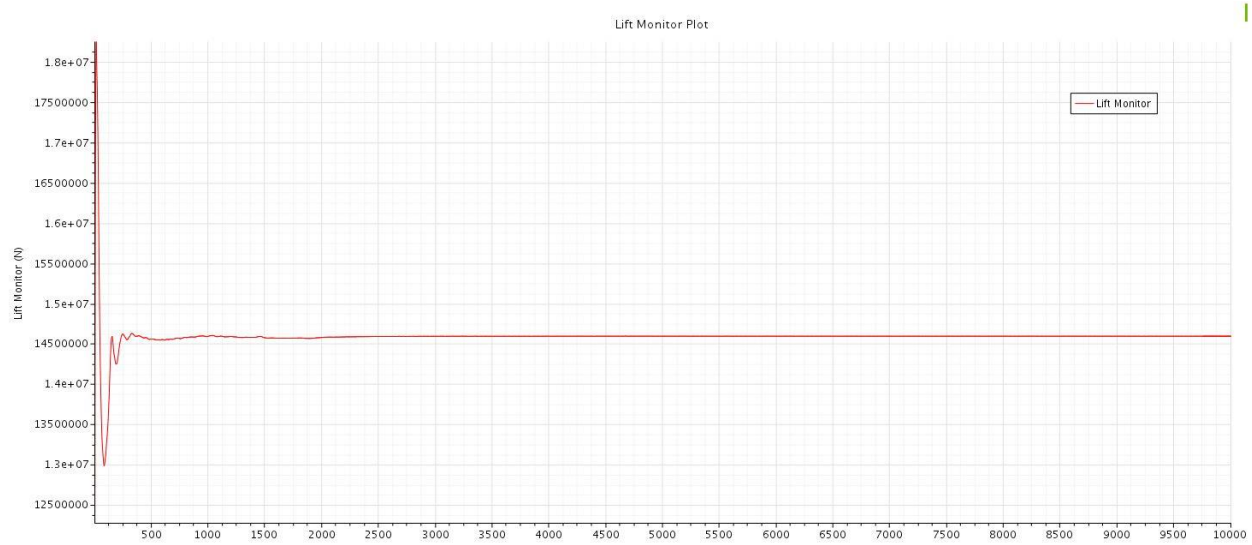

Figure 27 - 500K cells 100% scale X-37 Lift Plot

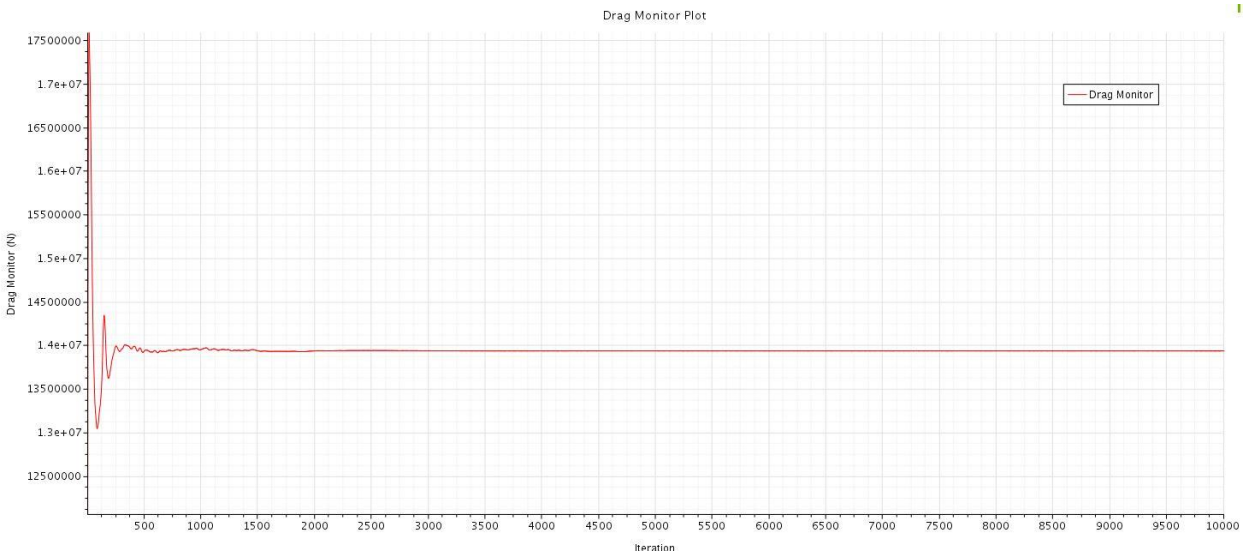

Figure 28 - 500K cells 100% scale X-37 Drag Plot

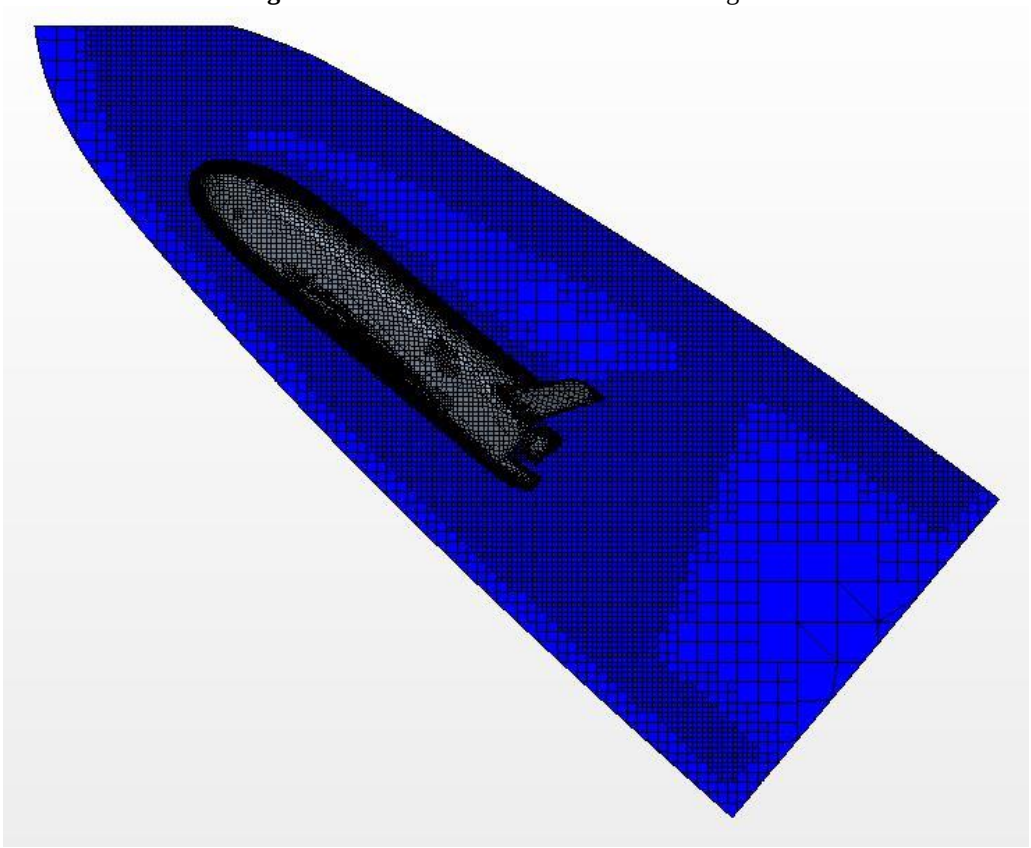

Figure 29 - 500K cells 100% scale X-37 full body Mesh

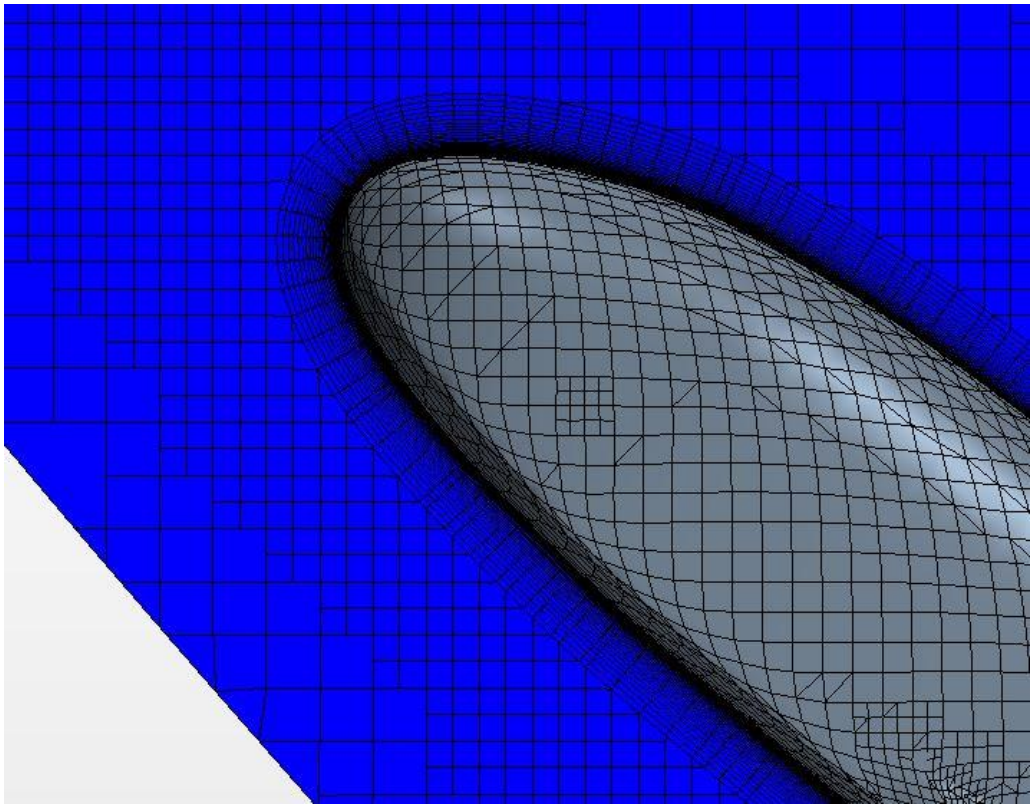

Figure 30 500K Cells 100% scale X-37 nose Mesh

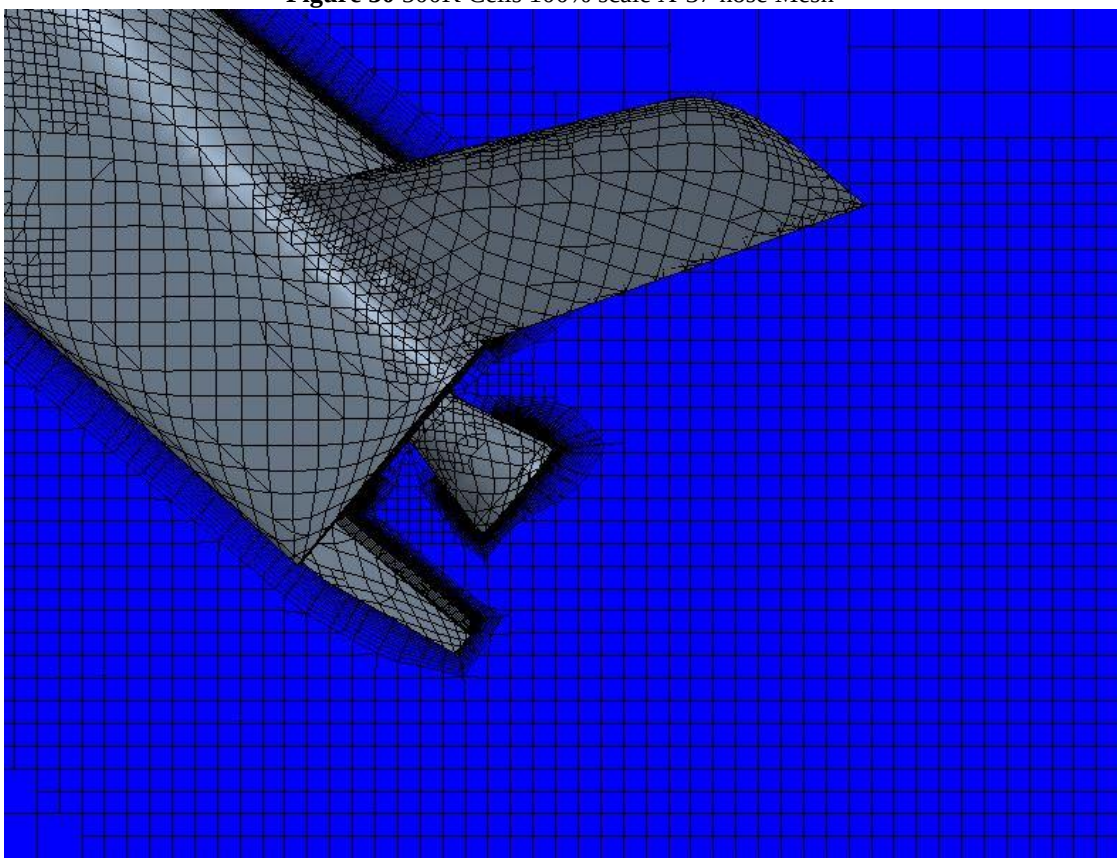

Figure 31 500K Cells 100% scale X-37 tail Mesh

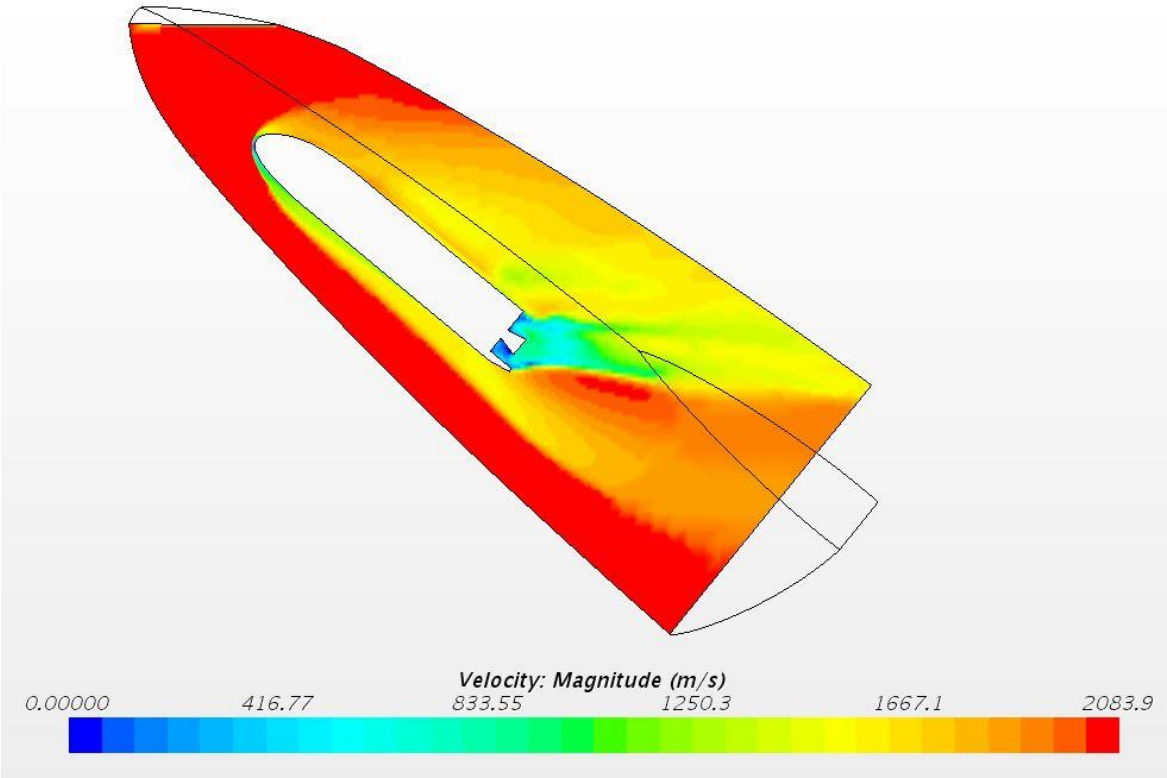

Figure 32 500K cells 100% scale X-37 full body Velocity

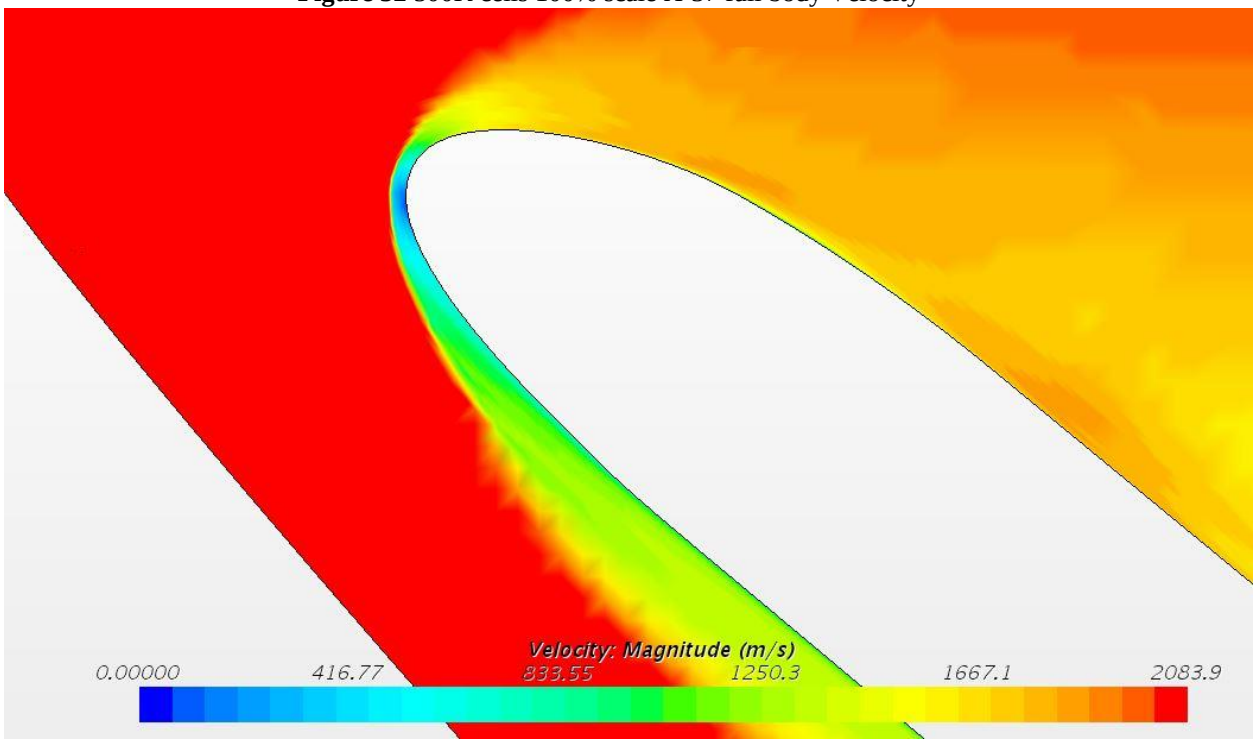

Figure 33 500K cells 100% scale X-37 nose Velocity

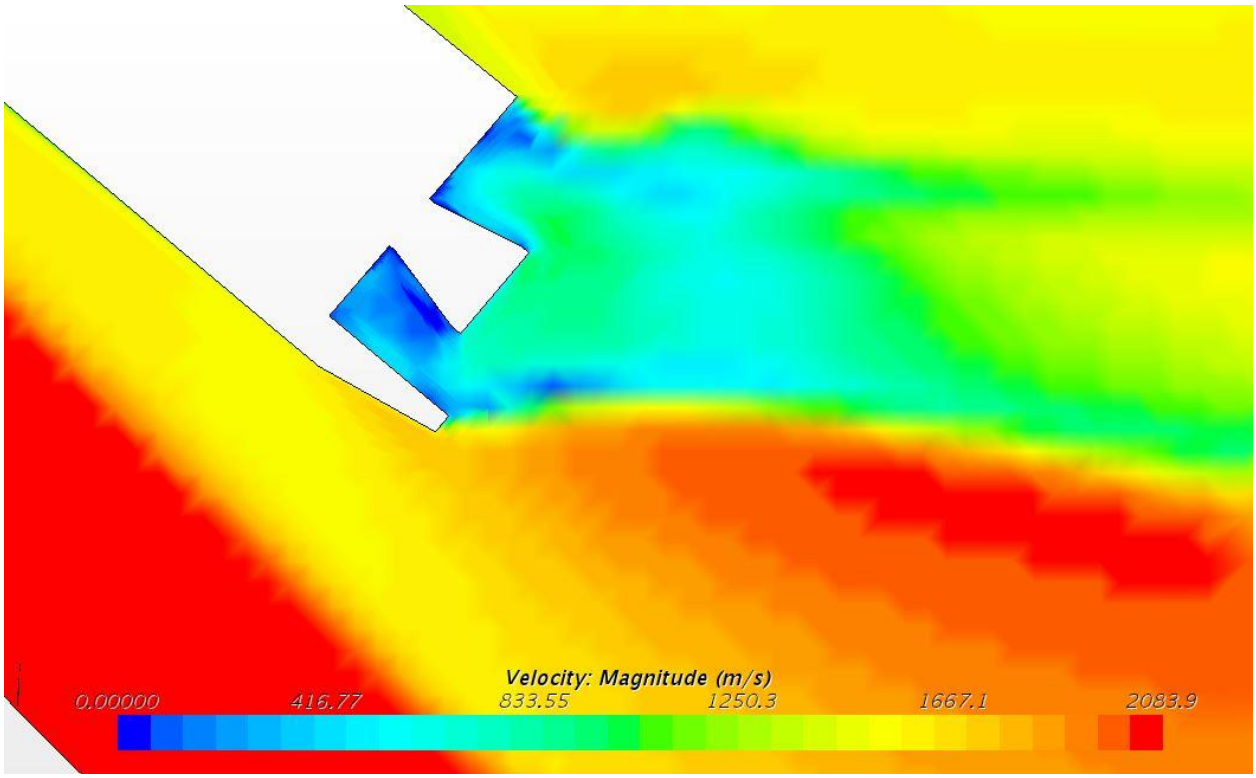

Figure 34 500K cells 100% scale X-37 tail Velocity

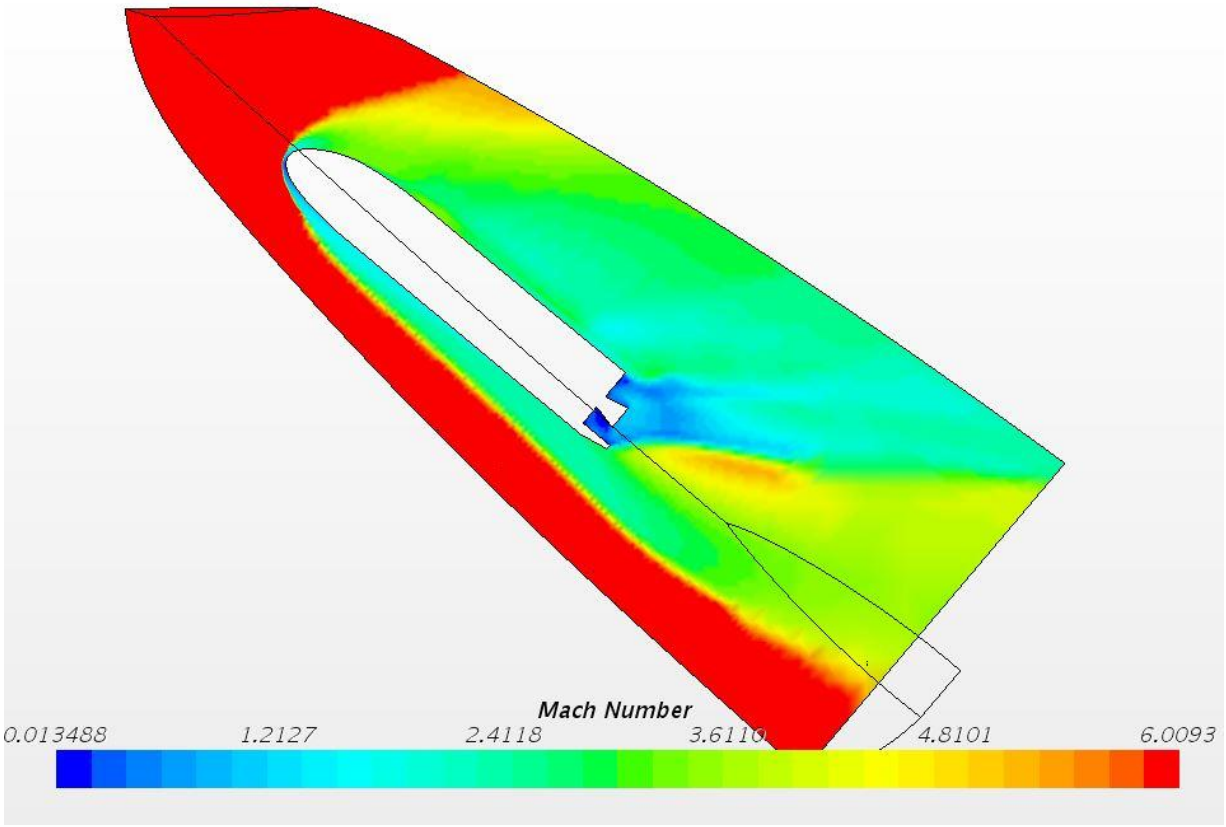

Figure 35 500K cells 100% scale X-37 full body Mach Number

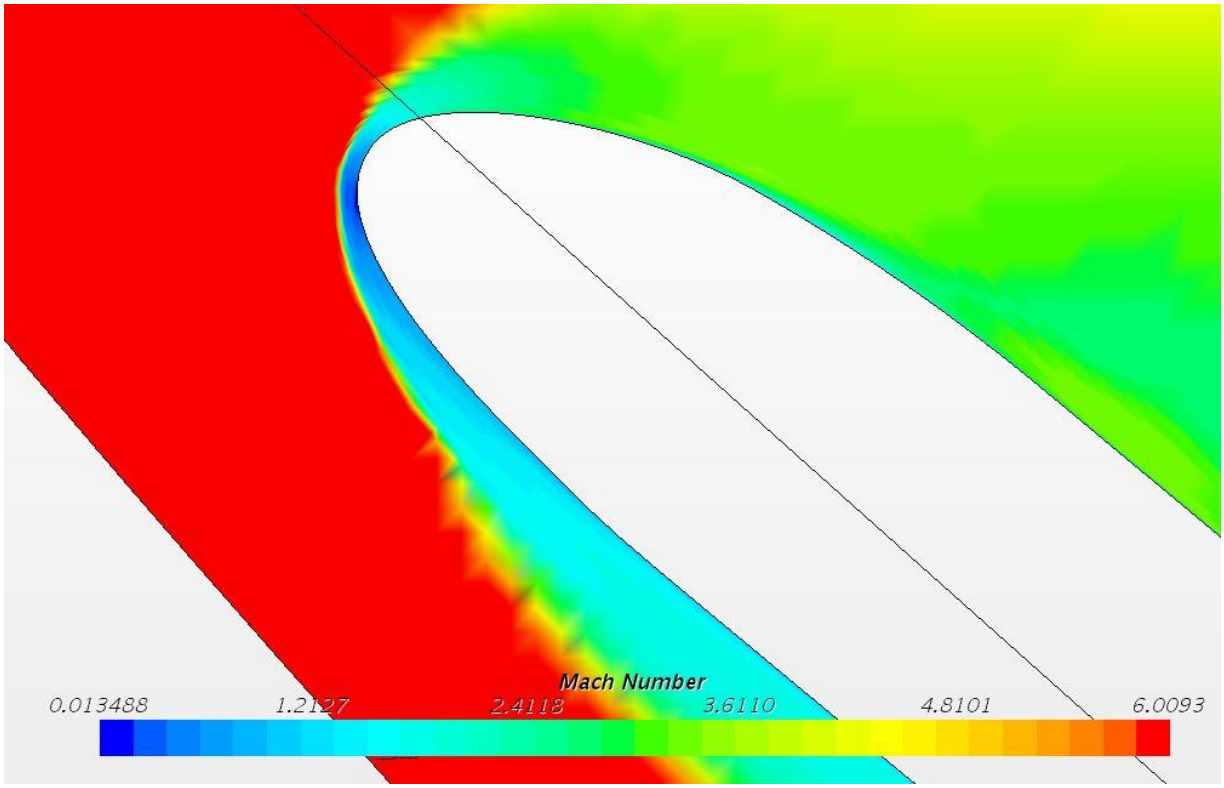

Figure 36 500K cells 100% scale X-37 nose Mach Number

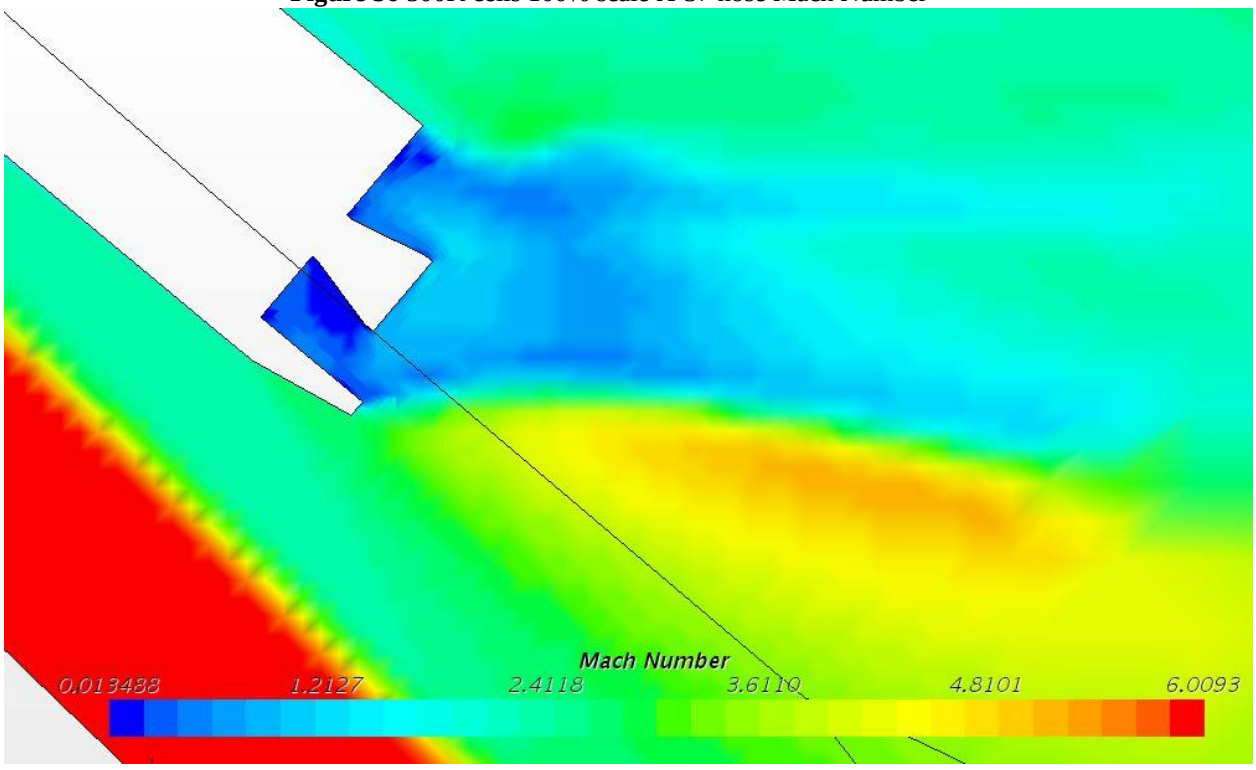

Figure 37 500K cells 100% scale X-37 tail Mach Number

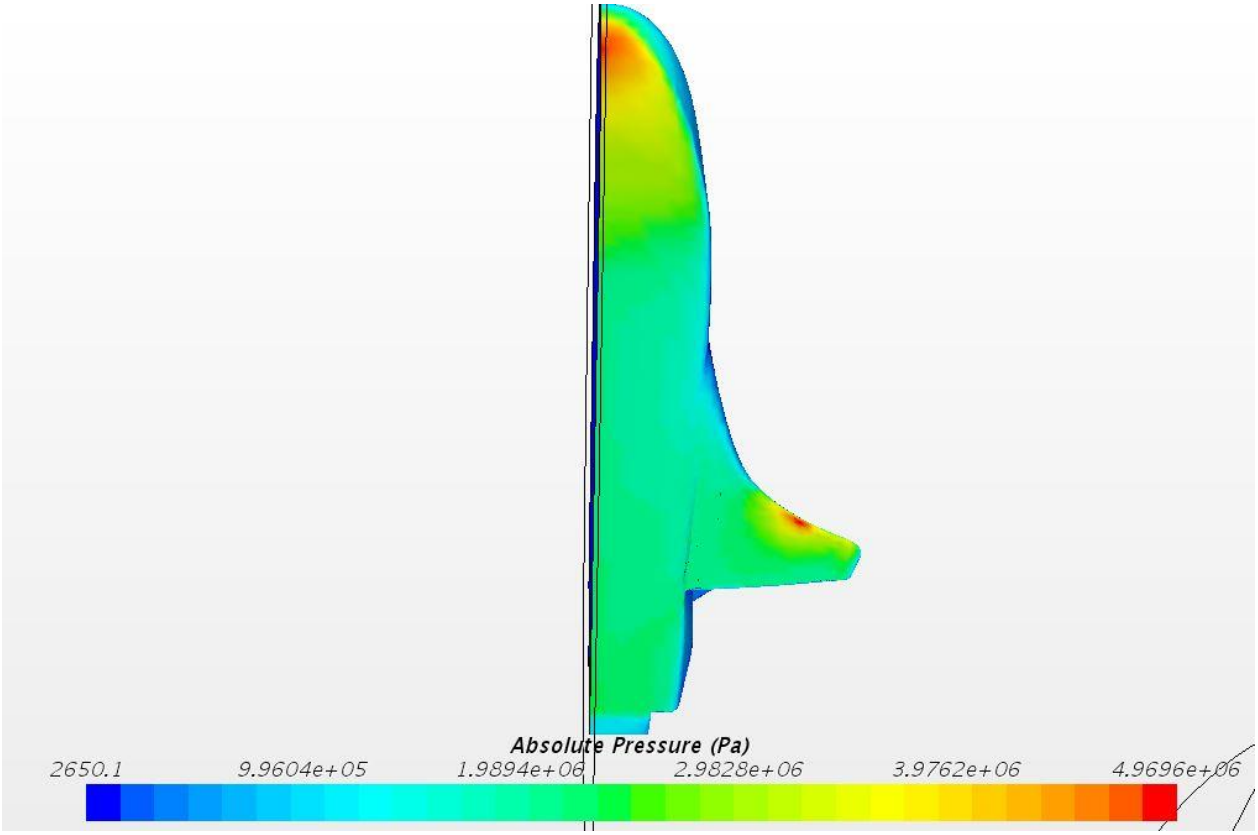

Figure 38 500K cells 100% scale X-37 bottom Absolute Pressure

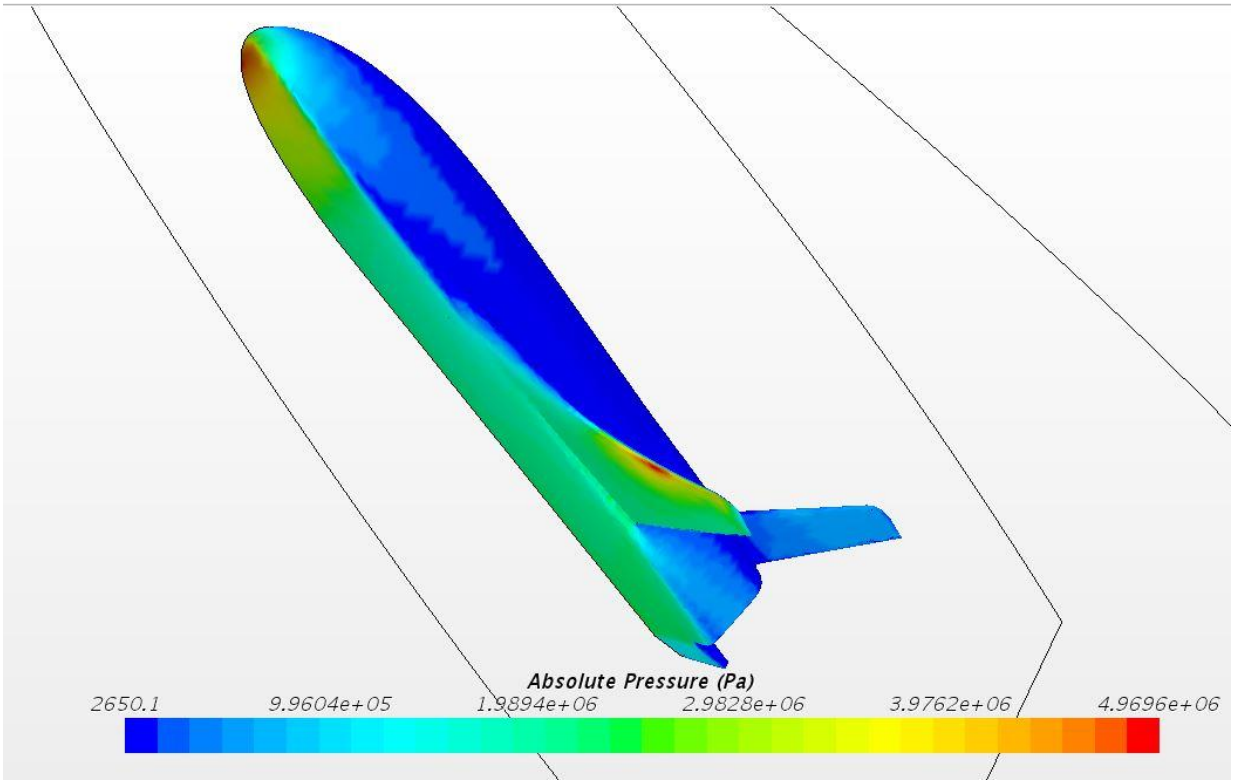

Figure 39 500K cells 100% scale X-37 3-D Absolute Pressure

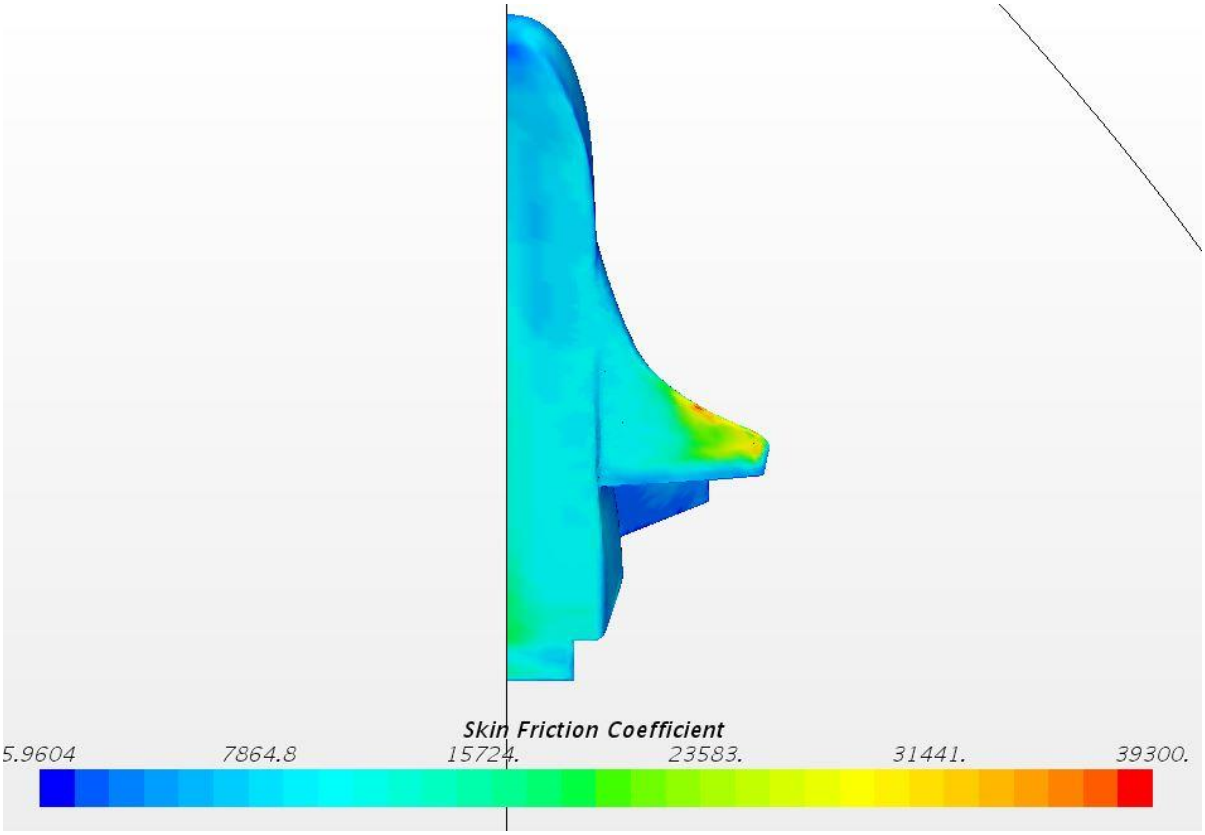

Figure 40 500K cells 100% scale X-37 bottom Skin Friction Coefficient

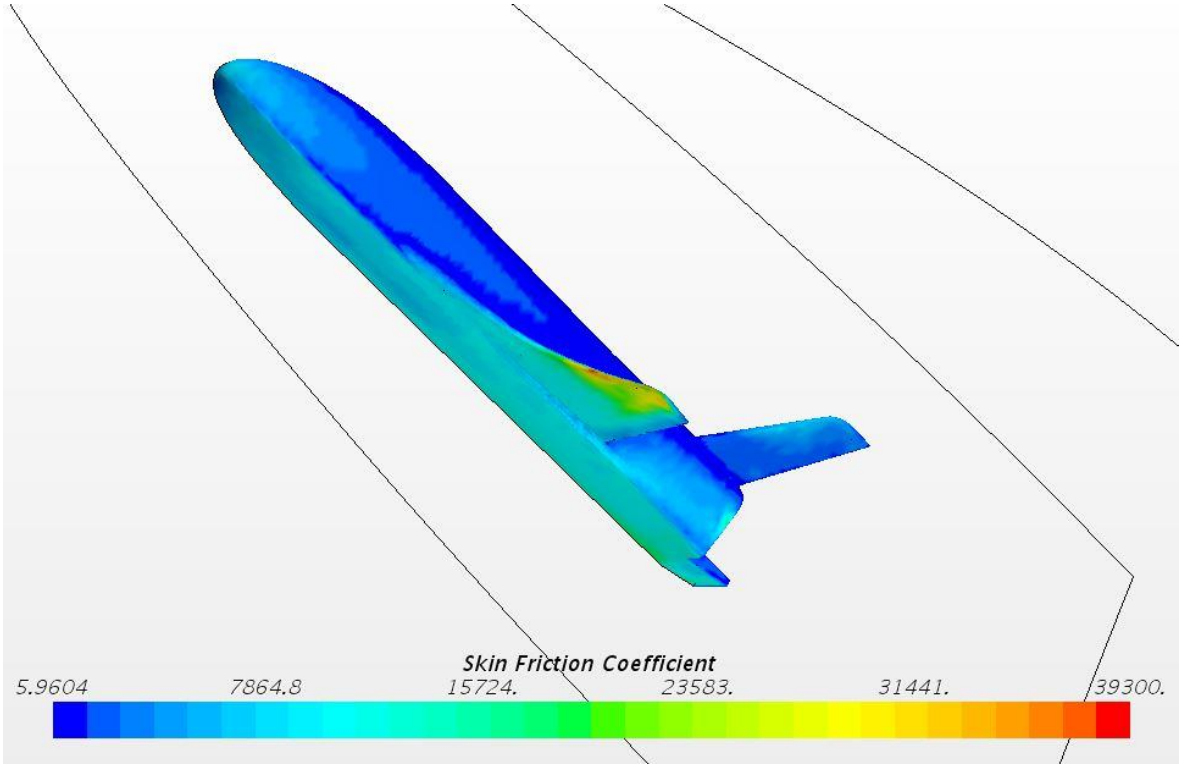

Figure 41 500K cells 100% scale X-37 3-D Skin Friction Coefficient

7.3.2 100% X-37 at 1 Million Cells

A 100% scale model of the X-37 is tested at 1049517 Cells. Figure 45 displays the mesh generated with Figure 46 and Figure 47 providing focus on the mesh near the nose and tail of the vehicle. The CFD simulation ran for a total of 7,000 iterations and seemed to converge towards a stable solution as seen in Figure 42. The Base cell size for the mesh was designated at 0.62 meters. The cone area behind the tail as well as the refinement area around the vehicle body were set to 20% of the base size (0.124m). The Far-field area outside of the refinement area was set to 300% of the base size (1.86m). The mesh was generated with 30 prism layers stretching at a rate of 1.1 the size of the previous layer, from the surface of the vehicle. The absolute thickness of these prism layers was 30% of the base size (0.186m). The target cell size on the surface of the vehicle was 10% of base size (0.062m) and the minimum surface cell size was set to 5% of the base size (0.031m). The lift force of the vehicle was 14,660,778N, and the drag force of the vehicle was 13,969,214N. Using these values for lift force and drag force and equation 3.6, the lift-to-drag ratio can be calculated to be 1.050.

Figure 42 - One million cells 100% scale X-37 Residual Plot

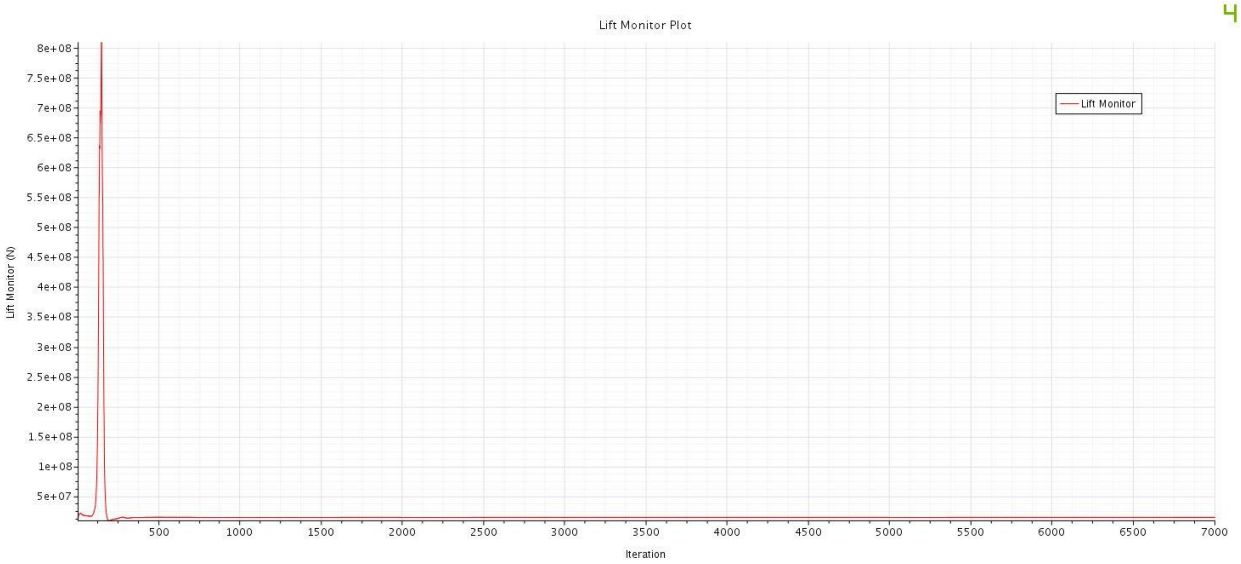

Figure 43 - One million cells 100% scale X-37 Lift Plot

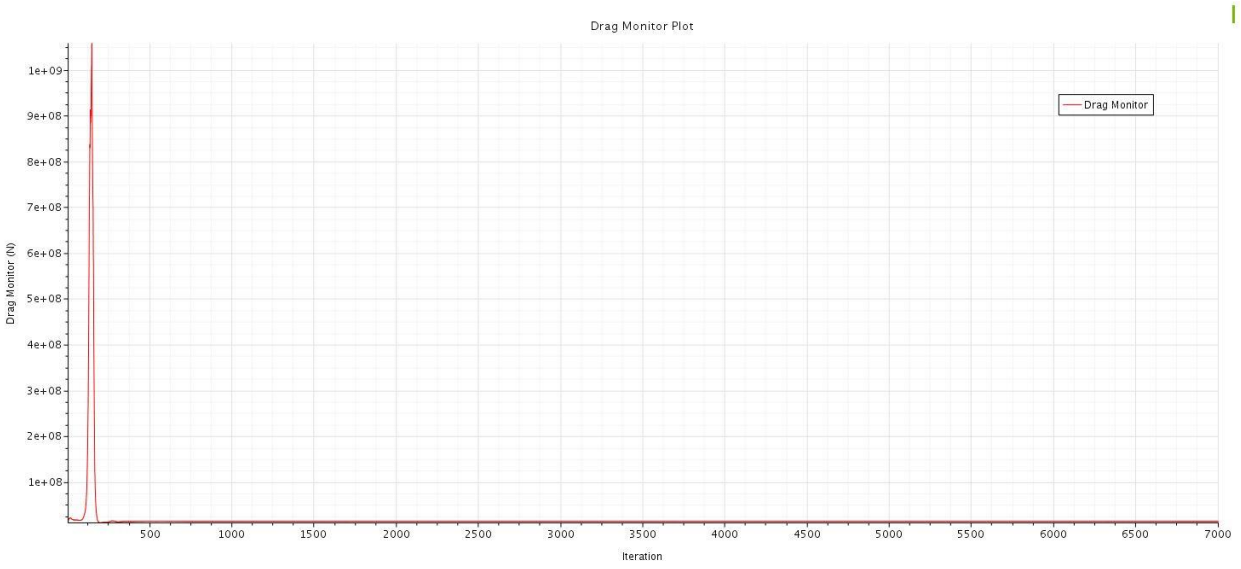

Figure 44 - One million cells 100% scale X-37 Drag Plot

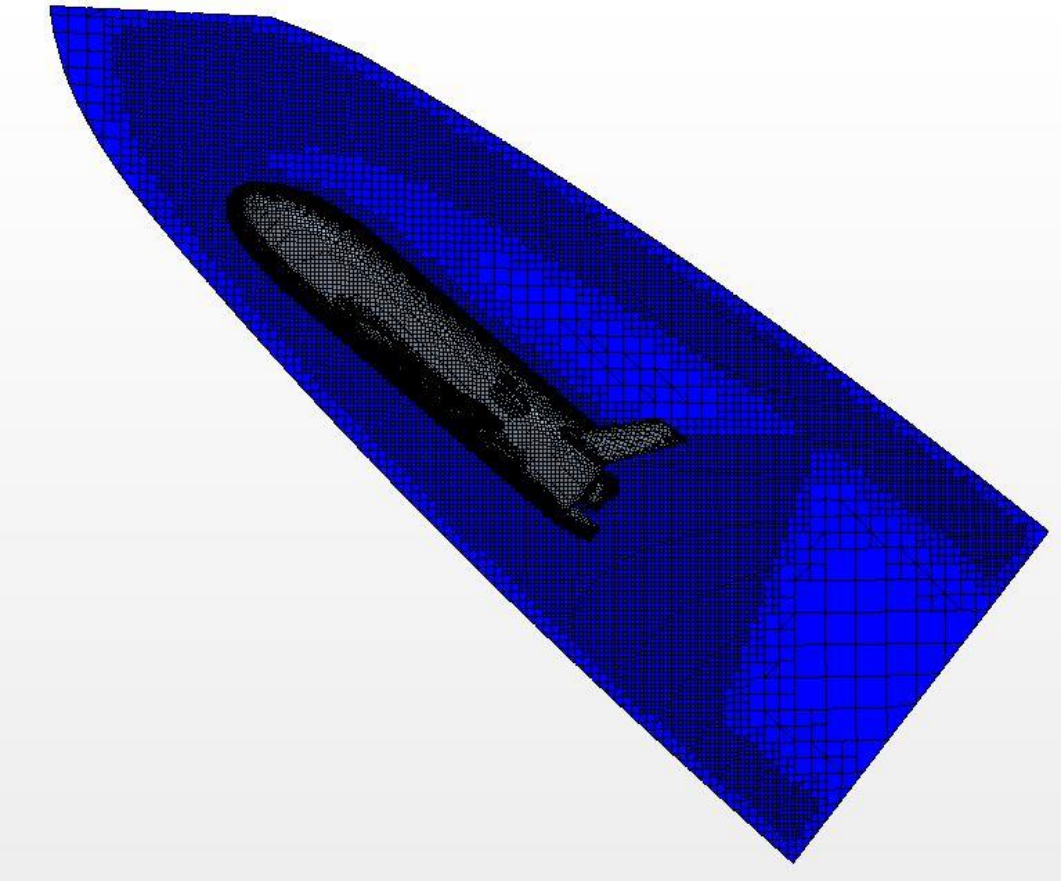

Figure 45 - One million cells 100% scale X-37 full body Mesh

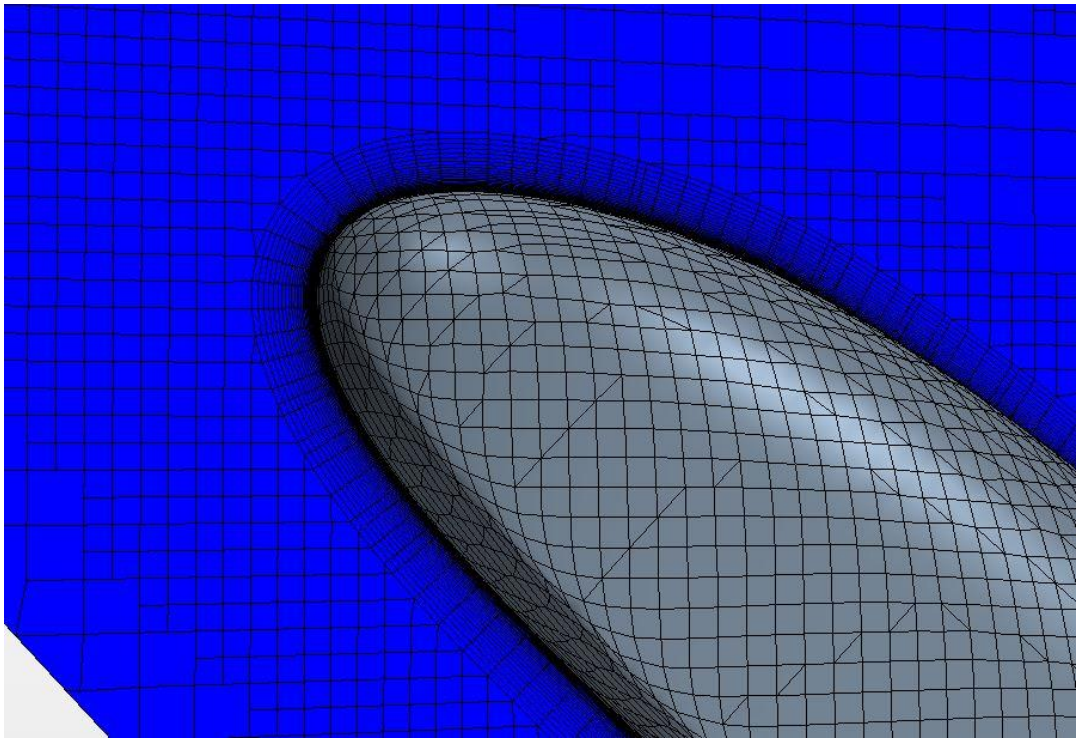

Figure 46 - One million cells 100% scale X-37 nose Mesh

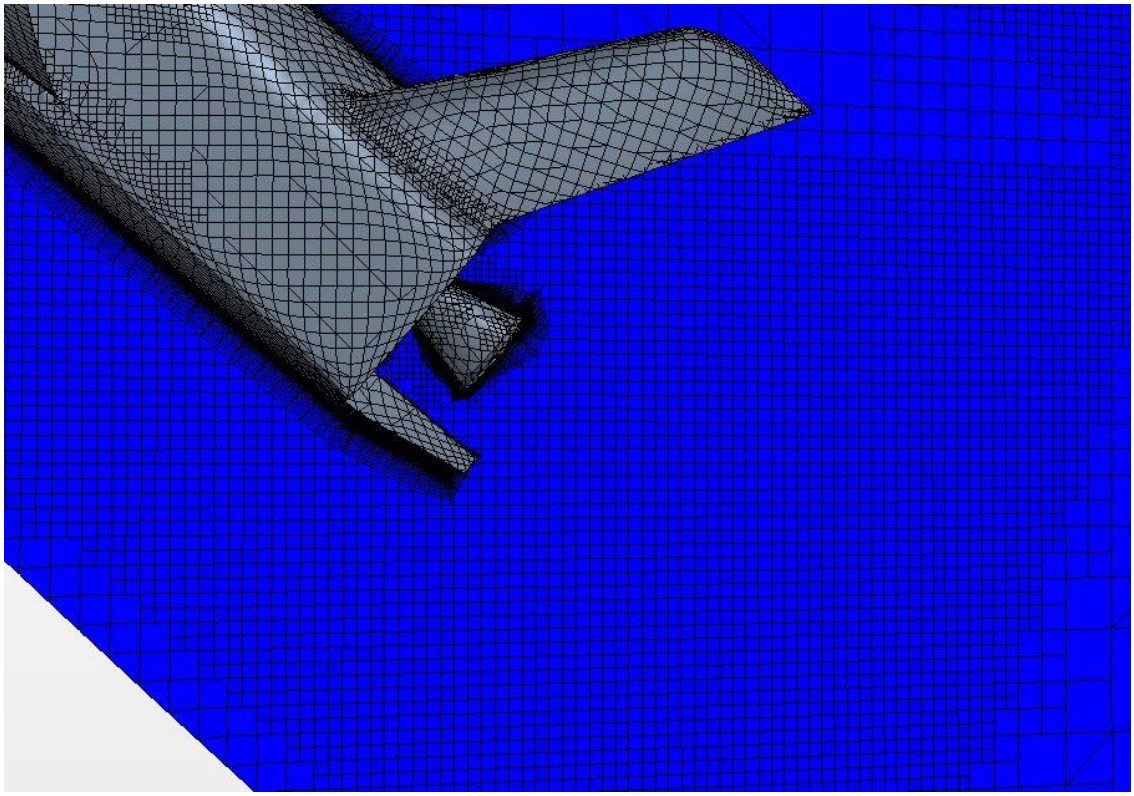

Figure 47 - One million cells 100% scale X-37 tail Mesh

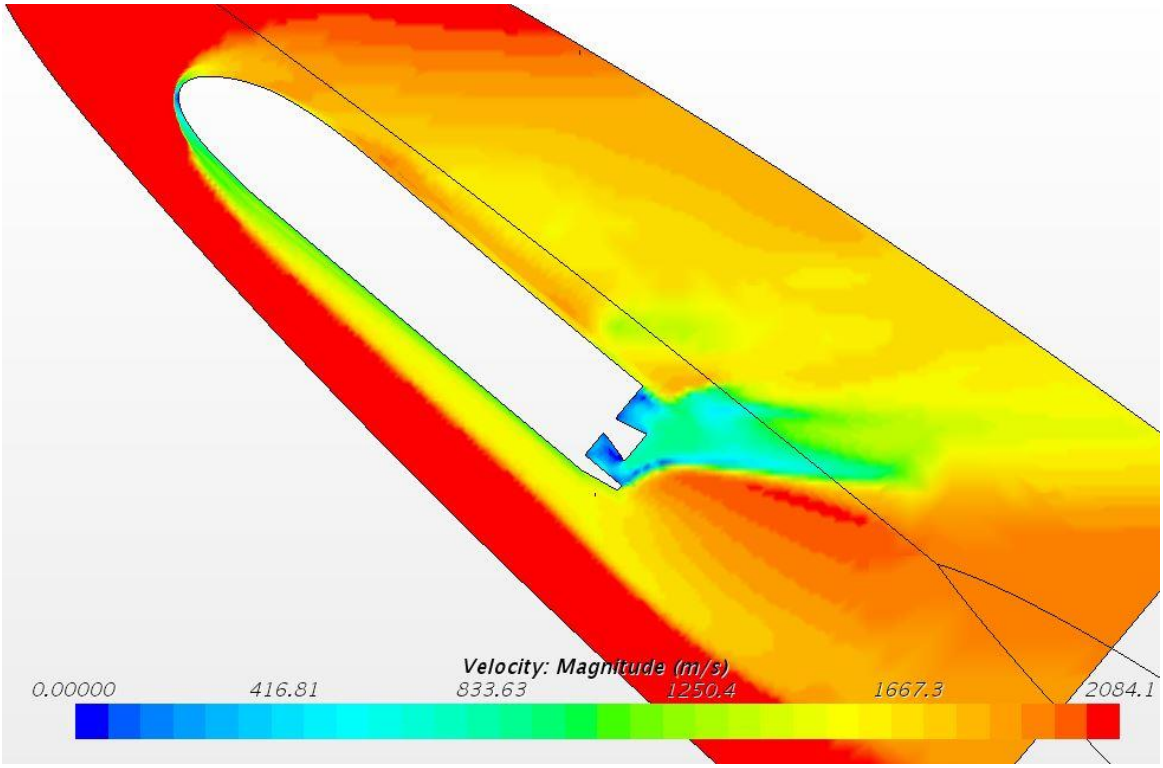

Figure 48 - One million cells 100% scale X-37 full body Velocity

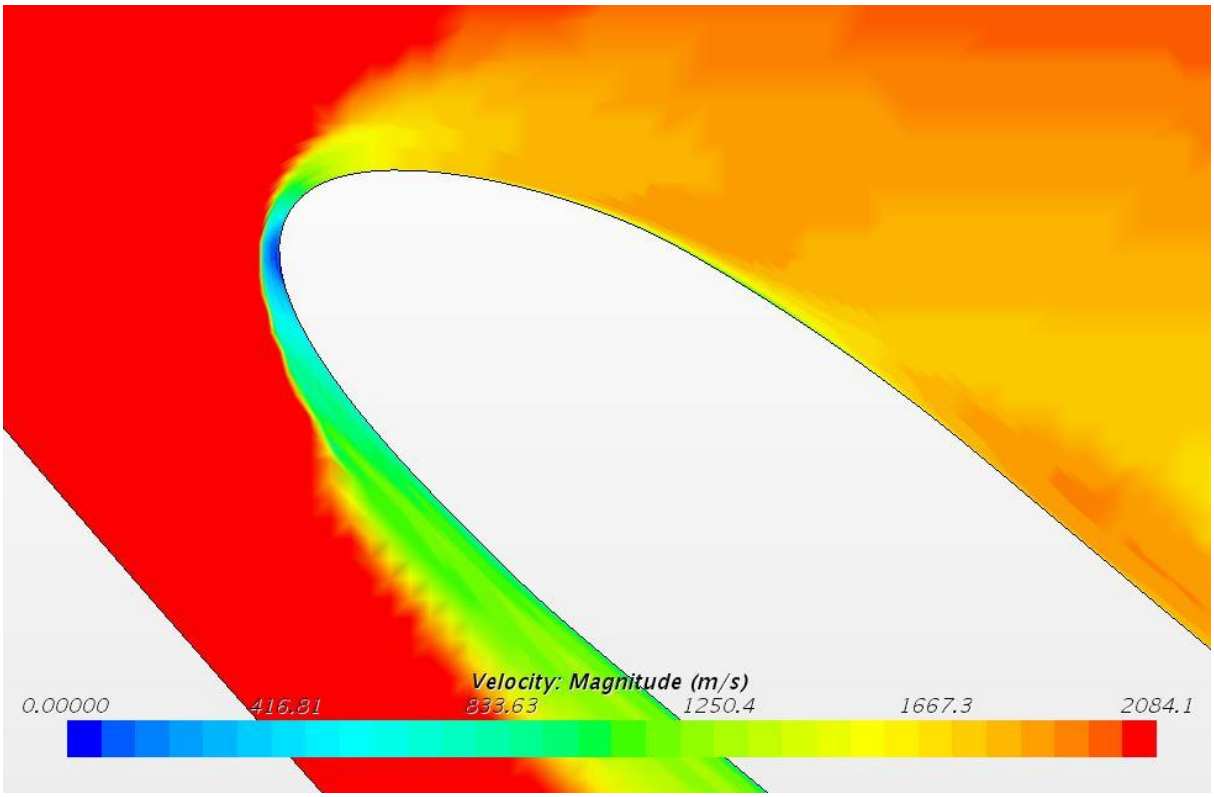

Figure 49 - One million cells 100% scale X-37 nose Velocity

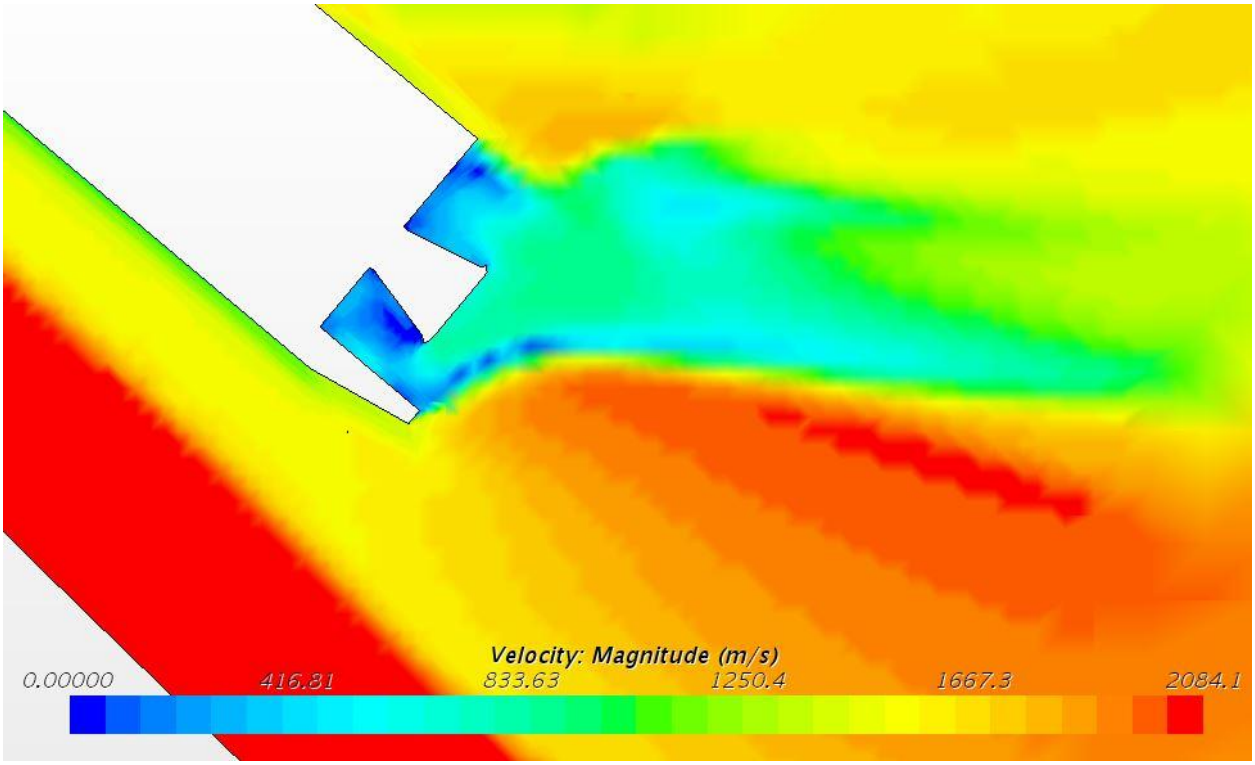

Figure 50 – One million cells 100% scale X-37 tail Velocity

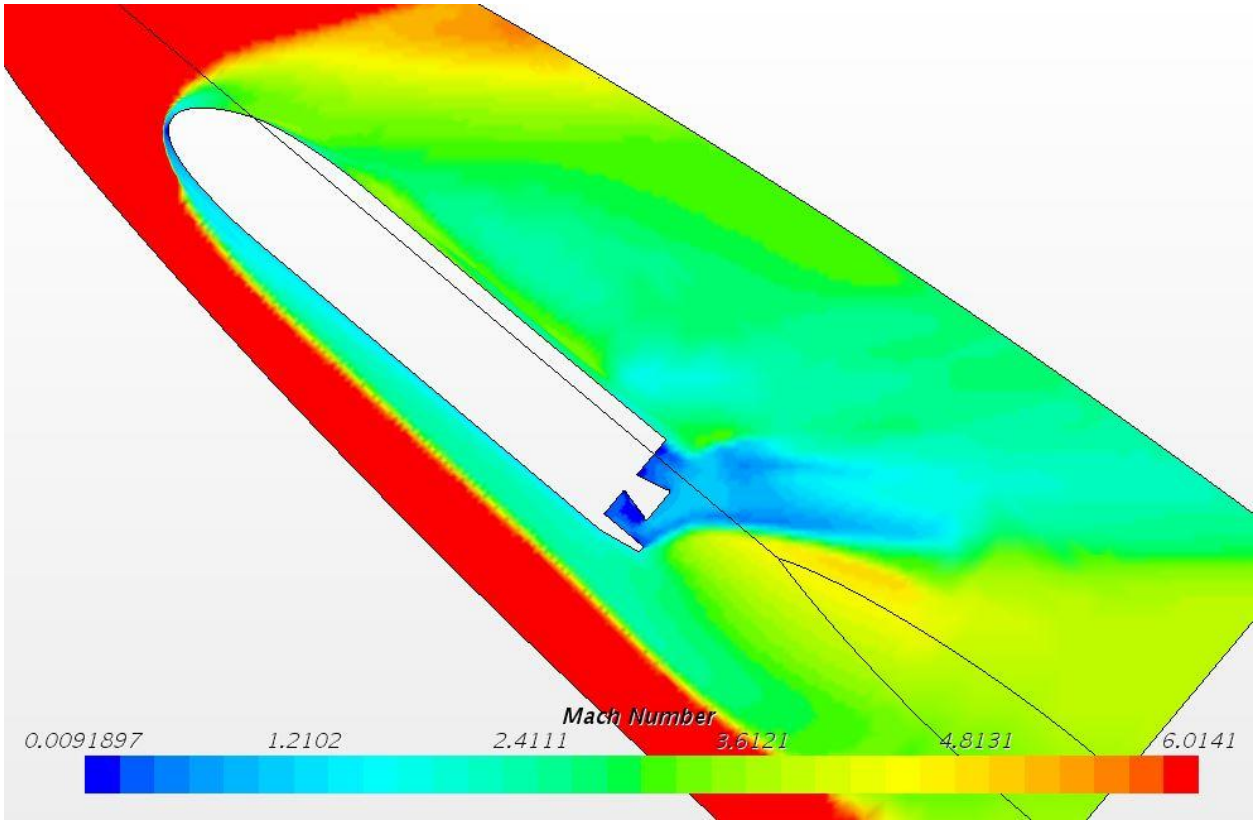

Figure 51 - One million cells 100% scale X-37 full body Mach Number

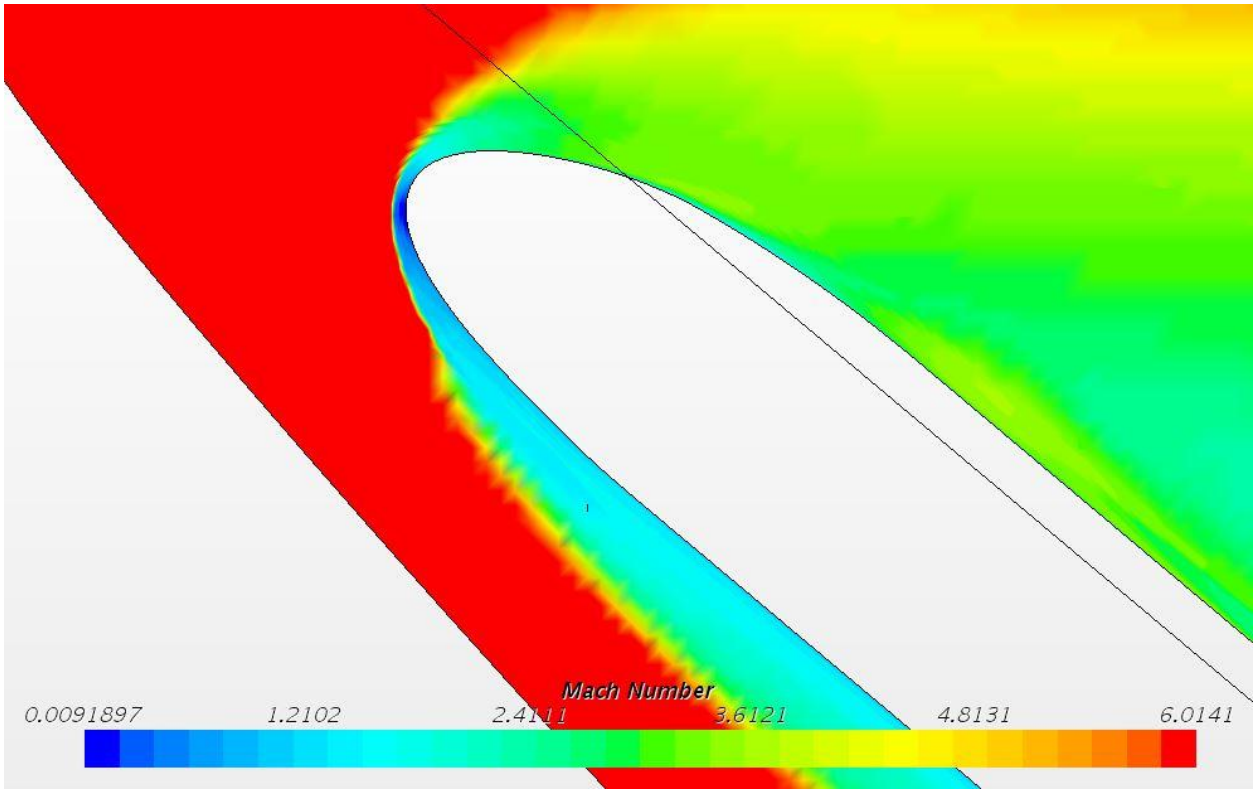

Figure 52 - One million cells 100% scale X-37 nose Mach Number

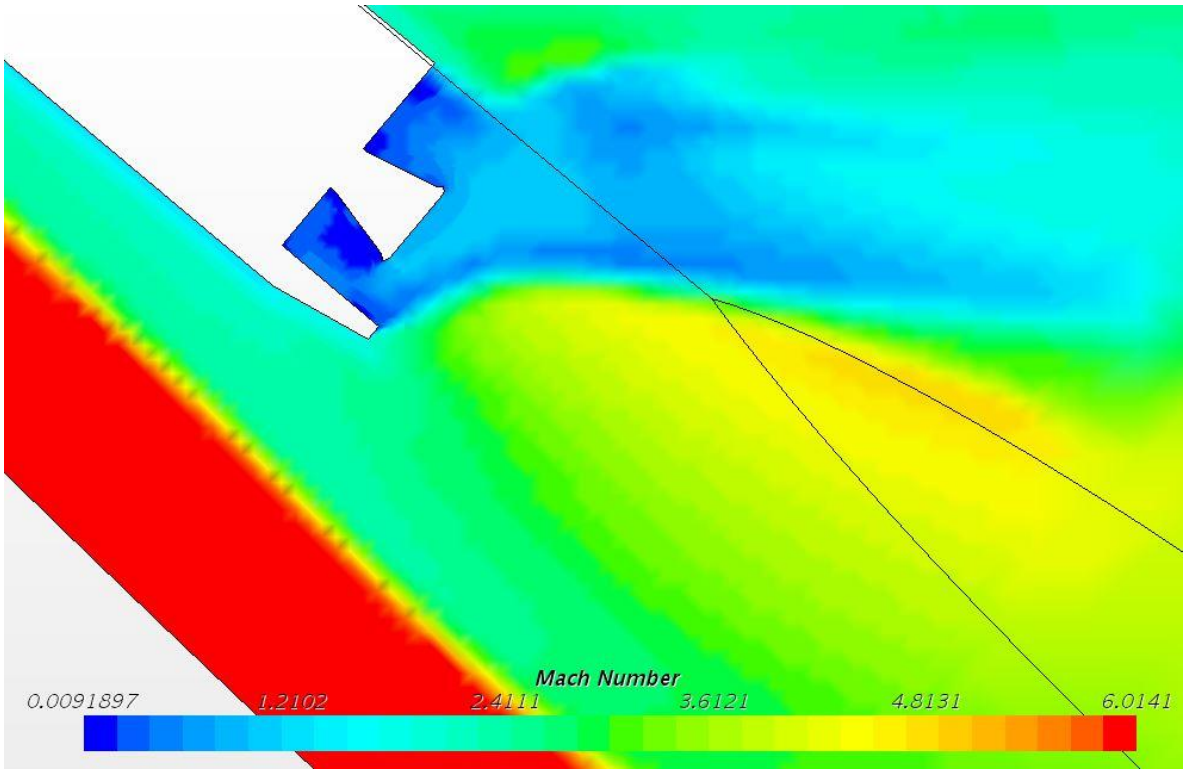

Figure 53 - One million cells 100% scale X-37 tail Mach Number

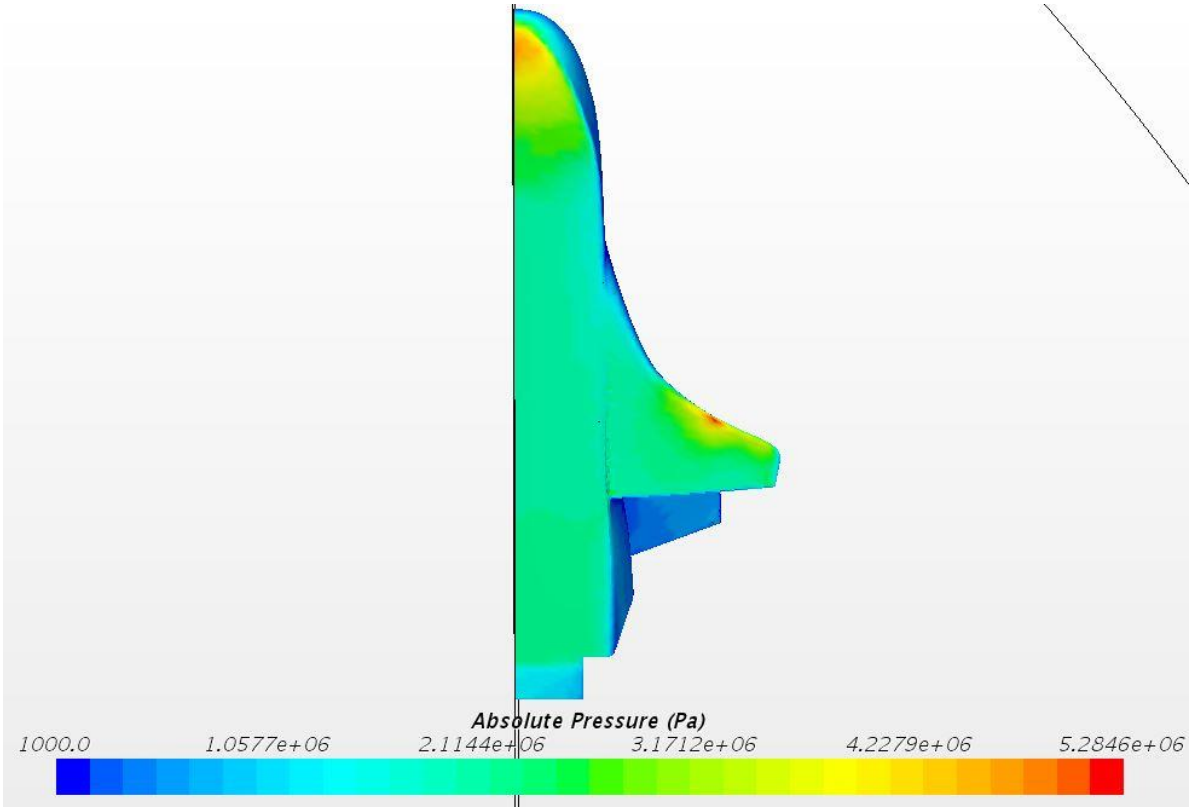

Figure 54 - One million cells 100% scale X-37 bottom Absolute Pressure

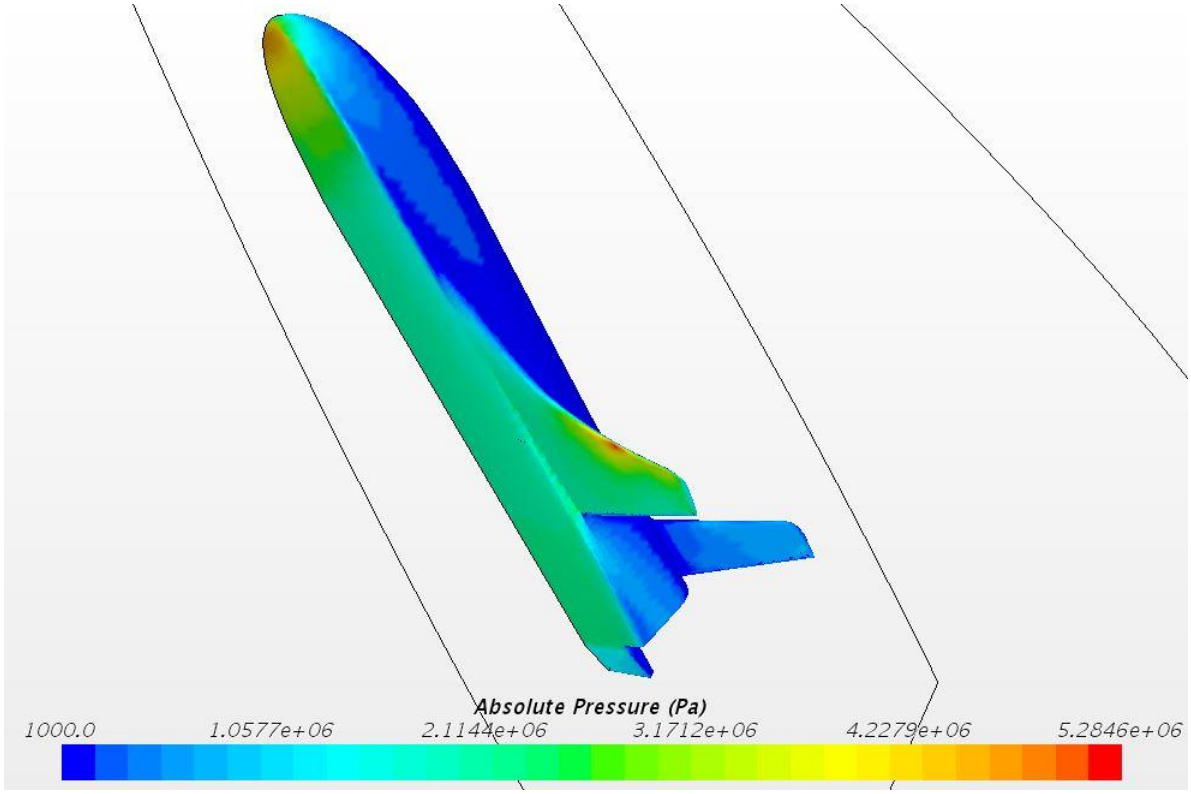

Figure 55 - One million cells 100% scale X-37 3-D Absolute Pressure

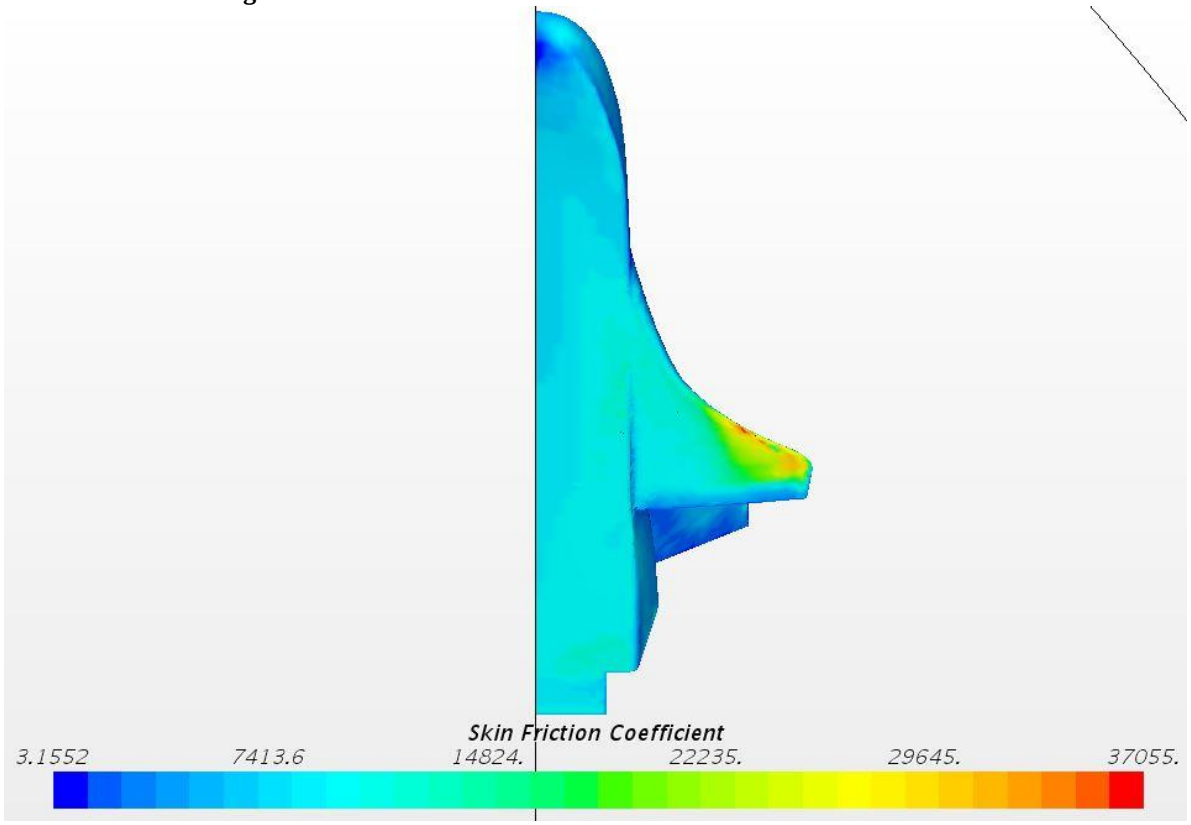

Figure 56 - One million cells 100% scale X-37 bottom Skin Friction Coefficient

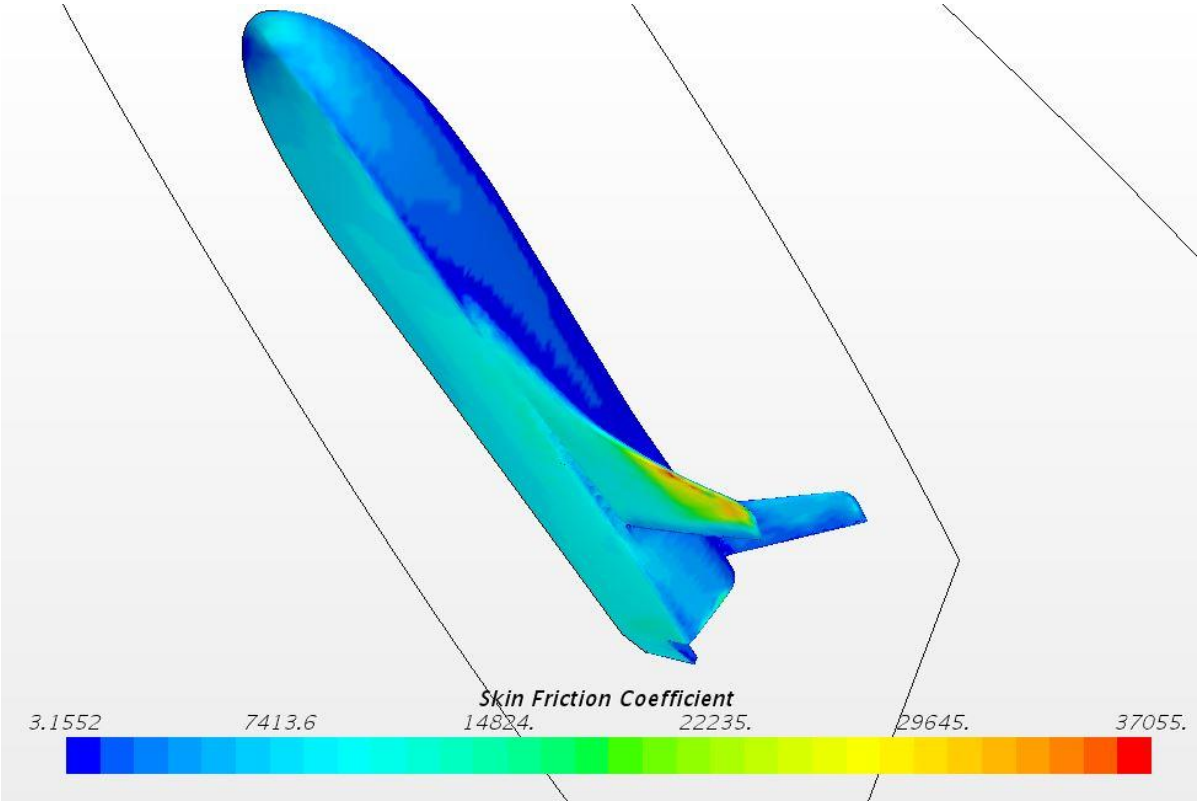

Figure 57 - One million cells 100% scale X-37 3-D Skin Friction Coefficient

7.3.3 100% X-37 at 2 Million Cells

A 100% scale model of the X-37 is tested at 1998012 Cells. Figure 61 displays the mesh generated with Figure 62 and Figure 63 providing focus on the mesh near the nose and tail of the vehicle. The CFD simulation ran for a total of 6,500 iterations and seemed to converge towards a stable solution as seen in Figure 58. The Base cell size for the mesh was designated at 0.478 meters. The cone area behind the tail as well as the refinement area around the vehicle body were set to 15% of the base size (0.0717m). The Far-field area outside of the refinement area was set to 300% of the base size (1.434m). The mesh was generated with 30 prism layers stretching at a rate of 1.1 the size of the previous layer, from the surface of the vehicle. The absolute thickness of these prism layers was 30% of the base size (0.1434m). The target cell size on the surface of the vehicle was 10% of base size (0.0478m) and the minimum surface cell size was set to 5% of the base size (0.0239m). The lift force of the vehicle was 14,737,326N, and the drag force of the vehicle was 14,033,323N. Using these values for lift force and drag force and equation 3.6, the lift-to-drag ratio can be calculated to be 1.050.

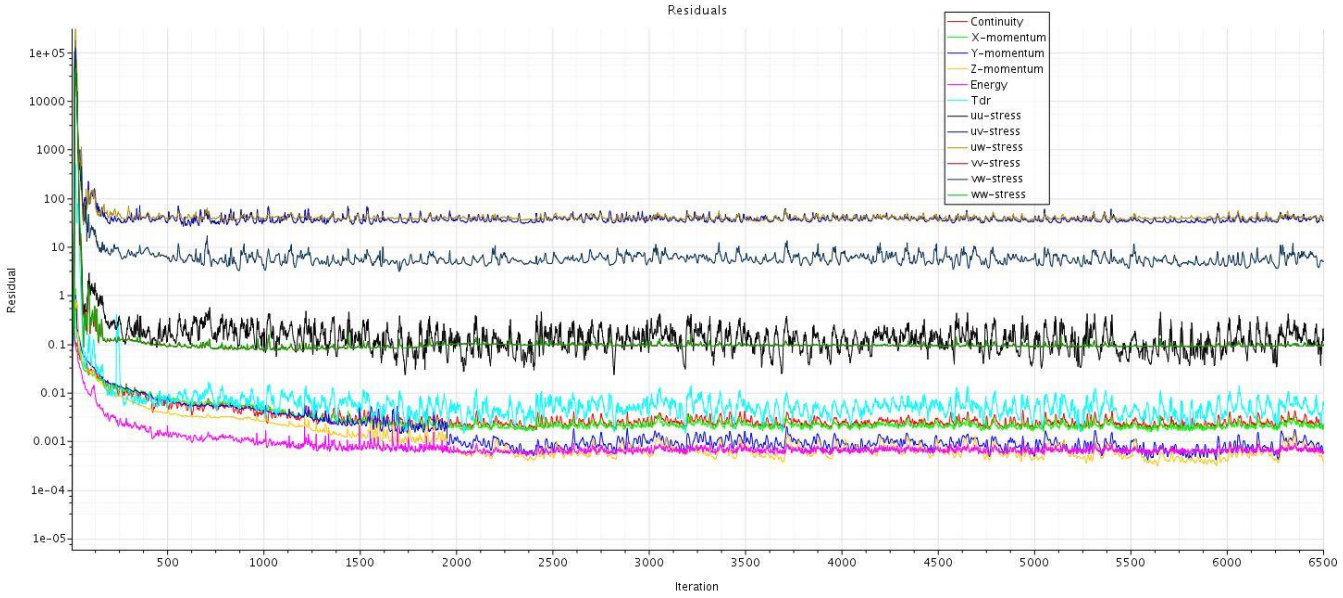

Figure 58 - Two million cells 100% scale X-37 Residual Plot

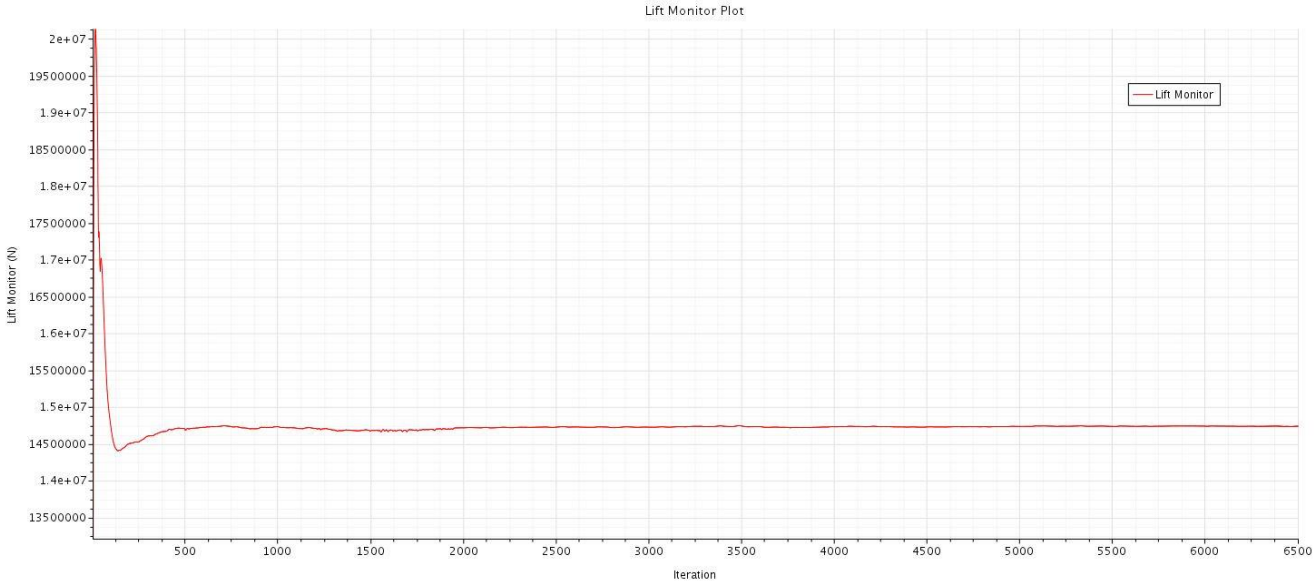

Figure 59 - Two million cells 100% scale X-37 Lift Plot

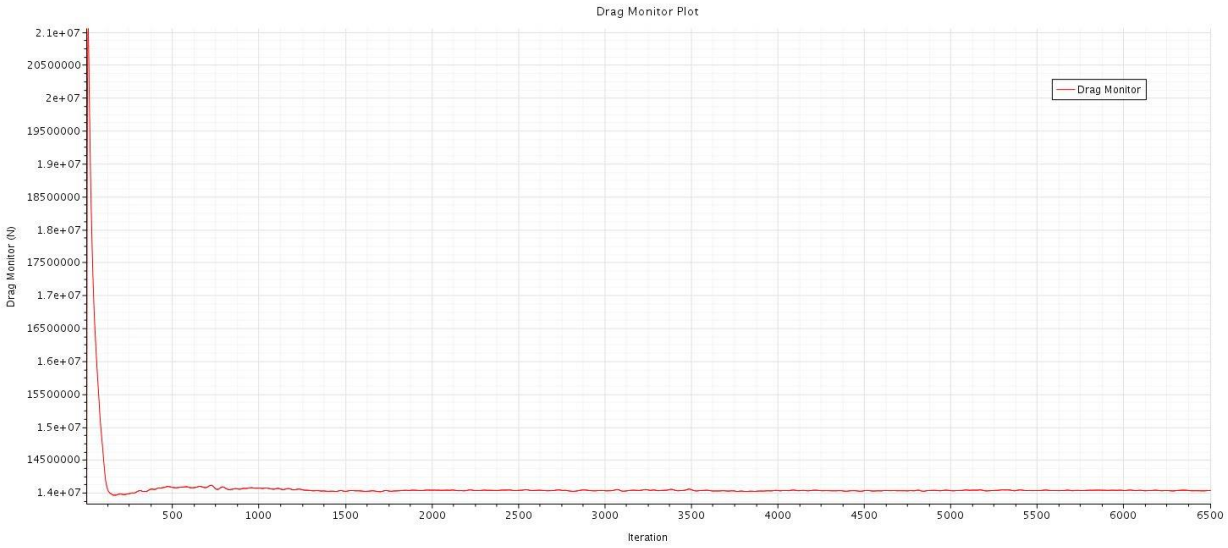

Figure 60 - Two million cells 100% scale X-37 Drag Plot

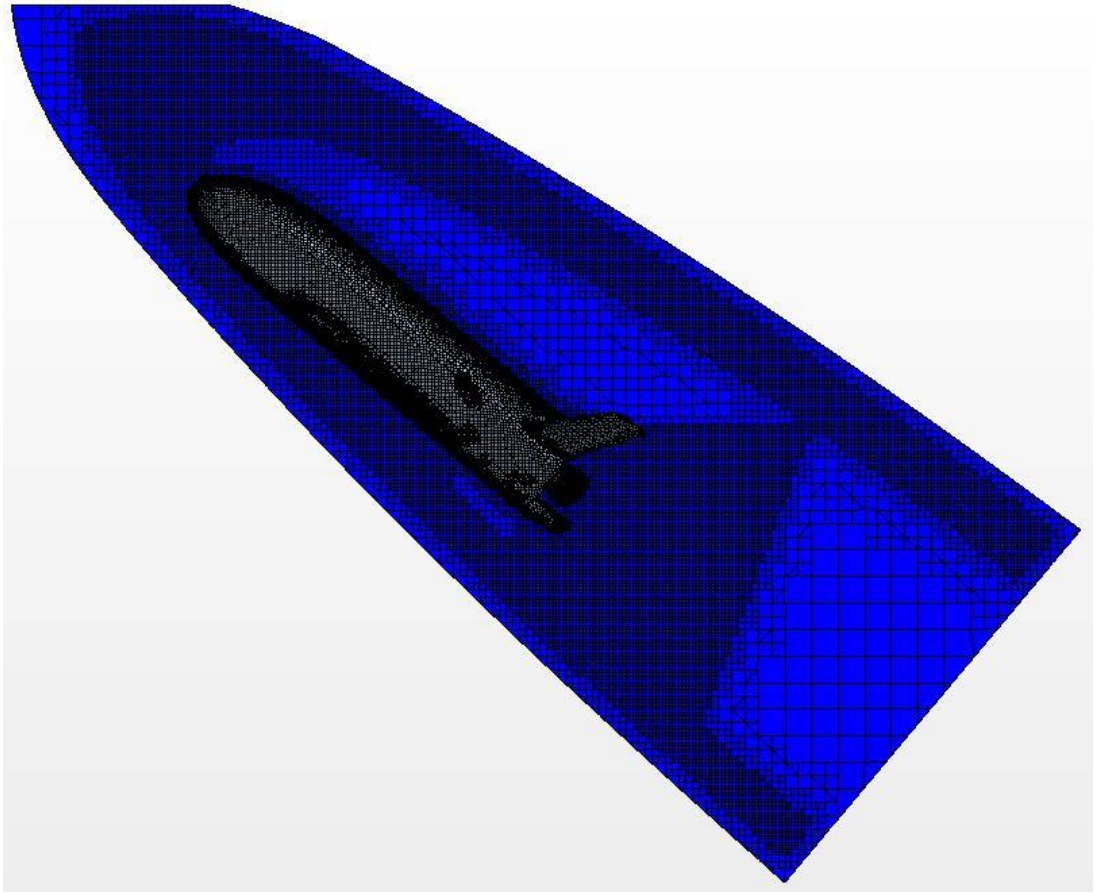

Figure 61 - Two million cells 100% scale X-37 full body Mesh

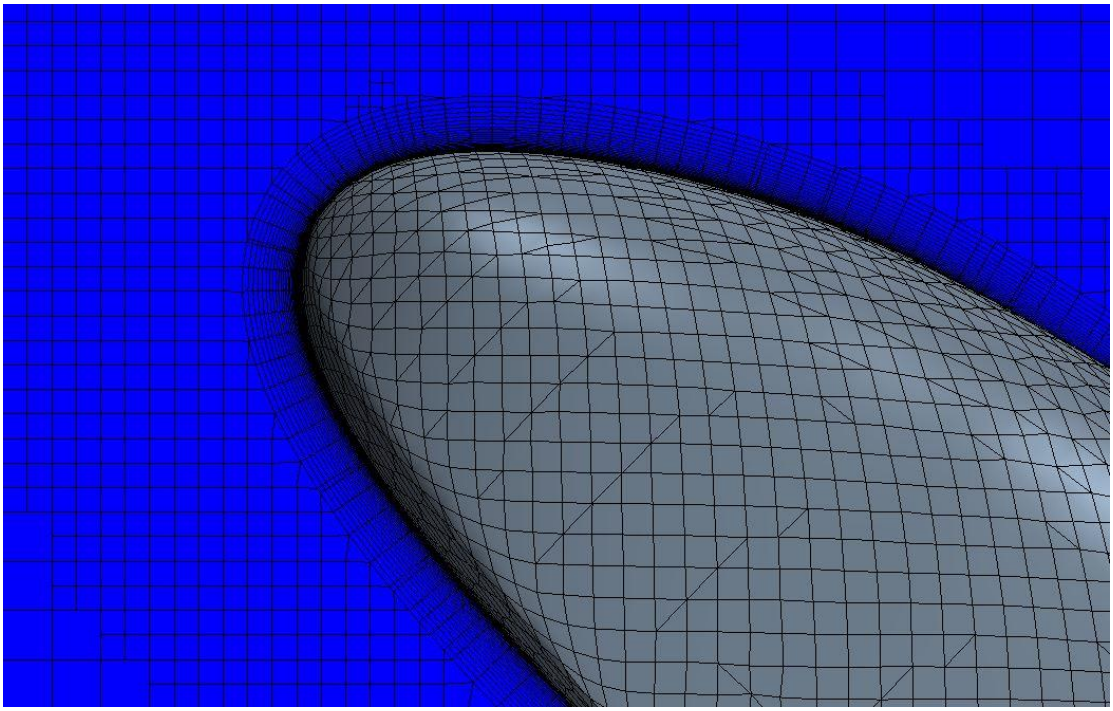

Figure 62 - Two million cells 100% scale X-37 nose Mesh

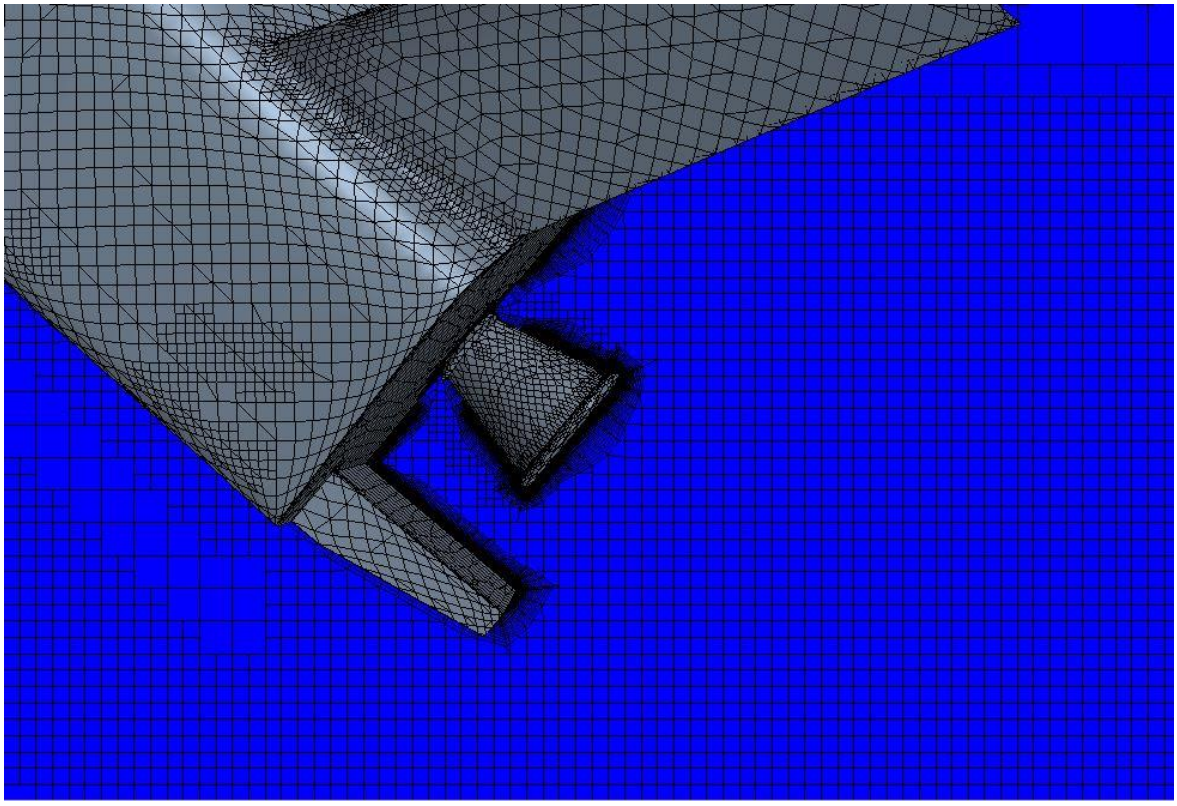

Figure 63 - Two million cells 100% scale X-37 tail Mesh

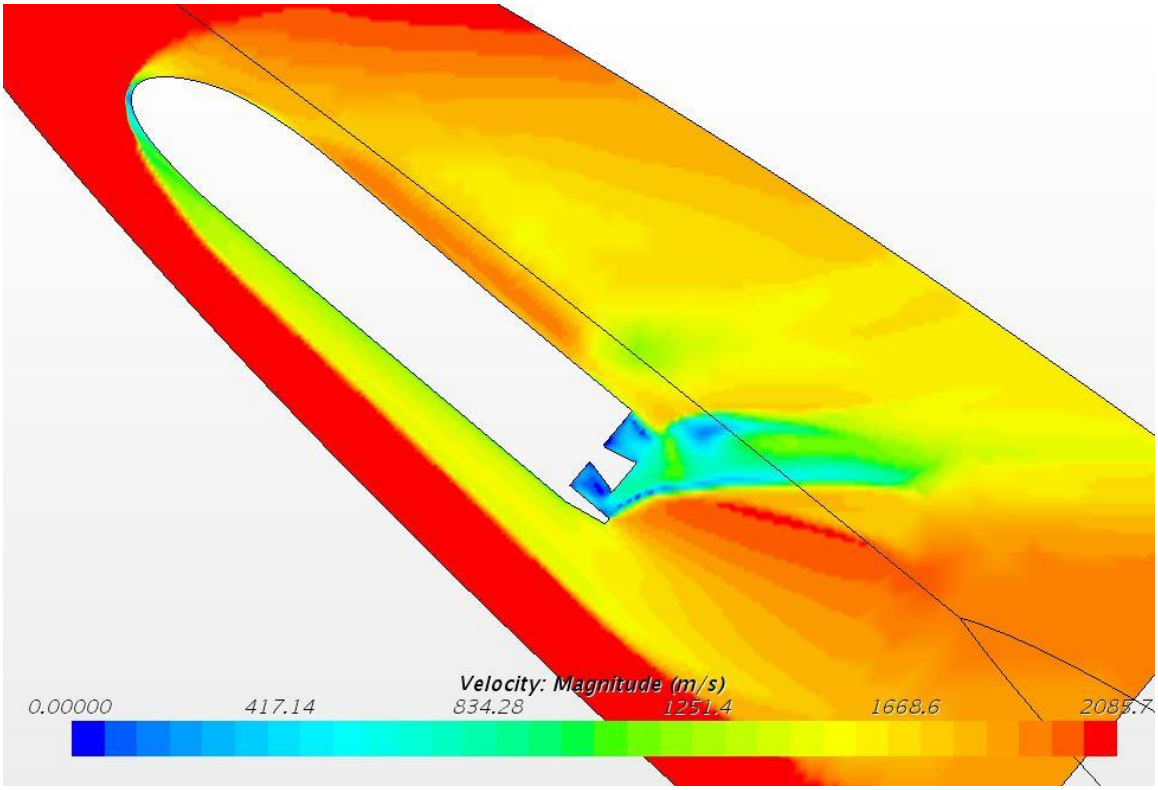

Figure 64 - Two million cells 100% scale X-37 full body Velocity

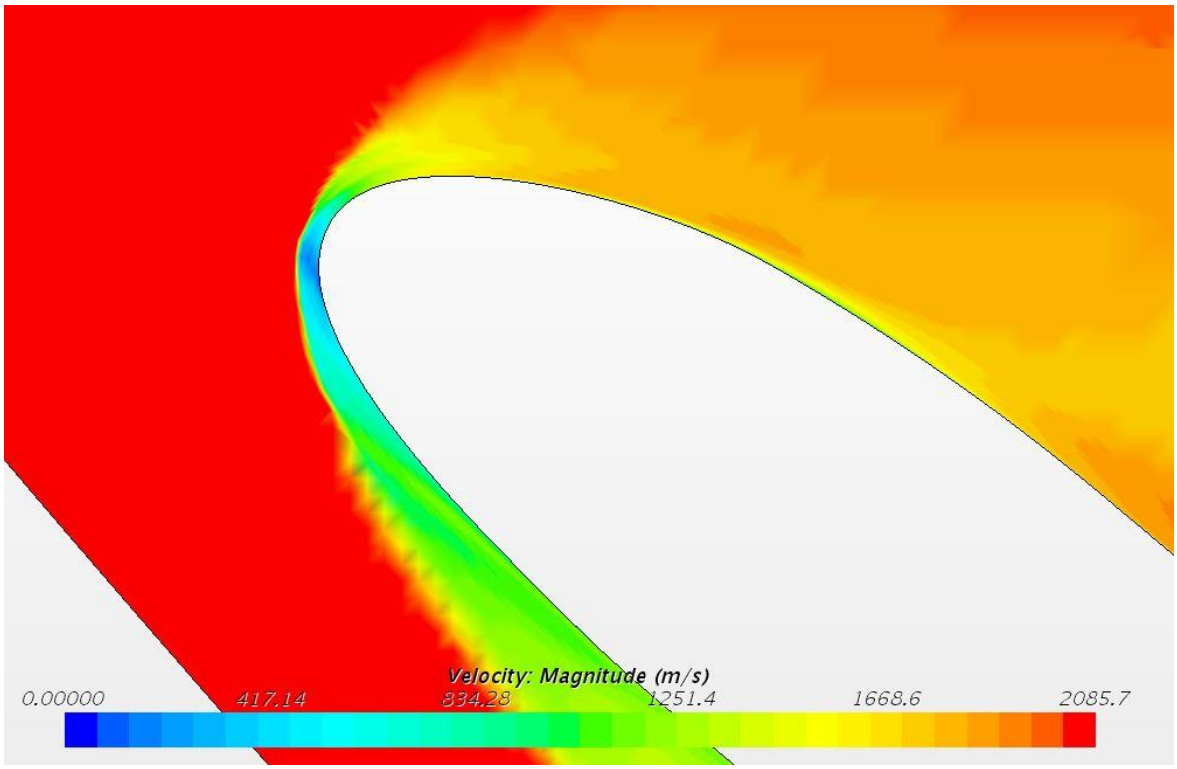

Figure 65 – Two million cells 100% scale X-37 nose Velocity

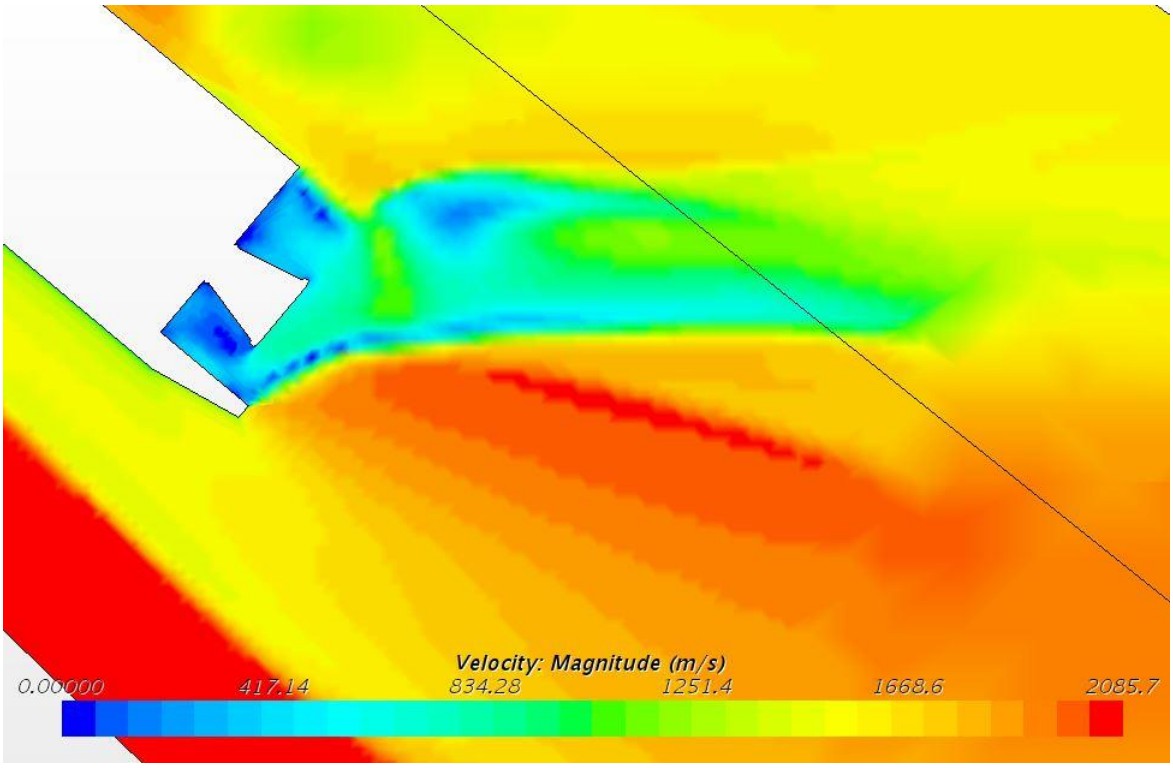

Figure 66 - Two million cells 100% scale X-37 tail Velocity

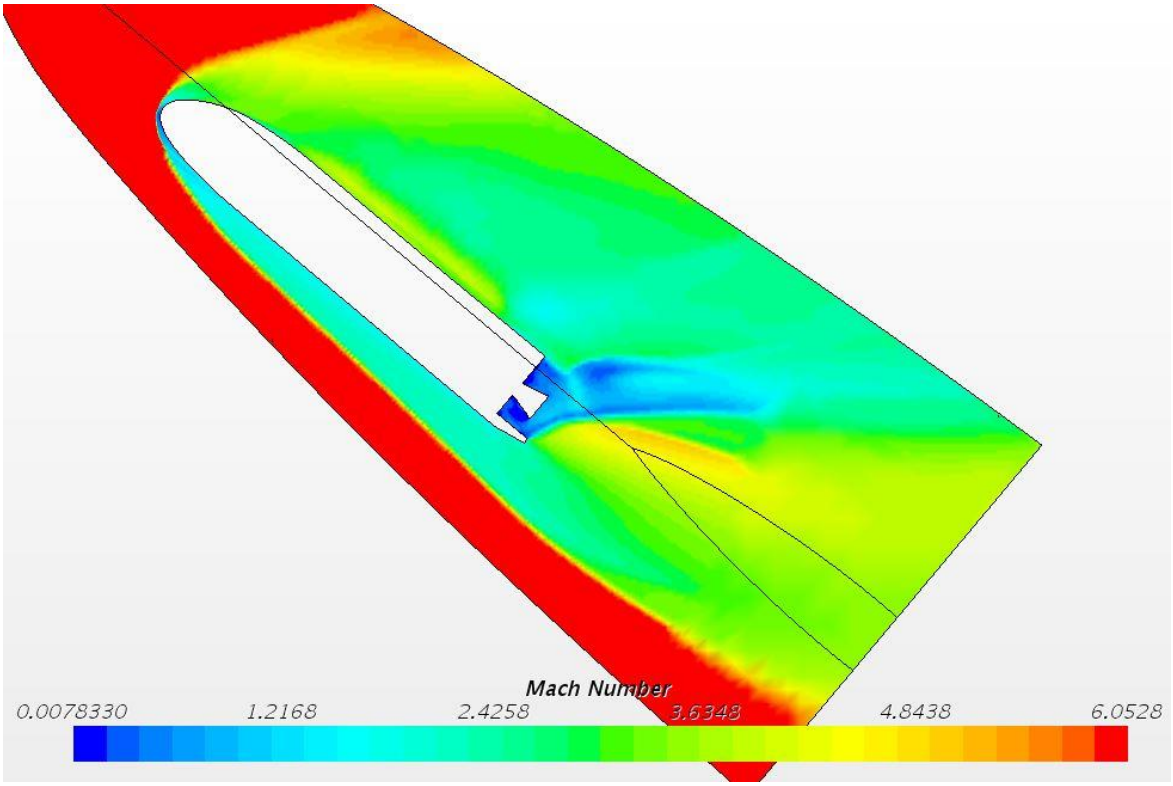

Figure 67 - Two million cells 100% scale X-37 full body Mach Number

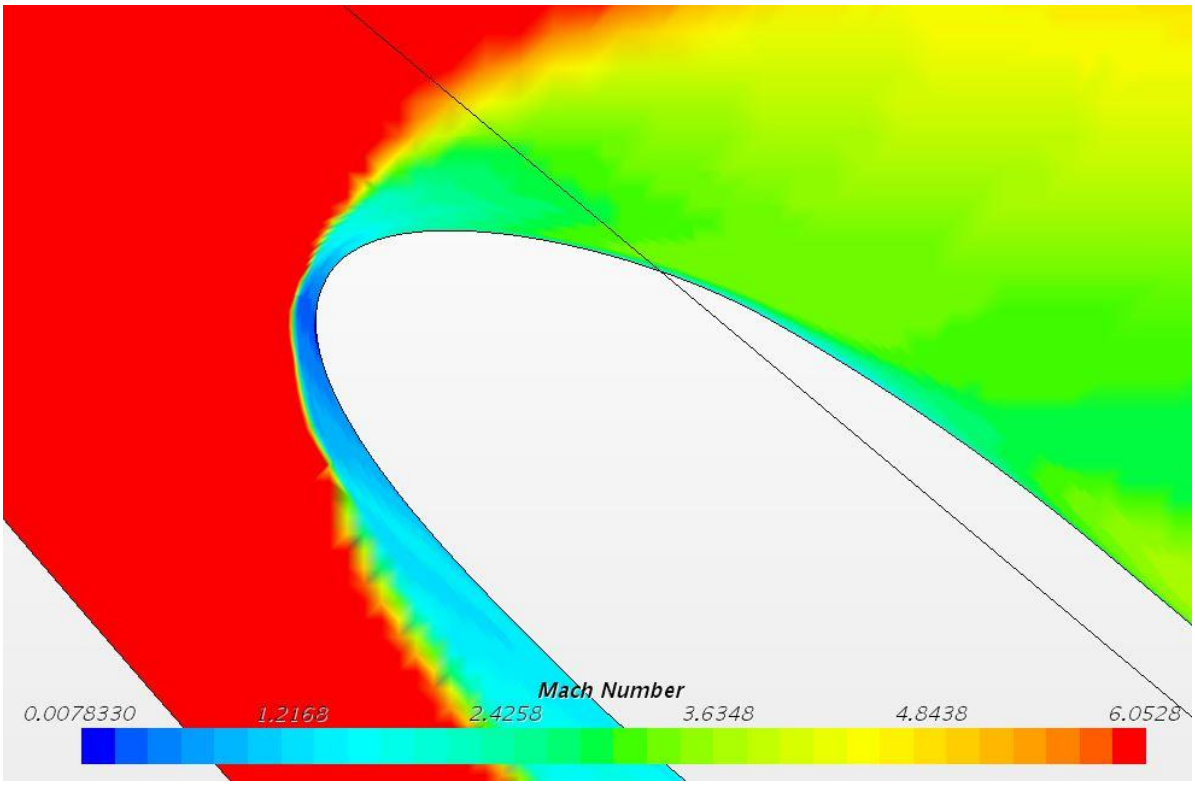

Figure 68 - Two million cells 100% scale X-37 nose Mach Number

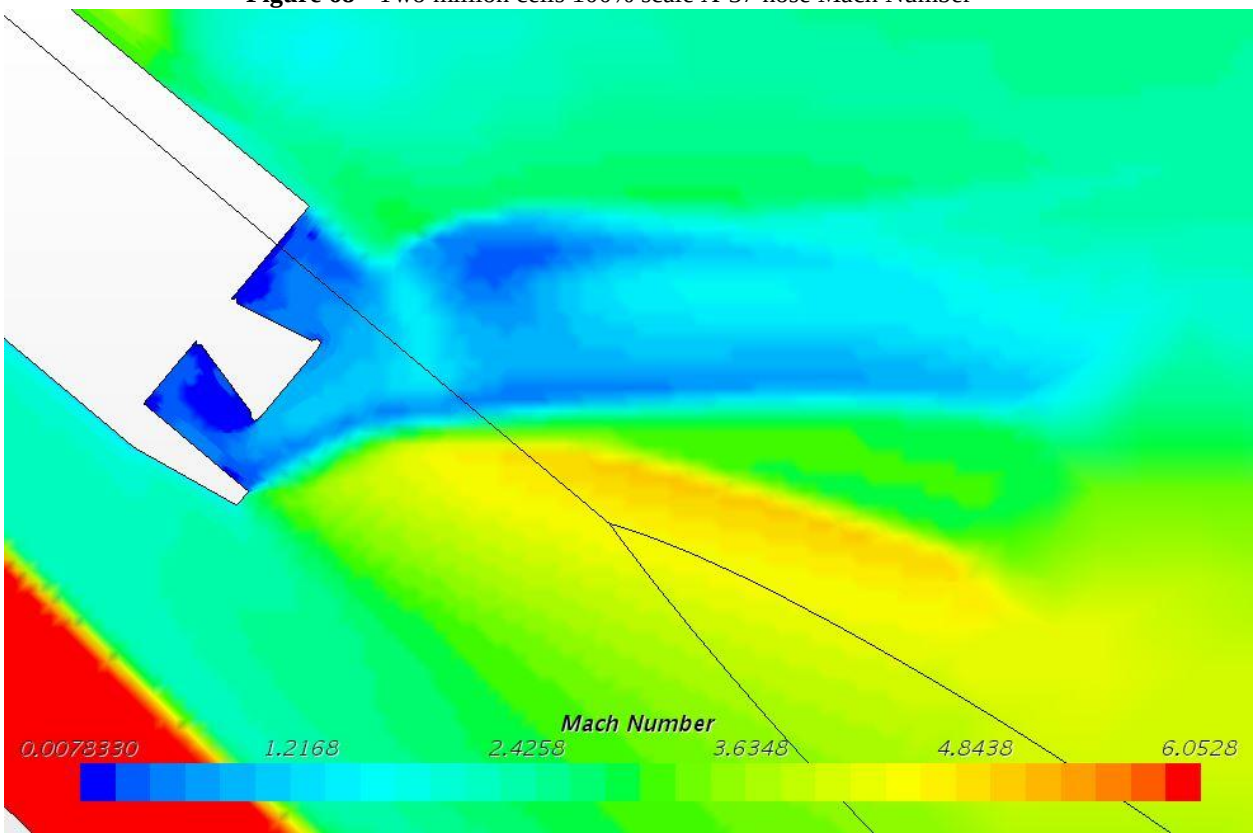

Figure 69 - Two million cells 100% scale X-37 tail Mach Number

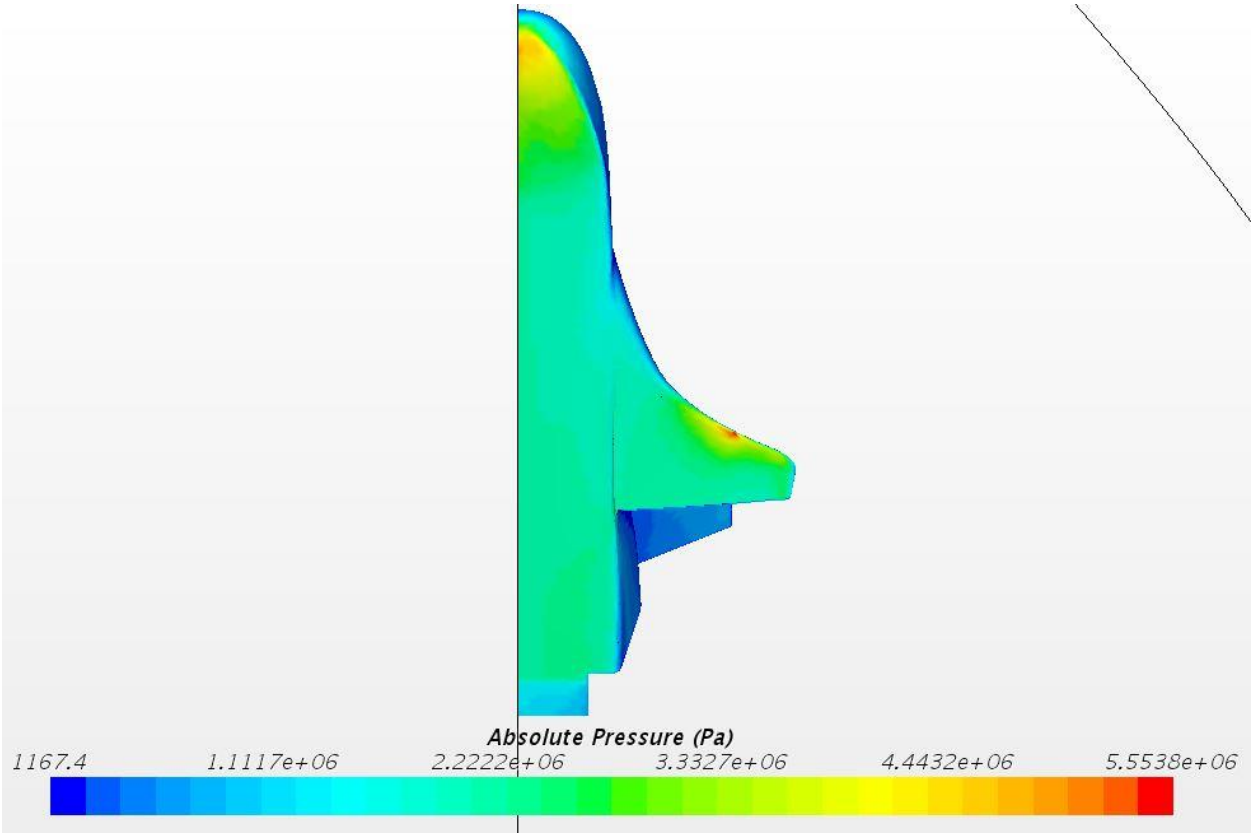

Figure 70 - Two million cells 100% scale X-37 bottom Absolute Pressure

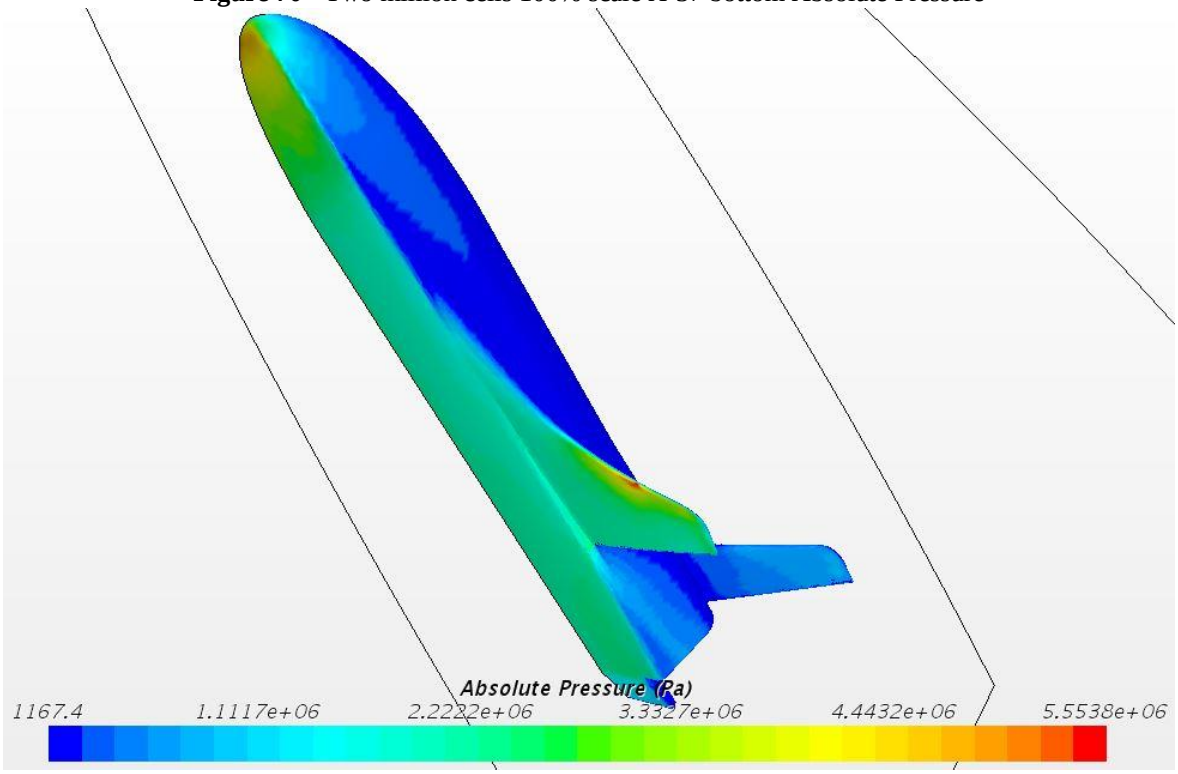

Figure 71 - Two million cells 100% scale X-37 3-D Absolute Pressure

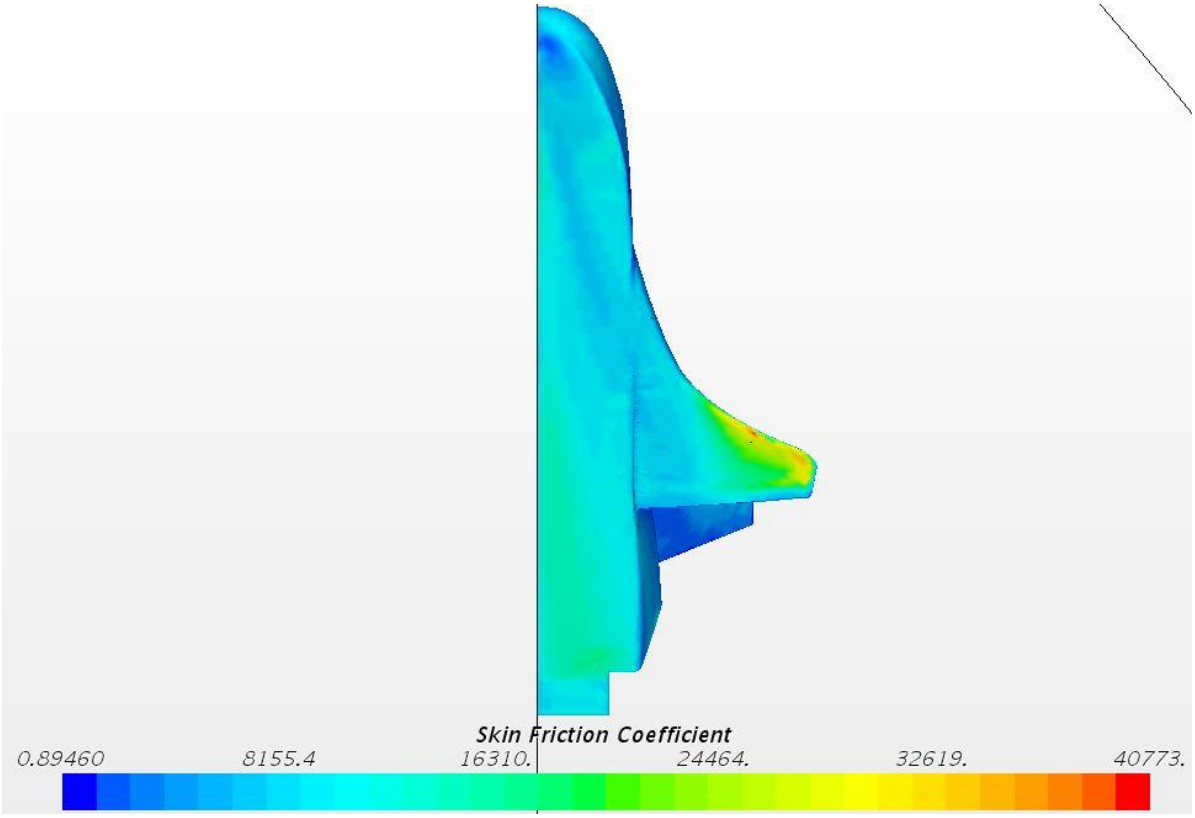

Figure 72 - Two million cells 100% scale X-37 bottom Skin Friction Coefficient

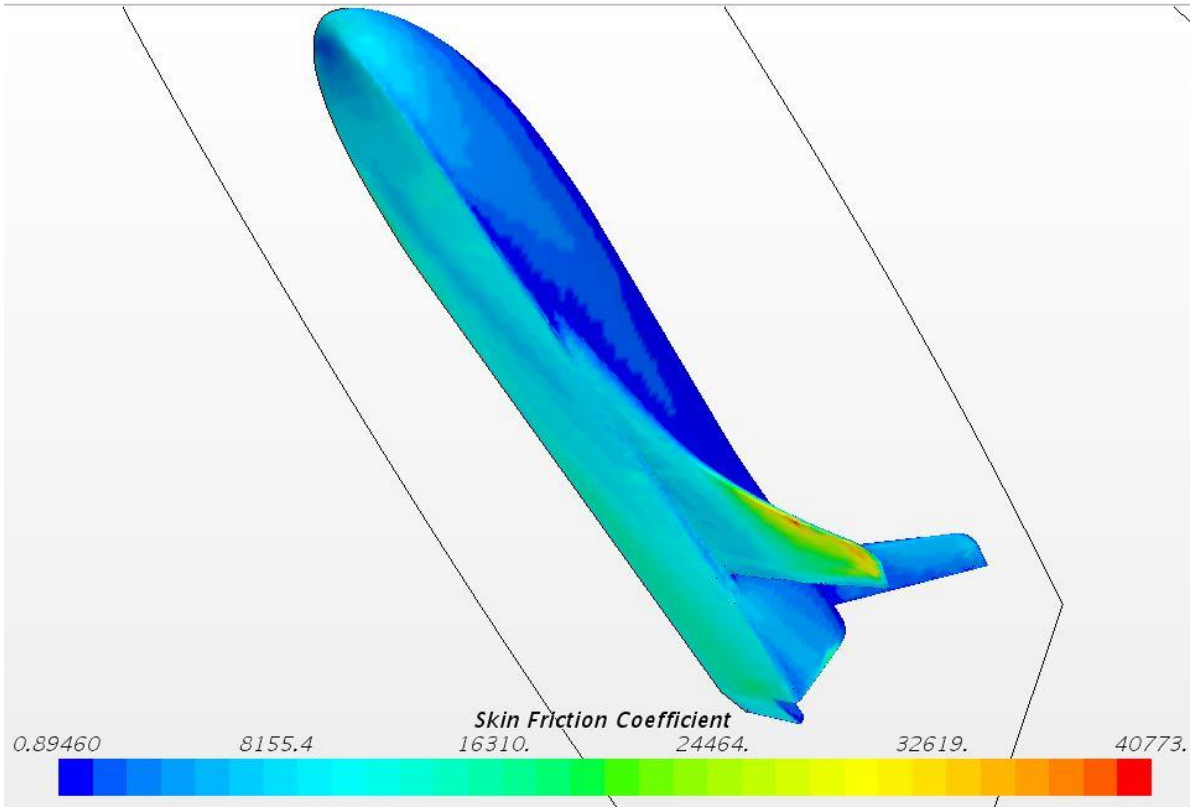

Figure 73 - Two million cells 100% scale X-37 3-D Skin Friction Coefficient

7.3.4 50% X-37 at 1 Million Cells

A 50% scale model of the X-37 is tested at 1011637 Cells. Figure 77 displays the mesh generated with Figure 78 and Figure 79 providing focus on the mesh near the nose and tail of the vehicle. The CFD simulation ran for a total of 6,500 iterations and seemed to converge towards a stable solution as seen in Figure 74. The Base cell size for the mesh was designated at 0.315 meters. The cone area behind the tail as well as the refinement area around the vehicle body were set to 15% of the base size (0.04725m). The Far-field area outside of the refinement area was set to 300% of the base size (0.945m). The mesh was generated with 30 prism layers stretching at a rate of 1.1 the size of the previous layer, from the surface of the vehicle. The absolute thickness of these prism layers was 30% of the base size (0.0945m). The target cell size on the surface of the vehicle was 10% of base size (0.0315m) and the minimum surface cell size was set to 5% of the base size (0.01575m). The lift force of the vehicle was 3,653,280N, and the drag force of the vehicle was 3,489,000N. Using these values for lift force and drag force and equation 3.6, the lift-to-drag ratio can be calculated to be 1.047.

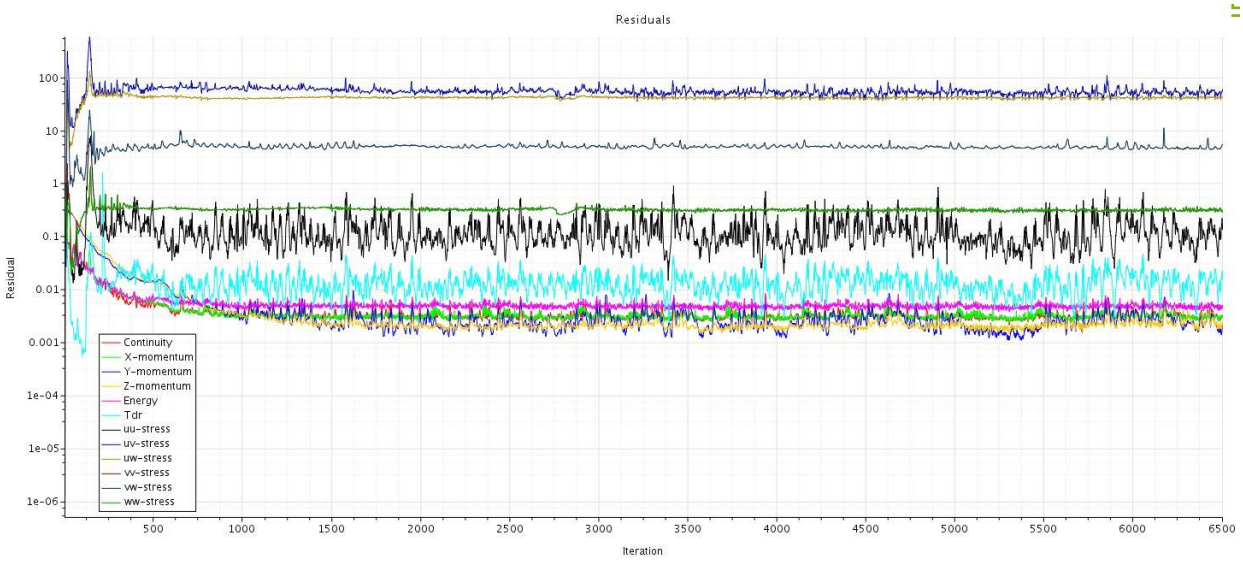

Figure 74 - One million cells 50% scale X-37 Residual Plot

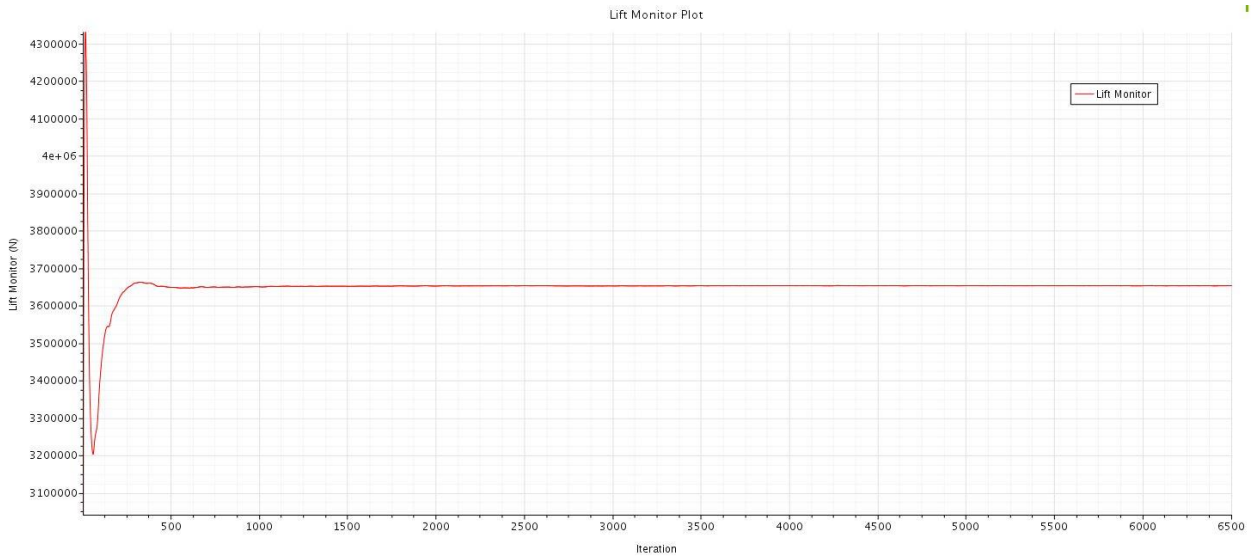

Figure 75 - One million cells 50% scale X-37 Lift Plot

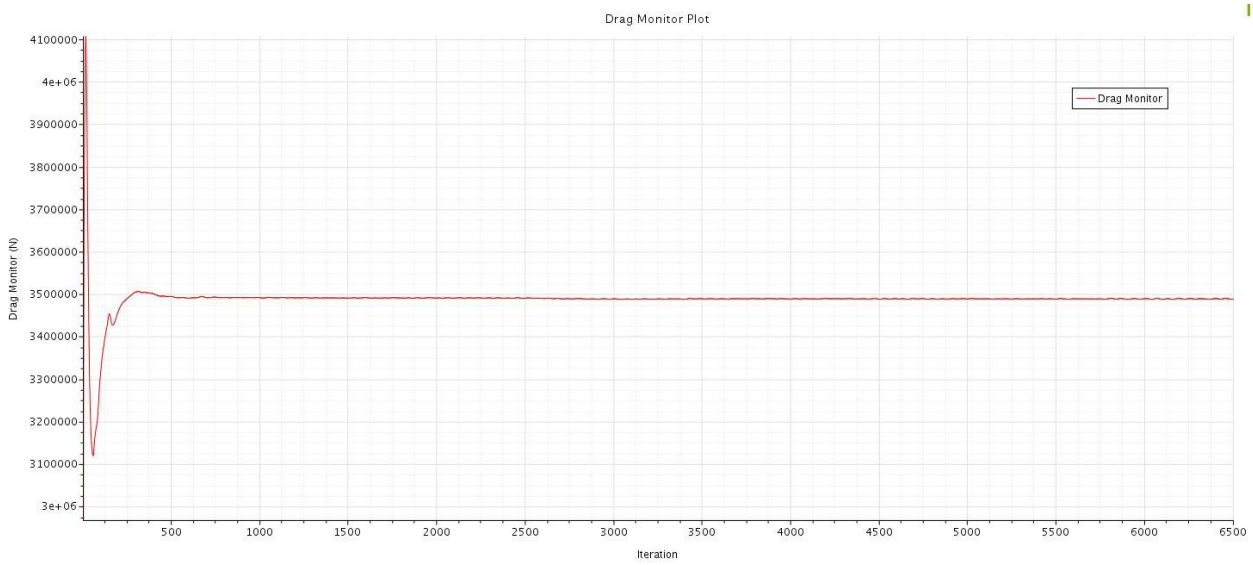

Figure 76 - One million cells 50% scale X-37 Drag Plot

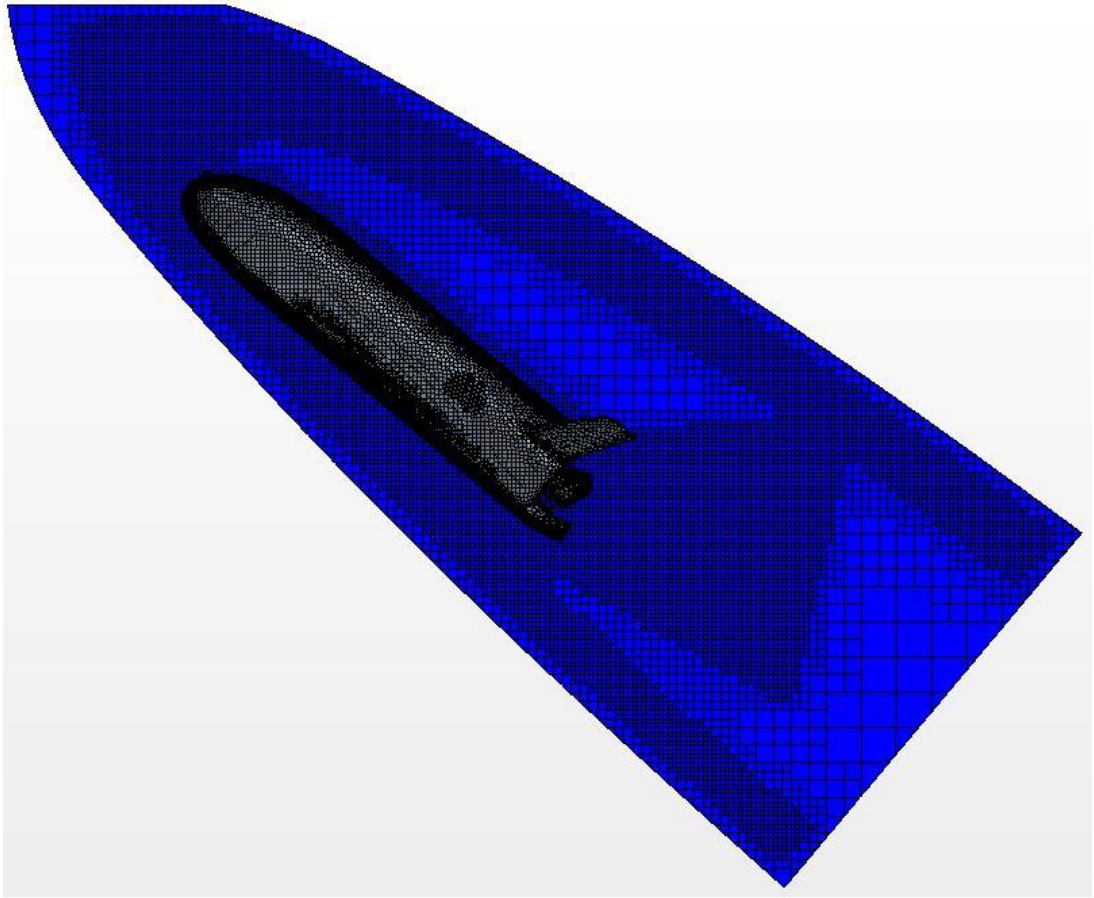

Figure 77 - One million cells 50% scale X-37 full body Mesh

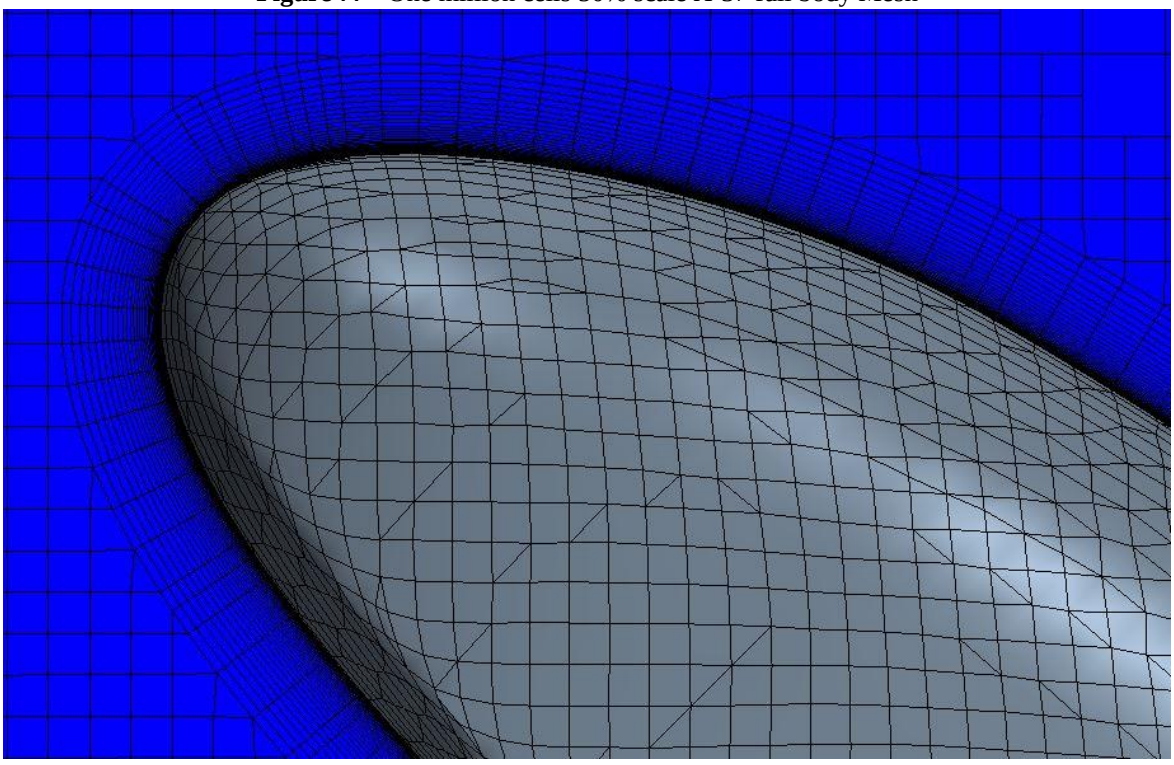

Figure 78 - One million cells 50% scale X-37 nose Mesh

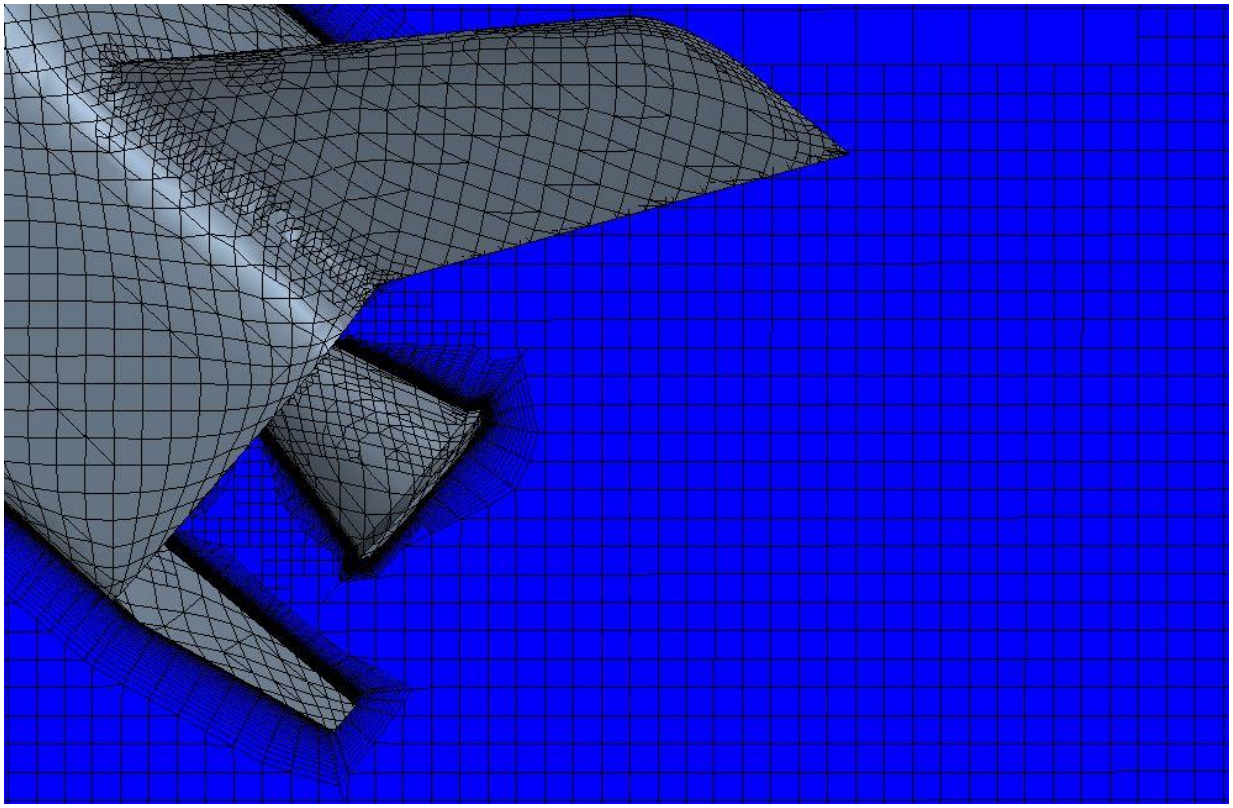

Figure 79 - One million cells 50% scale X-37 tail Mesh

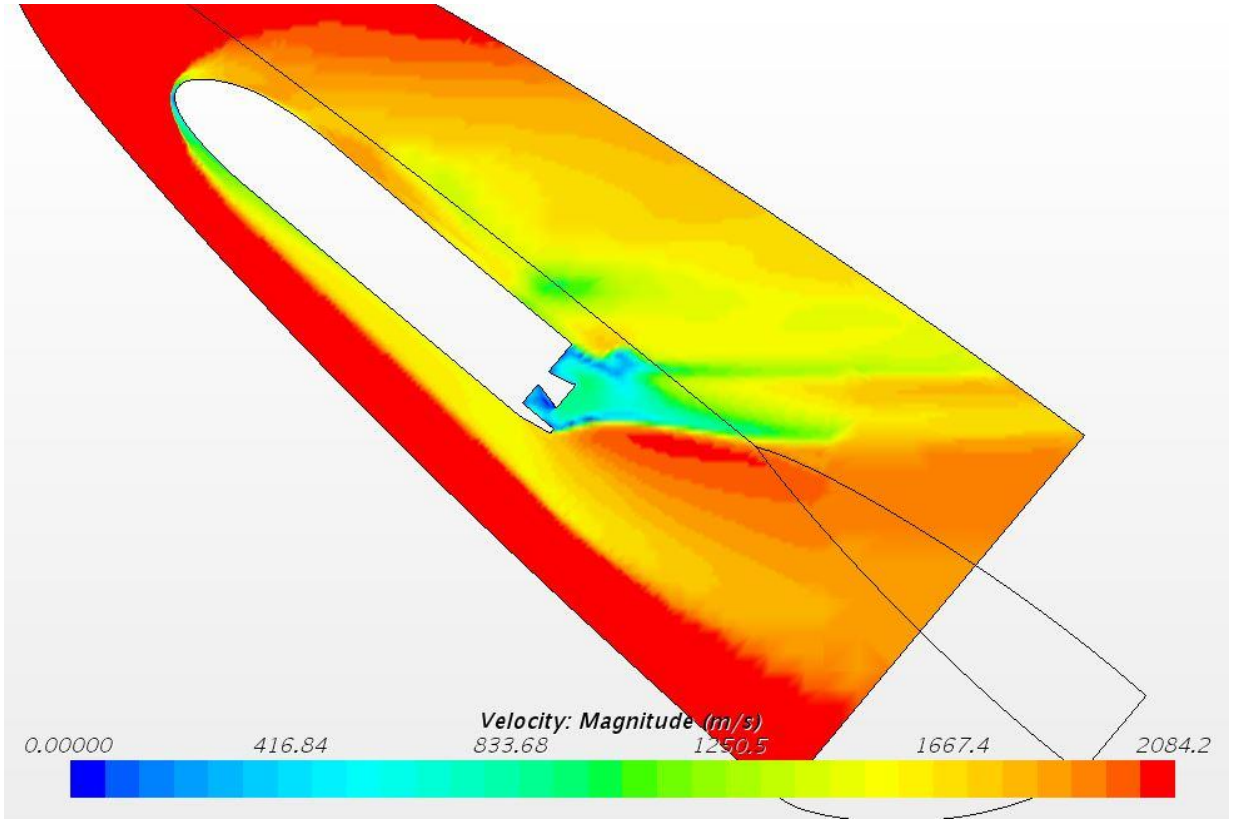

Figure 80 - One million cells 50% scale X-37 full body Velocity

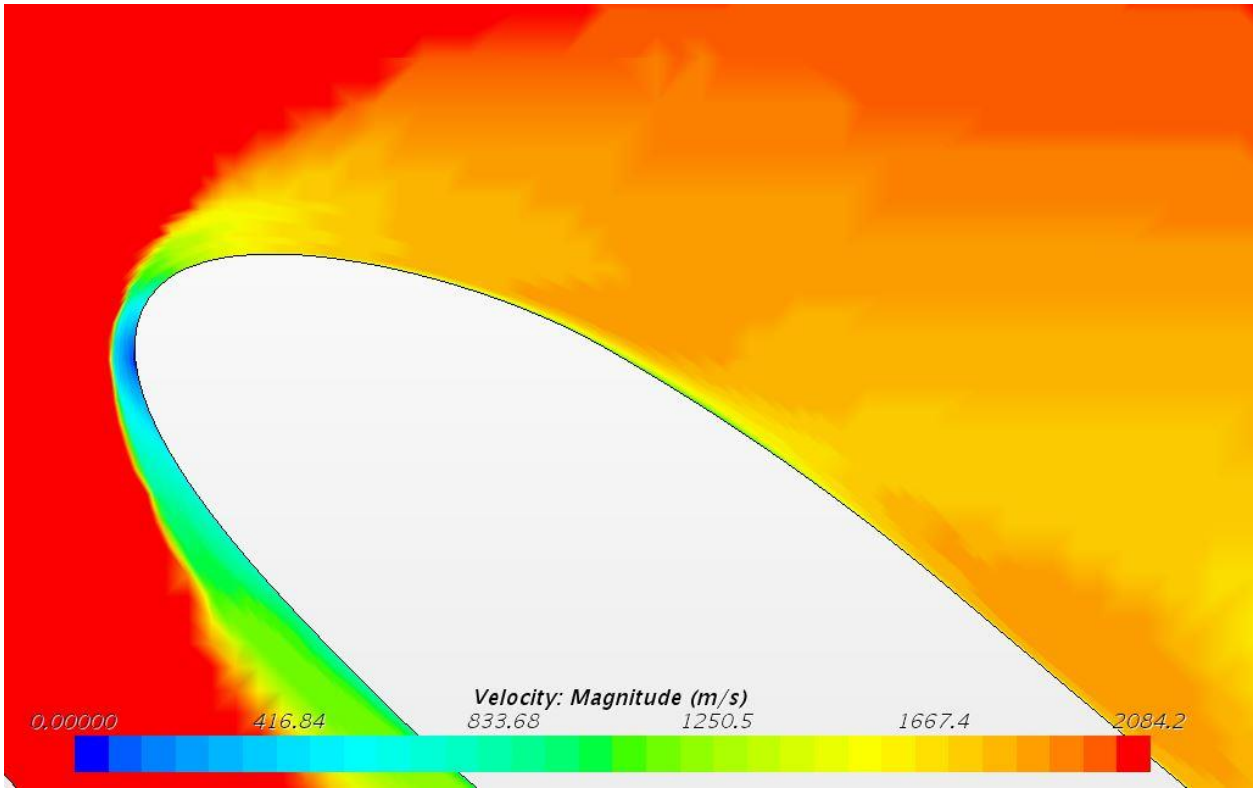

Figure 81 - One million cells 50% scale X-37 nose Velocity

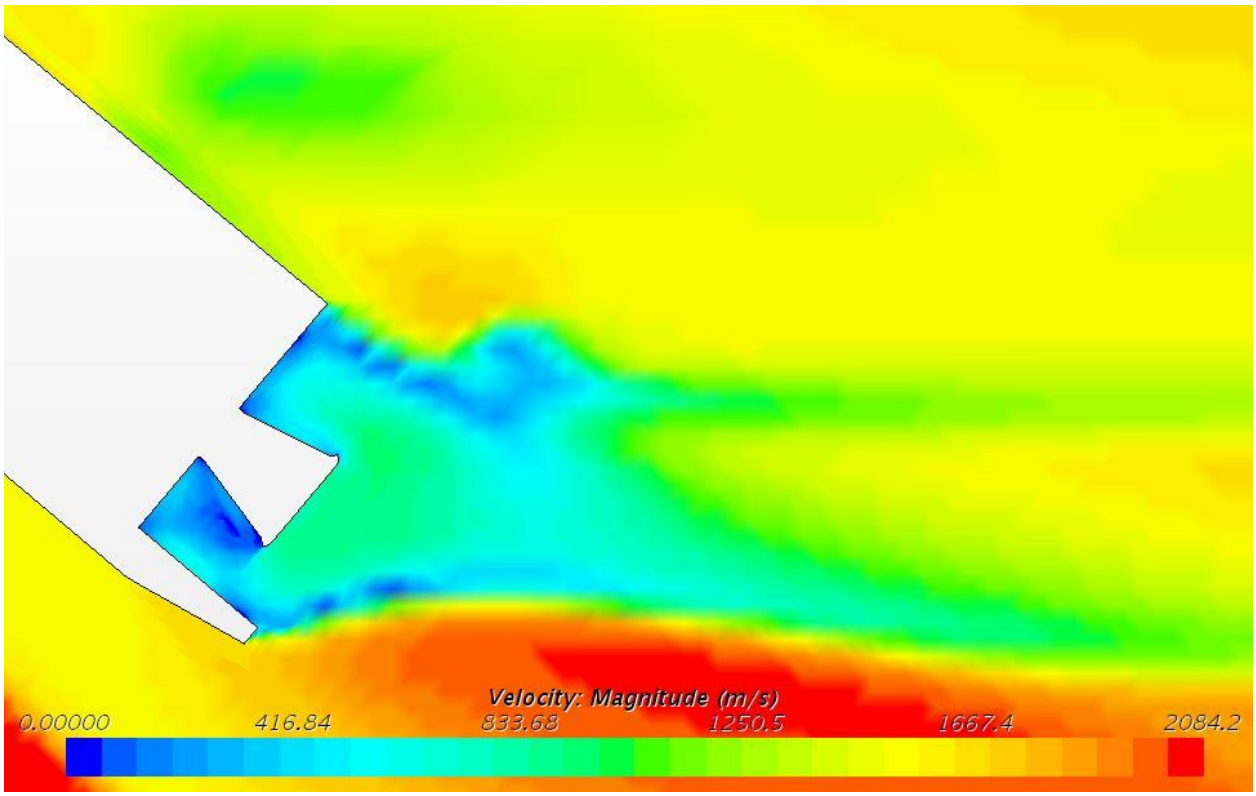

Figure 82 - One million cells 50% scale X-37 tail Velocity

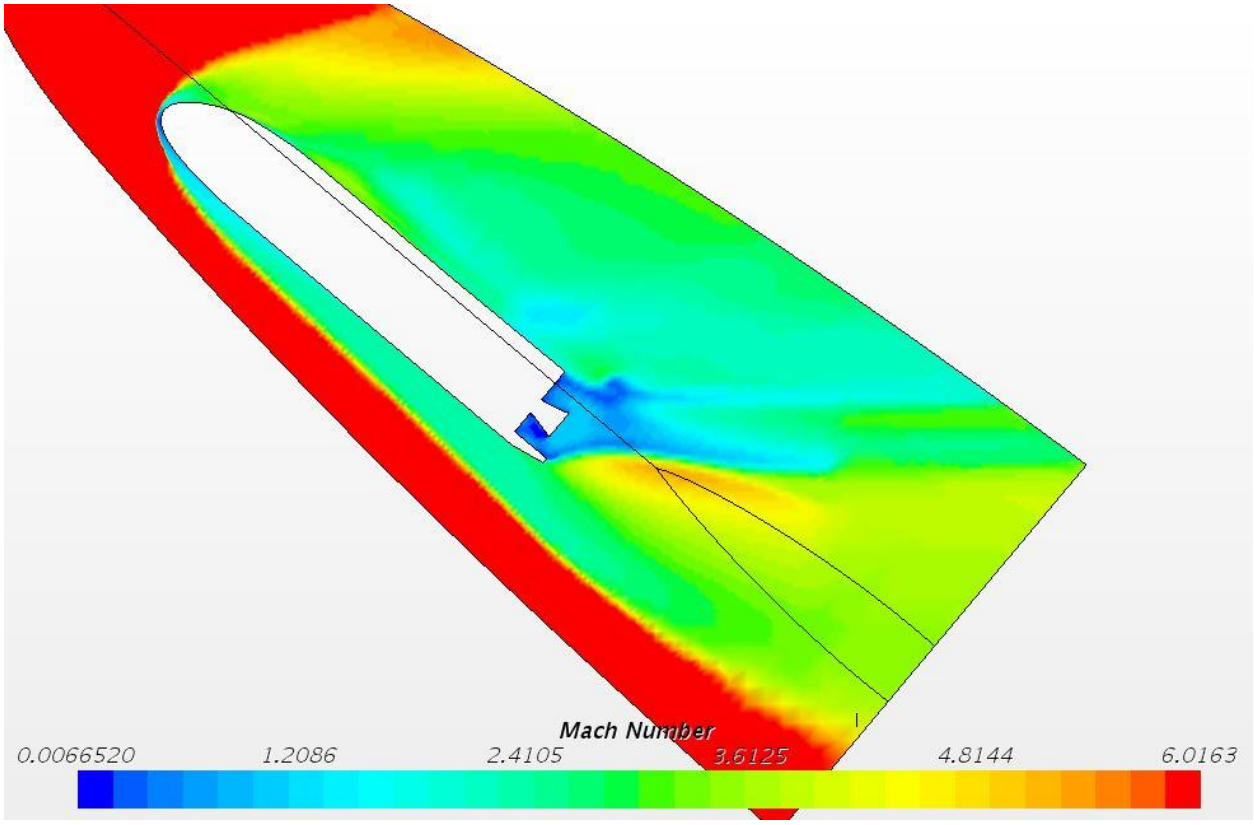

Figure 83 - One million cells 50% scale X-37 full body Mach Number

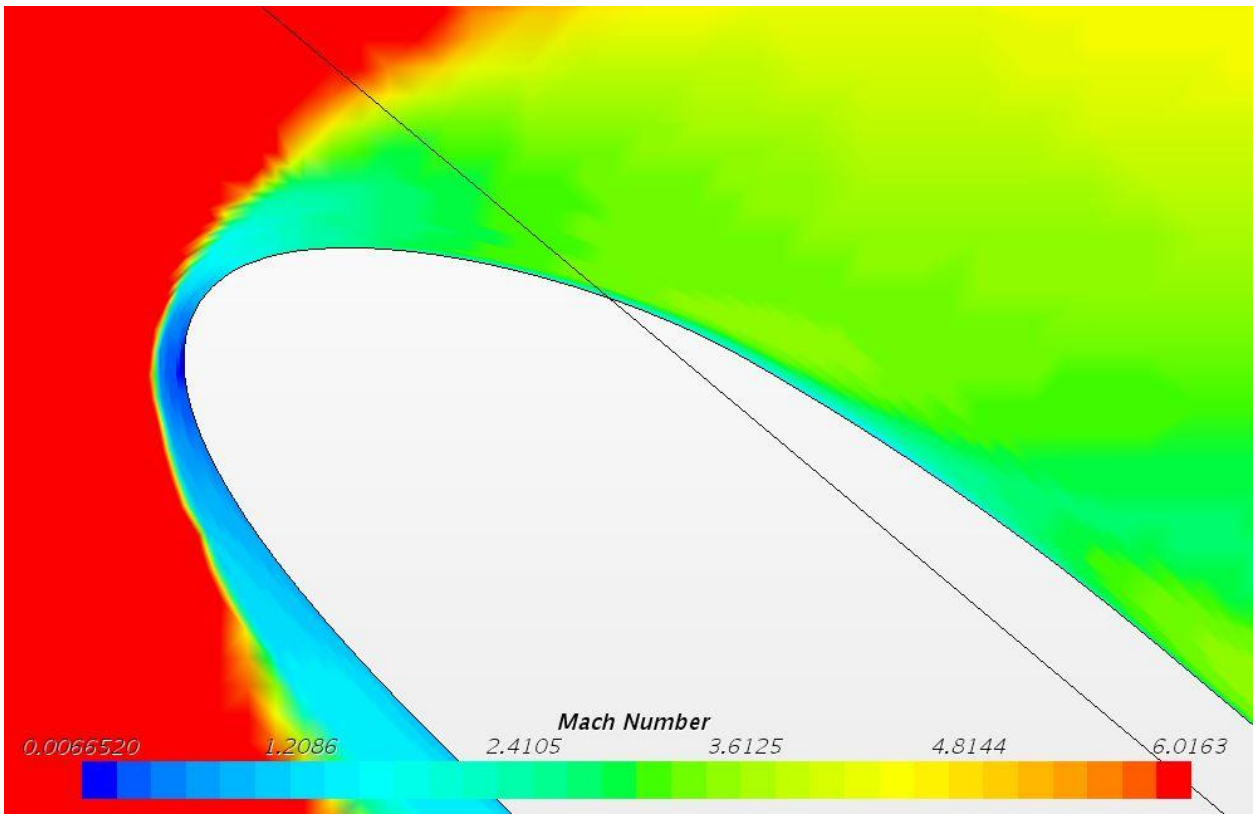

Figure 84 - One million cells 50% scale X-37 nose Mach Number

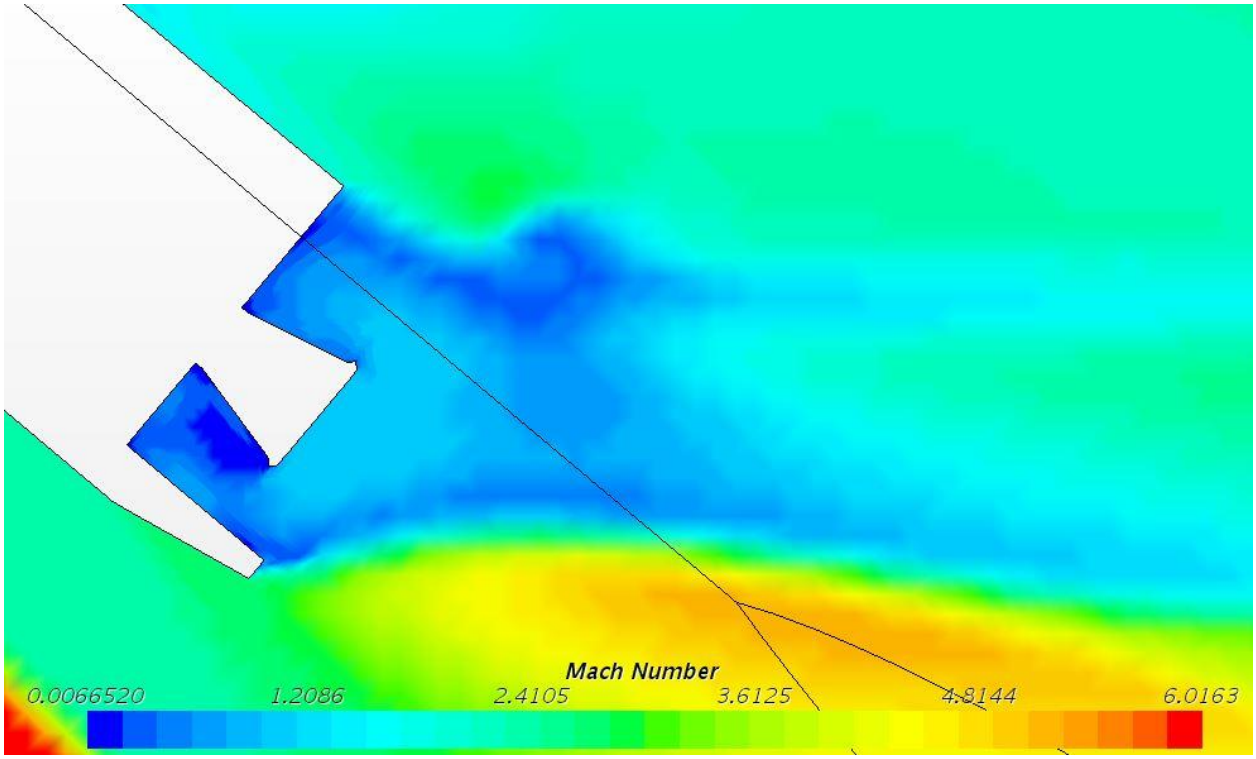

Figure 85 - One million cells 50% scale X-37 tail Mach Number

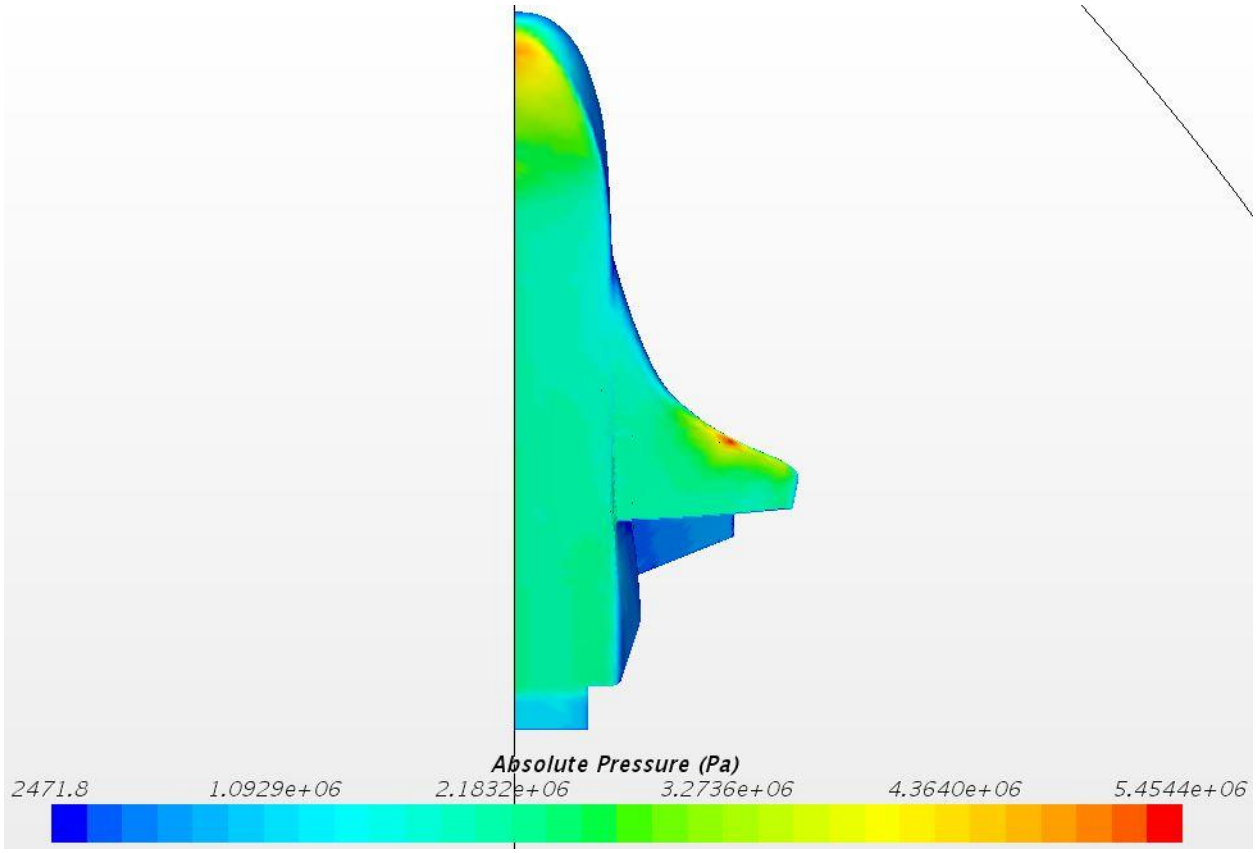

Figure 86 - One million cells 50% scale X-37 bottom Absolute Pressure

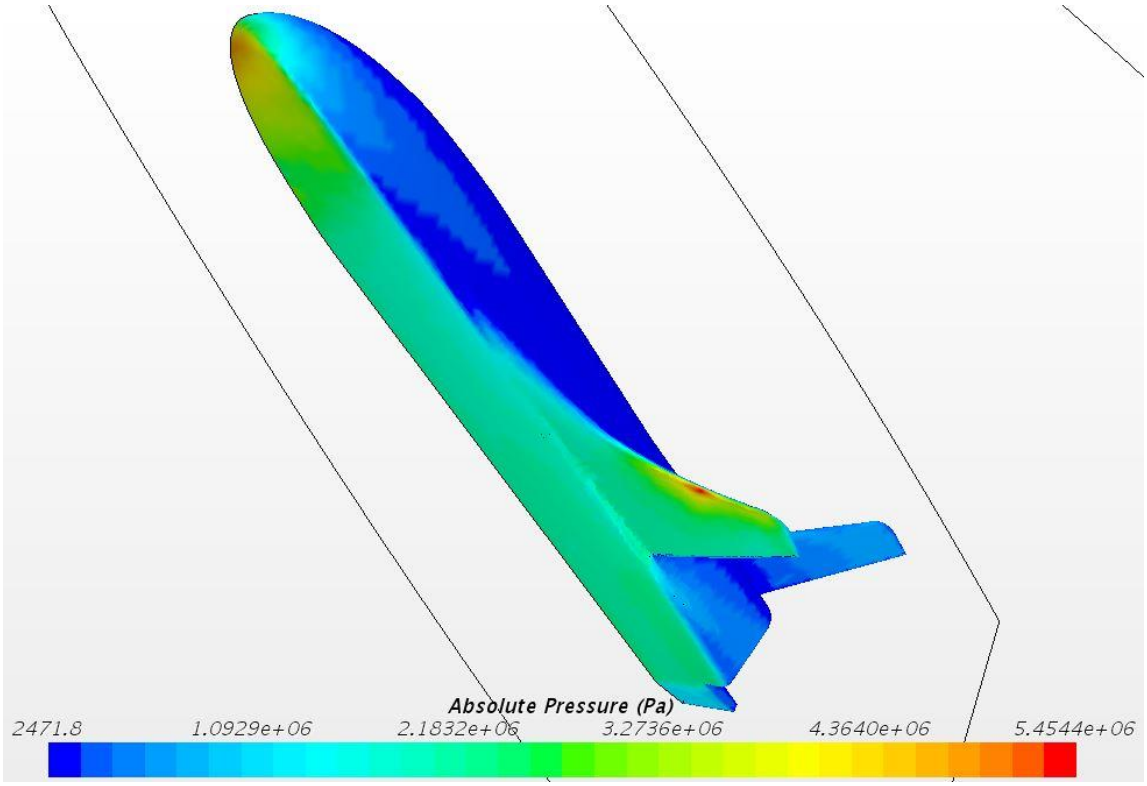

Figure 87 - One million cells 50% scale X-37 3-D Absolute Pressure

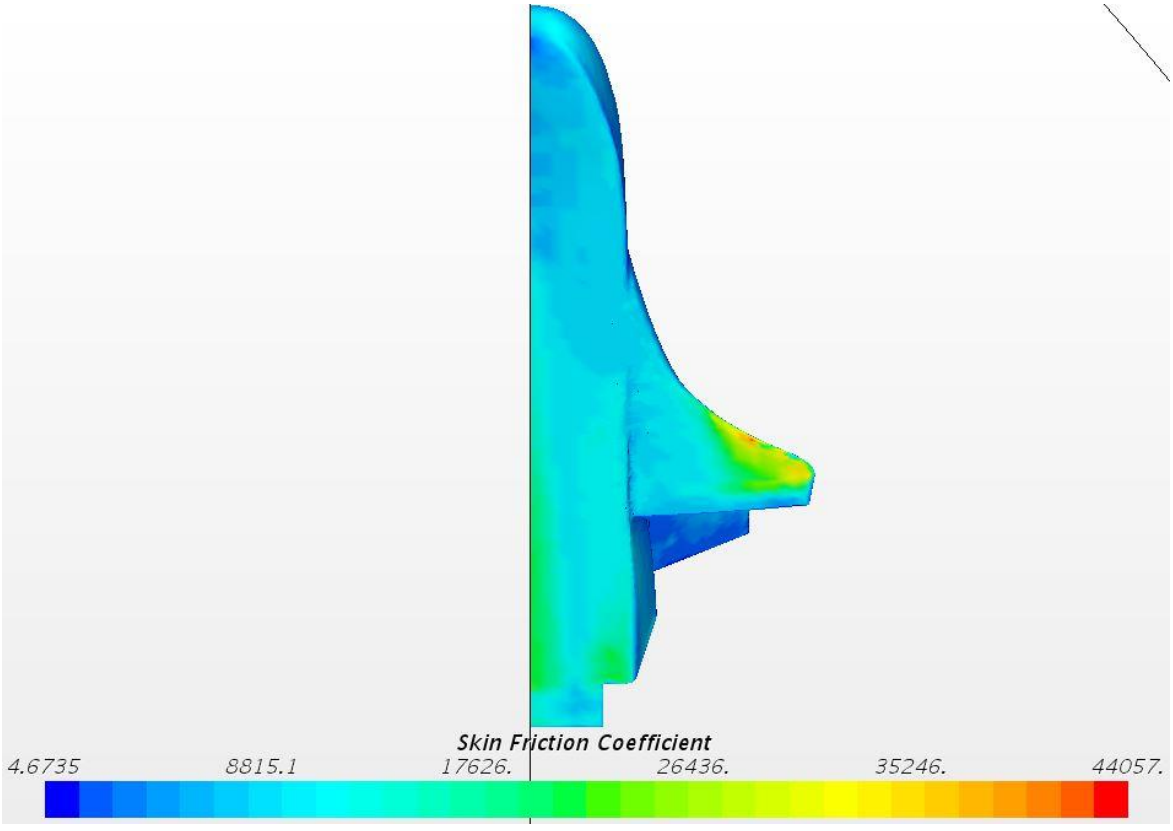

Figure 88 – One million cells 50% scale X-37 bottom Skin Friction Coefficient

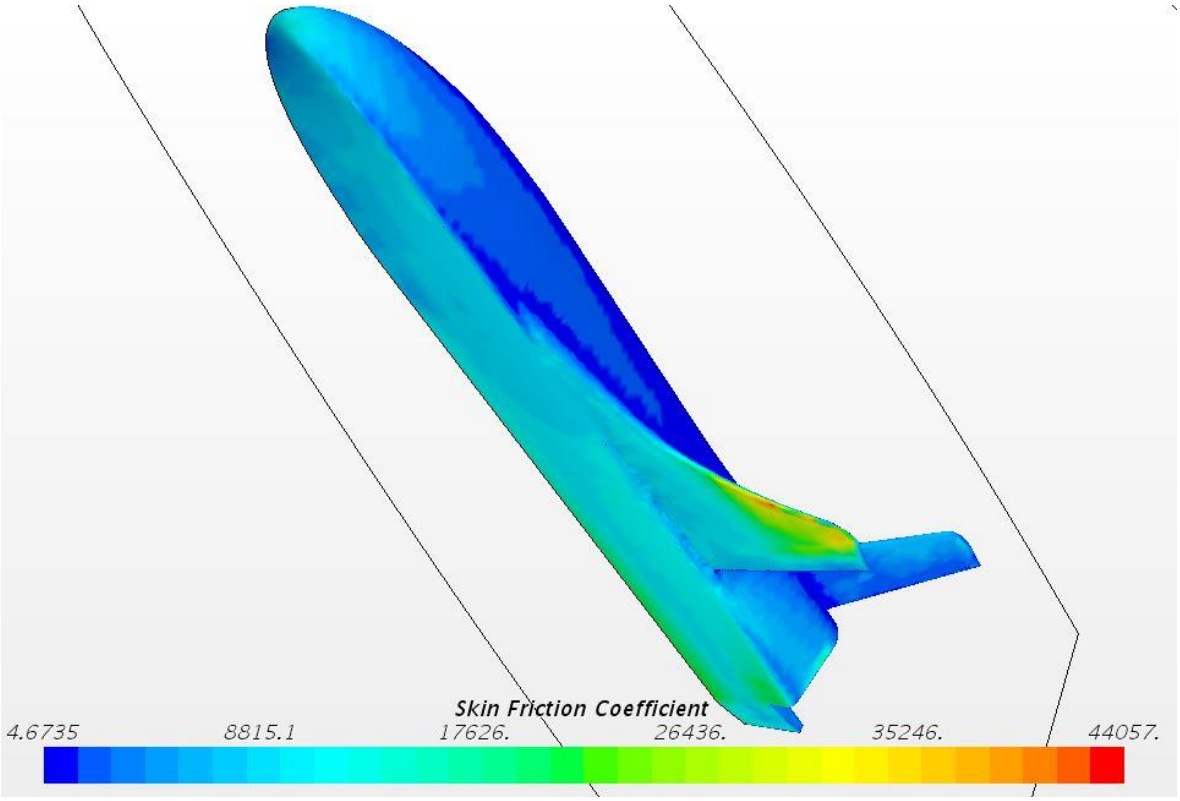

Figure 89 - One million cells 50% scale X-37 3-D Skin Friction Coefficient

7.3.5 25% X-37 at 500K Cells

A 25% scale model of the X-37 is tested at 572143 Cells. Figure 93 displays the mesh generated with Figure 94 and Figure 95 providing focus on the mesh near the nose and tail of the vehicle. The CFD simulation ran for a total of 5,883 iterations and seemed to converge towards a stable solution as seen in Figure 90. The Base cell size for the mesh was designated at 0.2 meters. The cone area behind the tail as well as the refinement area around the vehicle body were set to 15% of the base size (0.03m). The Far-field area outside of the refinement area was set to 300% of the base size (0.6m). The mesh was generated with 30 prism layers stretching at a rate of 1.1 the size of the previous layer, from the surface of the vehicle. The absolute thickness of these prism layers was 30% of the base size (0.06m). The target cell size on the surface of the vehicle was 10% of base size (0.02m) and the minimum surface cell size was set to 5% of the base size (0.01m). The lift force of the vehicle was 908,775N, and the drag force of the vehicle was 869,735N. Using these values for lift force and drag force and equation 3.6, lift-to-drag ratio can be calculated to be 1.045.

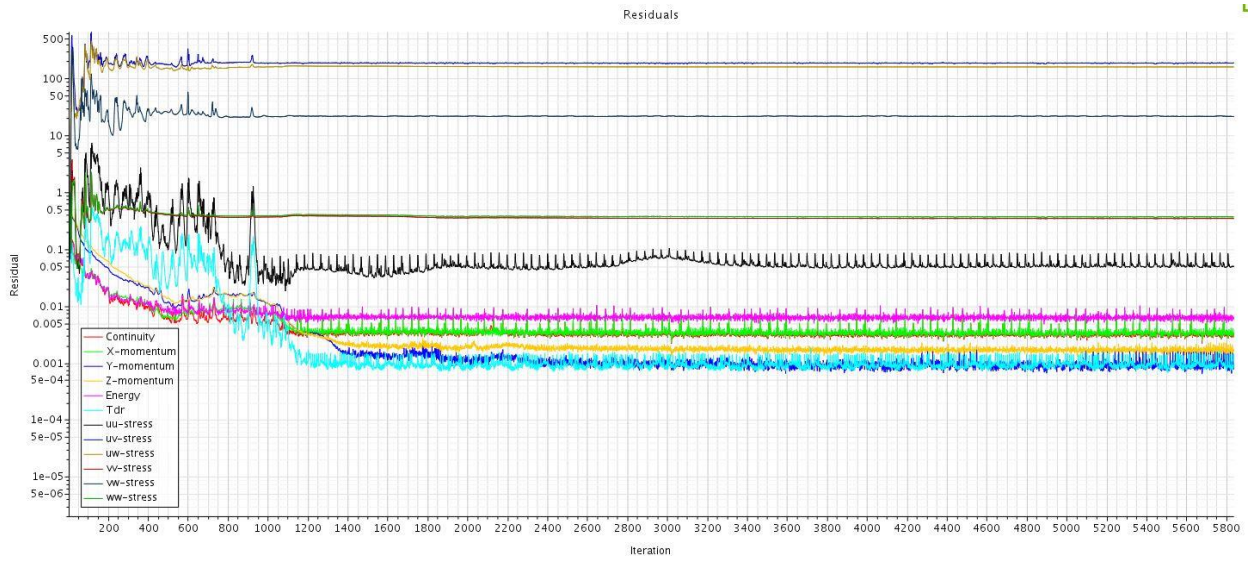

Figure 90 - 500K cells 25% scale X-37 Residual Plot

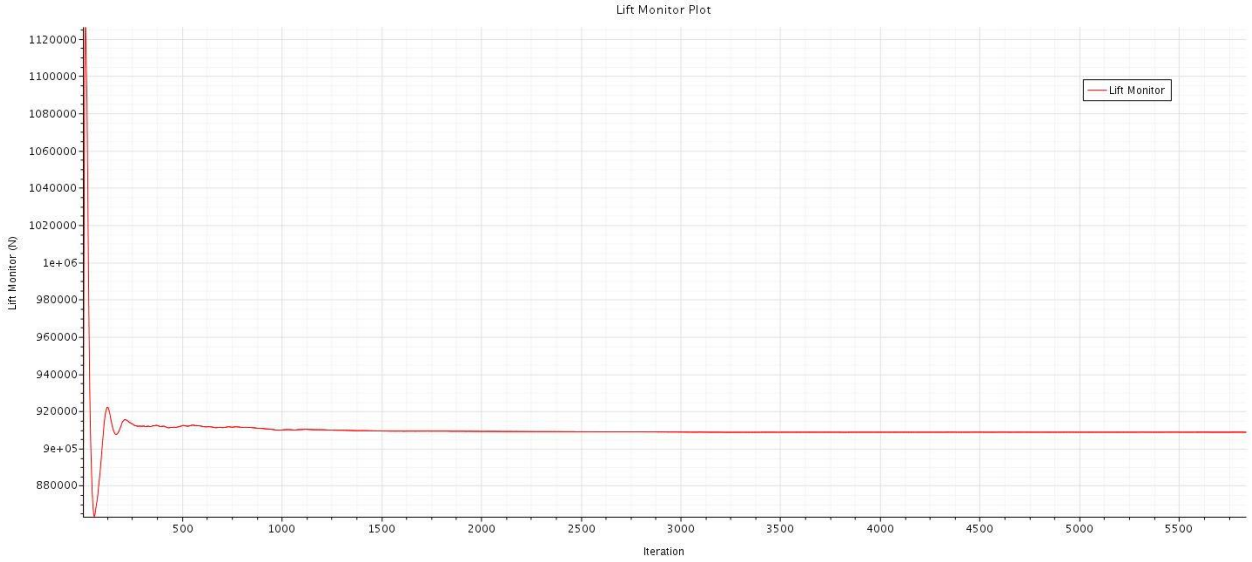

Figure 91 - 500K cells 25% scale X-37 Lift Plot

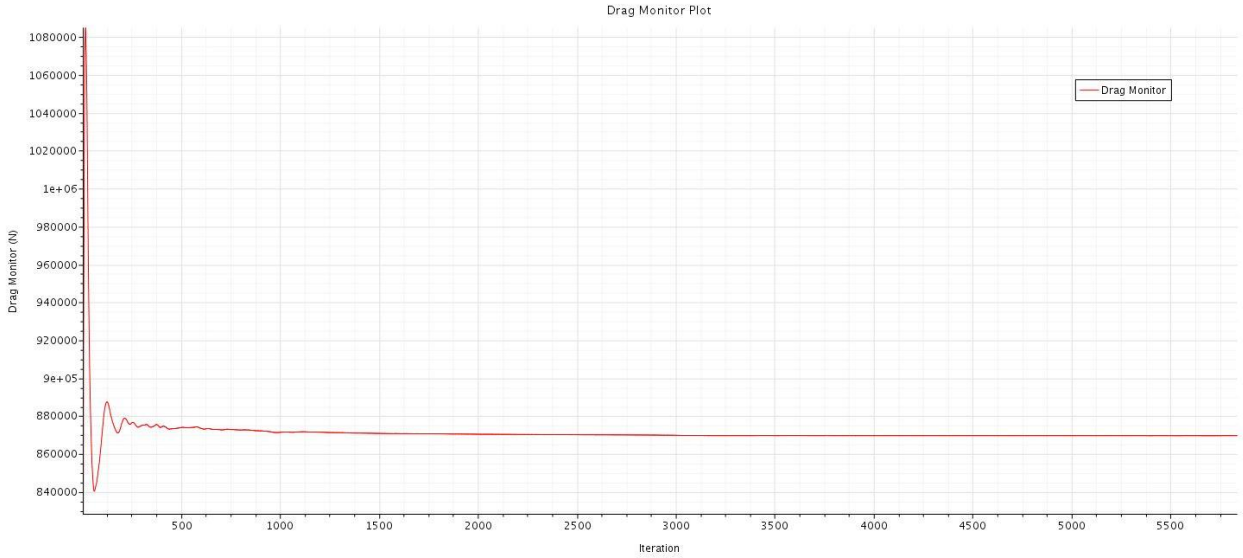

Figure 92 - 500K cells 25% scale X-37 Drag Plot

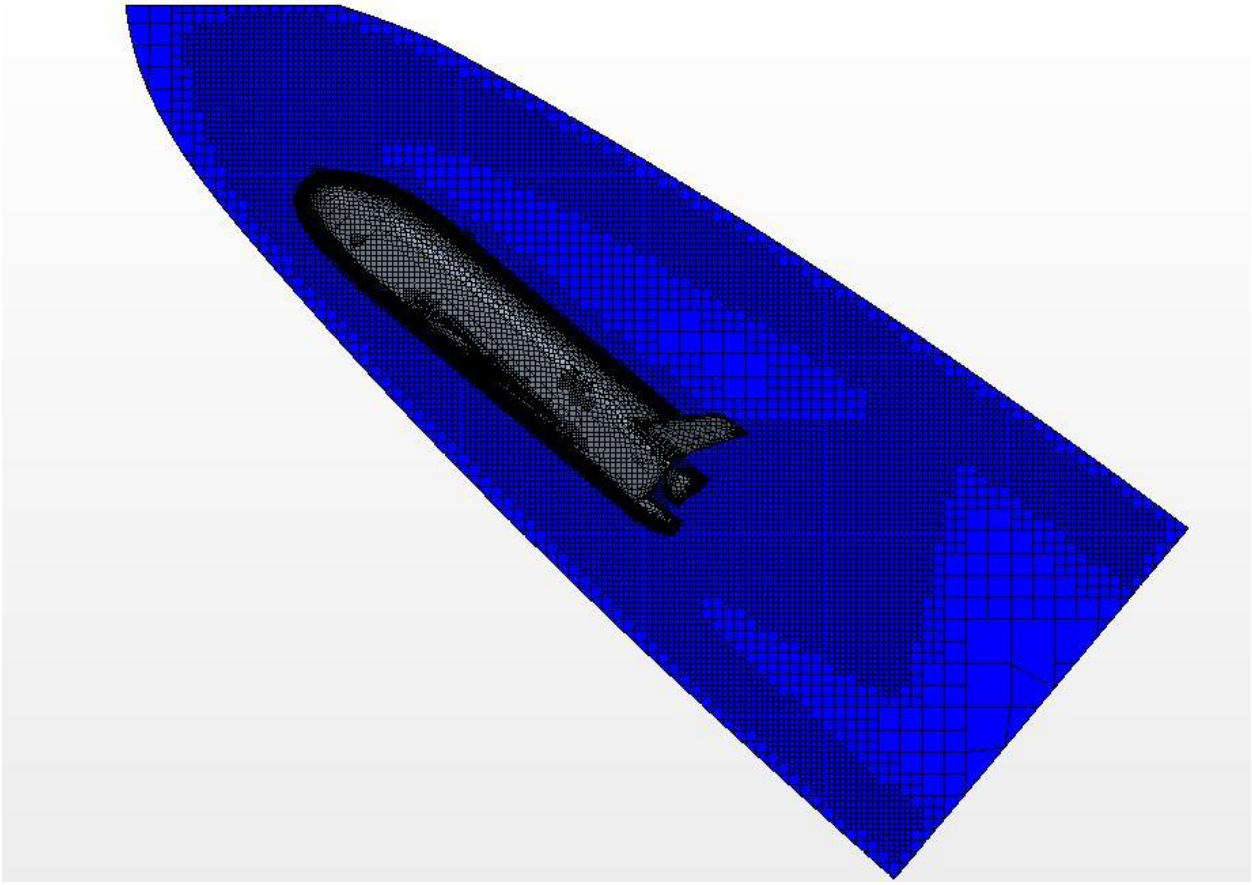

Figure 93 - 500K cells 25% scale X-37 full body Mesh

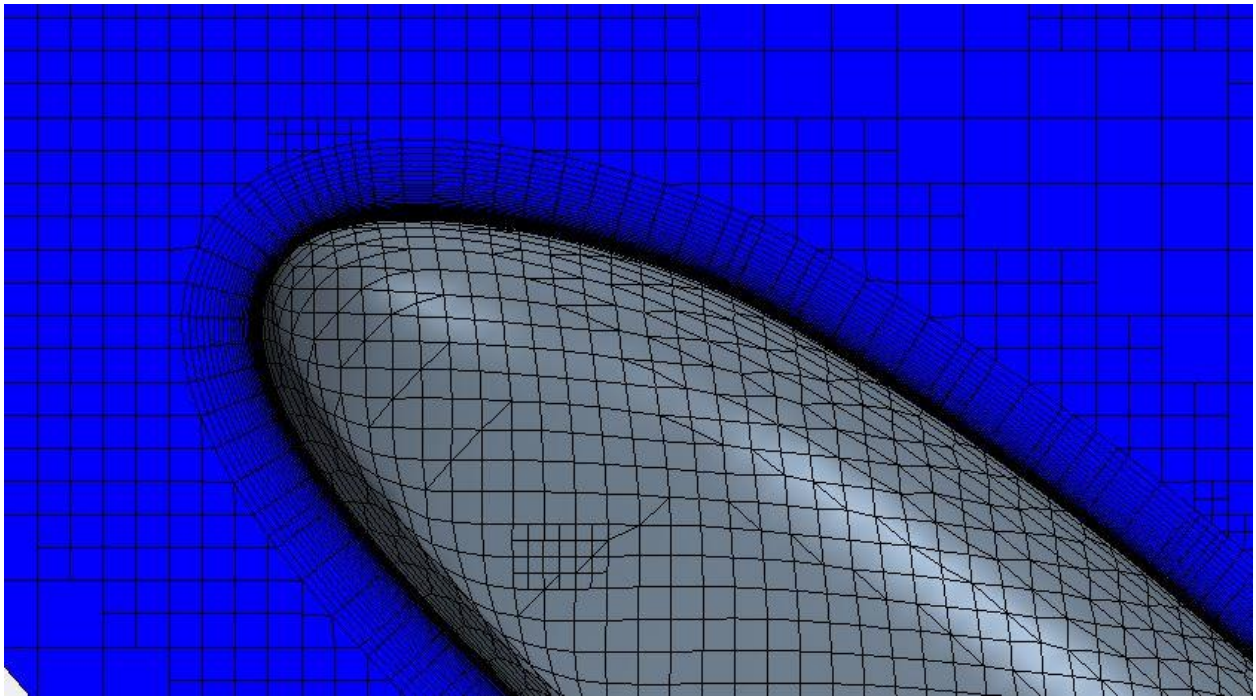

Figure 94 - 500K cells 25% scale X-37 nose Mesh

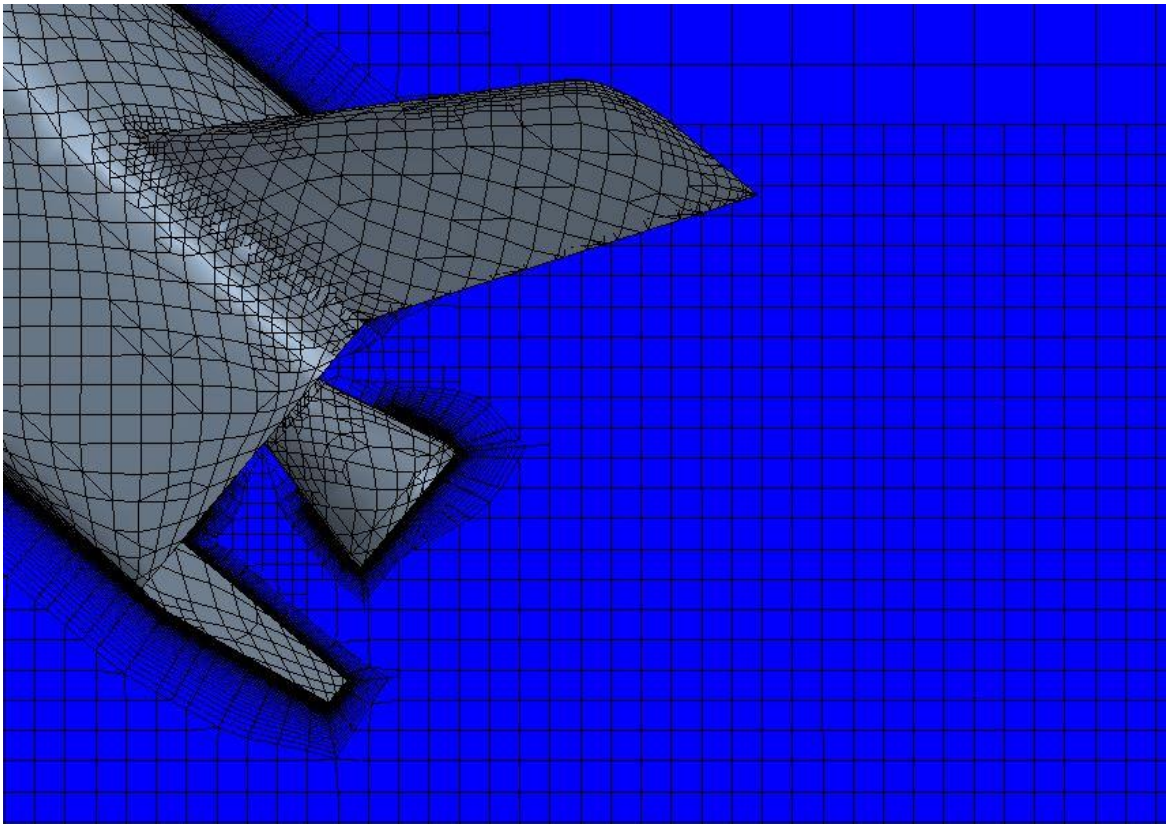

Figure 95 - 500K cells 25% scale X-37 tail Mesh

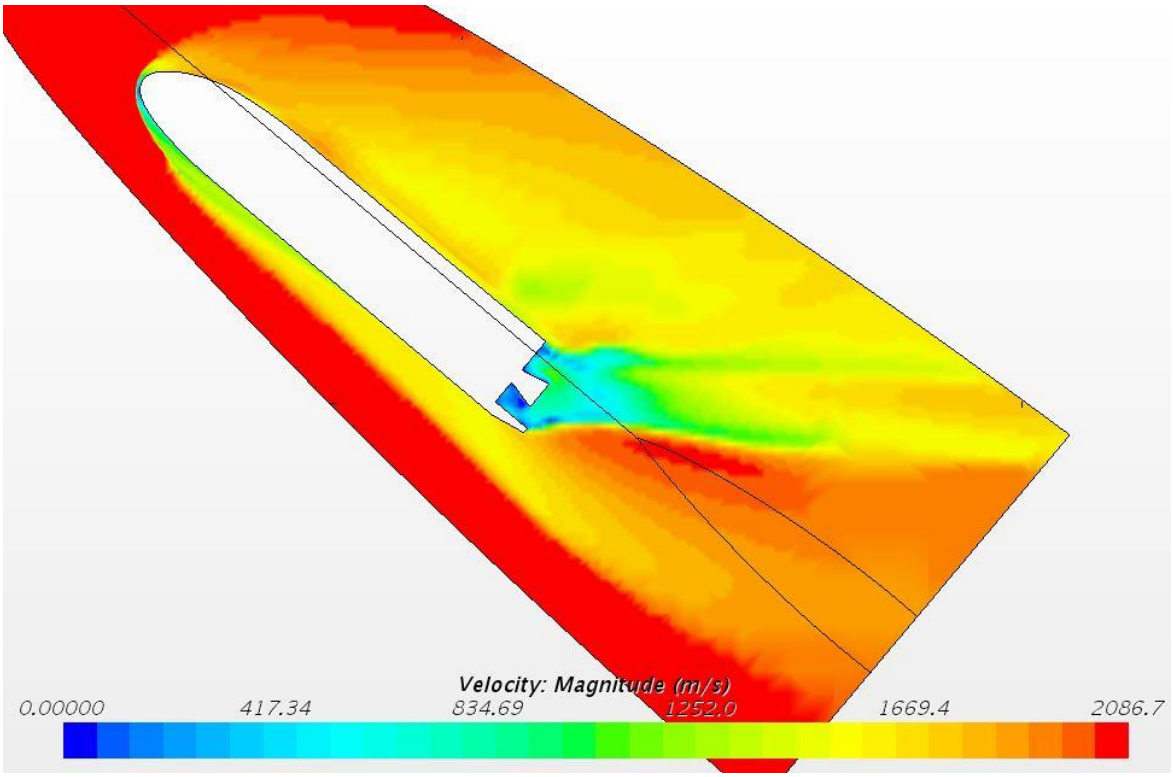

Figure 96 - 500K cells 25% scale X-37 full body Velocity

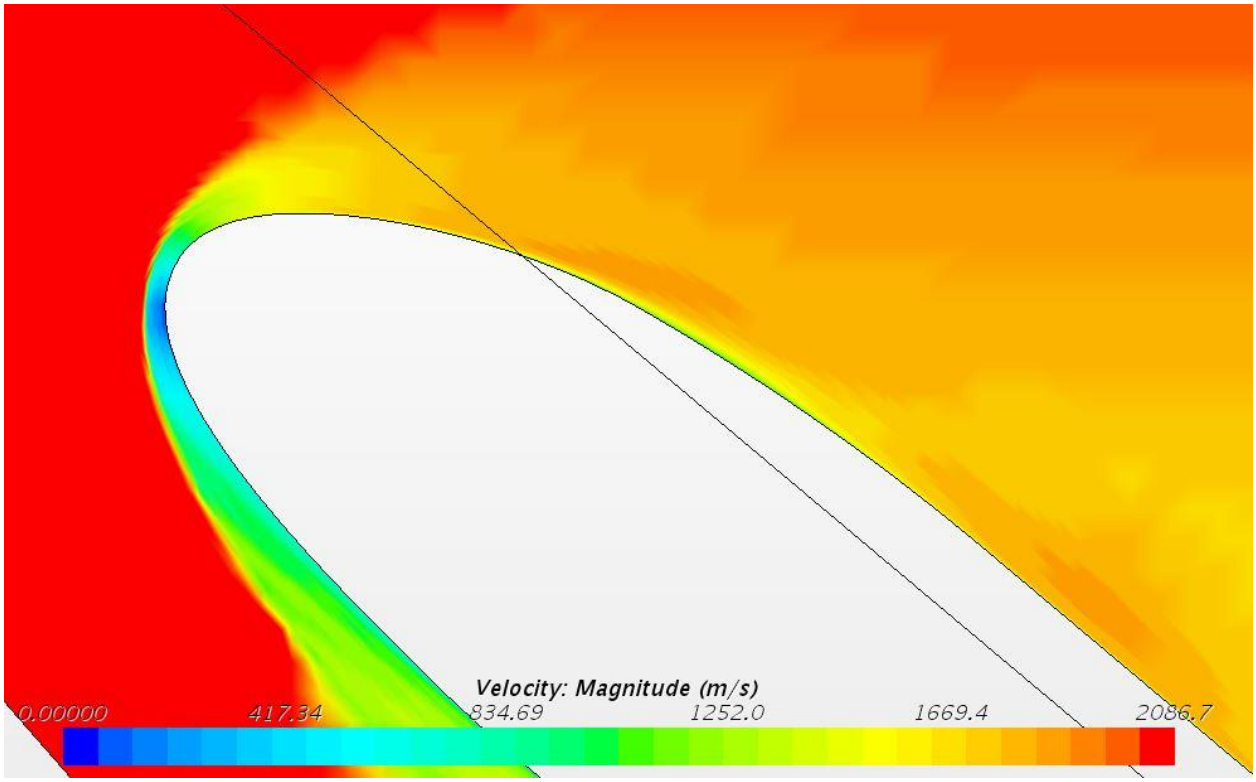

Figure 97 - 500K cells 25% scale X-37 nose Velocity

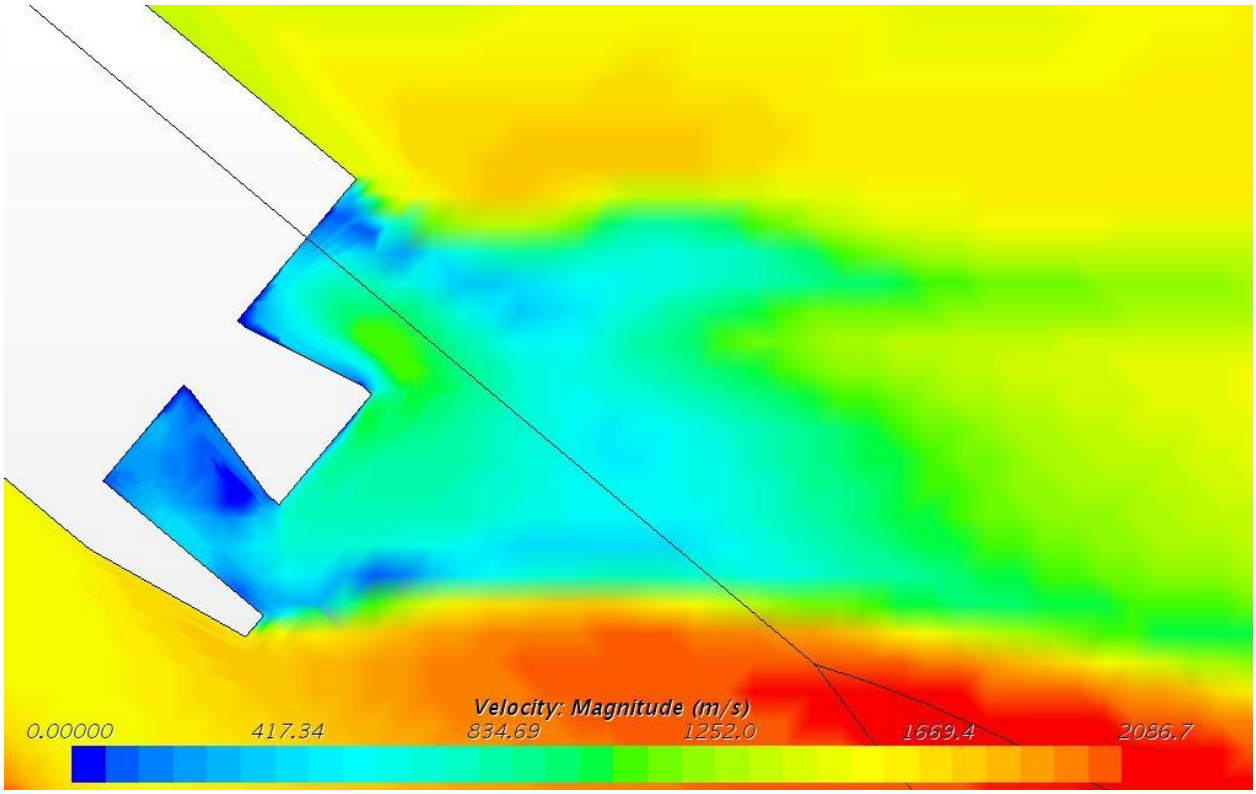

Figure 98 - 500K cells 25% scale X-37 tail Velocity

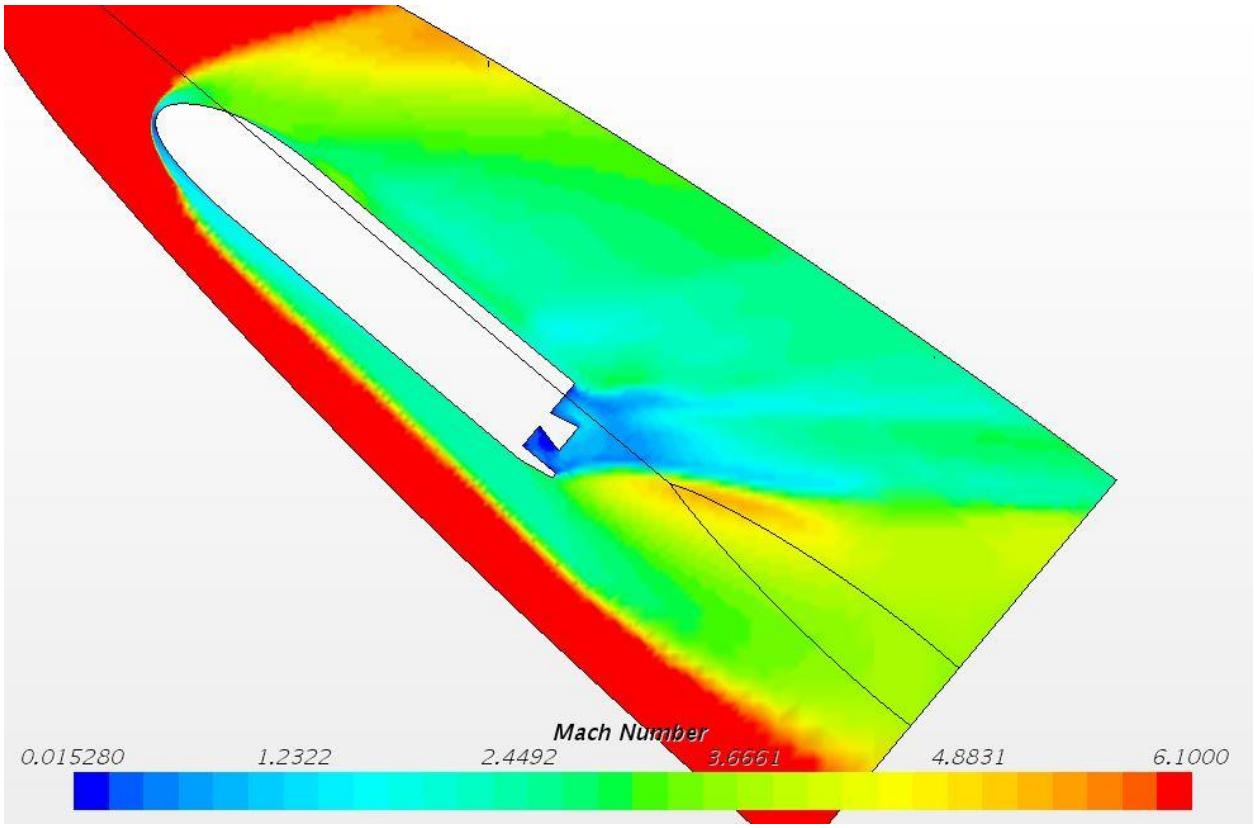

Figure 99 - 500K cells 25% scale X-37 full body Mach Number

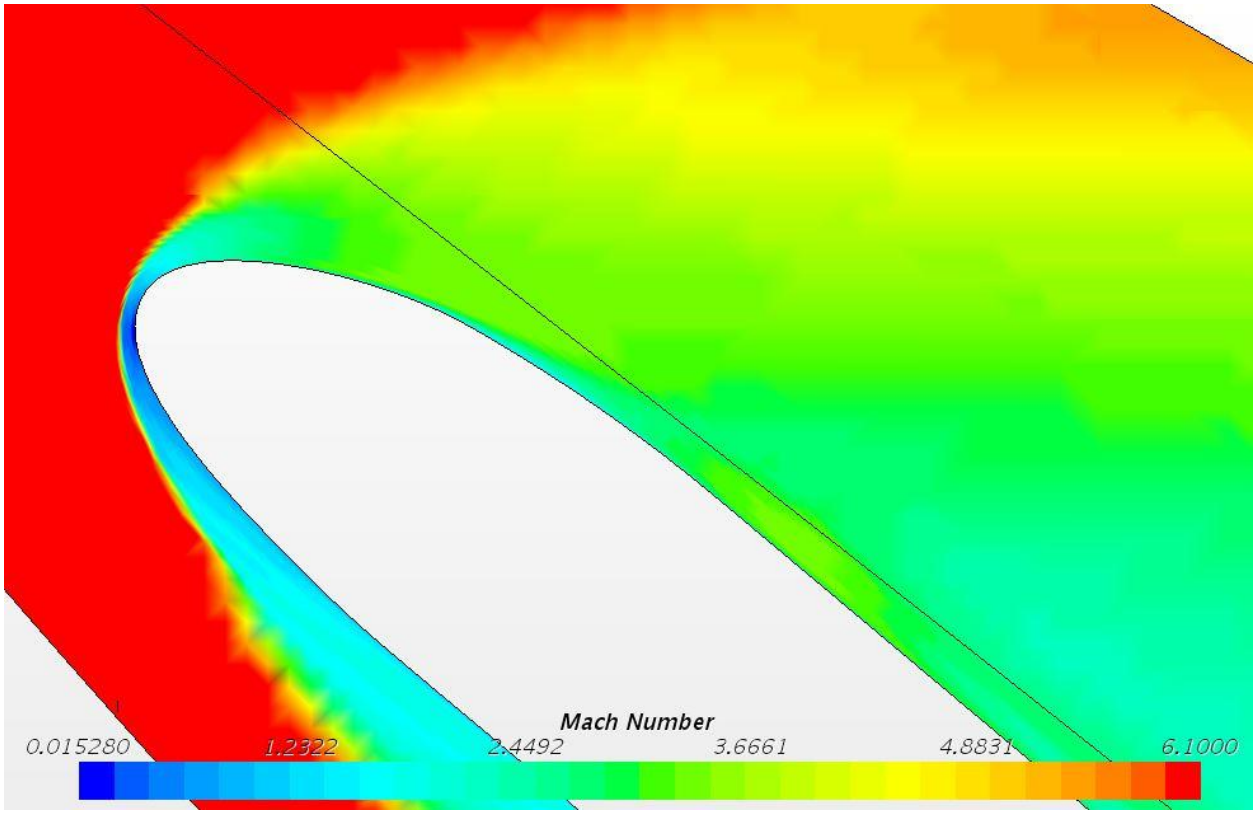

Figure 100 - 500K cells 25% scale X-37 nose Mach Number

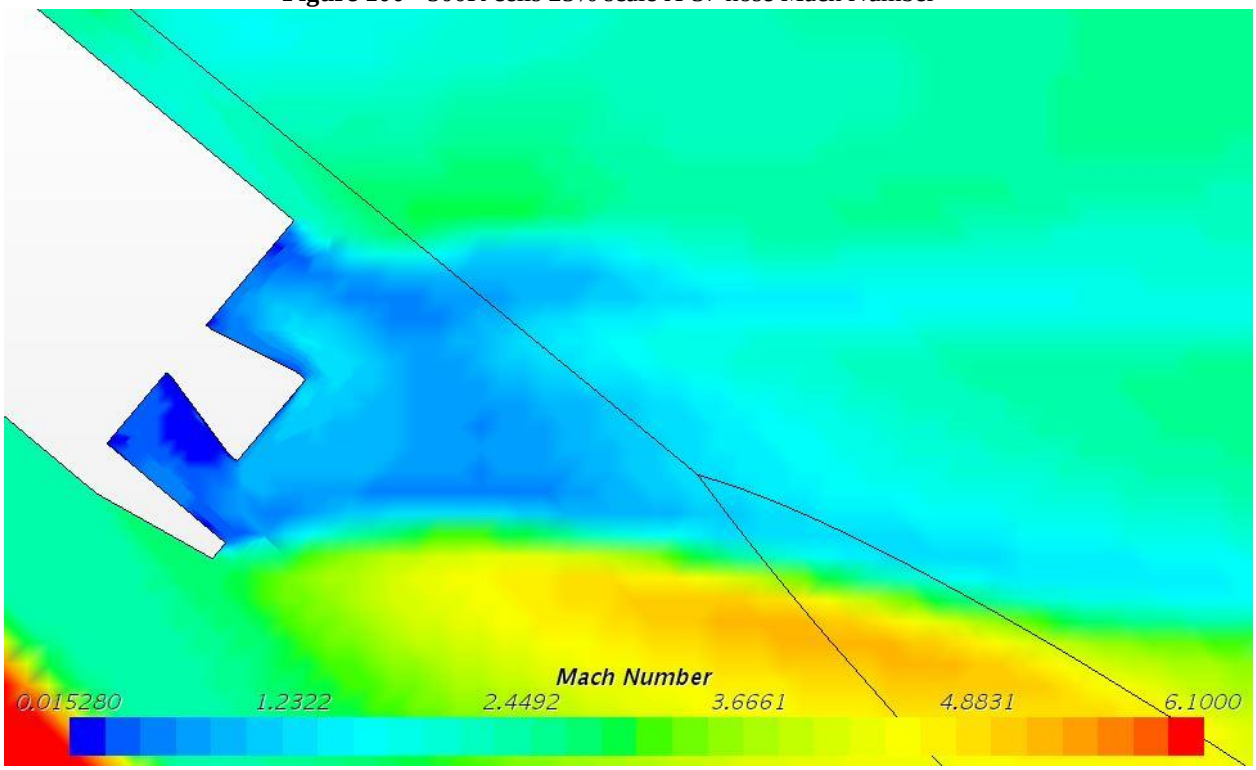

Figure 101 - 500K cells 25% scale X-37 tail Mach Number

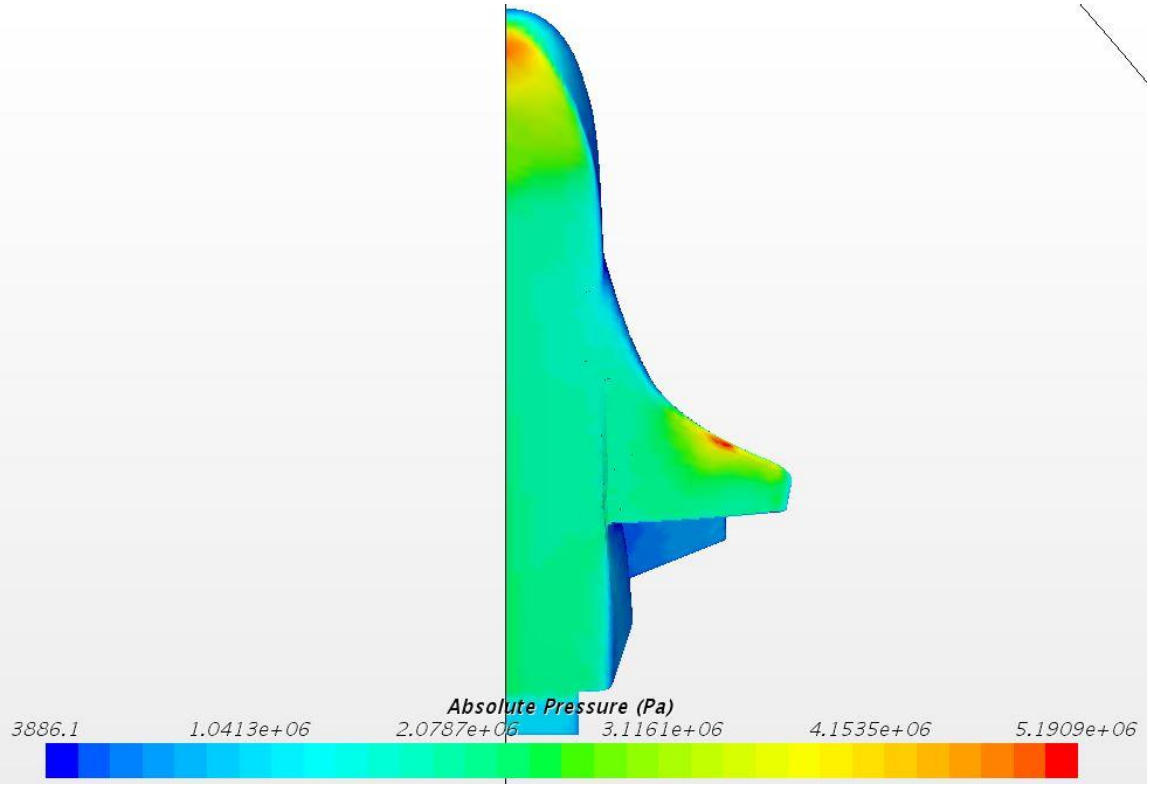

Figure 102 - 500K cells 25% scale X-37 bottom Absolute Pressure

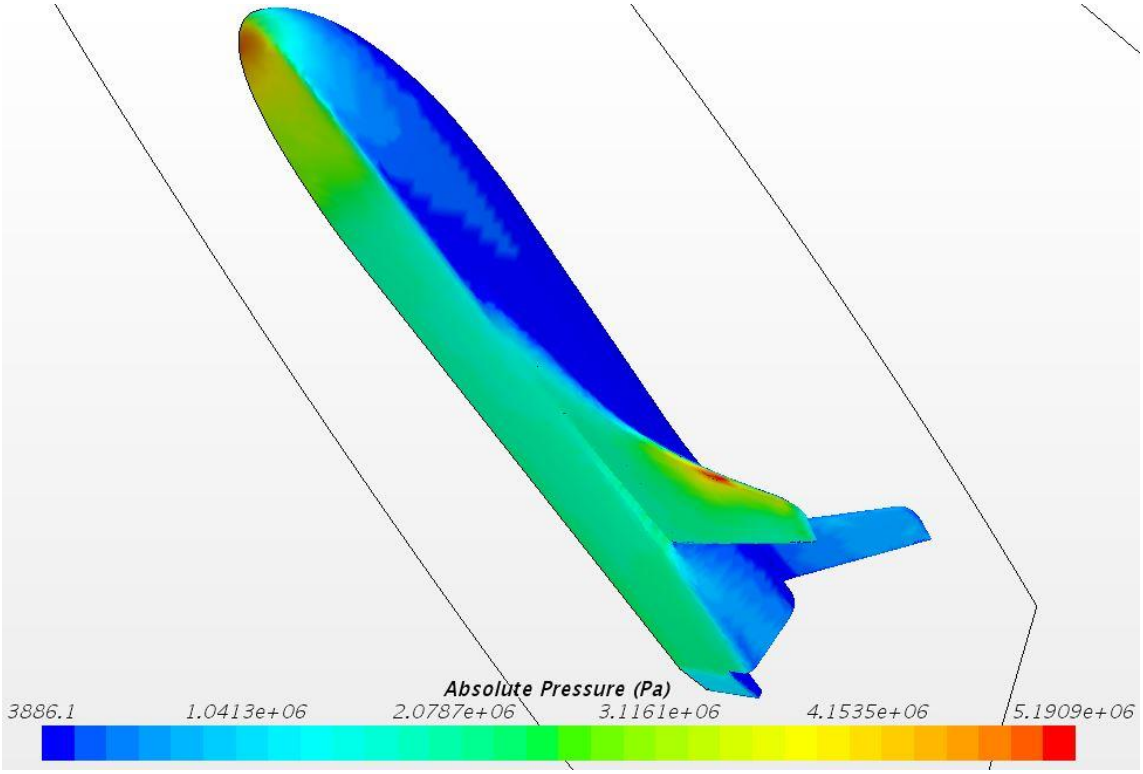

Figure 103 - 500K cells 25% scale X-37 3-D Absolute Pressure

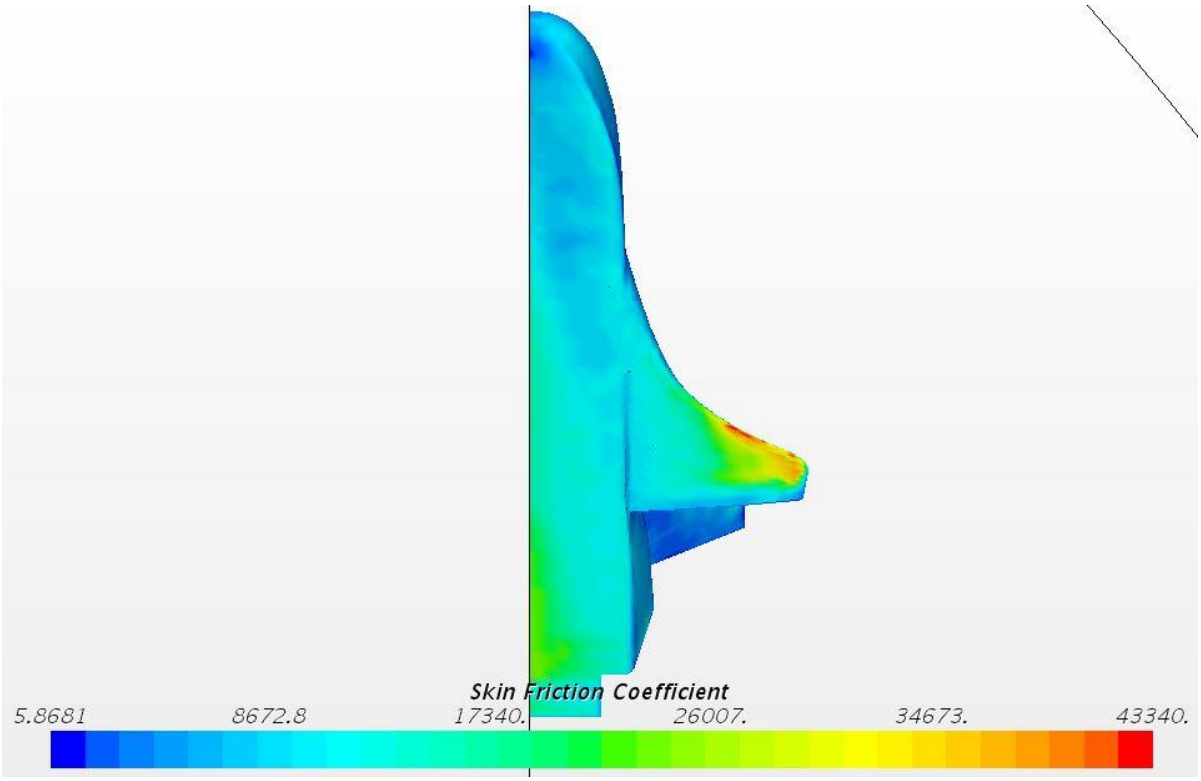

Figure 104 - 500K cells 25% scale X-37 bottom Skin Friction Coefficient

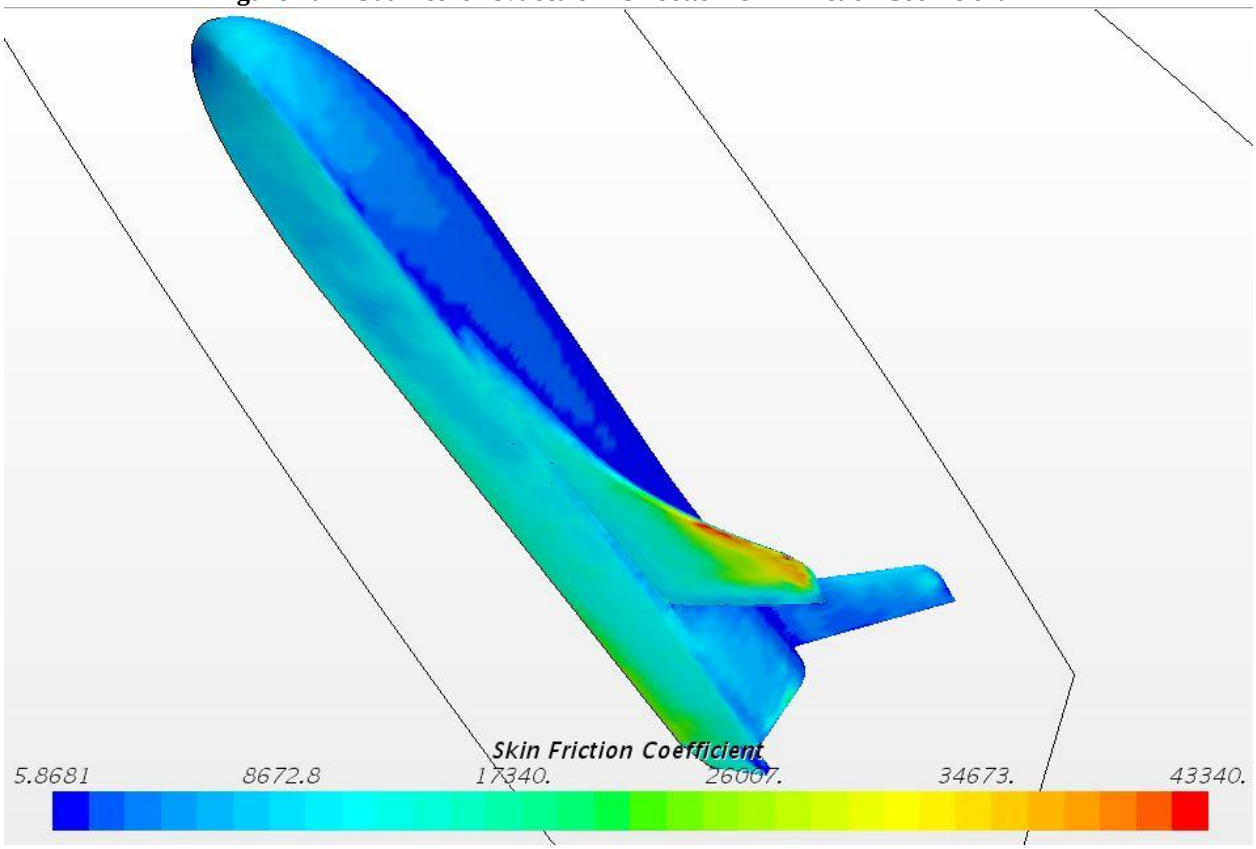

Figure 105 - 500K cells 25% scale X-37 3-D Skin Friction Coefficient

7.4 Space Shuttle Orbiter

The 100%, 50%, and 25% Space Shuttle Orbiter models were each run in their own CFD simulation at 1 Million cells. The test area that designated the outer area of the CFD simulation was the same as the one used in the X-37 runs, scaled up for the specific scale of SSO being run. This allowed the refinement area to be placed where the shocks appear in the CFD run. All models of the SSO were tested with the SSO at an angle of attack of 40 degrees in an effort to achieve a lift-to-drag ratio of 1. (Stone D, 1970)

7.4.1 100% SSO at 1 Million Cells

A 100% scale model of the SSO is tested at 1079000 Cells. Figure 109 displays the mesh generated with Figure 110 and Figure 111 providing focus on the mesh near the nose and tail of the vehicle. The CFD simulation ran for a total of 7,500 iterations and seemed to converge towards a stable solution as seen in Figure 106. The Base cell size for the mesh was designated at 2.4 meters. The cone area behind the tail as well as the refinement area around the vehicle body were set to 15% of the base size (0.36m). The Far-field area outside of the refinement area was set to 300% of the base size (7.2m). The mesh was generated with 33 prism layers stretching at a rate of 1.1 the size of the previous layer, from the surface of the vehicle. The absolute thickness of these prism layers was 40% of the base size (0.96m). The target cell size on the surface of the vehicle was 10% of base size (0.24m) and the minimum surface cell size was set to 5% of the base size (0.12m). The lift force of the vehicle was 248,358,901N, and the drag force of the vehicle was 224,073,593N. Using these values for lift force and drag force and equation 3.6, the lift-to-drag ratio can be calculated to be 1.108.

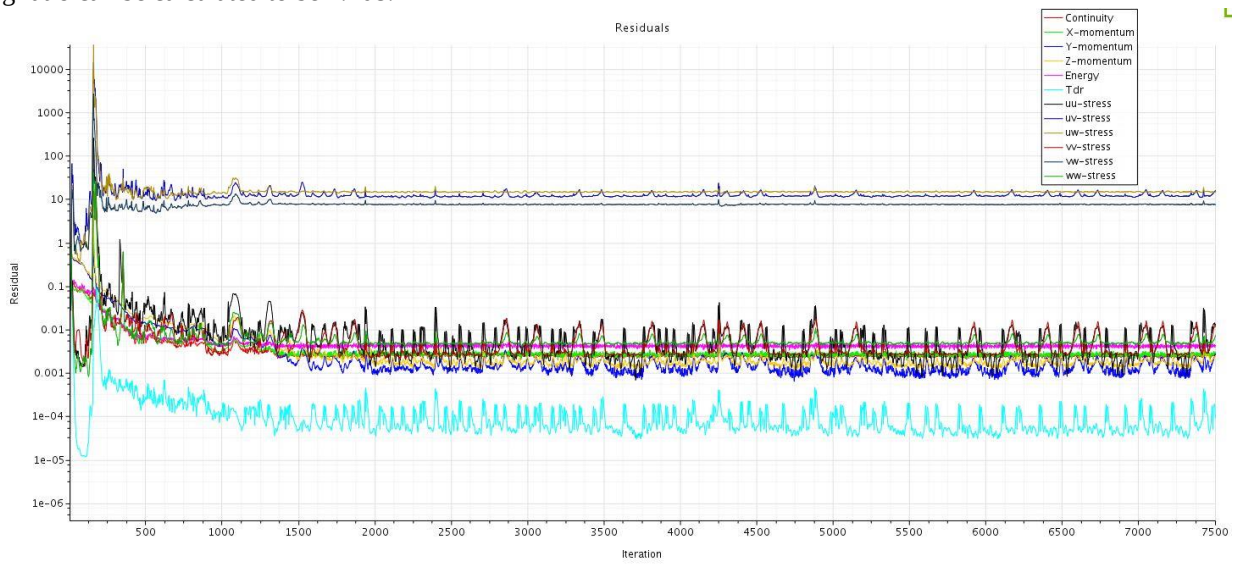

Figure 106 - One million cells 100% scale SSO Residual Plot

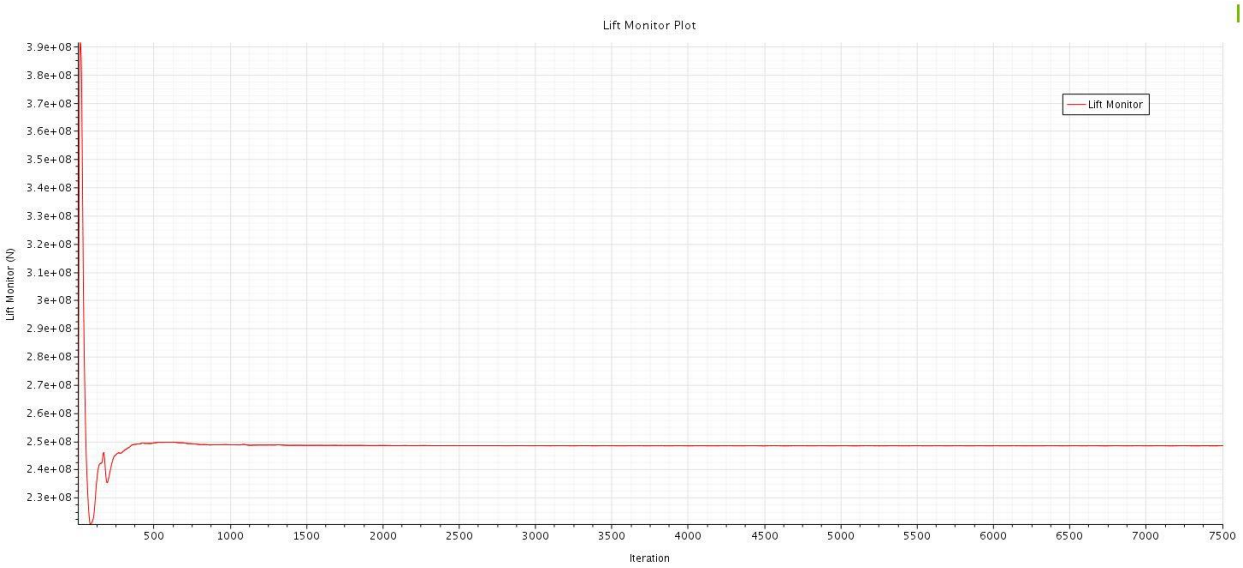

Figure 107 - One million cells 100% scale SSO Lift Plot

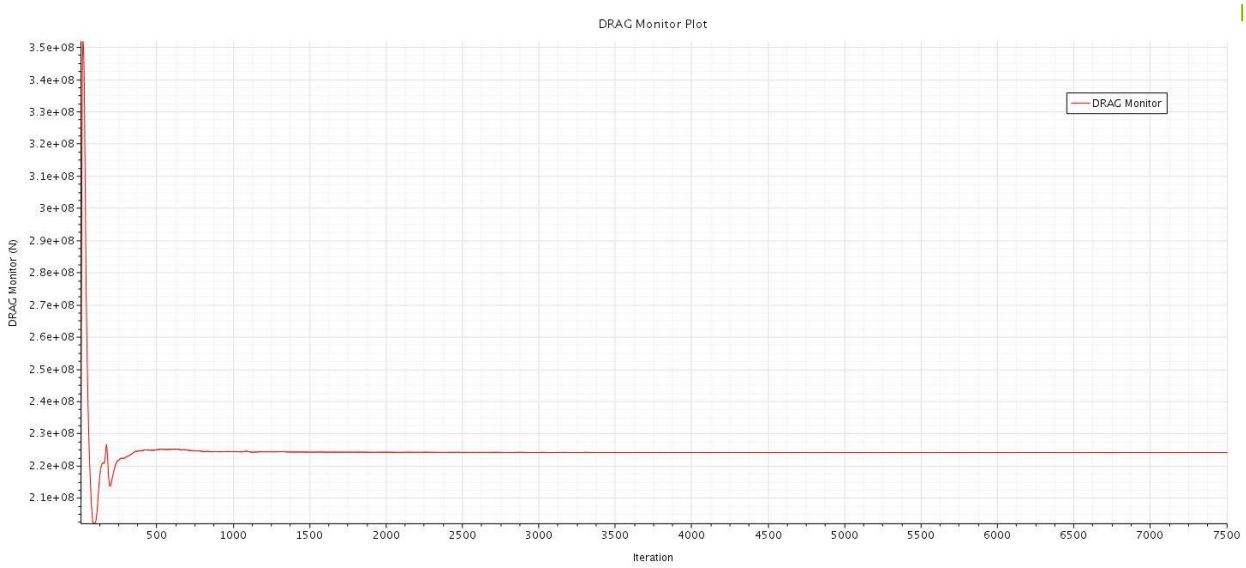

Figure 108 - One million cells 100% scale SSO Drag Plot

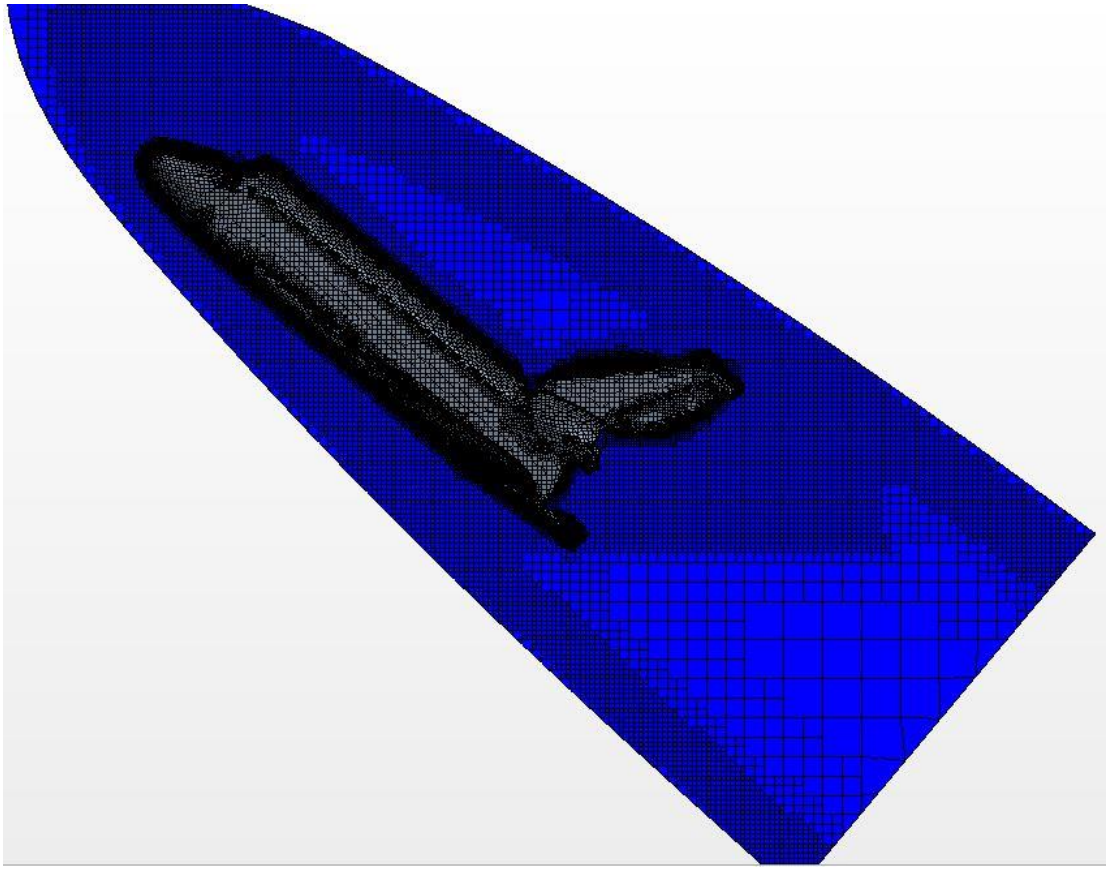

Figure 109 - One million cells 100% scale SSO full body Mesh

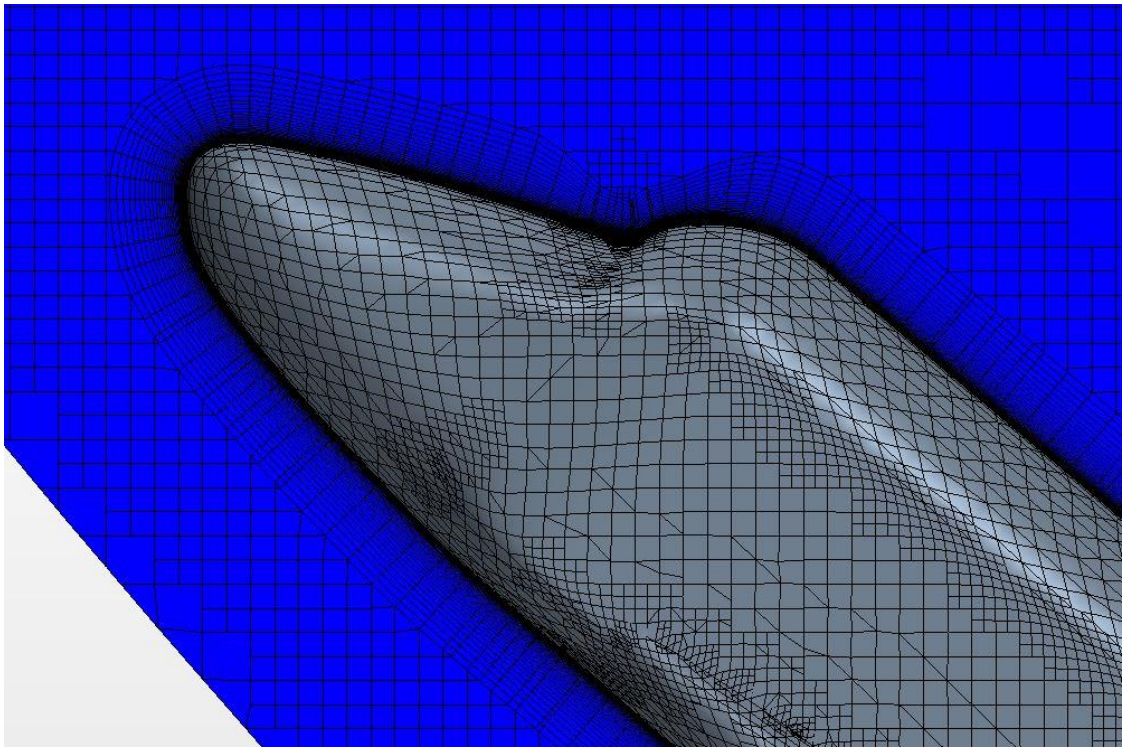

Figure 110 - One million cells 100% scale SSO nose Mesh

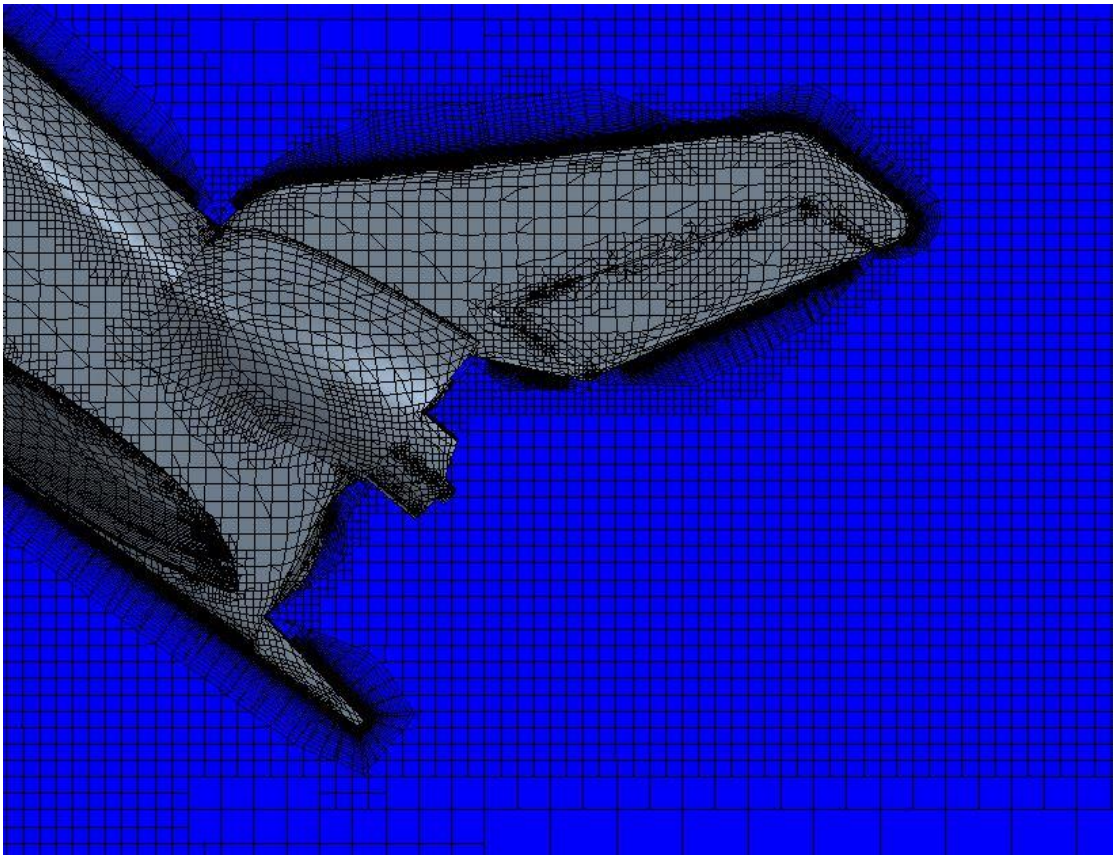

Figure 111 - One million cells 100% scale SSO tail Mesh

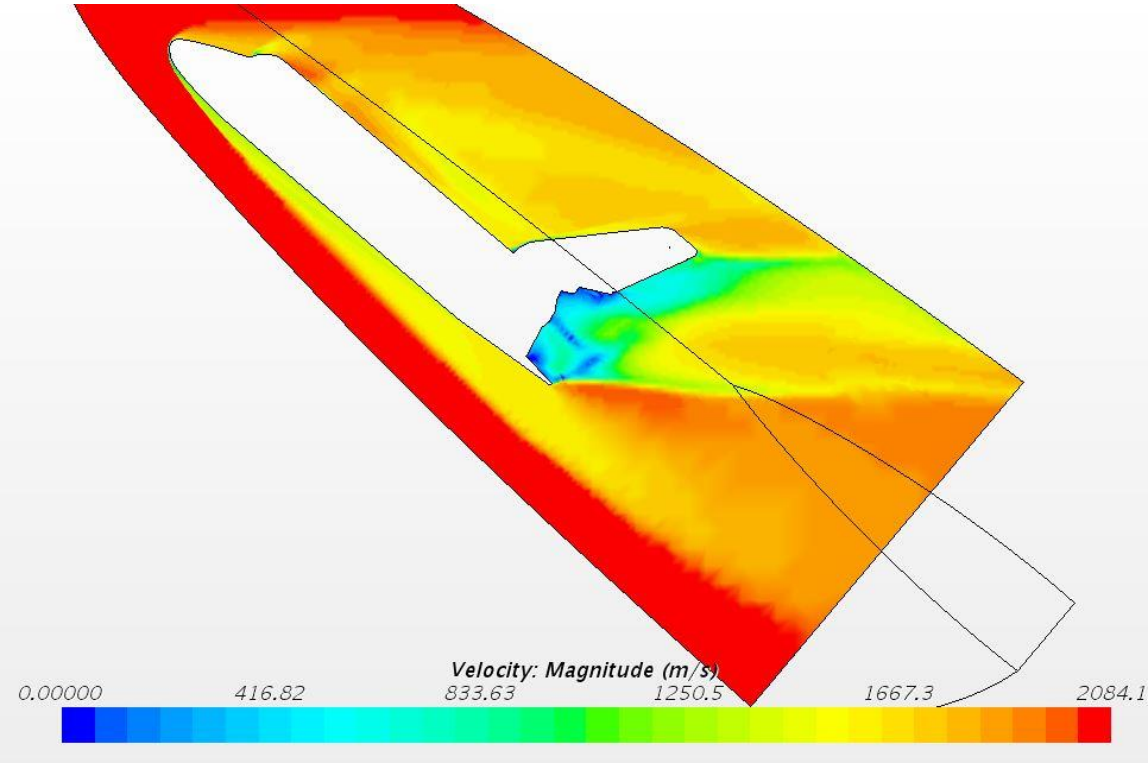

Figure 112 - One million cells 100% scale SSO full body Velocity

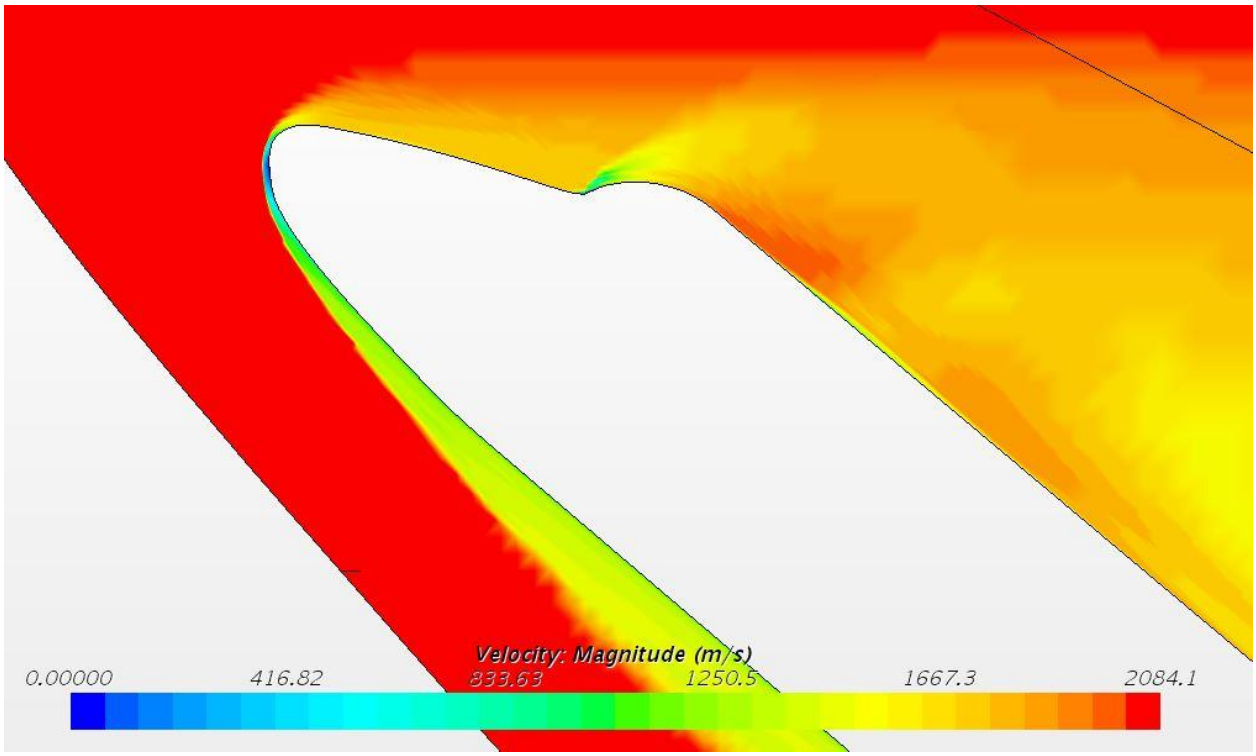

Figure 113 - One million cells 100% scale SSO nose Velocity

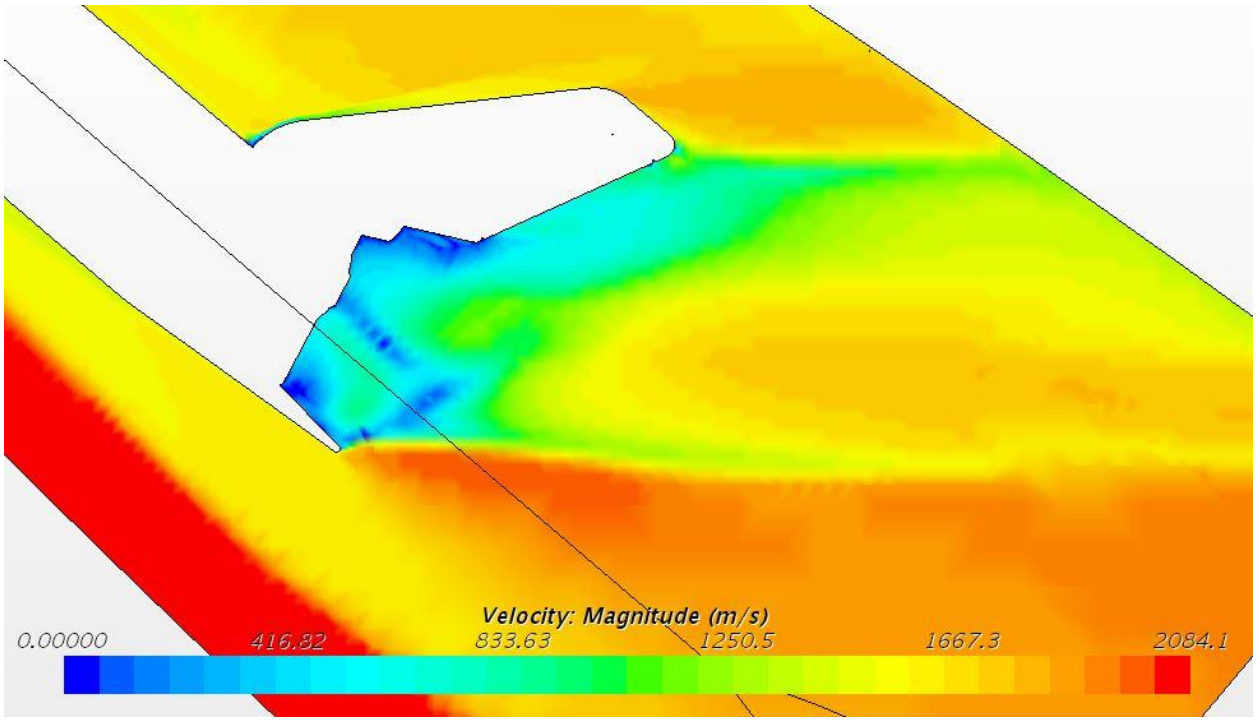

Figure 114 - One million cells 100% scale SSO tail Velocity

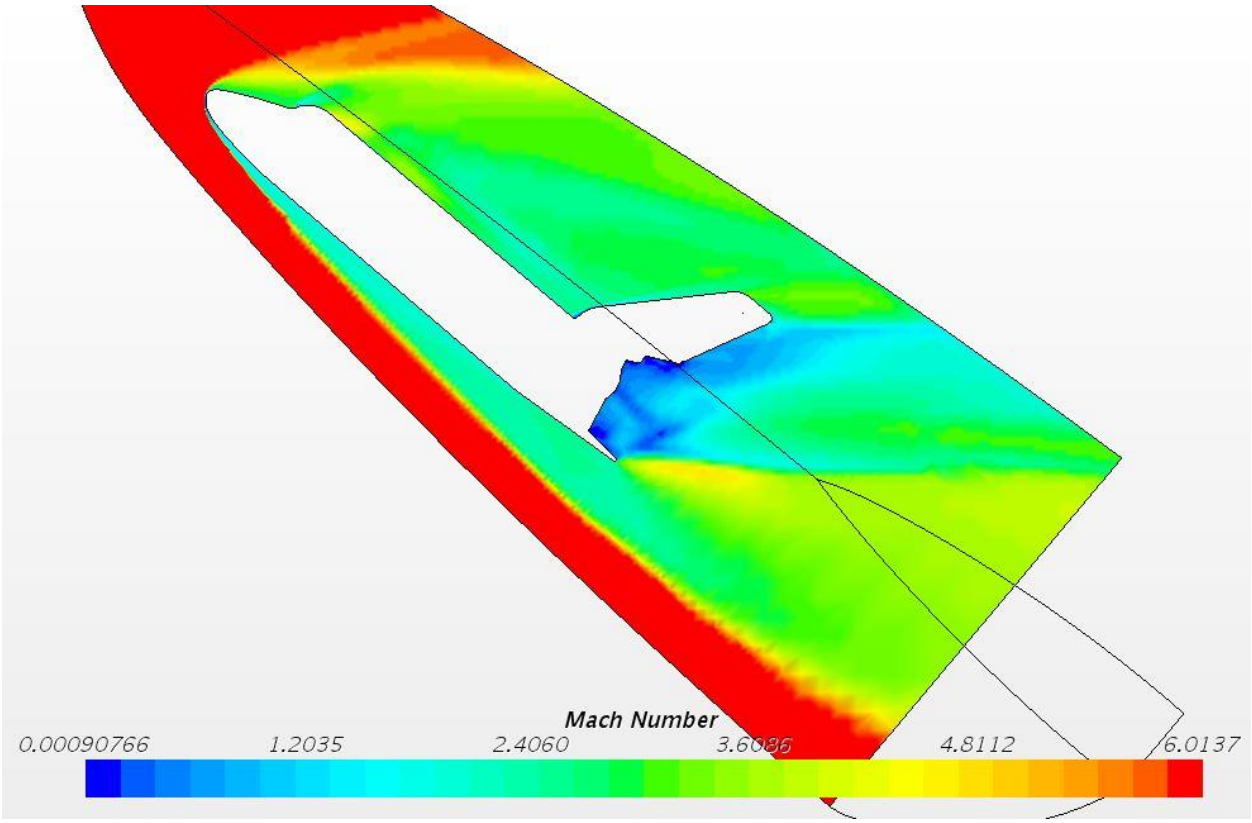

Figure 115 - One million cells 100% scale SSO full body Mach Number

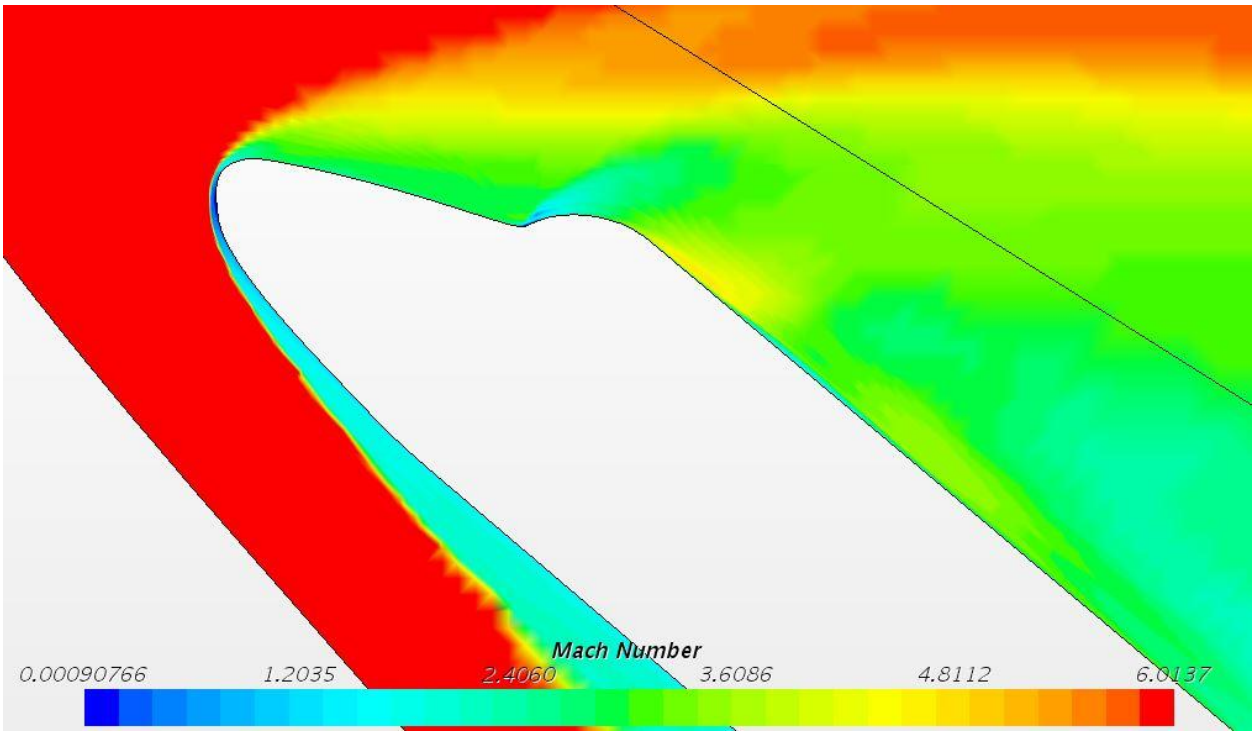

Figure 116 - One million cells 100% scale SSO nose Mach Number

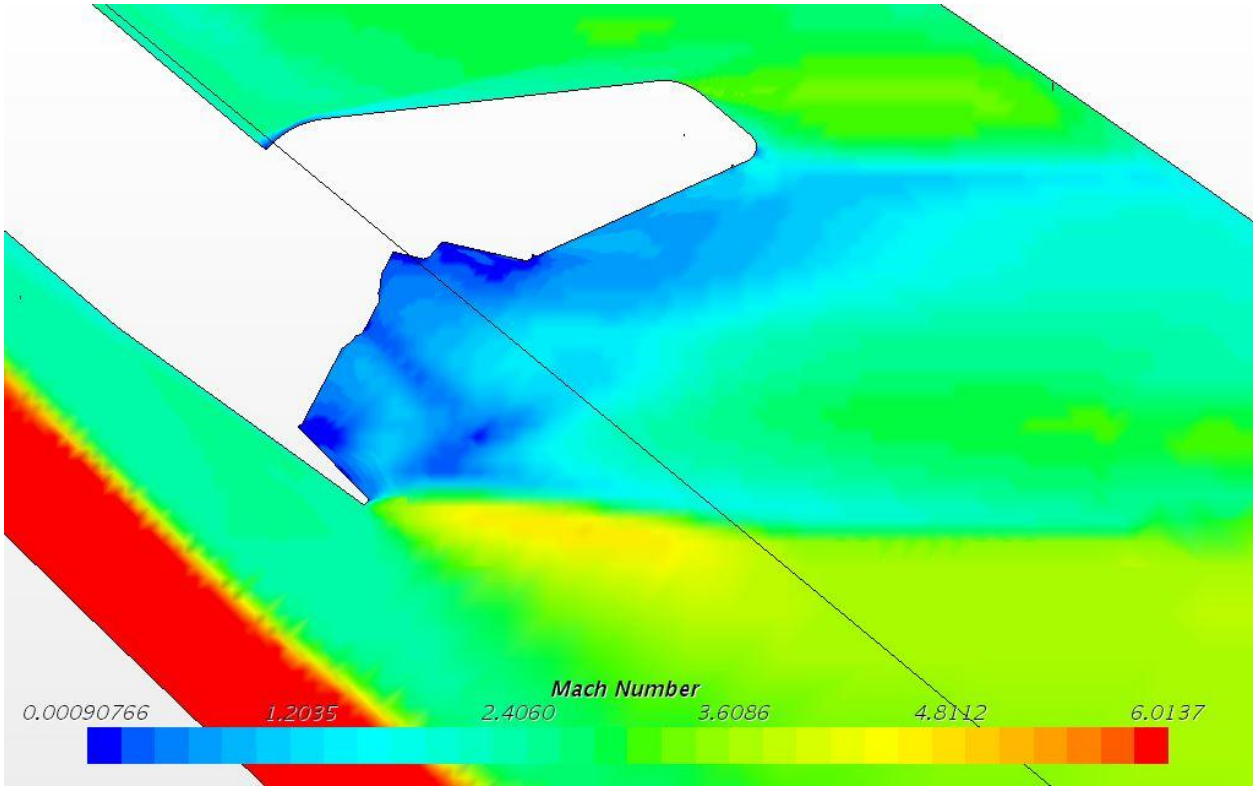

Figure 117 - One million cells 100% scale SSO tail Mach Number

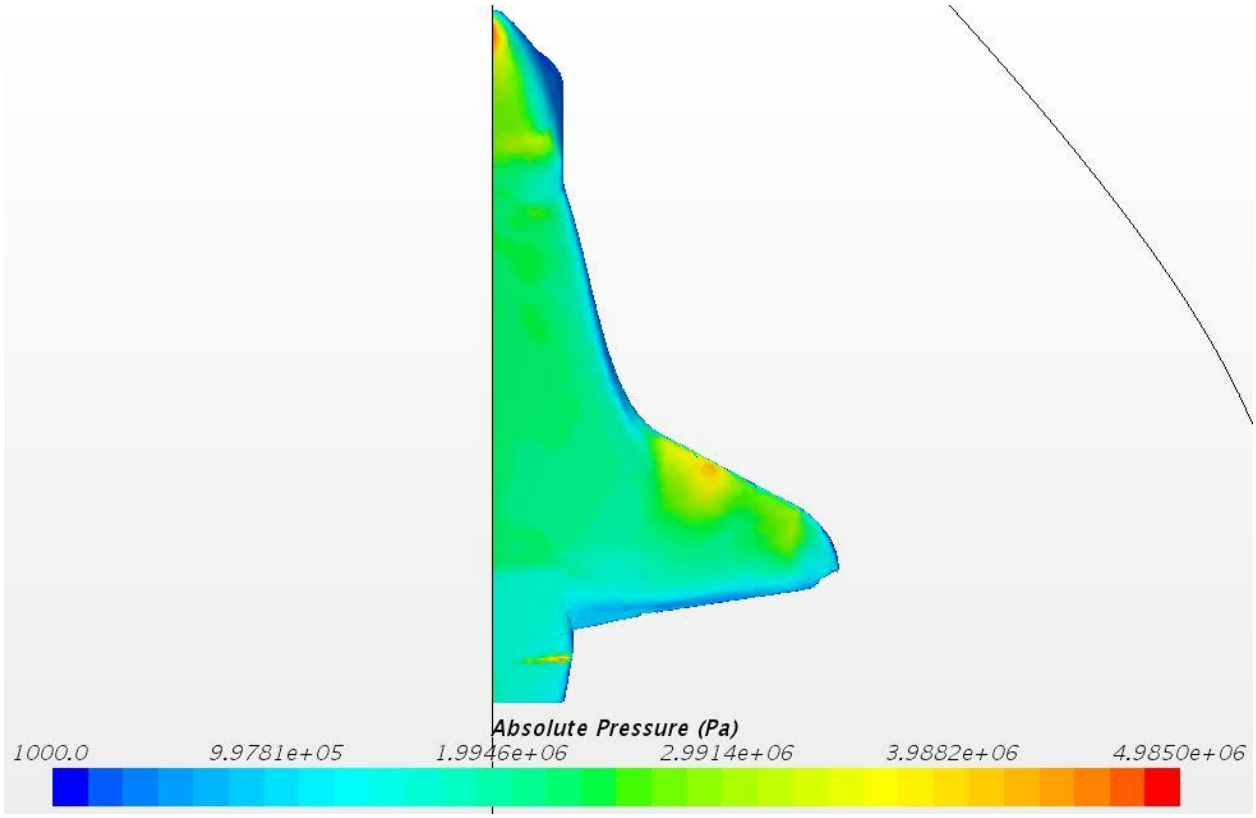

Figure 118 - One million cells 100% scale SSO bottom Absolute Pressure

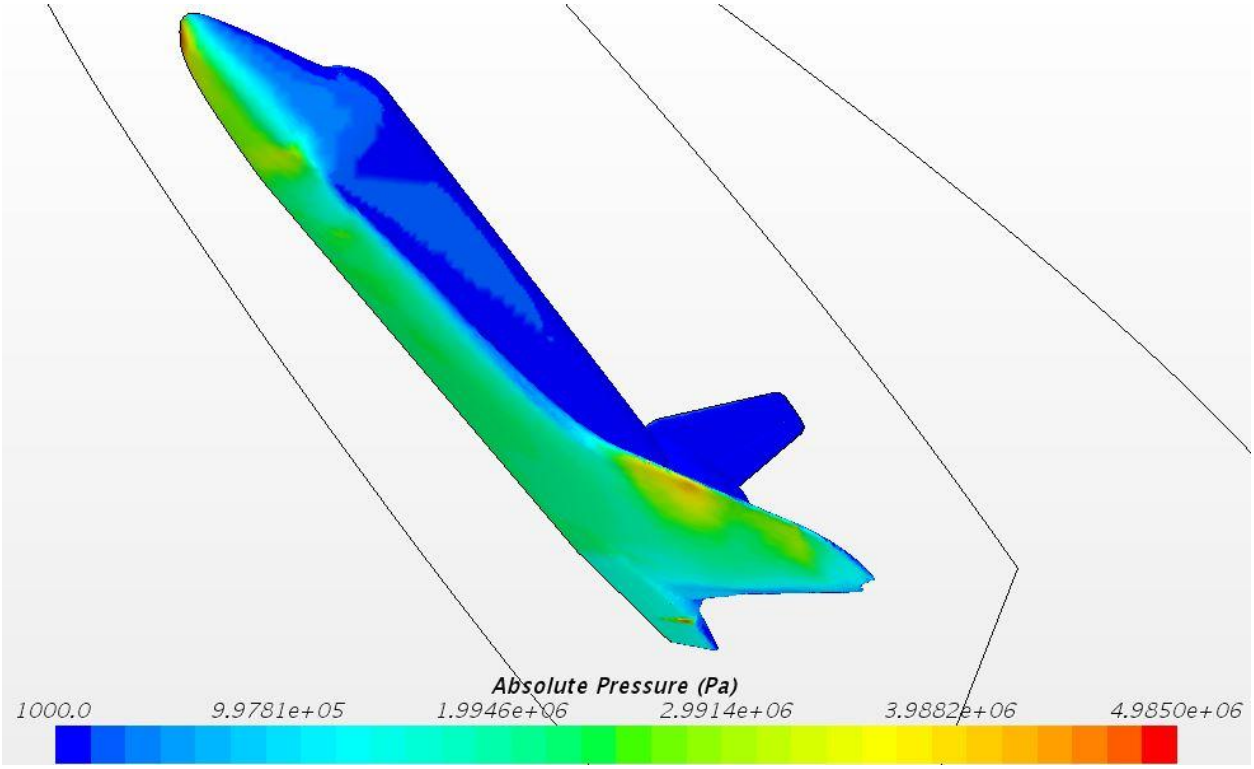

Figure 119 - One million cells 100% scale SSO 3-D Absolute Pressure

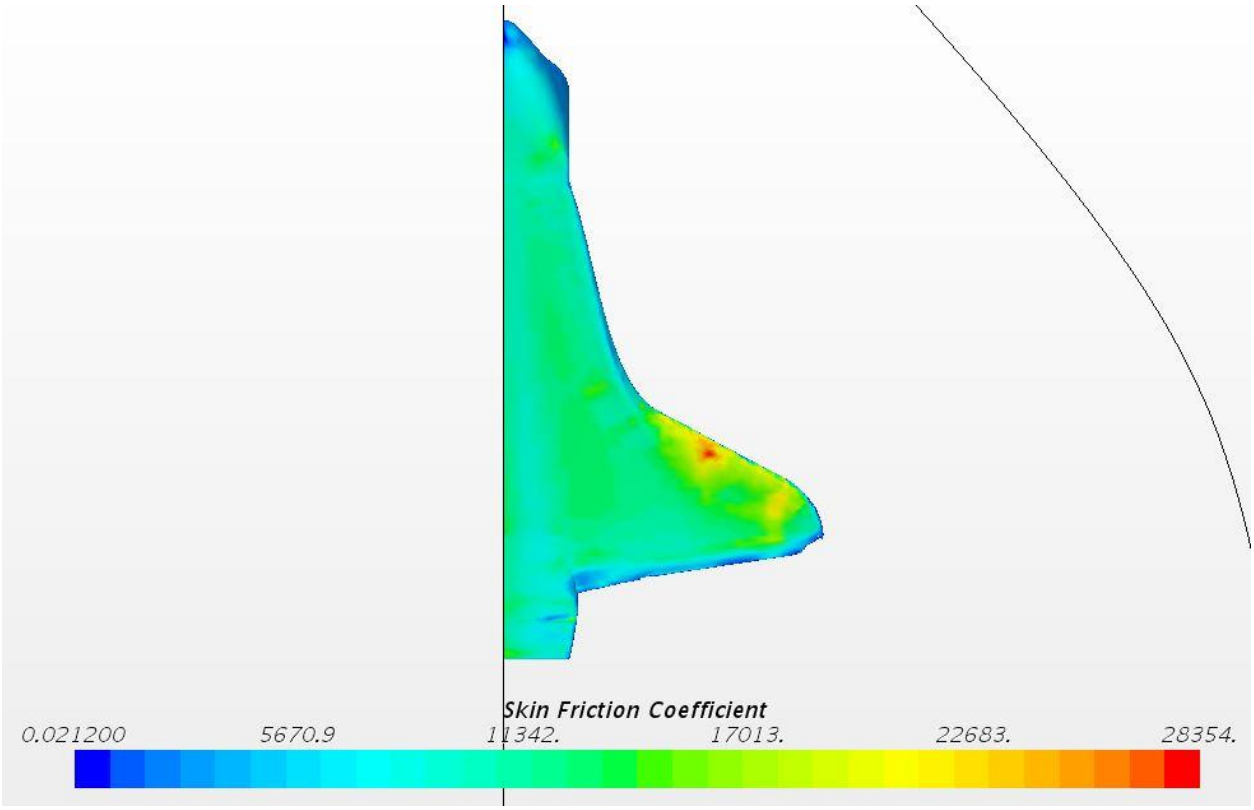

Figure 120 - One million cells 100% scale SSO Bottom Skin Friction Coefficient

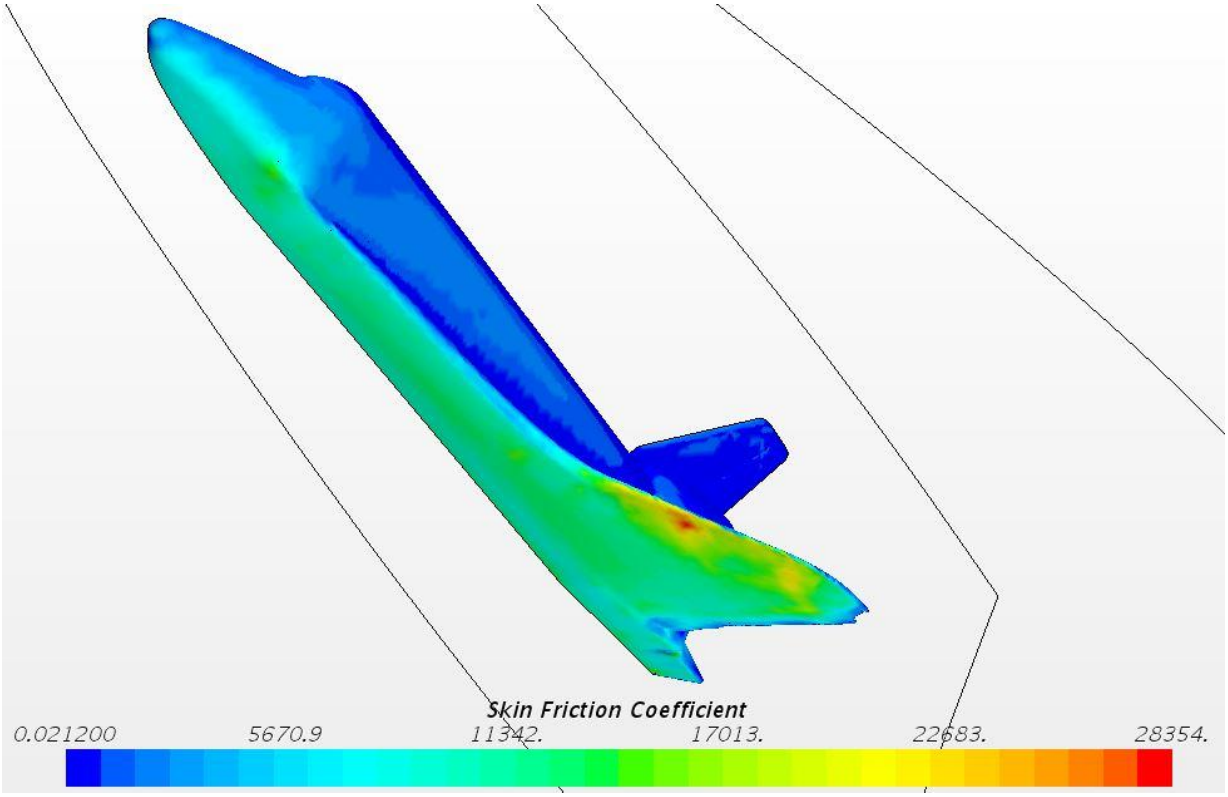

Figure 121- One million cells 100% Scale SSO 3-D Skin Friction Coefficient

7.4.2 50% SSO at 1 Million Cells

A 50% scale model of the SSO is tested at 1063909 Cells. Figure 125 displays the mesh generated with Figure 126 and Figure 127 providing focus on the mesh near the nose and tail of the vehicle. The CFD simulation ran for a total of 6,800 iterations and seemed to converge towards a stable solution as seen in Figure 122. The Base cell size for the mesh was designated at 1.2 meters. The cone area behind the tail as well as the refinement area around the vehicle body were set to 20% of the base size (0.24m). The Far-field area outside of the refinement area was set to 300% of the base size (3.6m). The mesh was generated with 30 prism layers stretching at a rate of 1.1 the size of the previous layer, from the surface of the vehicle. The absolute thickness of these prism layers was 40% of the base size (0.48m). The target cell size on the surface of the vehicle was 10% of base size (0.12m) and the minimum surface cell size was set to 5% of the base size (0.06m). The lift force of the vehicle was 62,208,957N, and the drag force of the vehicle was 56,116,800N. Using these values for lift force and drag force and equation 3.6, the lift-to-drag ratio can be calculated to be 1.109.

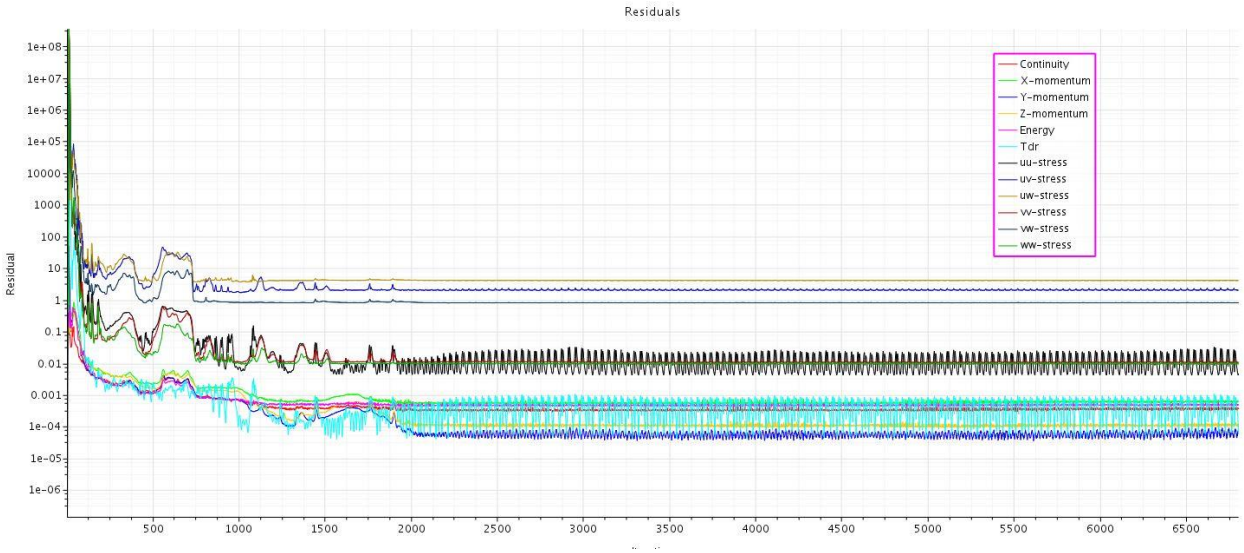

Figure 122 - One million cells 50% scale SSO Residual Plot

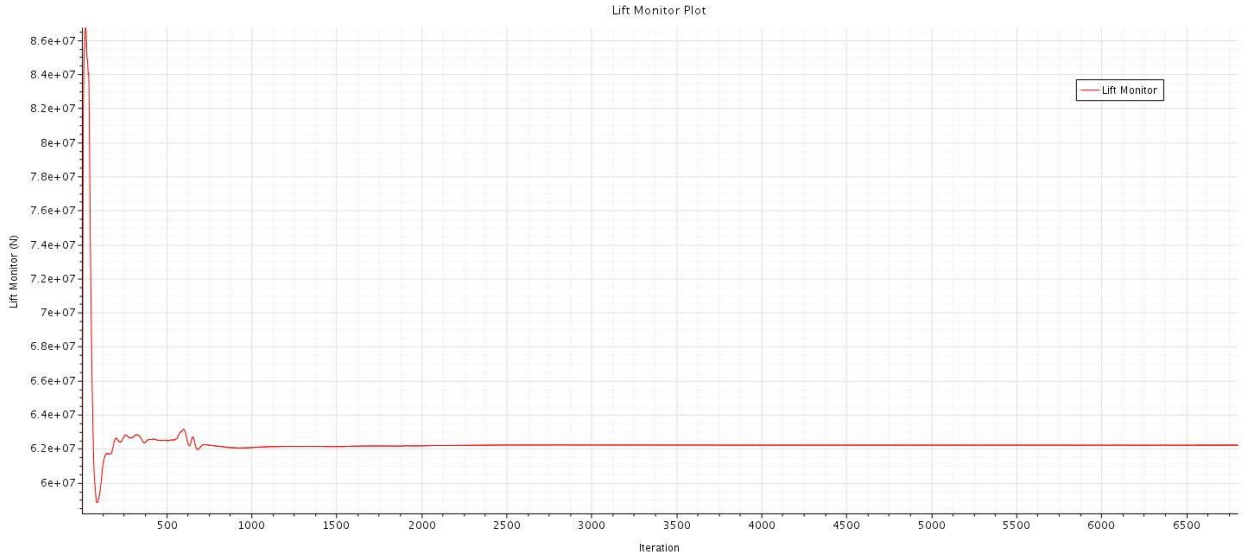

Figure 123 - One million cells 50% scale SSO Lift Plot

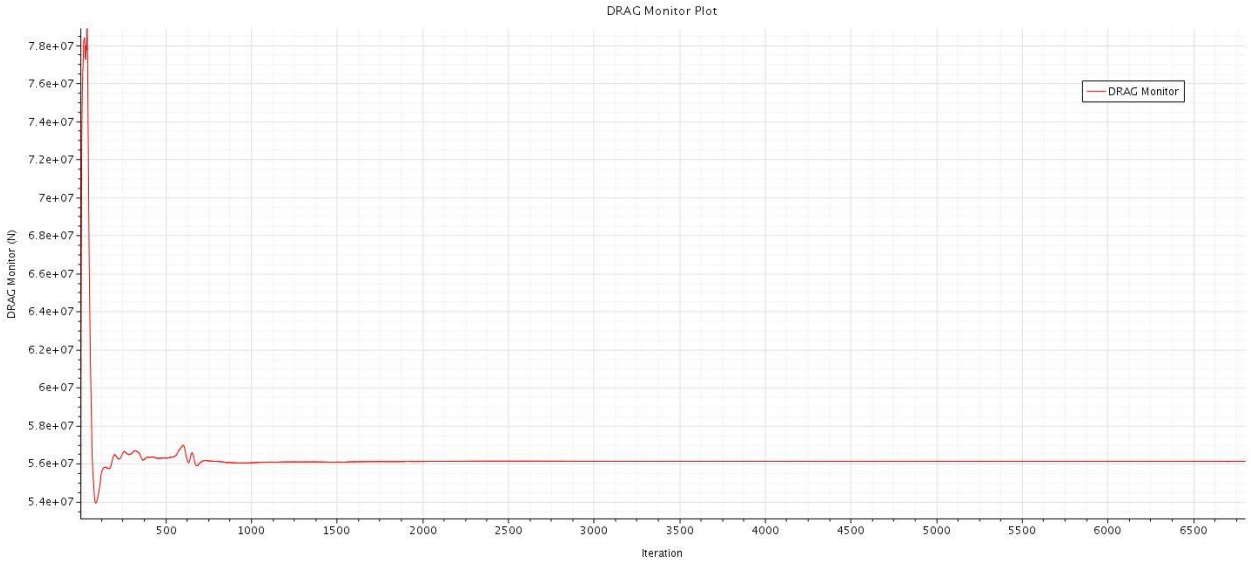

Figure 124 - One million cells 50% scale SSO Drag Plot

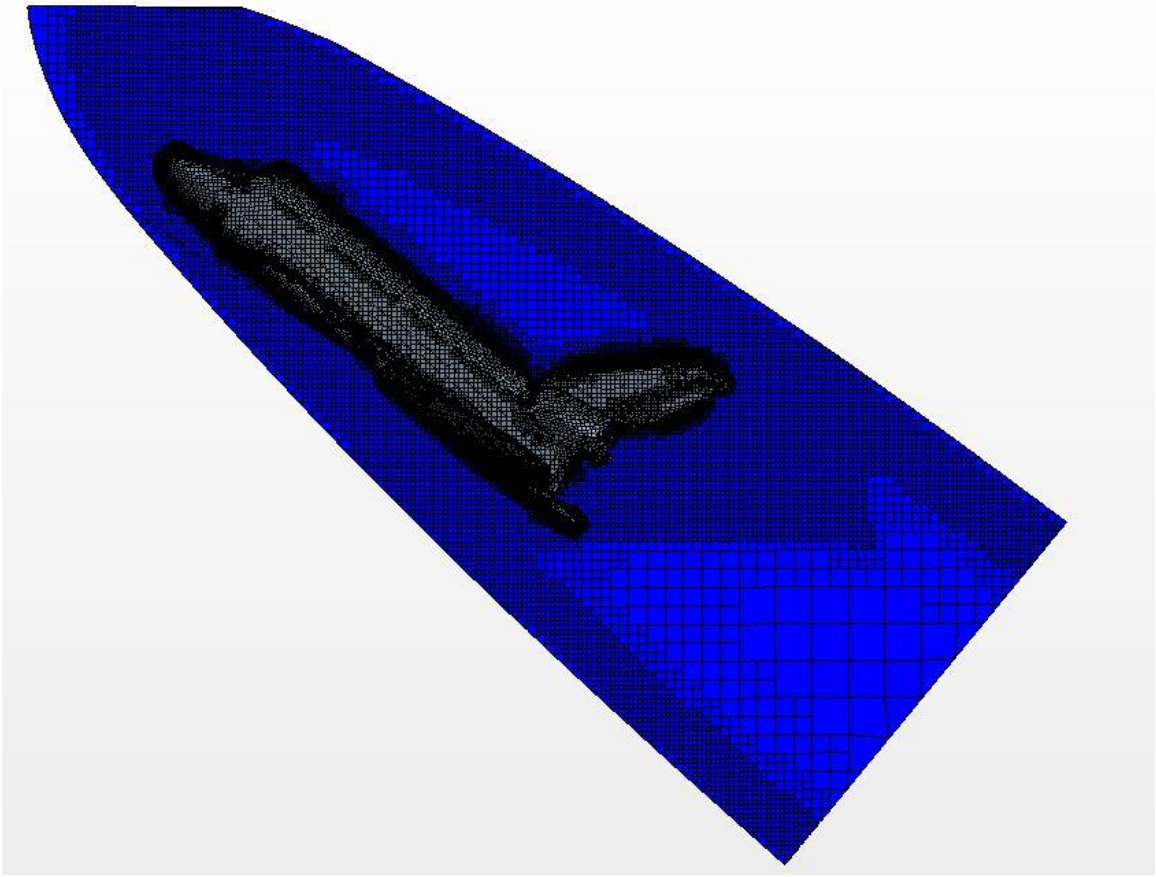

Figure 125 - One million cells 50% scale SSO full body Mesh

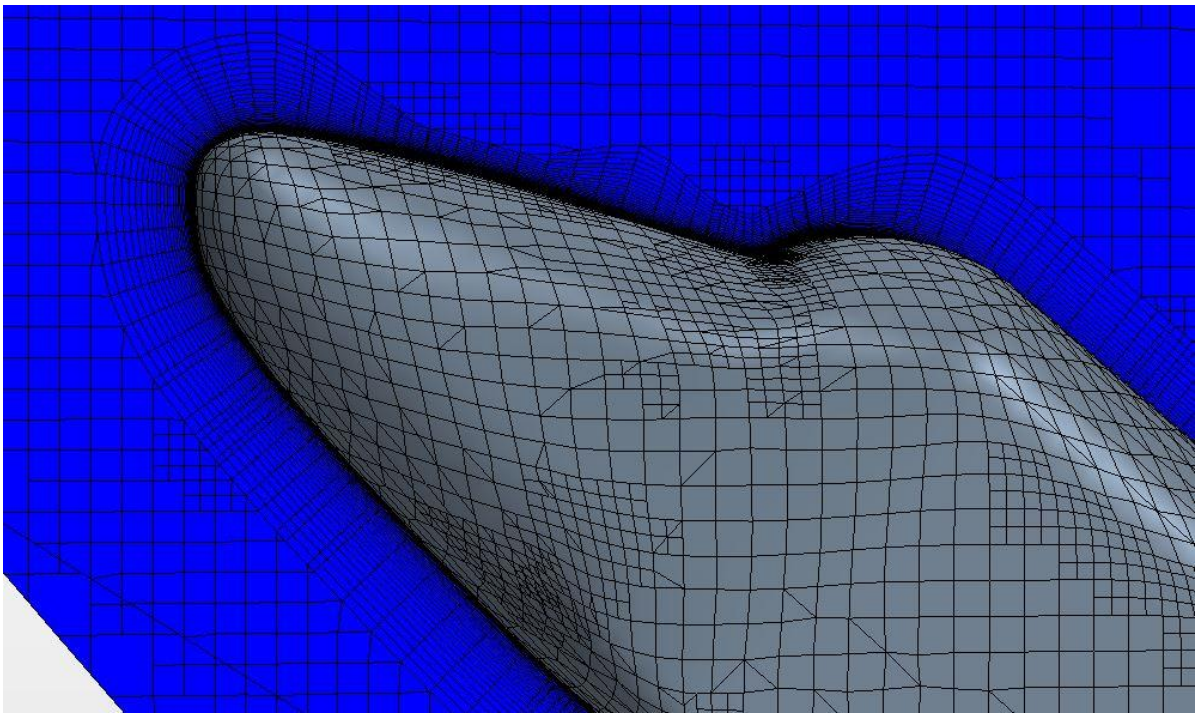

Figure 126 - One million cells 50% scale SSO nose Mesh

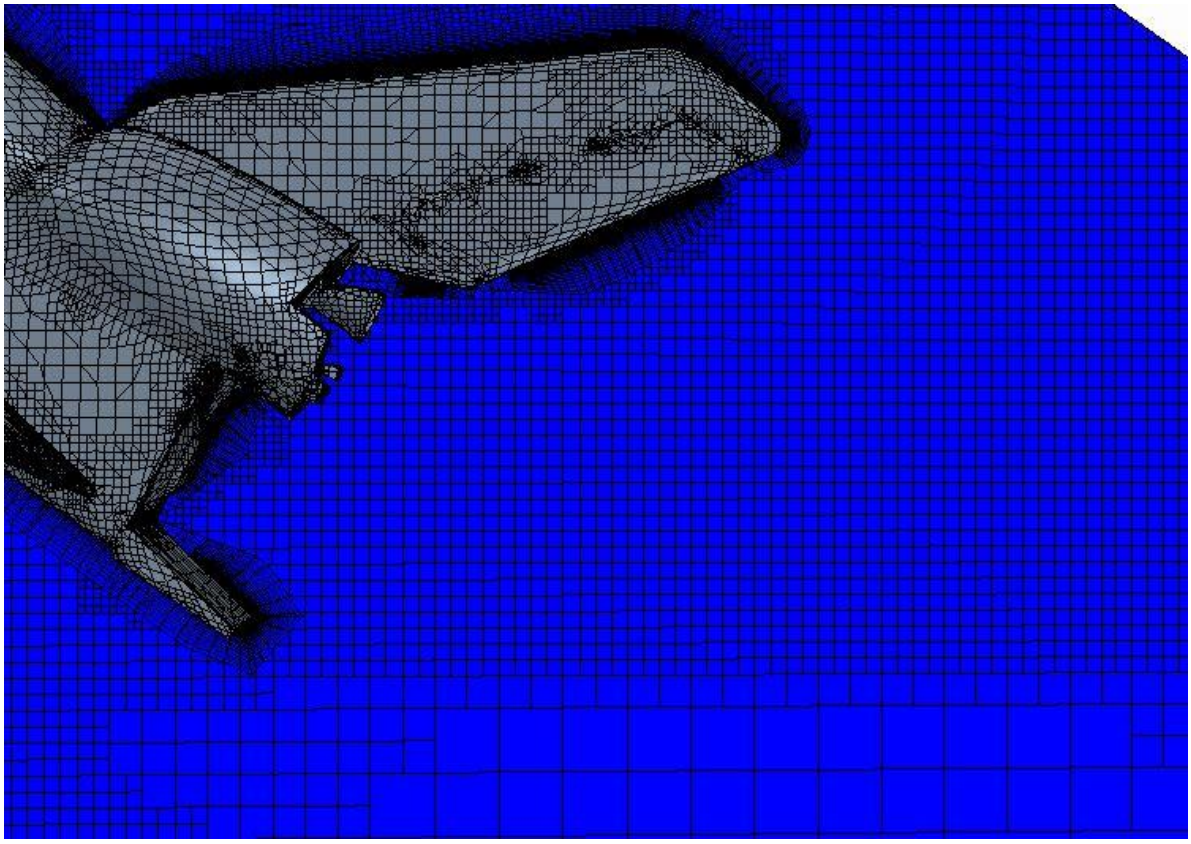

Figure 127 - One million cells 50% scale SSO tail Mesh

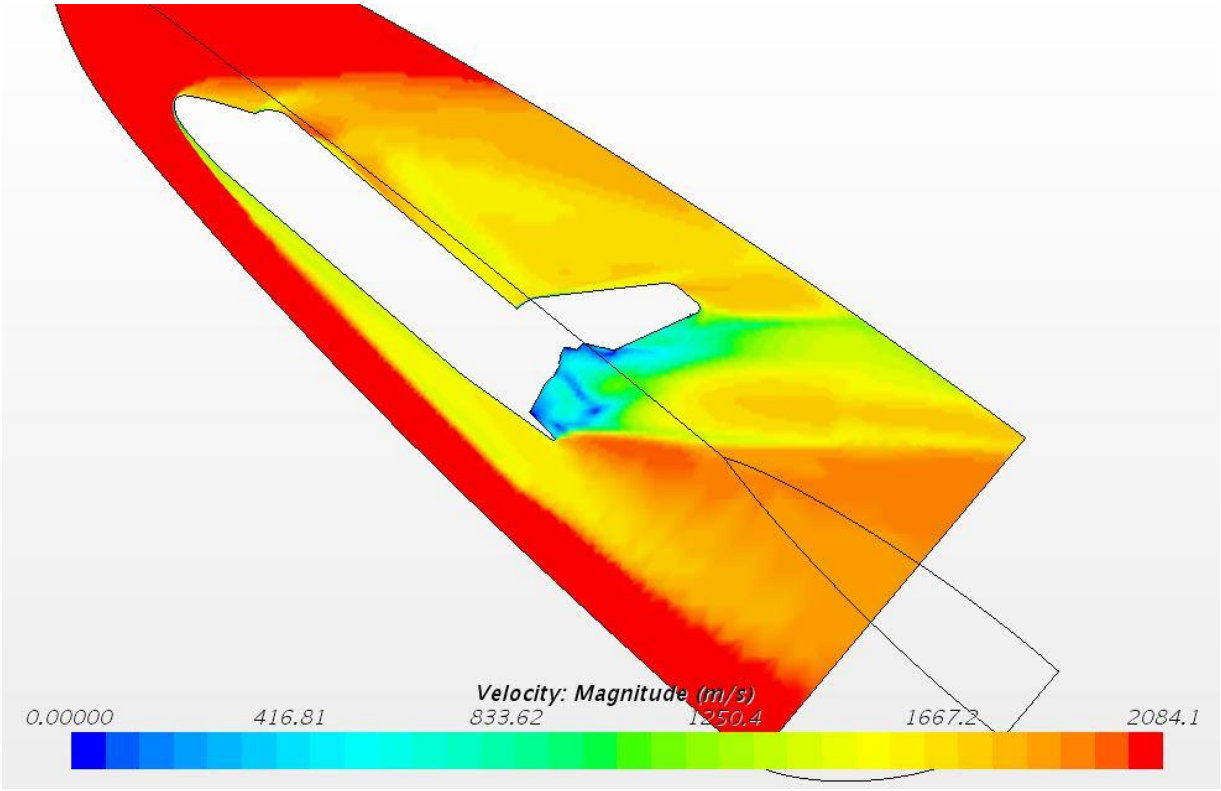

Figure 128 -One million cells 50% scale SSO full body Velocity

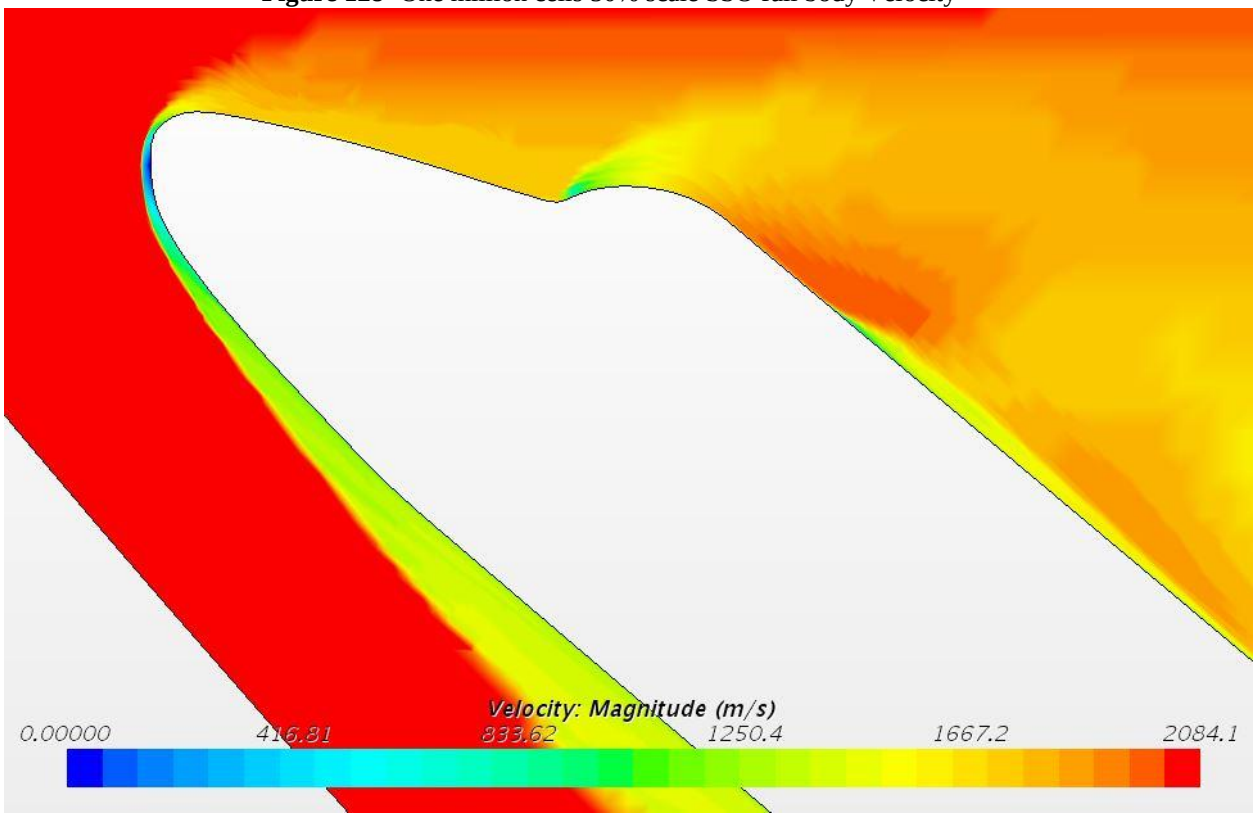

Figure 129 - One million cells 50% scale SSO nose Velocity

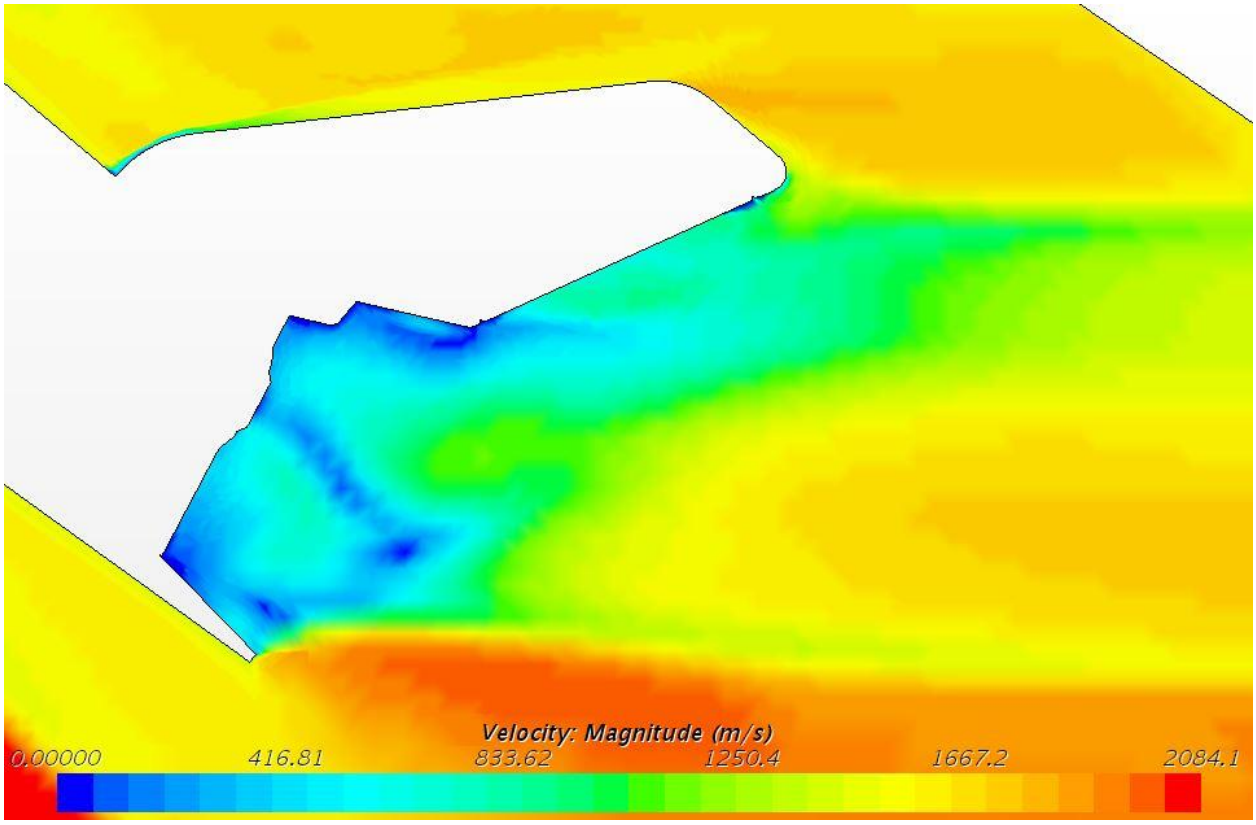

Figure 130 - One million cells 50% scale SSO tail Velocity

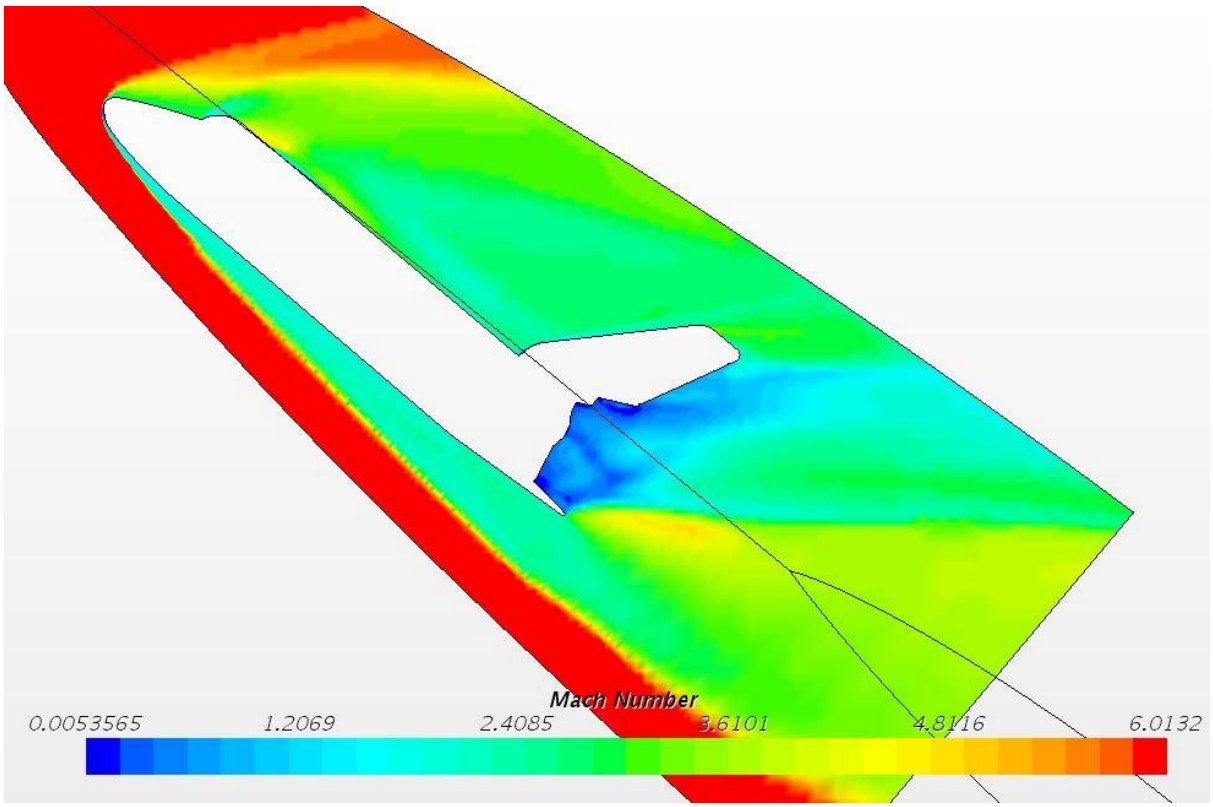

Figure 131 - One million cells 50% scale SSO full body Mach Number

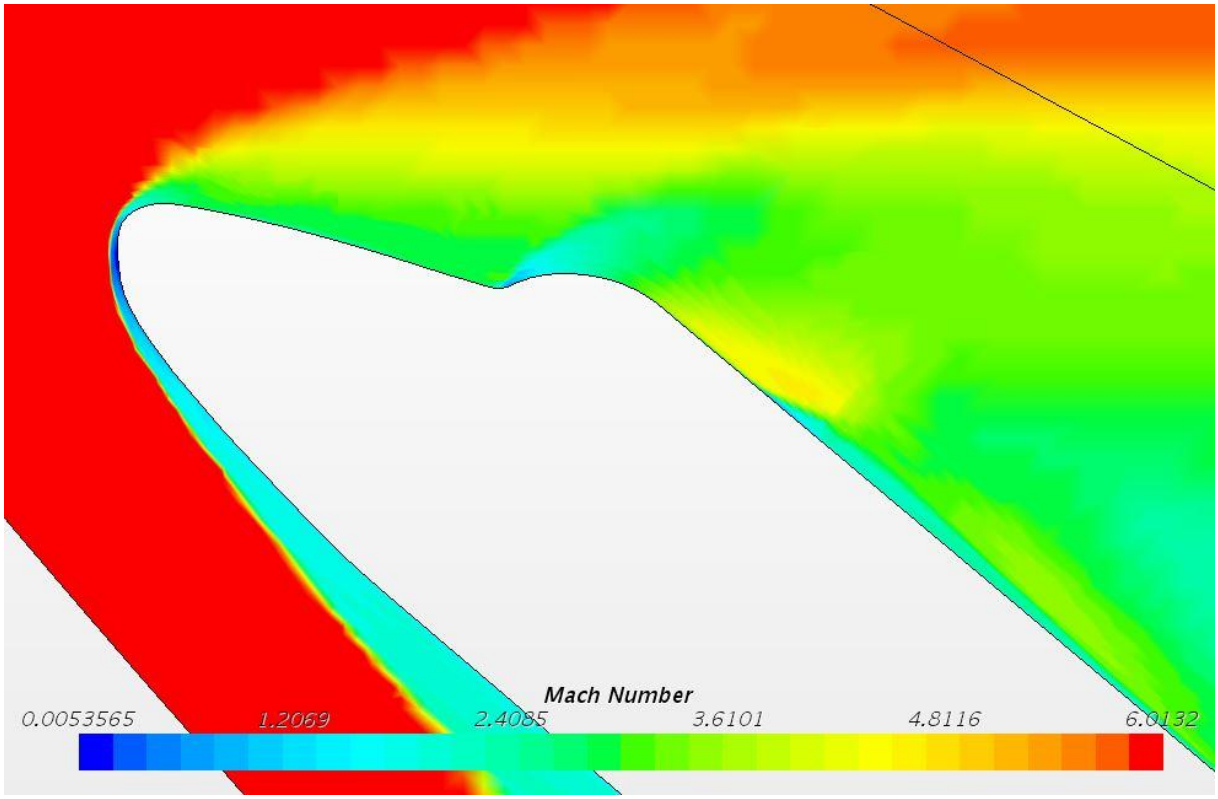

Figure 132 - One million cells 50% scale SSO nose Mach Number

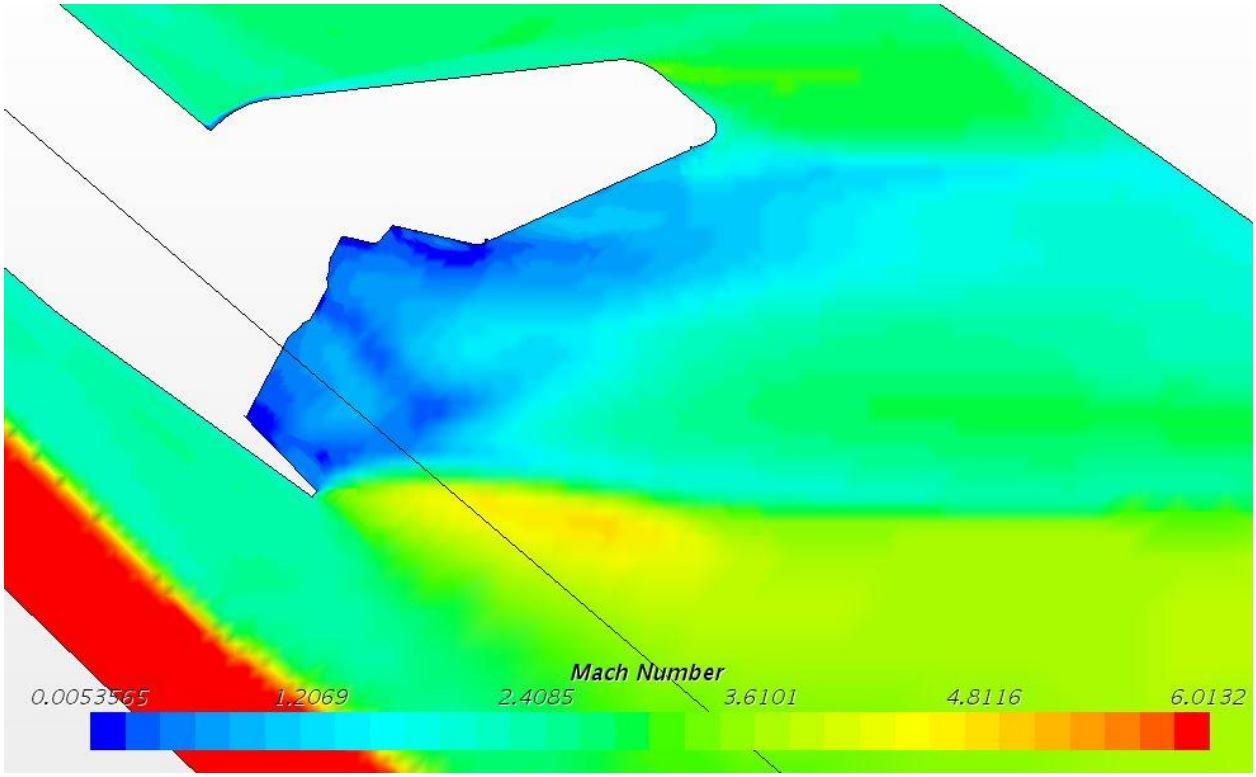

Figure 133 - One million cells 50% scale SSO tail Mach Number

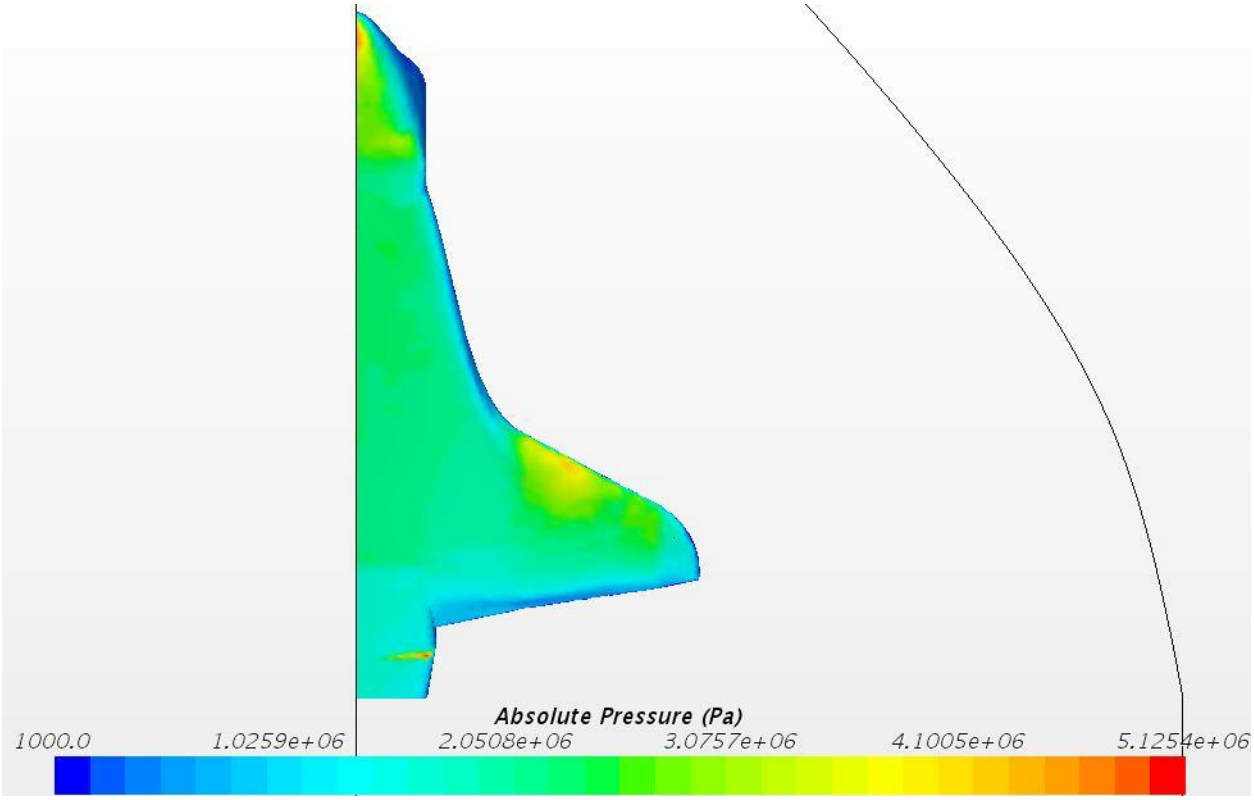

Figure 134 - One million cells 50% scale SSO bottom Absolute Pressure

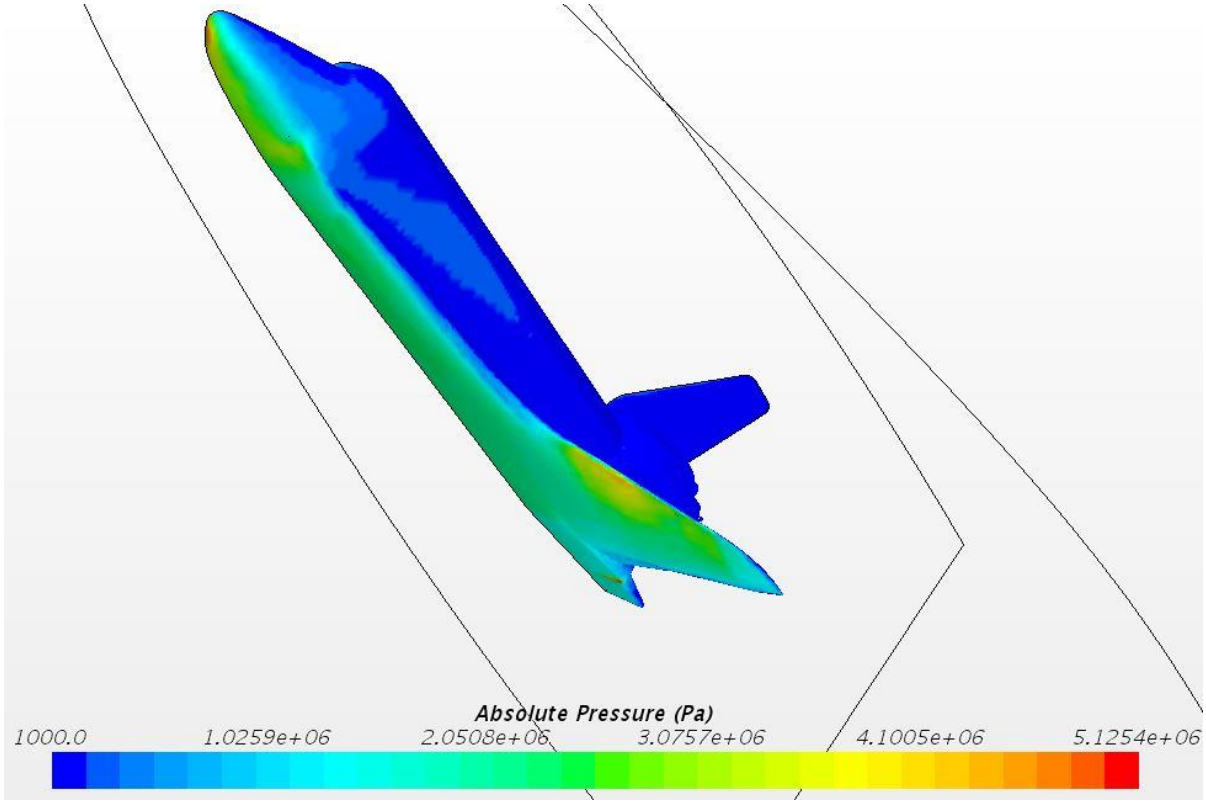

Figure 135 - One million cells 50% scale SSO 3-D Absolute Pressure

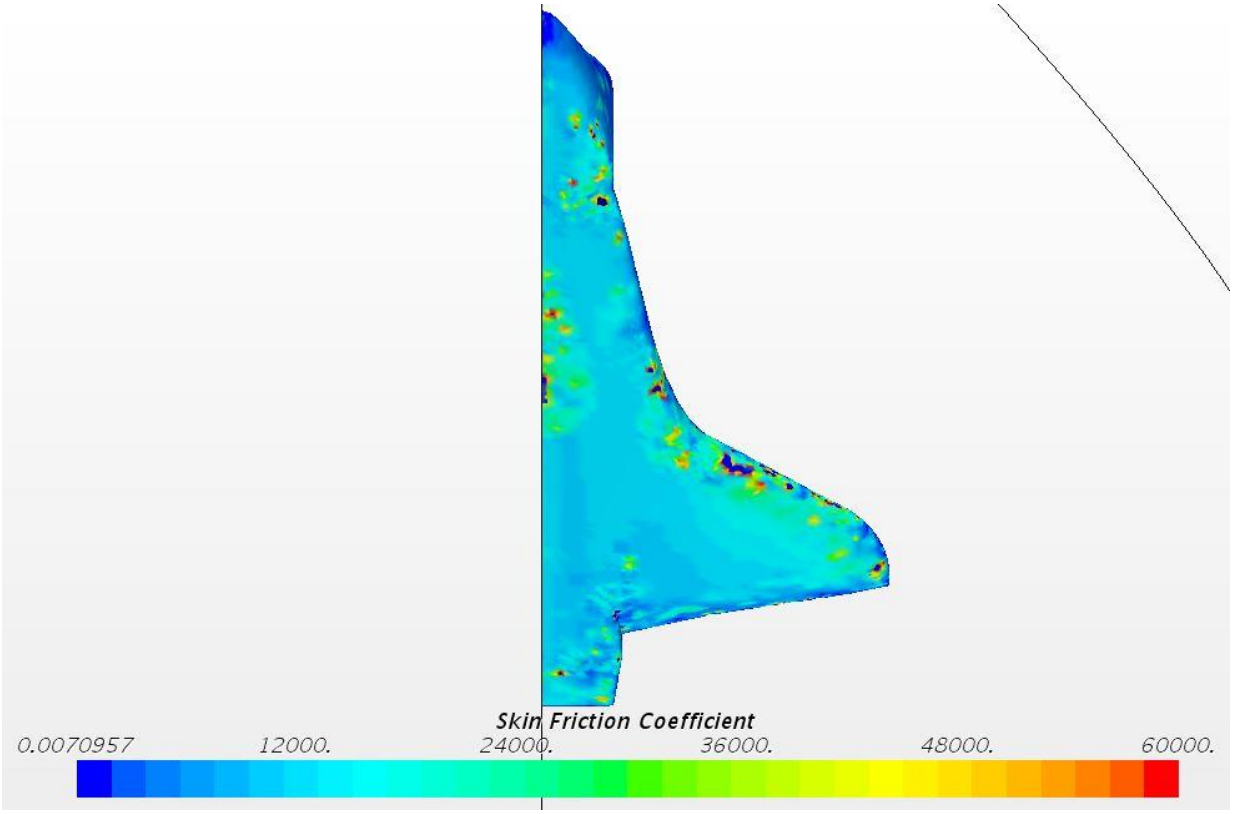

Figure 136 - One million cells 50% scale SSO bottom Skin Friction Coefficient

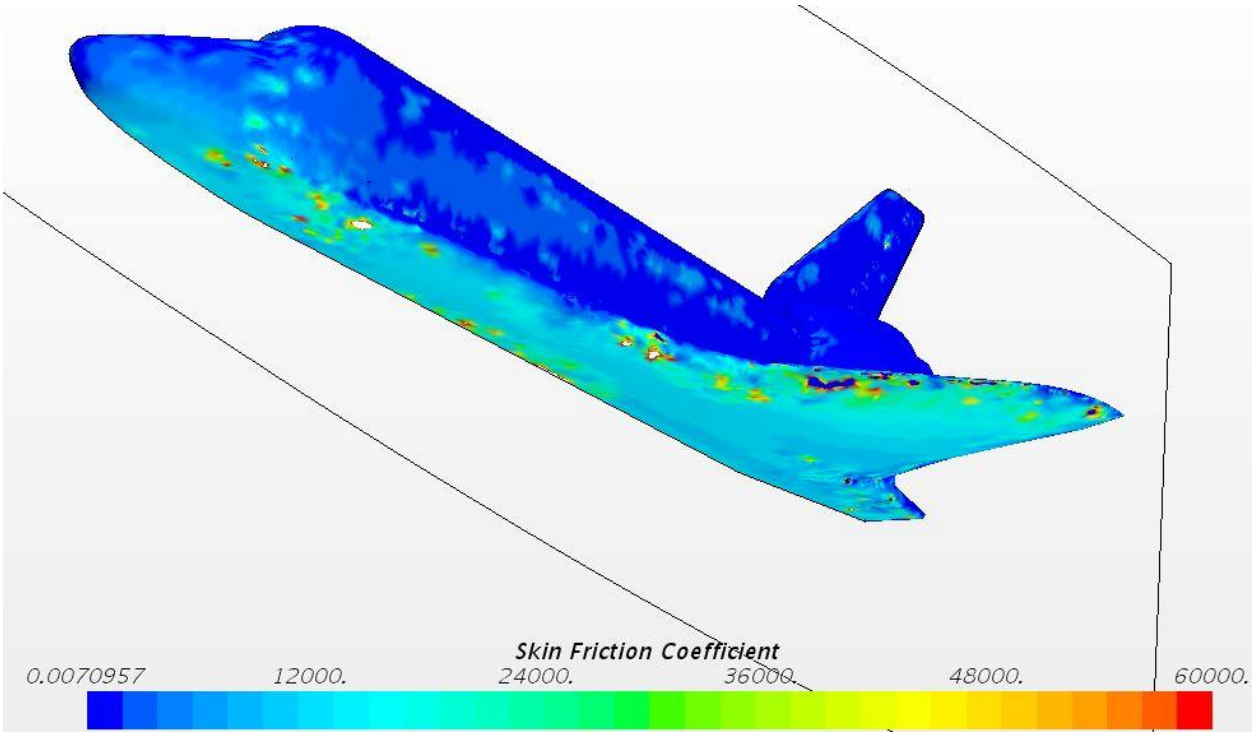

Figure 137 - One million cells 50% scale SSO 3-D Skin Friction Coefficient

7.4.3 25% SSO at 1 Million Cells

A 25% scale model of the SSO is tested at 1032032Cells. Figure 141 displays the mesh generated with Figure 142 and Figure 143 providing focus on the mesh near the nose and tail of the vehicle. The CFD simulation ran for a total of 6,800 iterations and seemed to converge towards a stable solution as seen in Figure 138. The Base cell size for the mesh was designated at 0.7 meters. The cone area behind the tail as well as the refinement area around the vehicle body were set to 10% of the base size (0.07m). The Far-field area outside of the refinement area was set to 300% of the base size (2.1m). The mesh was generated with 30 prism layers stretching at a rate of 1.1 the size of the previous layer, from the surface of the vehicle. The absolute thickness of these prism layers was 40% of the base size (0.28m). The target cell size on the surface of the vehicle was 10% of base size (0.07m) and the minimum surface cell size was set to 5% of the base size (0.035m). The lift force of the vehicle was 15,545,890N, and the drag force of the vehicle was 14,044,350N. Using these values for lift force and drag force and equation 3.6, the lift-to-drag ratio can be calculated to be 1.107.

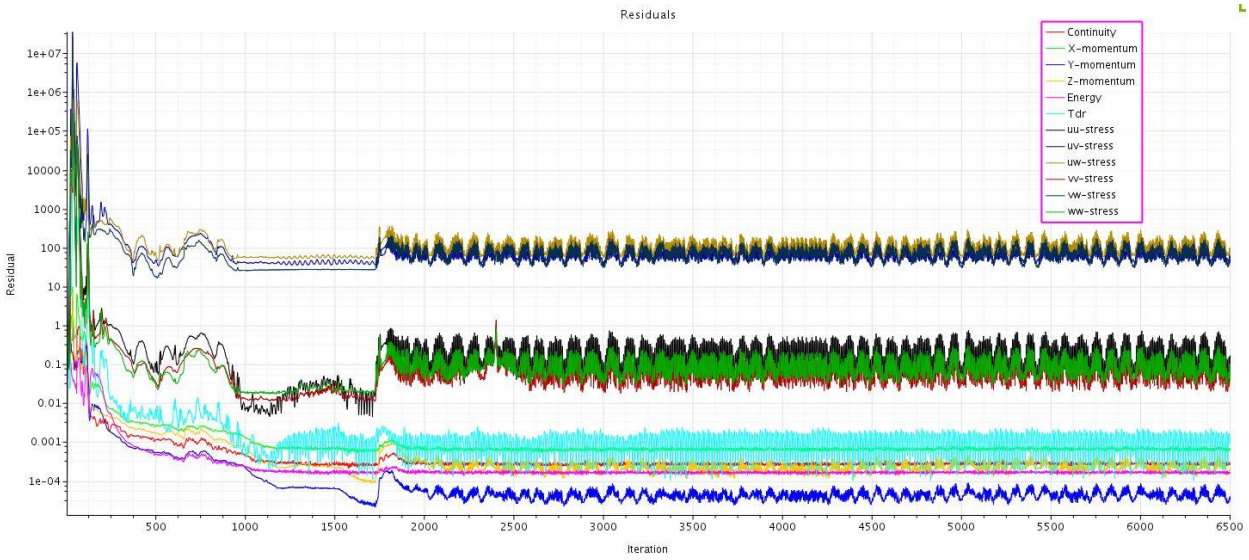

Figure 138 - One million cells 25% scale SSO Residual Plot

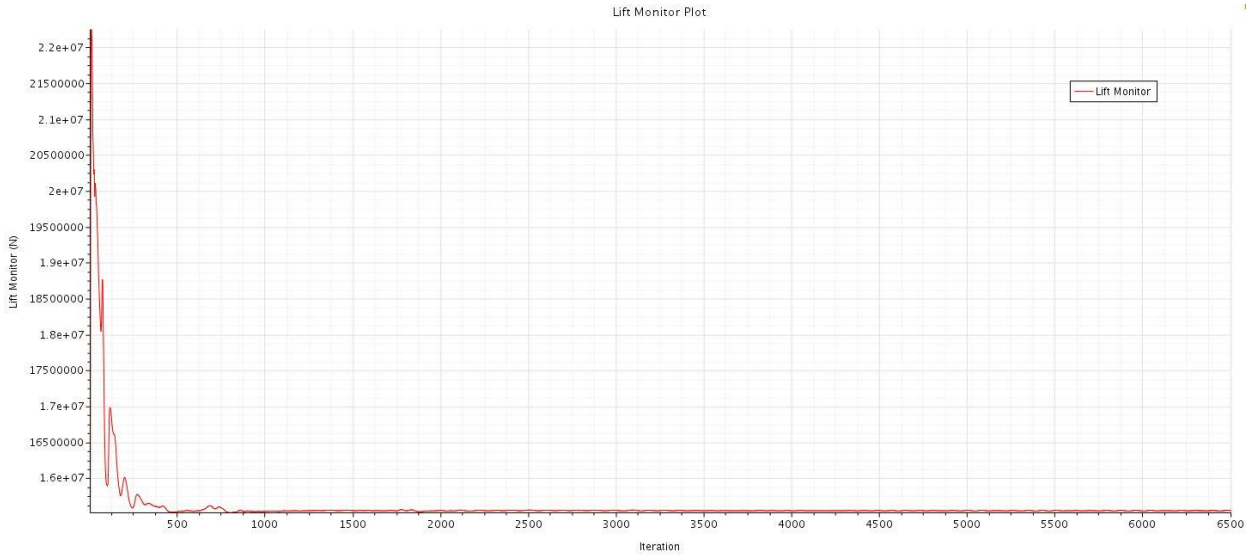

Figure 139 - One million cells 25% scale SSO Lift Plot

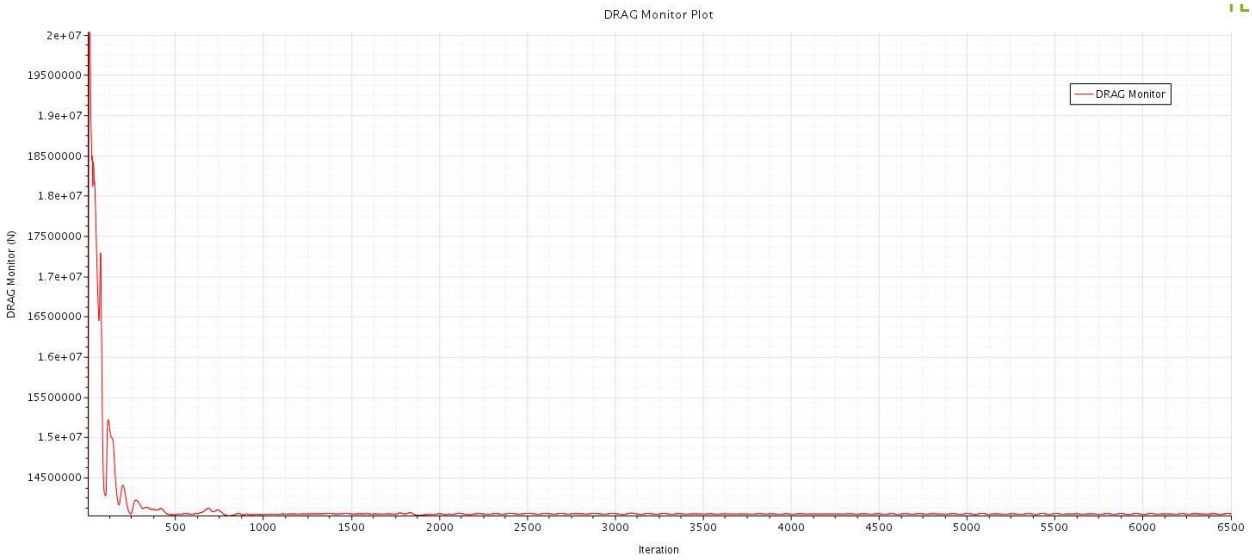

Figure 140 - One million cells 25% scale SSO Drag Plot

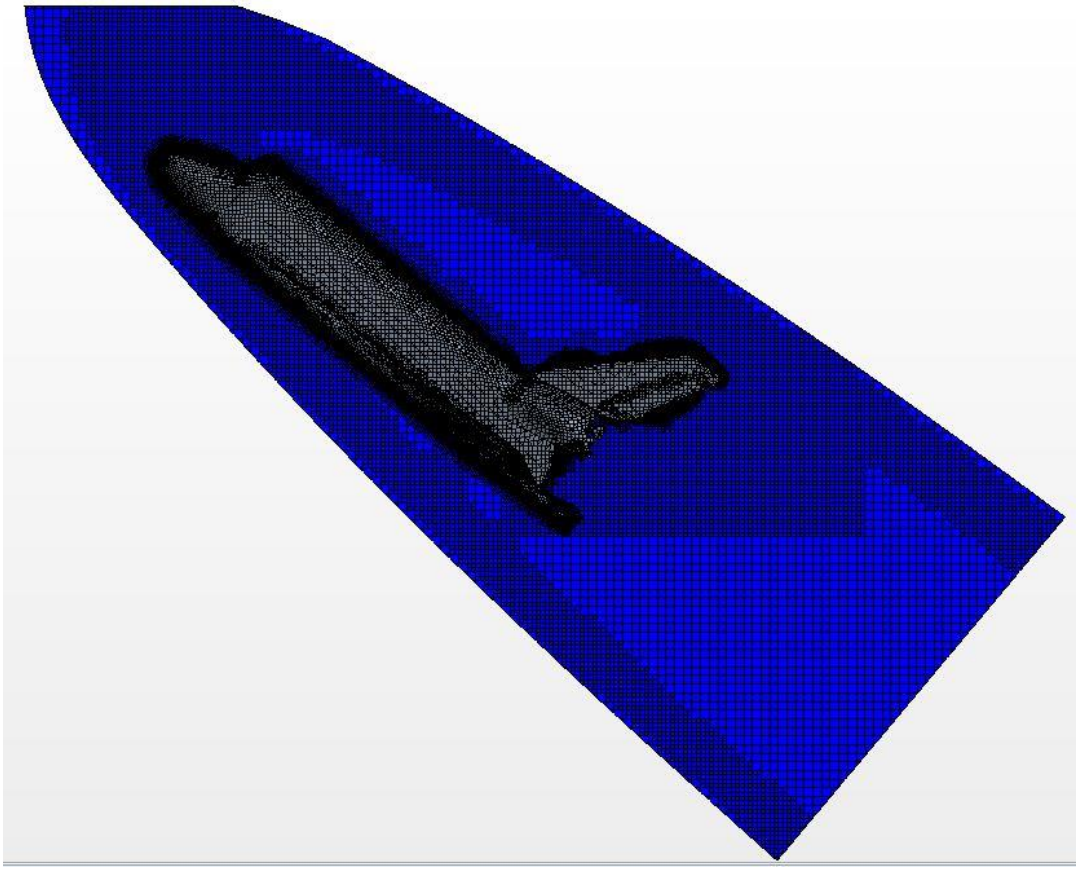

Figure 141 - One million cells 25% scale SSO full body Mesh

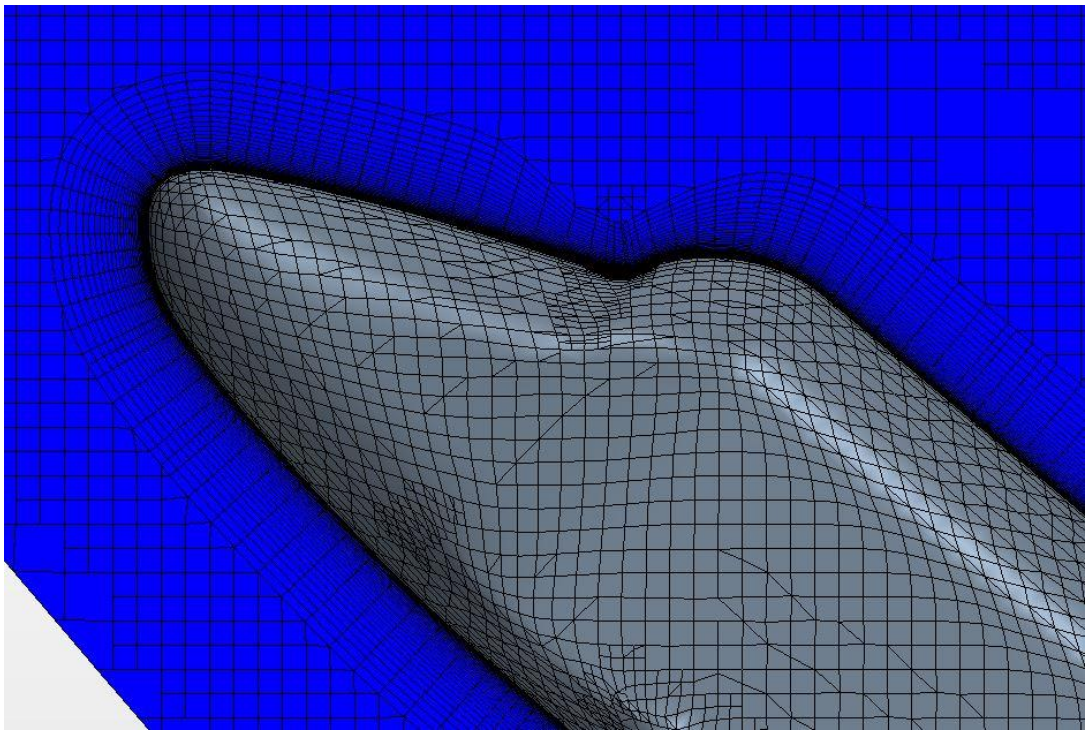

Figure 142 - One million cells 25% scale SSO nose Mesh

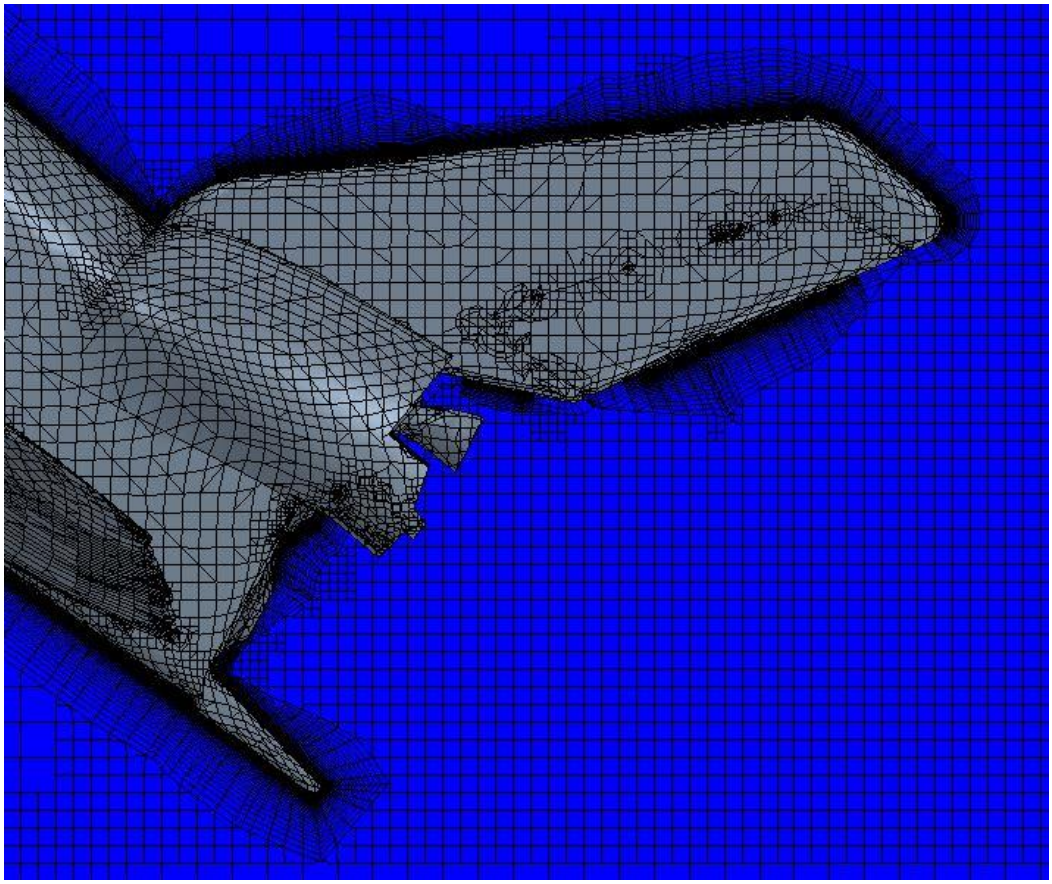

Figure 143 - One million cells 25% scale SSO tail Mesh

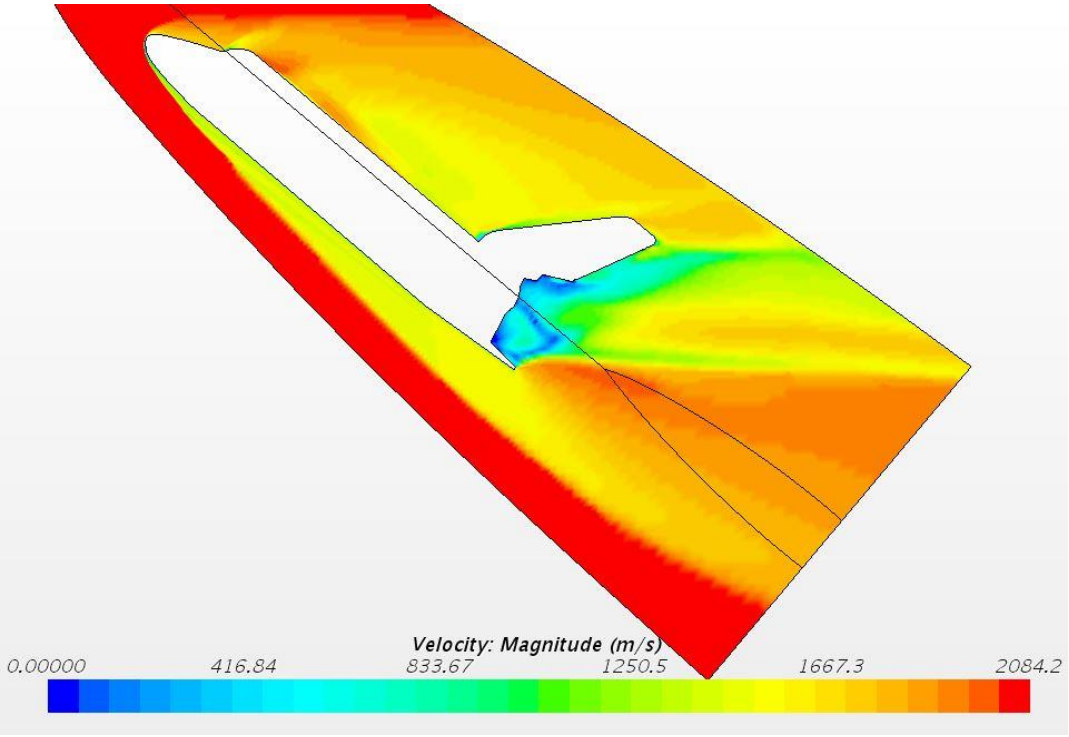

Figure 144 - One million cells 25% scale SSO full body Velocity

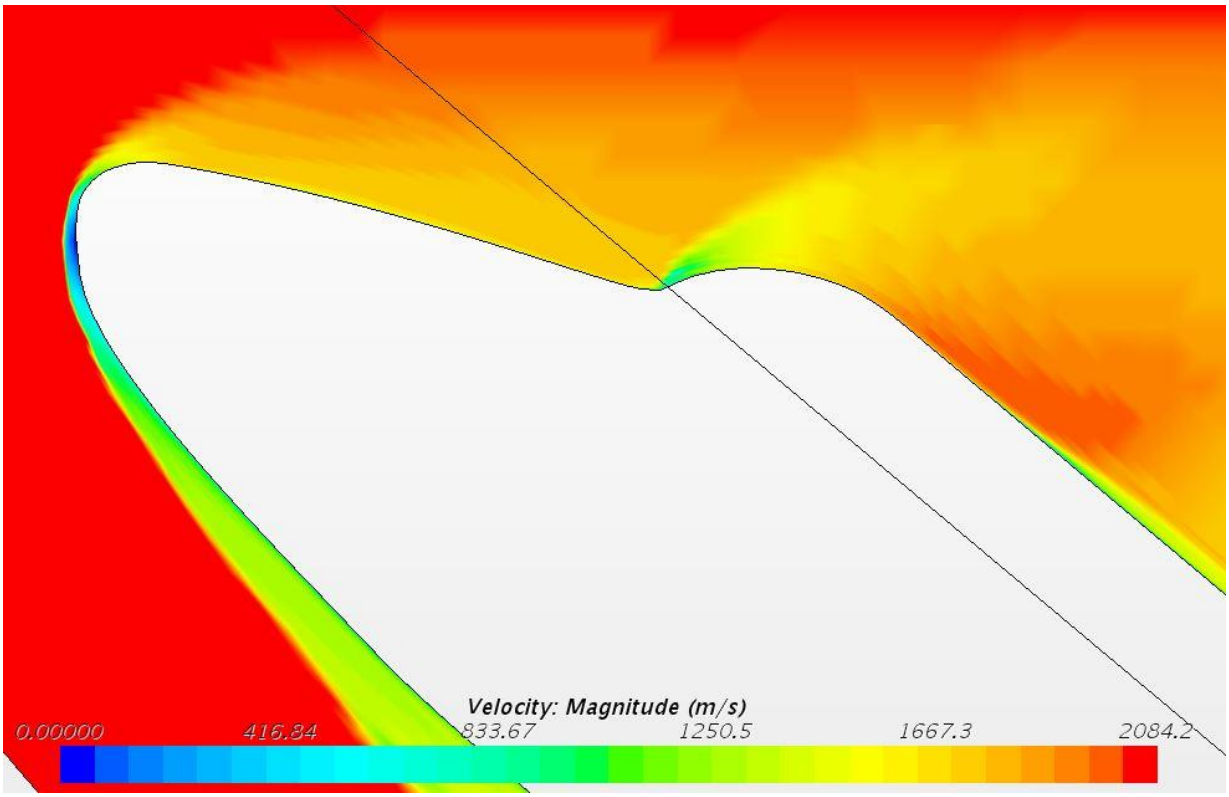

Figure 145 - One million cells 25% scale SSO nose Velocity

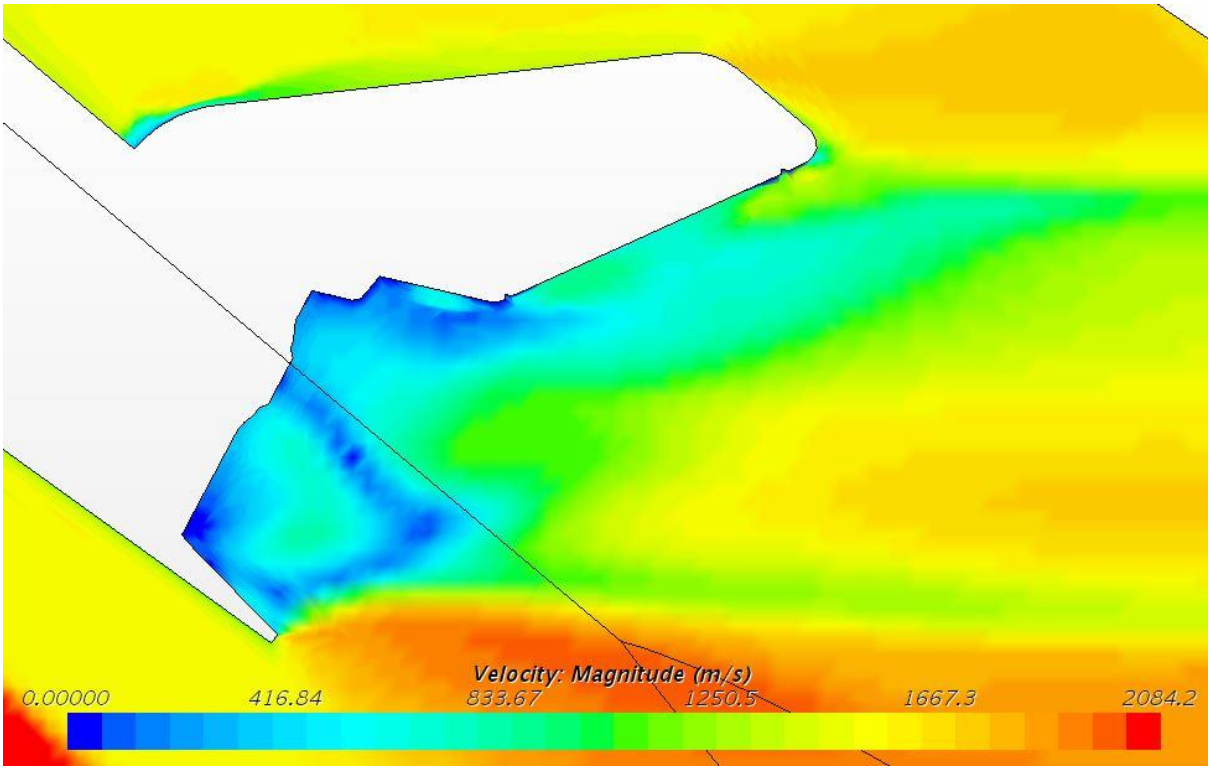

Figure 146 - One million cells 25% scale SSO tail Velocity

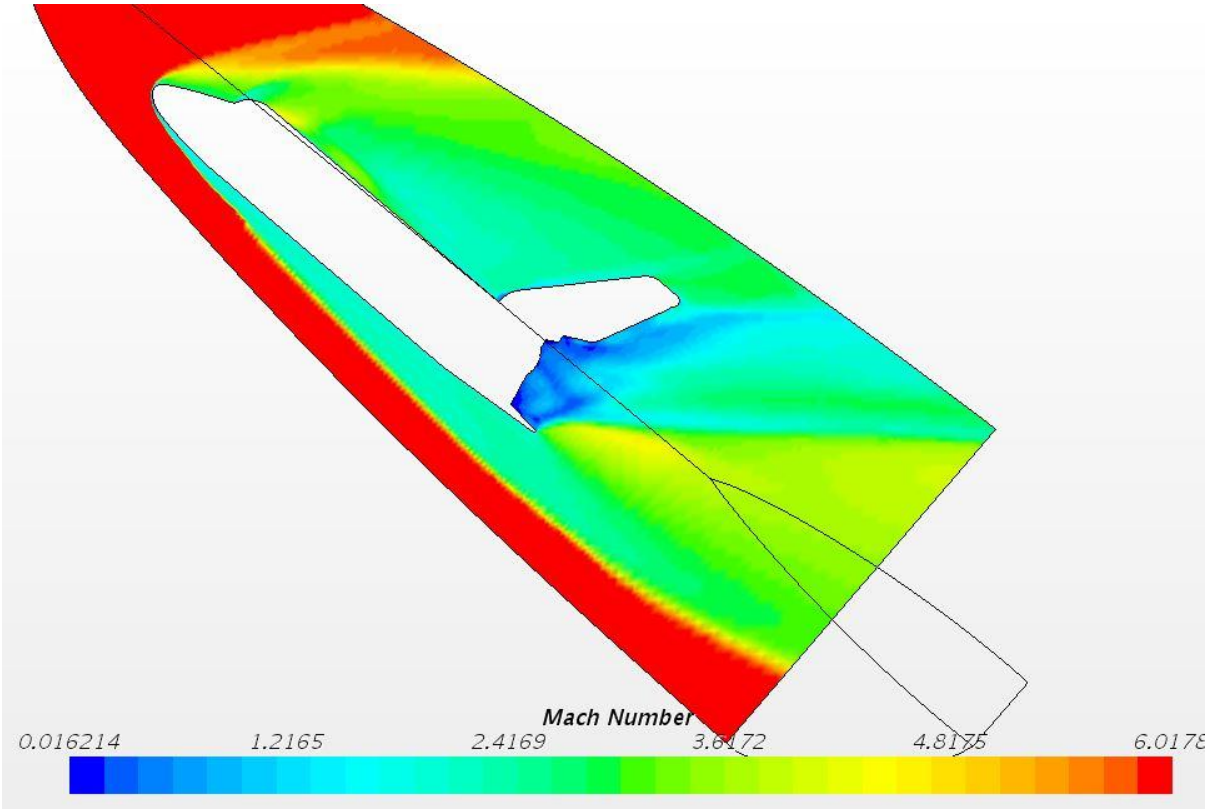

Figure 147 - One million cells 25% scale SSO full body Mach Number

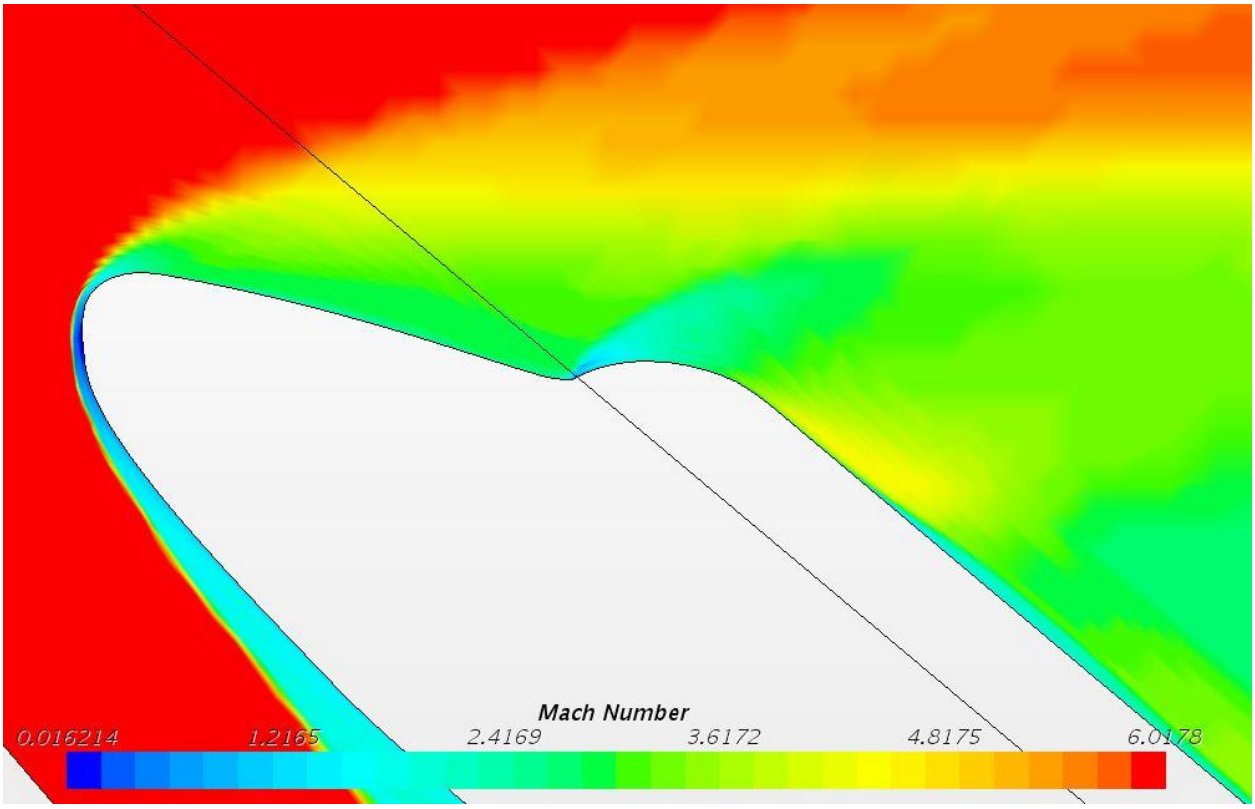

Figure 148 - One million cells 25% scale SSO nose Mach Number

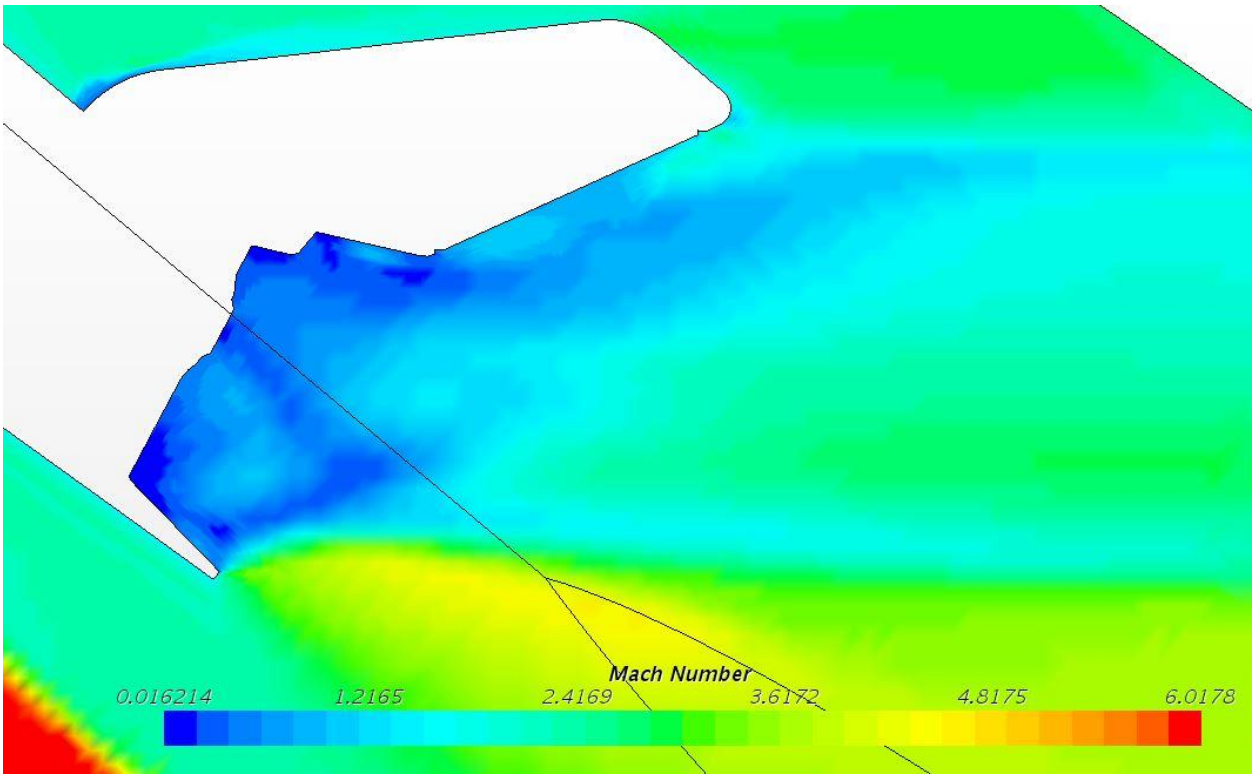

Figure 149 - One million cells 25% scale SSO tail Mach Number

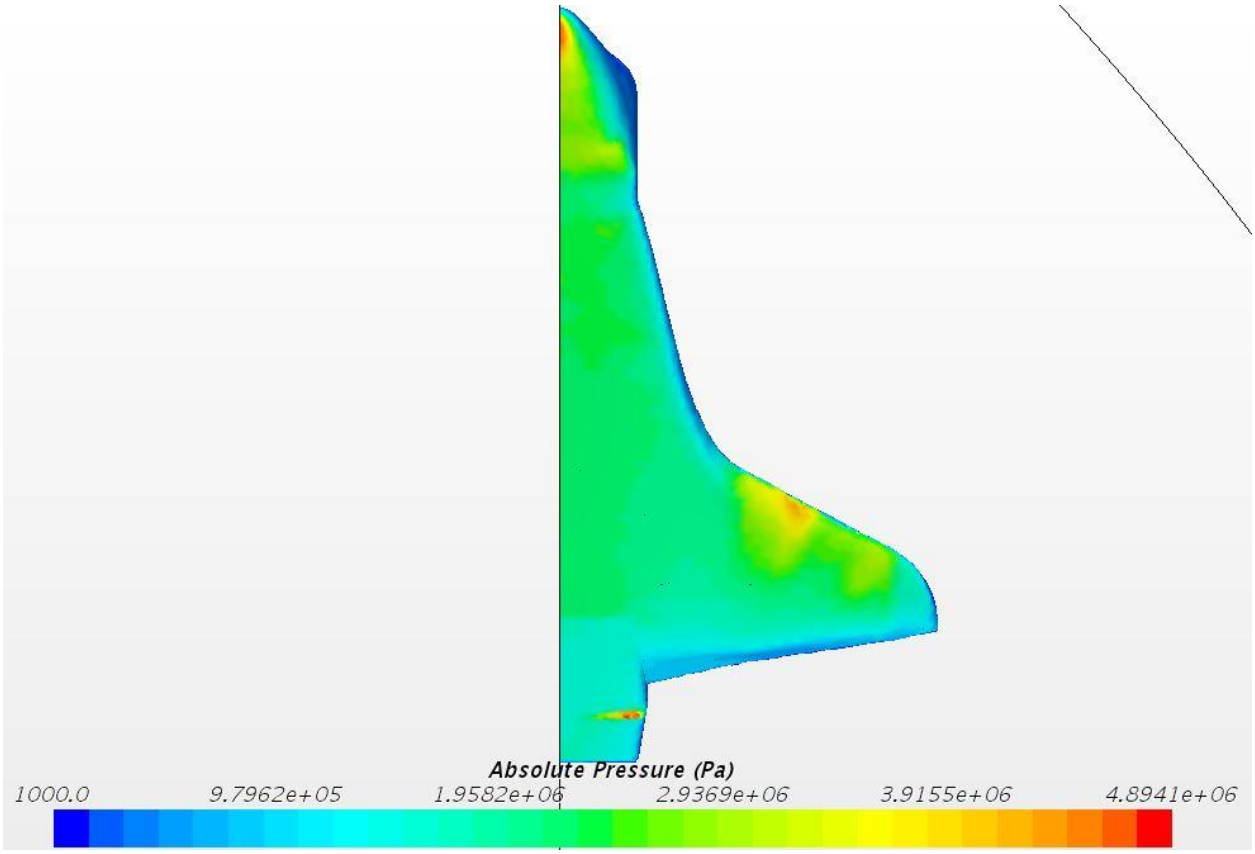

Figure 150 - One million cells 25% scale SSO bottom Absolute Pressure

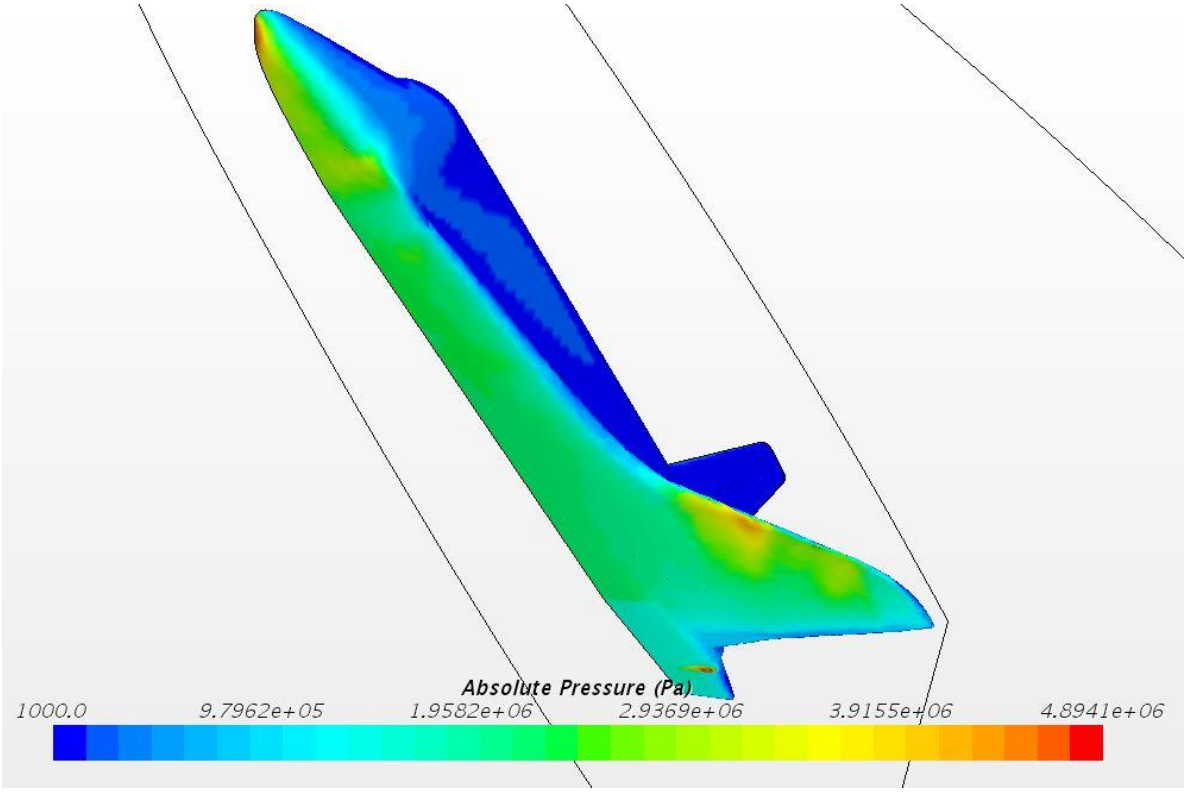

Figure 151 - One million cells 25% scale SSO 3-D Absolute Pressure

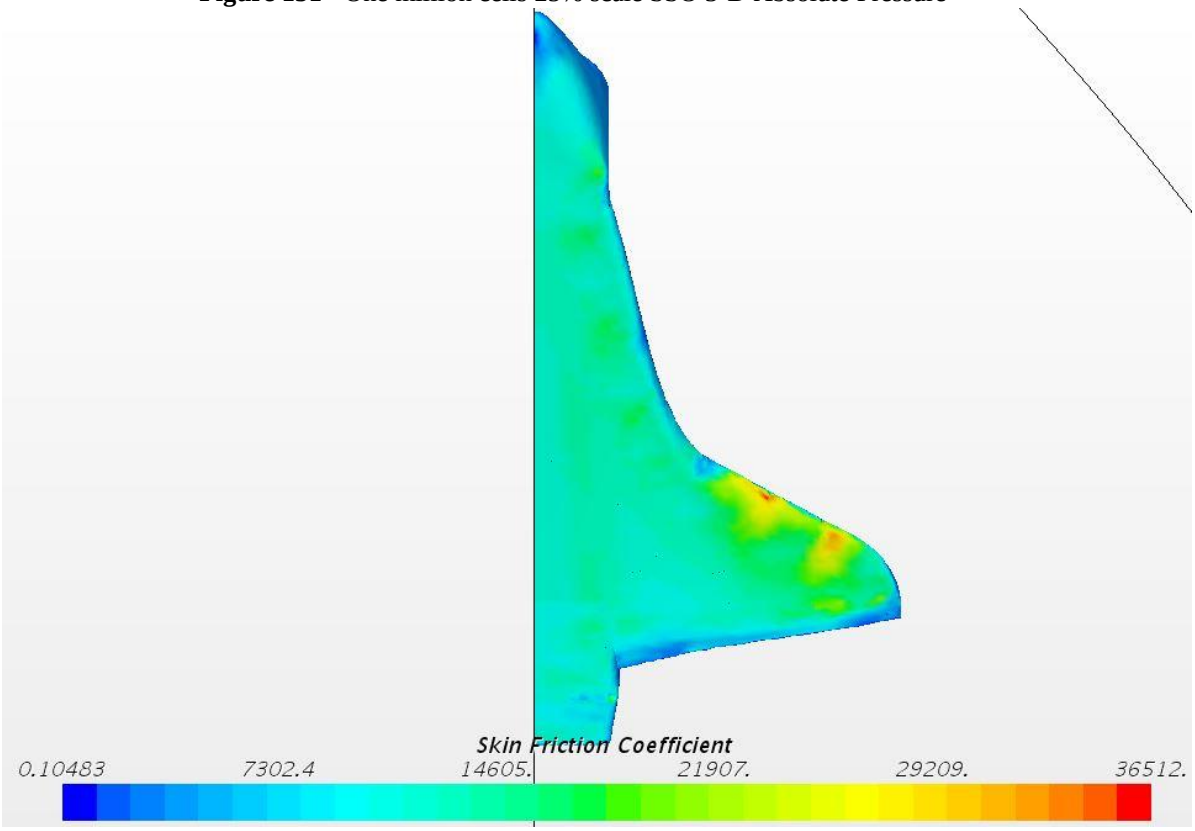

Figure 152 - One million cells 25% scale SSO bottom Skin Friction Coefficient

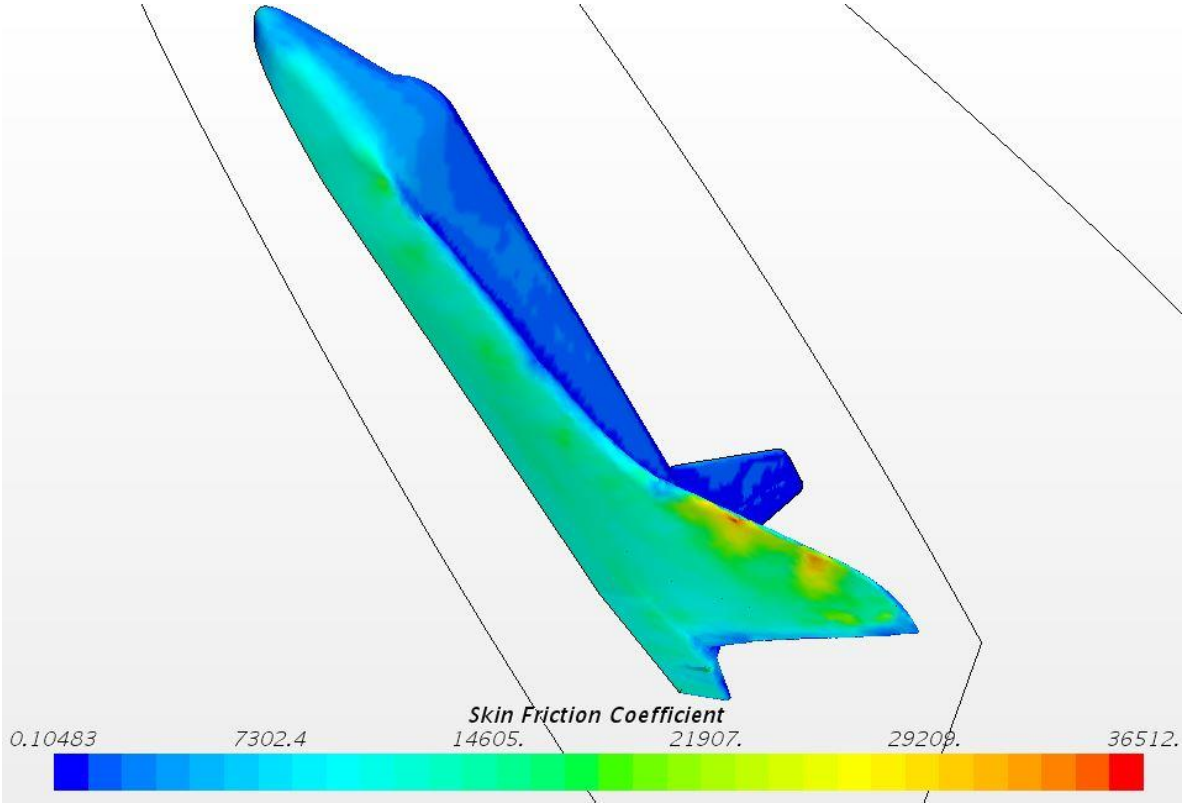

Figure 153 - One million cells 25% scale SSO 3-D Skin Friction Coefficient

8. Analysis

8.1 Space Shuttle Orbiter

The information collected in Chapter VII with the 100%, 50%, and 25% scale models of the SSO is compiled in Table 8.1 below.

Table 8.1 Data on SSO scale model simulations

Scale	Lift (N)	Drag (N)	L/D Ratio
100%	248,358,901	224,073,593	1.108
50%	62,208,957	56,116,800	1.109
25%	15,545,890	14,044,350	1.107

The lift-to-drag ratio for the three SSO runs are very close, deviating by a maximum of 0.02. This close calculation can be used to assume that the aerodynamic characteristics of the models, at least in regard to their lift and drag characteristics, was preserved through the scaling. As seen in Equations 3.7, the force of lift is calculated by multiplying the coefficient of lift by the product of density of the air, the area in the system, the velocity of freestream squared, and by 0.5. Equation 3.8 is in the same format except that it calculates the force of drag utilizing the coefficient of drag instead of the coefficient of lift. For these simulations, the coefficient of lift and coefficient of drag can be considered identical for the scaled vehicles, because they all share identical geometry. The initial conditions of the simulations are also identical so the only variable that this report is concerned with is the area used in the equation. Equation 3.9 provides a model of the relationship between the areas of different scale models and can be used to compare the force calculations between the scaled vehicles as they are directly related.

Utilizing Equation 3.9, the relationship between the Force values for the 100% and 50% SSO models can be calculated.

$$Area_{100\%}: Area_{50\%} = 1.0: \left(\frac{.5}{1.0}\right)^2 = 1: (.5^2) = 1: 0.25 \quad (8.1)$$

This calculation shows that the area of the 50% scale model is a quarter of the size of the area of the 100% scale model. As it relates to the Force calculations of the vehicles and the direct relation between area and Force calculated, the Force of Lift of the 50% model should be a quarter of that of the 100% model.

$$\frac{F_{Lift(50\%)}}{F_{Lift(100\%)}} = \frac{62{,}208{,}957N}{248{,}358{,}901N} = 25.05\% \quad (8.2)$$

$$\frac{F_{Drag(50\%)}}{F_{Drag(100\%)}} = \frac{56{,}116{,}800N}{224{,}073{,}593N} = 25.04\% \quad (8.3)$$

Equations 8.2 and 8.3 confirm that the force of lift and force of drag for the 50% scale SSO model are approximately 25% that of the 100% scale SSO model. This is in line with what would be expected based on the calculation done in equation 8.1. This same process can be repeated on the 25% scale SSO model.

$$Area_{100\%}: Area_{25\%} = 1.0: \left(\frac{.25}{1.0}\right)^2 = 1: (0.25^2) = 1: 0.0625 \quad (8.4)$$

According to Equation 8.4, the area of the 100% scale SSO model is 16 times larger than the 25% scale SSO model is. This means that the Forces between the two scale models should also share this same relation.

$$\frac{F_{Lift(25\%)}}{F_{Lift(100\%)}} = \frac{15{,}545{,}890N}{248{,}358{,}901N} = 6.259\% \quad (8.5)$$

$$\frac{F_{Drag(25\%)}}{F_{Drag(100\%)}} = \frac{14{,}044{,}350N}{224{,}073{,}593N} = 6.267\% \quad (8.6)$$

Equations 8.5 and 8.6 showcase a relationship of 6.259% and 6.267% respectively compared to the 6.25% relationship that should have been expected due to the area. The difference is small, however it is possible that this disparity was the result of the scaling itself, with a slightly larger percentage of it's body having to deal with the viscous nature of air compared to the larger models, where the area affected would be slightly smaller as a percentage of the body of the model. This is something that is inconclusive however and requires further study.

8.2 X-37

The information collected in Chapter 7 with the 100%, 50%, and 25% scale models of the X-37 OTV is compiled in Table 8.2 below.

Table 8.2 Data on X-37 scale model simulations

Scale	Cells	Lift (N)	Drag (N)	L/D Ratio
100%	500K	14,594,747	13,934,500	1.047
100%	1M	14,660,778	13,969,214	1.050
100%	2M	14,737,326	14,033,323	1.050
50%	1M	3,653,280	3,489,000	1.047
25%	500K	908,775	869,735	1.045

The lift-to-drag ratio for the five X-37 OTV runs deviate by a maximum of 0.005 between the highest and lowest values with an average of 1.0478. This similarity in lift-to-drag ratios along with the identical geometry can be used to assume identical coefficients of lift and drag. The initial conditions of the simulations are identical so the

only variable that this report is concerned with is the area used in the equation. As with the SSO models, Equation 3.9 provides a model of the relationship between the areas of different scale models and is used to compare the force calculations between the scaled vehicle.

Table 8.2 also showcases the similarities and differences in the three simulations of the X-37 OTV at 500K, 1M, and 2M cells. It seems that the lift-to-drag ratio is not changed with the increase in cells after 1 million, however the forces for both lift and drag are increased, although in a relatively small percentage. Due to time and computational constraints however, additional tests and refinement attempts on the mesh could not be made within the confines of this report.

Utilizing Equations 8.1 and 8.4, the area comparisons between the 100% scale model and the 50% and 25% scale models can be calculated to be 1:0.25 and 1:0.0625 respectively. The area ratios can now be used to compare the forces output by the CFD simulations shown in Table 8.2. The 50% scale X-37 OTV model will be compared against the 1M cell 100% scale X-37 OTV model to ensure the cell count is consistent. In the same way, the 25% scale X-37 OTV model will be compared with the 500K cell 100% scale X-37 OTV model.

$$\frac{F_{Lift(50\%)}}{F_{Lift(100\%)}} = \frac{3{,}653{,}280N}{14{,}660{,}778N} = 24.92\% \quad (8.7)$$

$$\frac{F_{Drag(50\%)}}{F_{Drag(100\%)}} = \frac{3{,}489{,}000N}{13{,}969{,}214N} = 24.98\% \quad (8.8)$$

Equations 8.7 and 8.8 are close to the expected 25%, with the largest discrepancy being a .08% difference with regards to force of lift. This isn't a large difference in percentage and may be due to the slight oscillation of the lift and drag forces as the simulations continued in their iterations. This same process can be repeated on the 25% scale X-37 OTV model with the 500K cell simulations. Using the area relation as defined in equation 8.4, the relation between the 100% scale X-37 OTV model and the 25% scale X-37 OTV model should mimic the 1:0.0625 ratio.

$$\frac{F_{Lift(25\%)}}{F_{Lift(100\%)}} = \frac{908{,}775N}{14{,}594{,}747N} = 6.23\% \quad (8.9)$$

$$\frac{F_{Drag(25\%)}}{F_{Drag(100\%)}} = \frac{869{,}735\text{N}}{13{,}934{,}500N} = 6.24\% \quad (8.10)$$

Equations 8.9 and 8.10 output the relation of 6.23% and 6.24% for the lift force and drag force respectively. Both of these values are slightly off from the expected 6.25%, however the largest difference is only 0.02% which may be due to the size of the vehicle in relation to the viscous flow, or simply the lack of resolution in the mesh. For the purposes of this report, the difference is small enough that it is possibly due to a number of error factors and cannot be conclusively assigned a significant reason for the deviation. Future work would have to be done with a focus on the accuracy of the lift force and drag force plots, as well as official models for the X-37 OTV rather than those constructed from images.

9. Future Work

For future work on this subject, several areas will need to be revisited and some concepts expanded. For the parts of this report that need to be revisited, the 25% scale model of the X-37 OTV will need to be tested at 1 million cells. This was not done within this report due to time constraints and the numerous errors that occurred in attempting to perform that CFD simulation. Future CFD runs of these models for purposes of comparison should

also be run at a standardized number of iterations. The current results were generated once the Residuals output of each run were determined to have stabilized, assuming no additional changed to the other outputs would occur. Standardization of the iterations each run would allow that variable to be removed when comparing the different models and simulations.

Additional work needs to be performed on the Surface Wrapper tool utilized in STAR-CCM+ for future iterations, as it caused small pockets to form on the models being tested, causing small areas to experience unusually high temperatures, or skin friction coefficients. This can be seen in the 3-dimensional images of each model as there are small spots on the wing where the value is much higher than the surrounding area. In addition to better work with the surface wrapper tool, this report can be revisited through the utilization of models supplied by the official government organization or companies that hold the designs. The models used in this report were constructed based on available images that allow for mistakes in their design and dimensions. Despite the problems that resulted in the three-dimensional figures for absolute pressure and temperature for both the X-37 and SSO, the areas of high temp and pressure actually in line with other CFD renderings. (Grantz A.C, 2011) The use of official models would mitigate the errors in results and allow the report to provide better data with regard to the SSO and X-37 OTV.

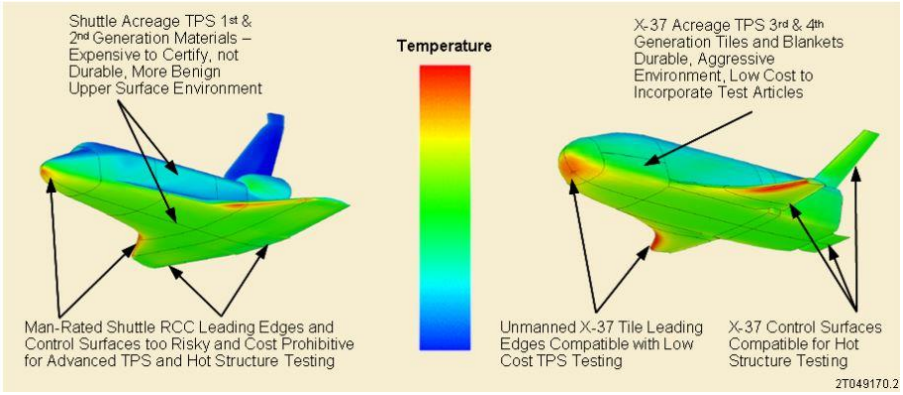

Figure 154 - 3-D renderings of SSO and X-37 OTV Temperature
(Reprinted from Grantz, A. C. (2011, September 27). X-37B Orbital Test Vehicle and Derivatives. https://pdfs.semanticscholar.org/b3f5/f5df7f1e8df80876cd8ff6c0fac1c04059ce.pdf)

Future reports on this topic can also expand the scope of this topic, through the modeling of non-earth atmospheres, as well as testing designed at various points of re-entry. The use of non-earth atmospheres in this type of CFD simulation would allow for information to be gathered on potential re-entry modeling of other planets in our solar system like Mars. These tests can provide information on whether or not the designs of reusable re-entry vehicles such as the X-37 OTV and SSO can be used on other planets. Testing in other stages of re-entry will allow for more information on what the effect of scaling will have on re-entry vehicles through the entire descent.

10. Summary

This report focused on the Space Shuttle Orbiter and the X-37 Orbital Test Vehicle and how scaling the geometries of these vehicles would affect them in a Hypersonic CFD simulation with the exact same Initial conditions. Models for these vehicles were constructed through the use of the CAD program Solidworks utilizing publicly available images and dimensions as models supplied from official sources proved unable to be tested. Despite restrictions in the computational resources and time available to run the simulations, the CFD software STAR-CCM+ was utilized to run a total of eight final runs, five of the X-37 OTV at various scales and mesh resolutions, and three of the SSO, all with similar mesh resolutions but varying scale. The results of these simulations were compared and confirmed to have similar lift-to-drag ratio, and displayed lift and drag forces proportional to their expected values. There were slight discrepancies in the values calculated however the cause for these variances is unknown and possibly a result of human error or as the result of a simulation failing to completely stabilize. Utilizing the equations of lift-to-drag ratio, solid relations can be made between the scaled vehicles and their respective Forces generated.

References

Anderson, J. D., Jr. (2006). Hypersonic and high-temperature gas dynamics (2nd ed.). Reston, VA: American Institute of Aeronautics and Astronautics.

Anderson, J. D., Jr. (2017). Fundamentals of aerodynamics (5th ed.). New York, NY: McGraw Hill Education.

Baker, D. (2017, June 03). Book Excerpt: Space Shuttle Owners' Workshop Manual. Retrieved March 20, 2018, from https://www.wired.com/2011/04/shuttle-manual-excerpt/

Dunbar, B. (2017, August 01). The Aeronautics of the Space Shuttle. Retrieved October 20, 2017, from https://www.nasa.gov/audience/forstudents/9-12/features/F_Aeronautics_of_Space_Shuttle.html

Dunbar, B. (n.d.). X-37 [fact sheet] (05/03). Retrieved from https://www.nasa.gov/centers/marshall/news/background/facts/x37facts2.html

Figure 2. Orbiter Vehicle Dimensions. [Report of the PRESIDENTIAL COMMISSION on the Space Shuttle Challenger Accident]. (n.d.). Retrieved April 6, 2018, from https://history.nasa.gov/rogersrep/v3o378b.htm

Grantz, A. C. (2011, September 27). X-37B Orbital Test Vehicle and Derivatives. Retrieved February 25, 2018, from https://pdfs.semanticscholar.org/b3f5/f5df7f1e8df80876cd8ff6c0fac1c04059ce.pdf

NASA.(n.d.). *Space Shuttle Era Facts* [Fact Sheet]. Retrieved February 12, 2018, from https://www.nasa.gov/pdf/566250main_2011.07.05%20SHUTTLE%20ERA%20FACTS.pdf

Navier-Stokes Equations. (2015, May 5). Retrieved January 20, 2018, from https://www.grc.nasa.gov/www/k-12/airplane/nseqs.html

Seemangal, R., & Seemangal, R. (2017, June 08). SpaceX to Launch Secretive Robotic Spaceplane for US Air Force. Retrieved February 1, 2018, from https://observer.com/2017/06/spacex-to-launch-secretive-robotic-spaceplane-for-u-s-air-force/

Space Shuttle as a Glider. (n.d.). Retrieved March 3, 2018, from https://www.grc.nasa.gov/www/k-12/airplane/glidshuttle.html

Space Shuttle orbiter 4-view diagram. [4 views of the Space Shuttle Orbiter]. (n.d.). Retrieved May 1, 2018, from https://www.dfrc.nasa.gov/Gallery/Graphics/STS/index.html

Space Task Group, "The Post-Apollo Space Program: Directions for the Future," [Editorial]. (1969, September). NASA Historical Reference Collection, History Office. Retrieved February 10, 2018, from https://www.hq.nasa.gov/office/pao/History/taskgrp.html

Stone,D. (September 1970). *Aerodynamic Characteristics of a Fixed-Wing Manned Space Shuttle Concept at a MACH Number of 6.0* [Memorandum] Hampton, VA. : NASA Langley Research Center Retrieved from https://ntrs.nasa.gov/archive/nasa/casi.ntrs.nasa.gov/19700029474.pdf

X-37B Orbital Test Vehicle. (2015, April 17). Retrieved November 11, 2017, from https://www.af.mil/About-Us/Fact-Sheets/Display/Article/104539/x-37b-orbital-test-vehicle/

X-37 Technology Demonstrator: Blazing the trail for the next generation of space transportation systems [Fact Sheet] Retrieved 4 March, 2018, from https://www.nasa.gov/centers/marshall/pdf/100431main_x37-historical.pdf

Appendix A: Temperature and Pressure Figures for SSO and X-37 CFD Simulations

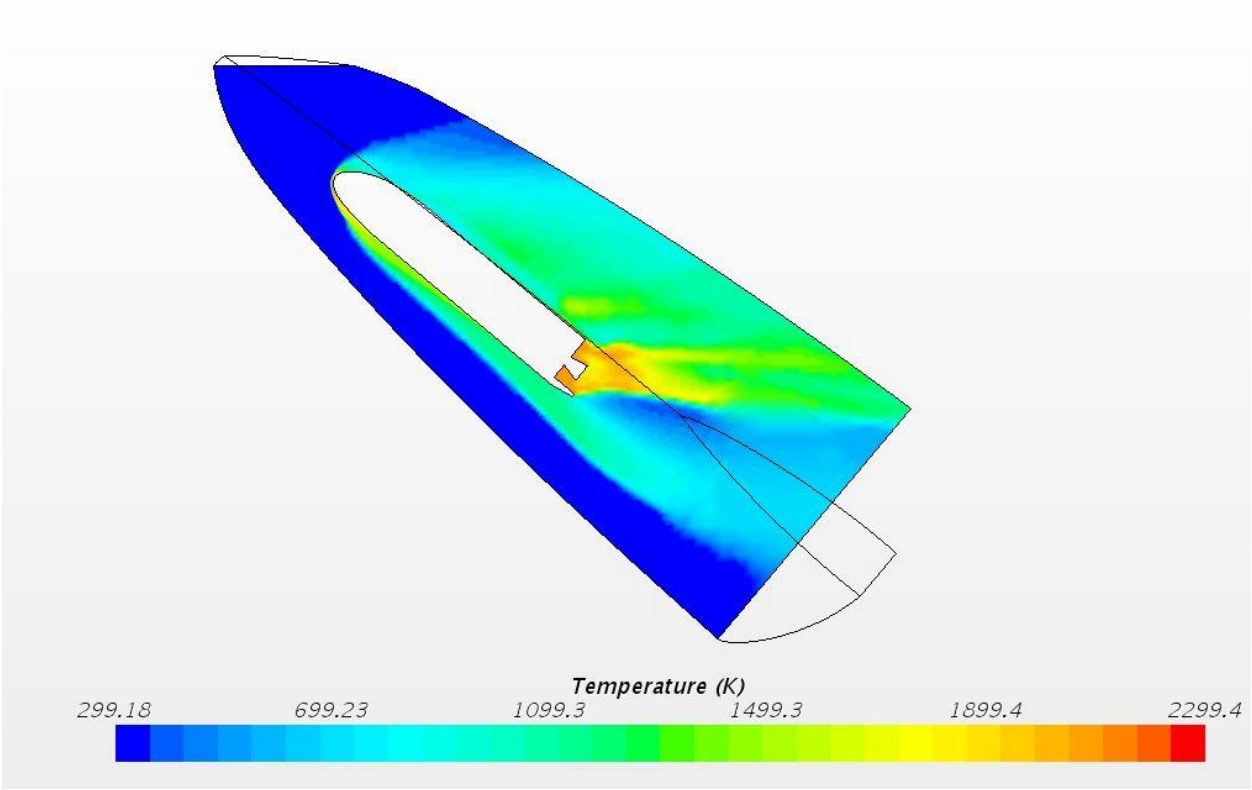

Figure A.1 - 500K cells 100% scale X-37 Temperature full body

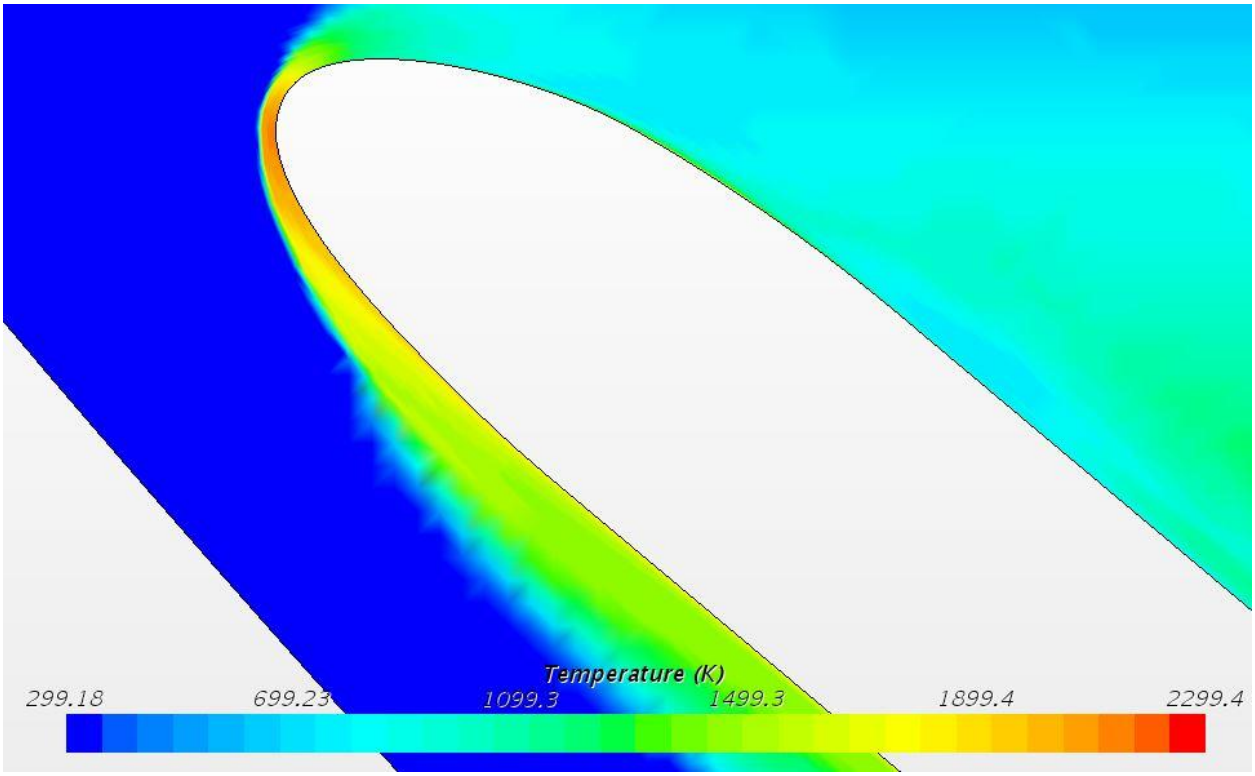

Figure A.2 - 500K cells 100% scale X-37 Temperature nose

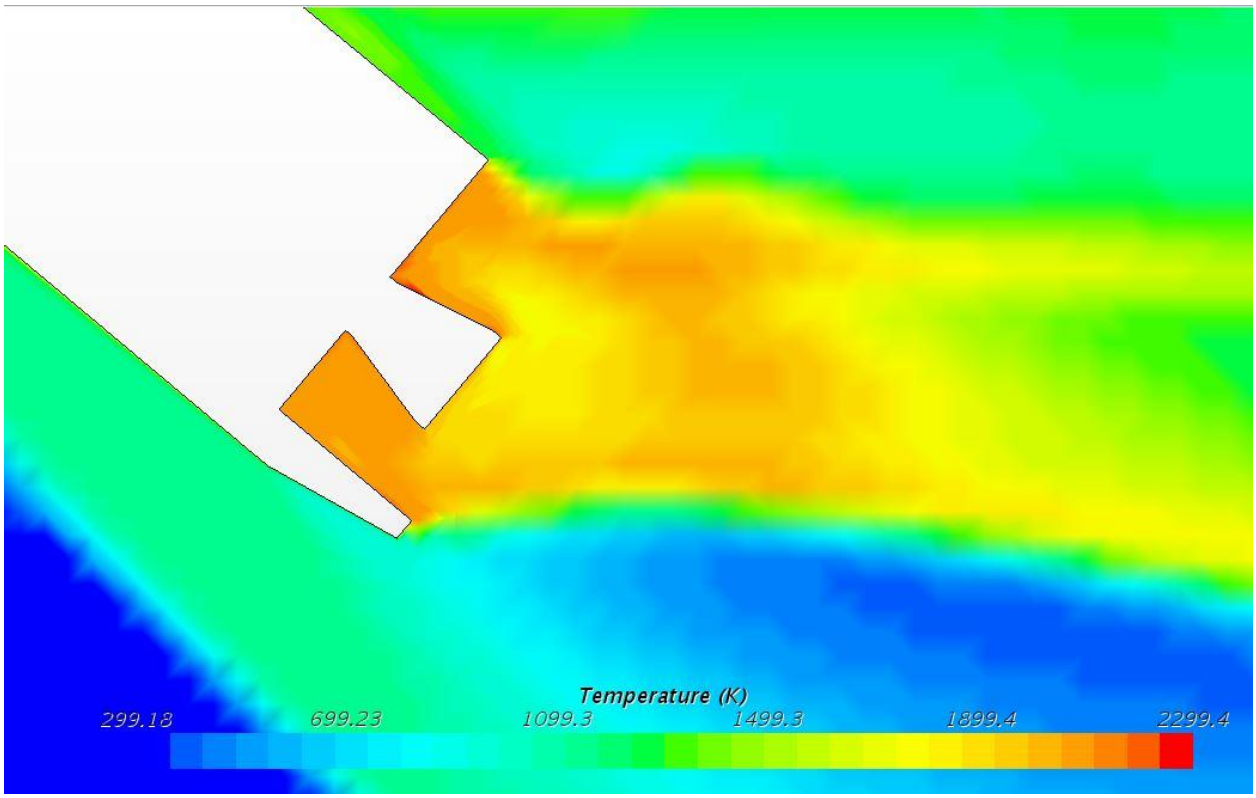

Figure A.3 - 500K cells 100% scale X-37 Temperature tail

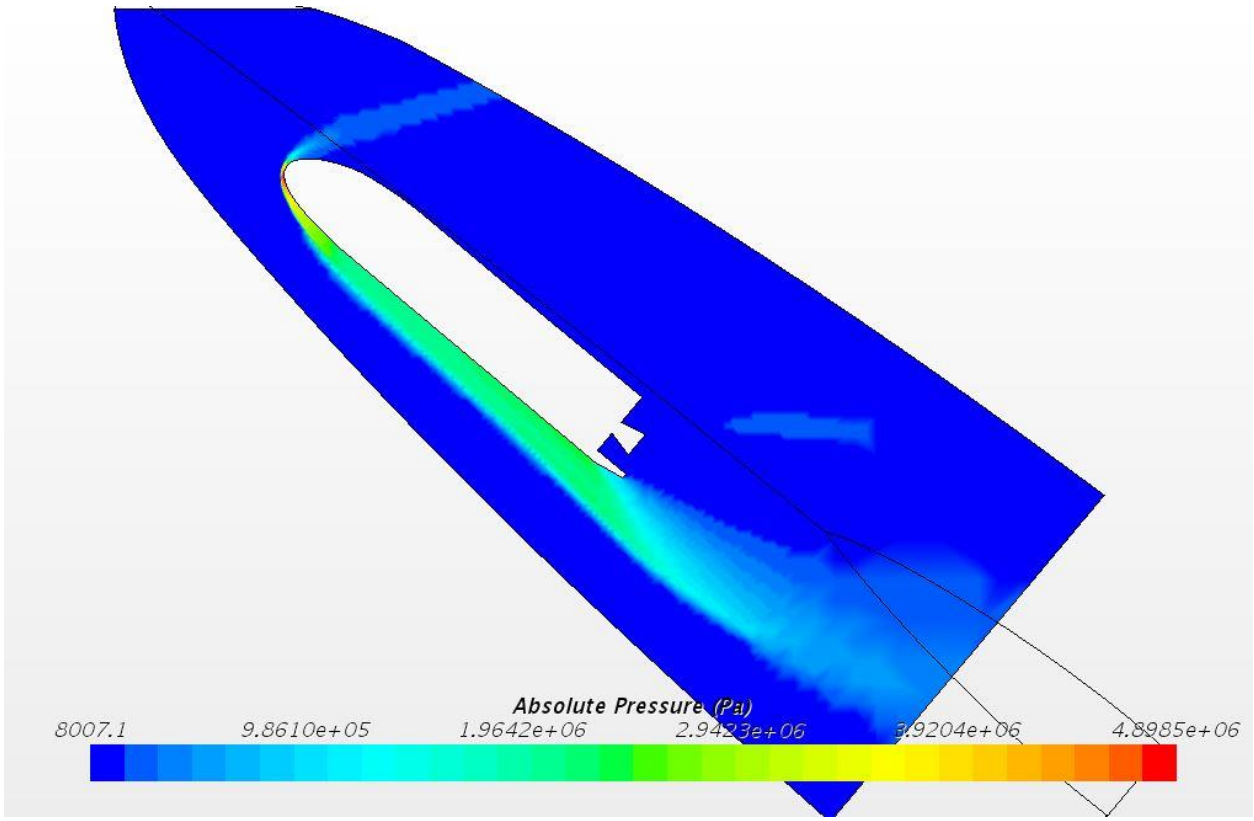

Figure A.4 - 500K cells 100% scale X-37 Absolute Pressure full body

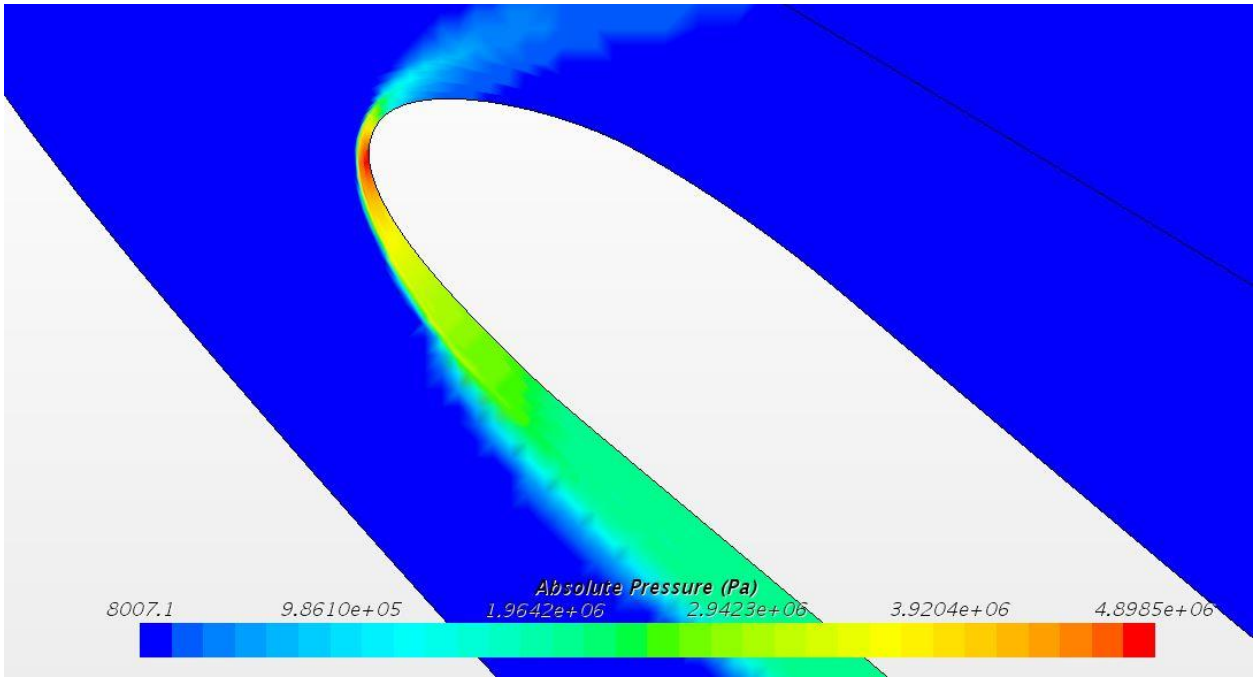

Figure A.5 - 500K cells 100% scale X-37 Absolute Pressure nose

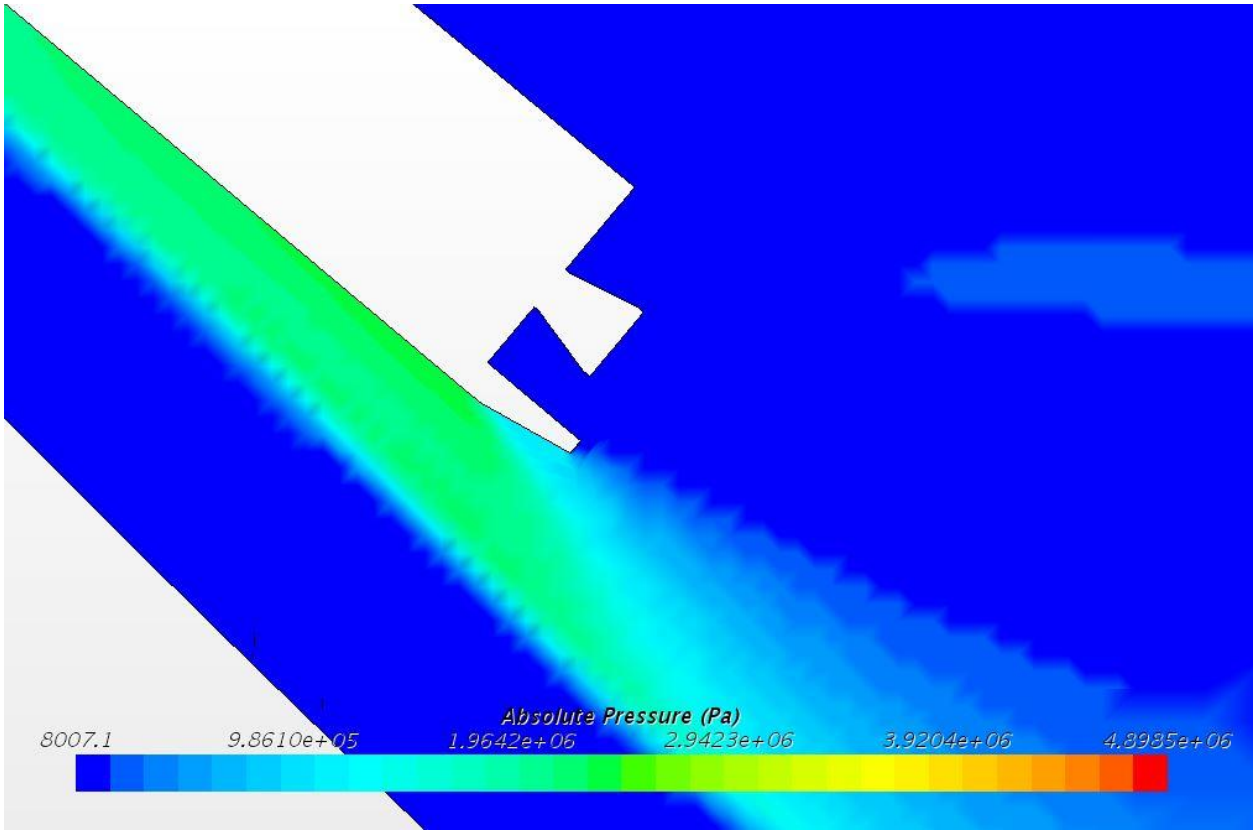

Figure A.6 - 500K cells 100% scale X-37 Absolute Pressure tail

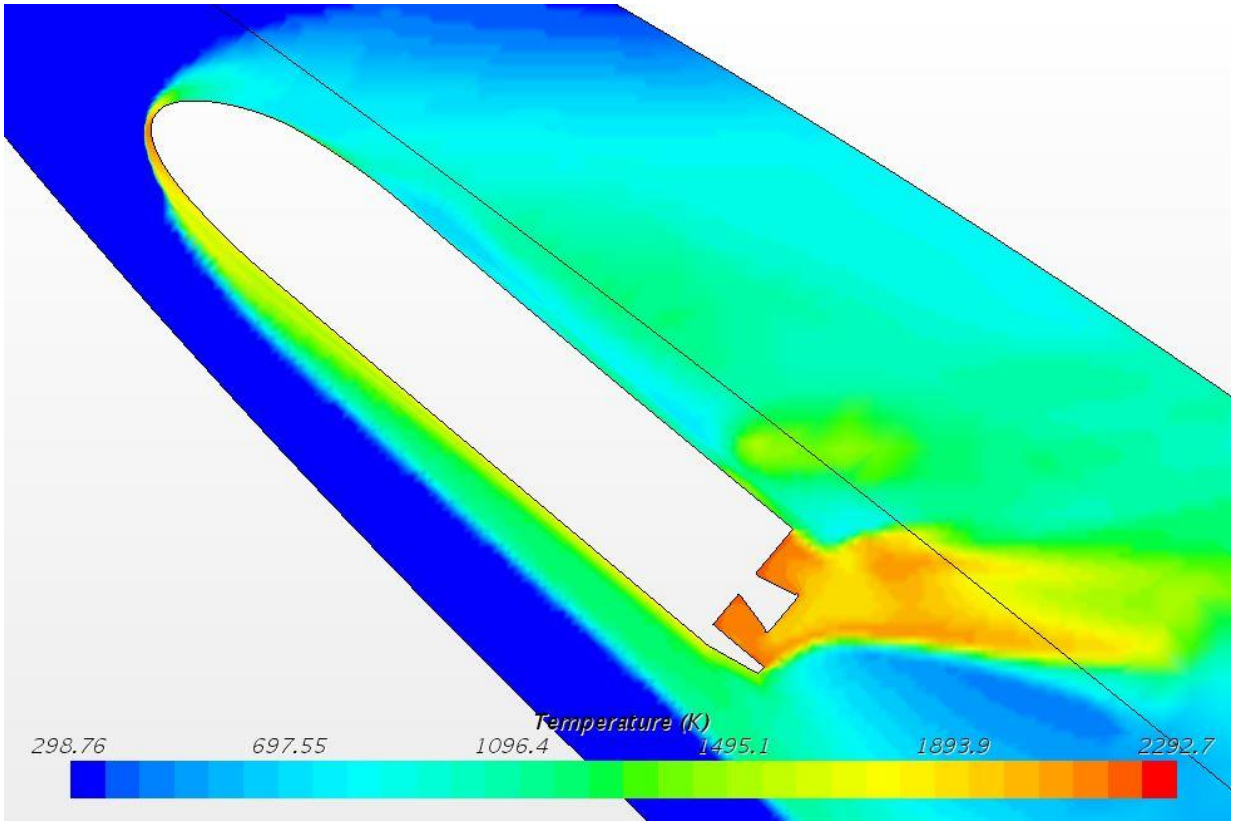

Figure A.7 - One million cells 100% scale X-37 Temperature full body

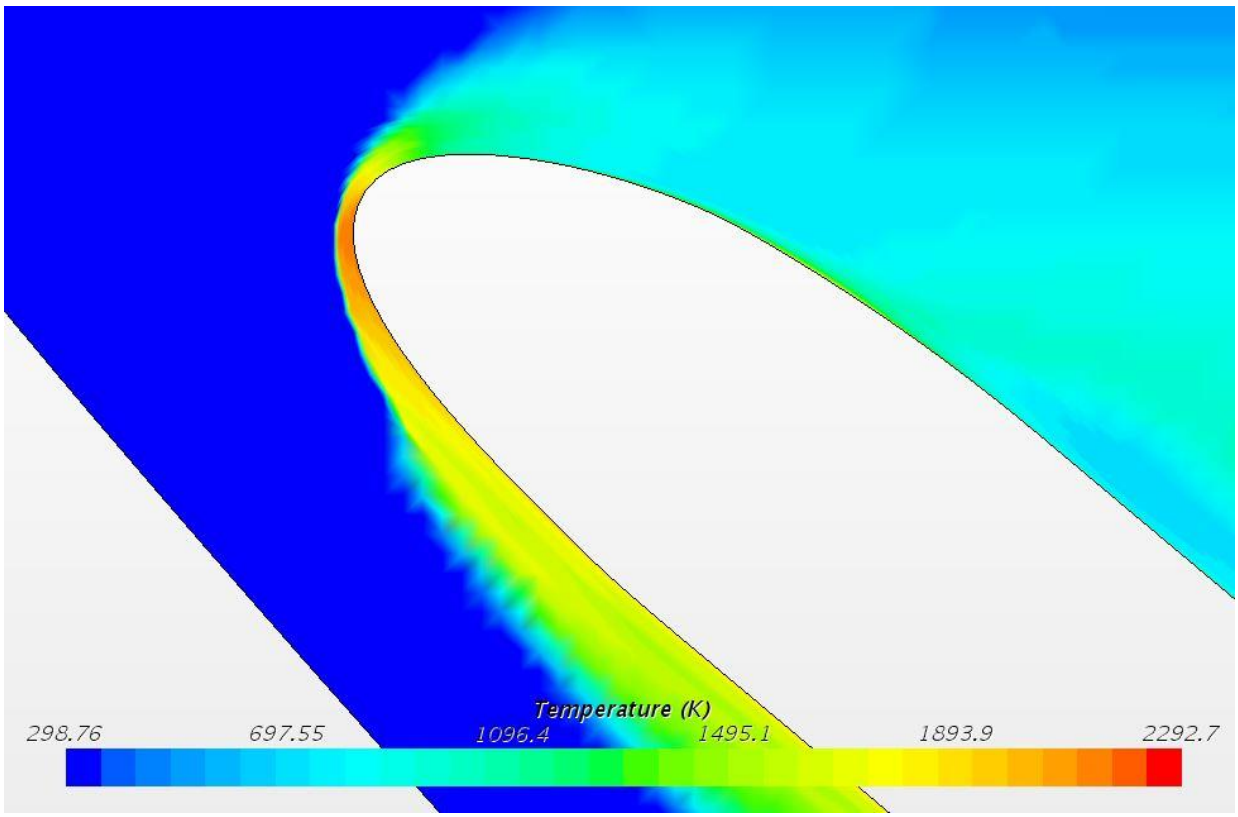

Figure A.8 - One million cells 100% scale X-37 Temperature nose

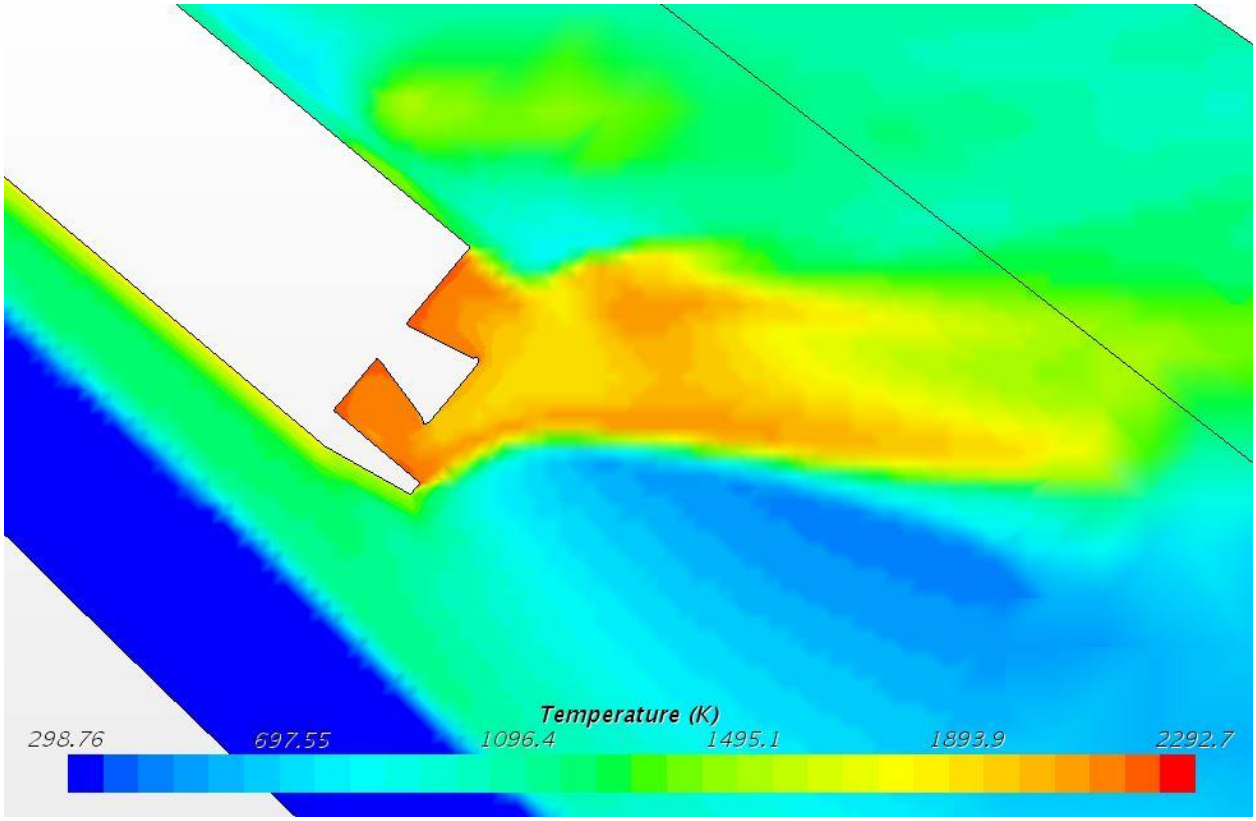

Figure A.9 - One million cells 100% scale X-37 Temperature tail

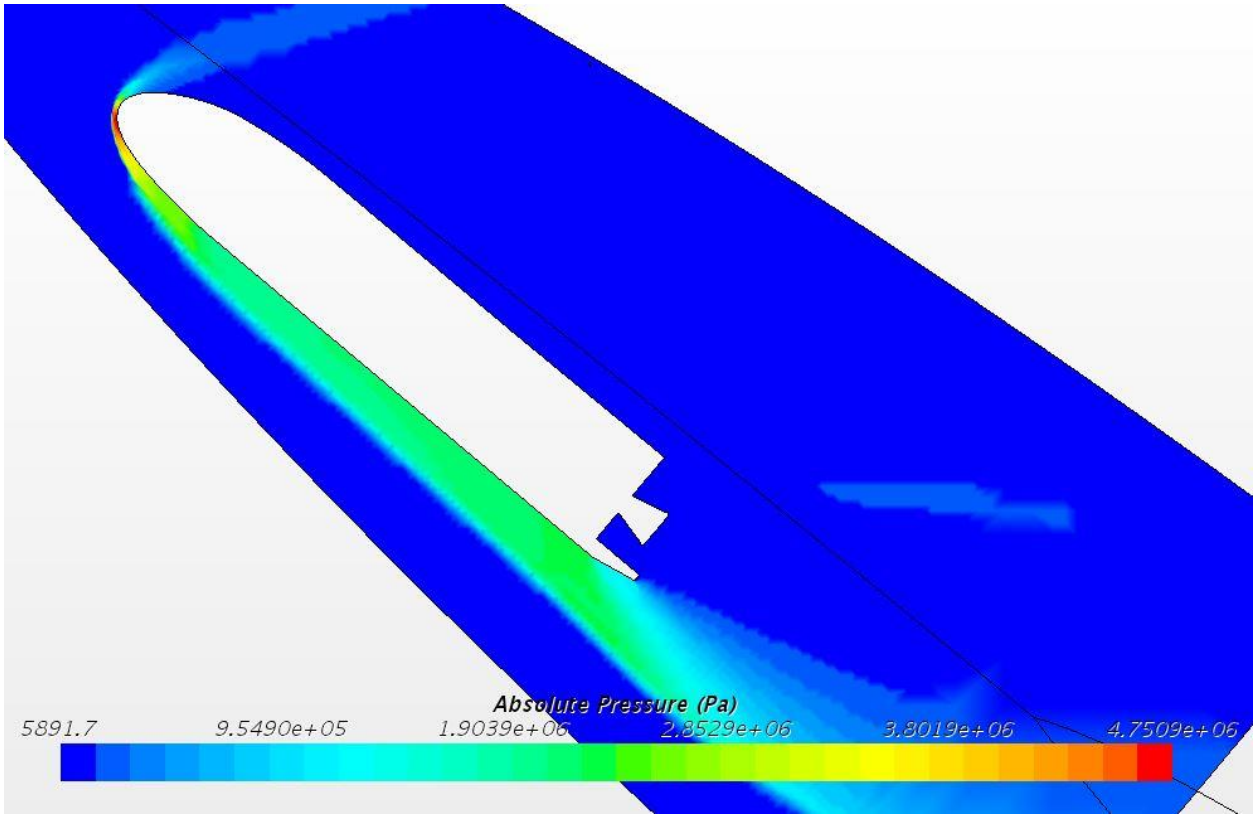

Figure A.10 - One million cells 100% scale X-37 Absolute Pressure full body

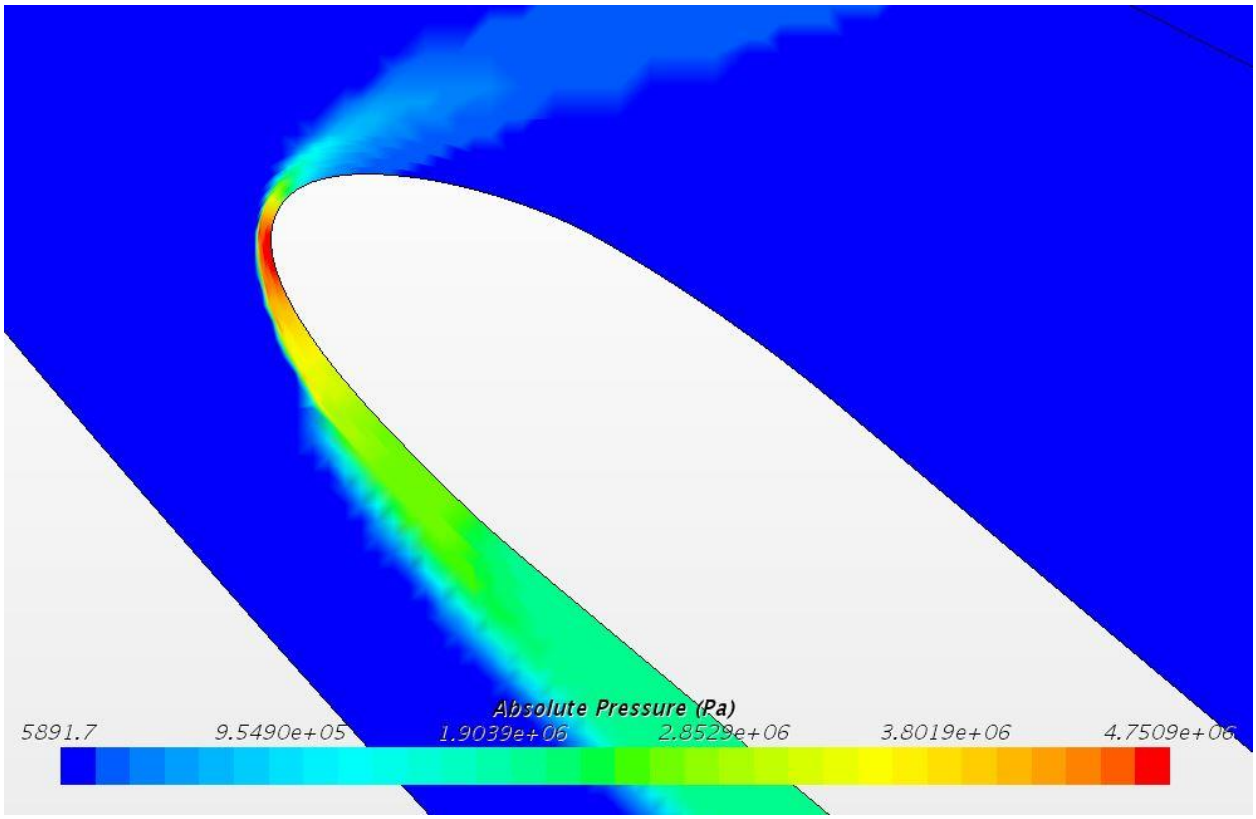

Figure A.11 - One million cells 100% scale X-37 Absolute Pressure nose

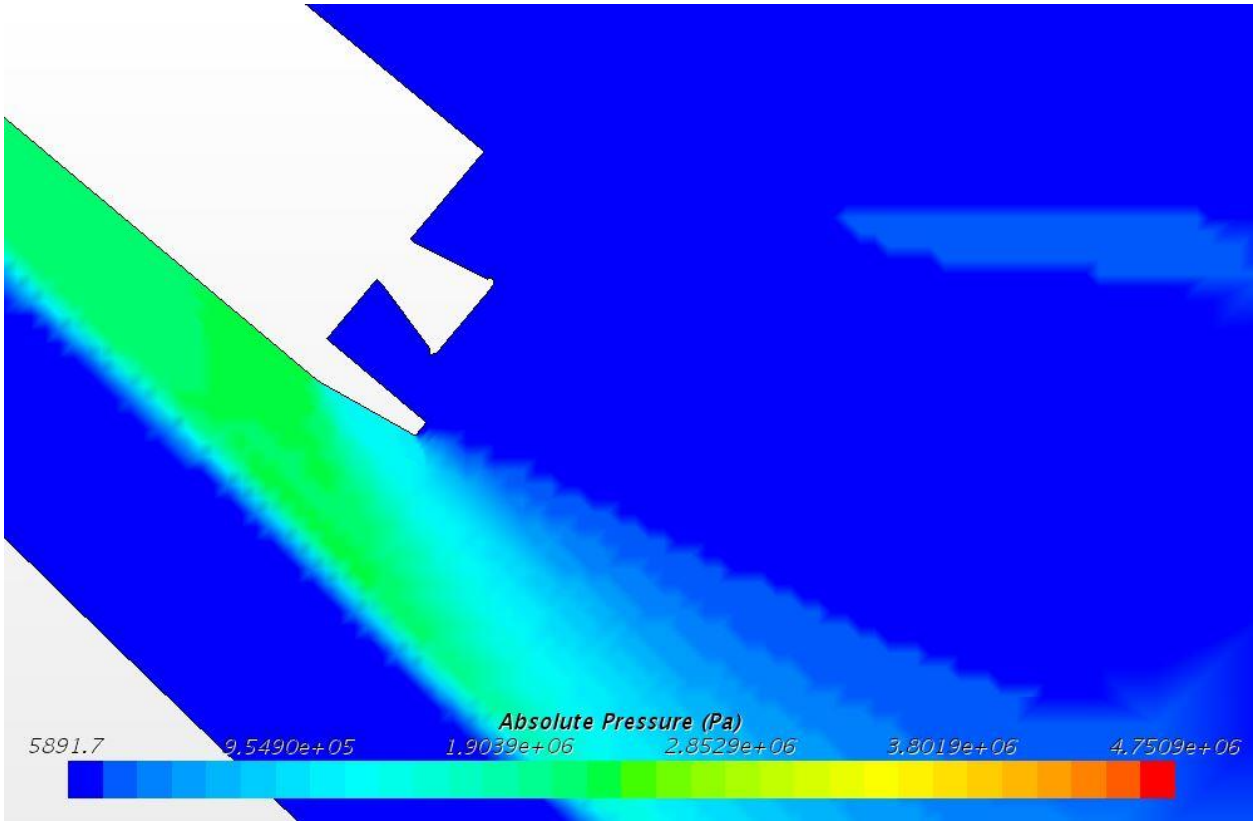

Figure A.12 - One million cells 100% scale X-37 Absolute Pressure tail

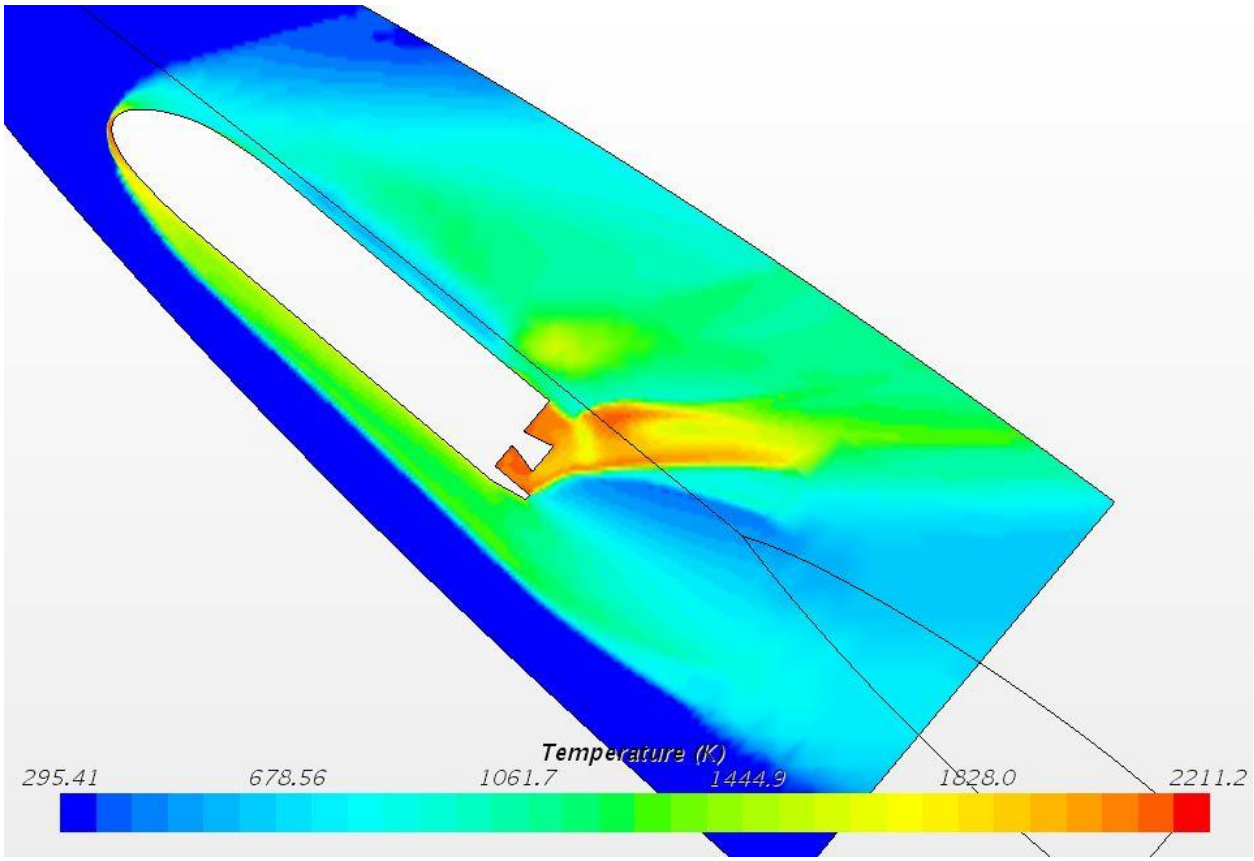

Figure A.13 - Two million cells 100% scale X-37 Temperature full body

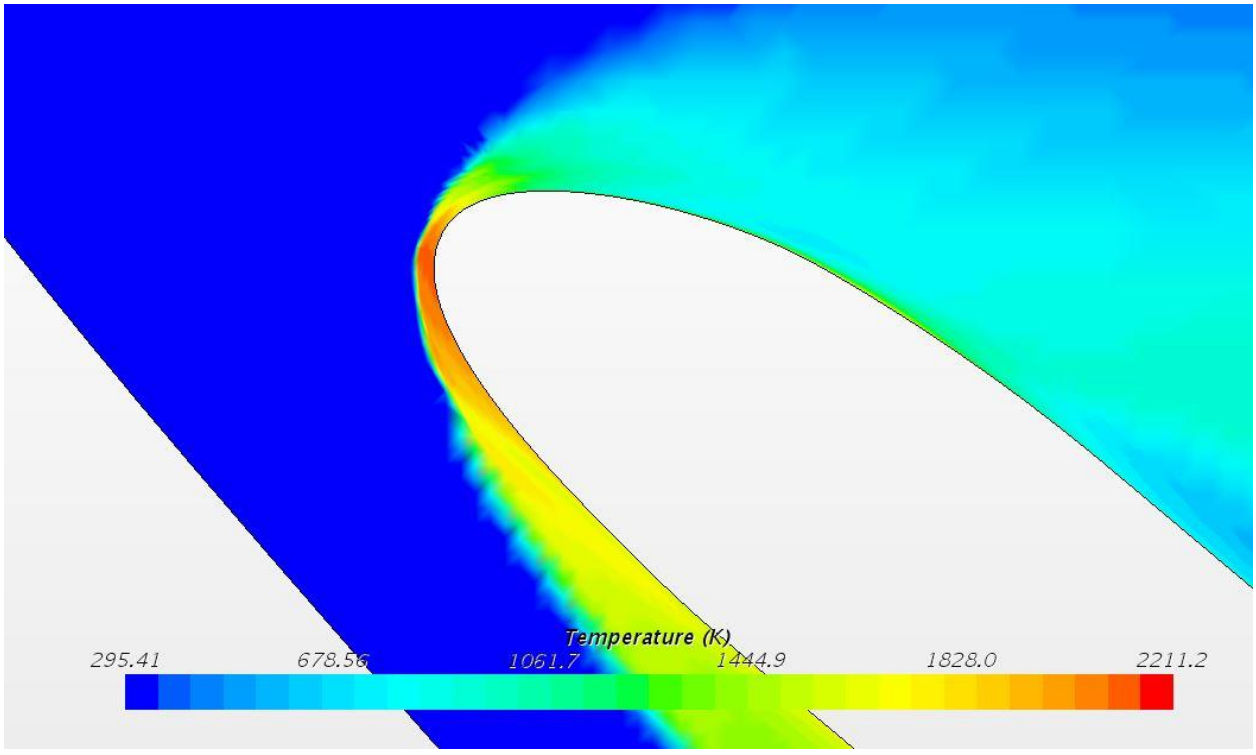

Figure A.14 - Two million cells 100% scale X-37 Temperature nose

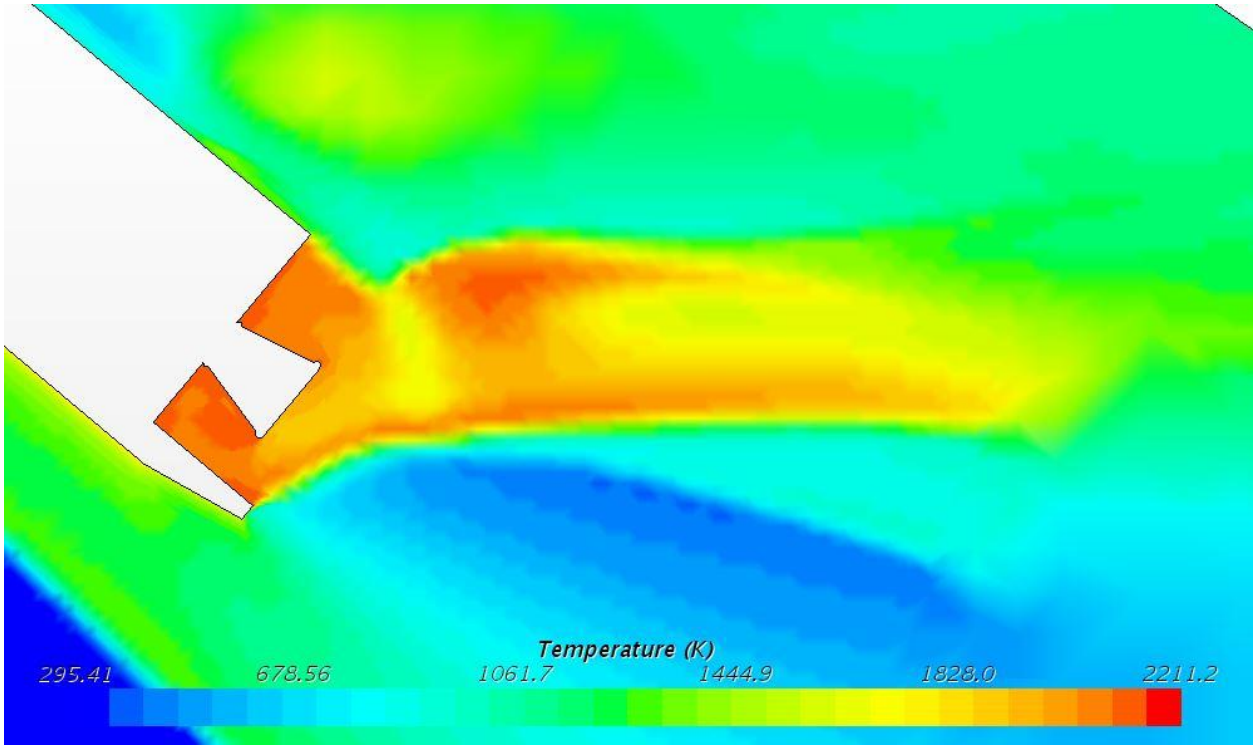

Figure A.15 - Two million cells 100% scale X-37 Temperature tail

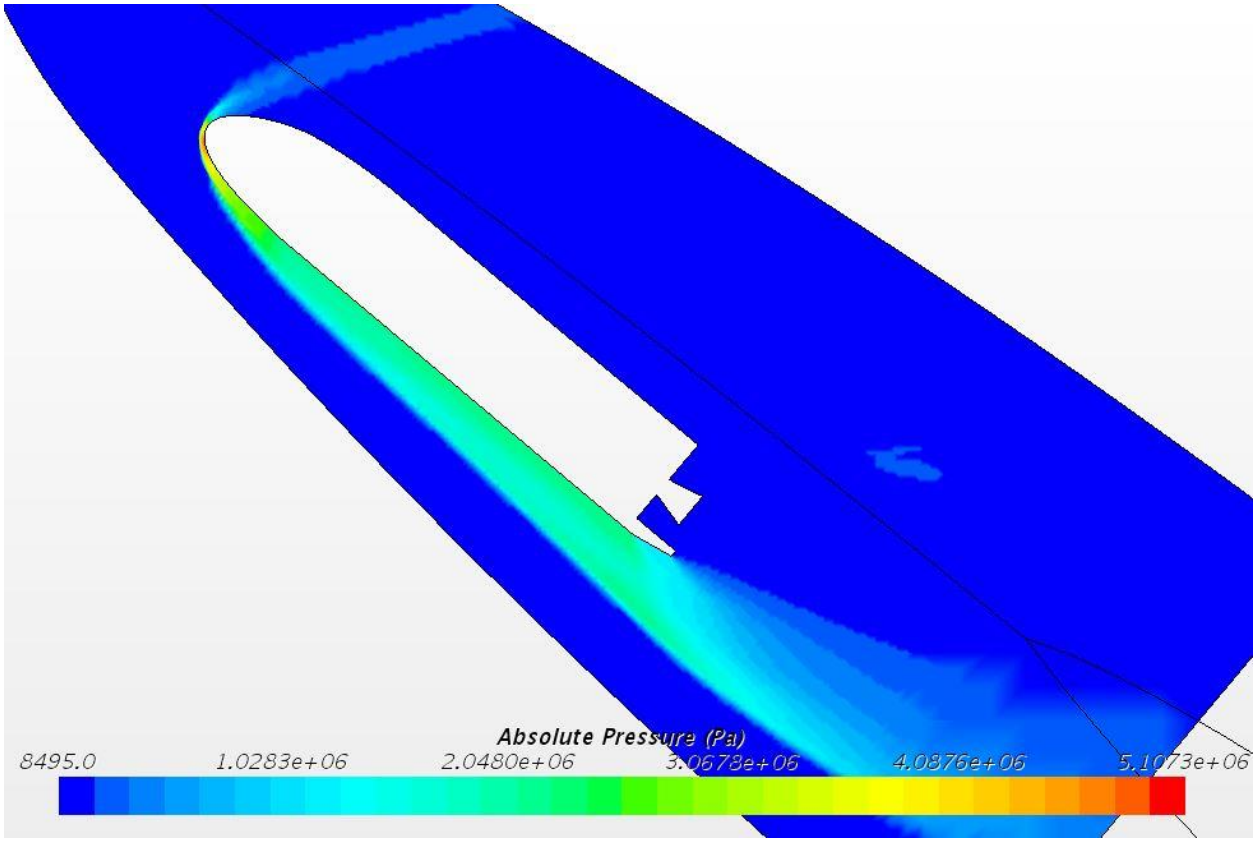

Figure A.16 - Two million cells 100% scale X-37 Absolute Pressure full body

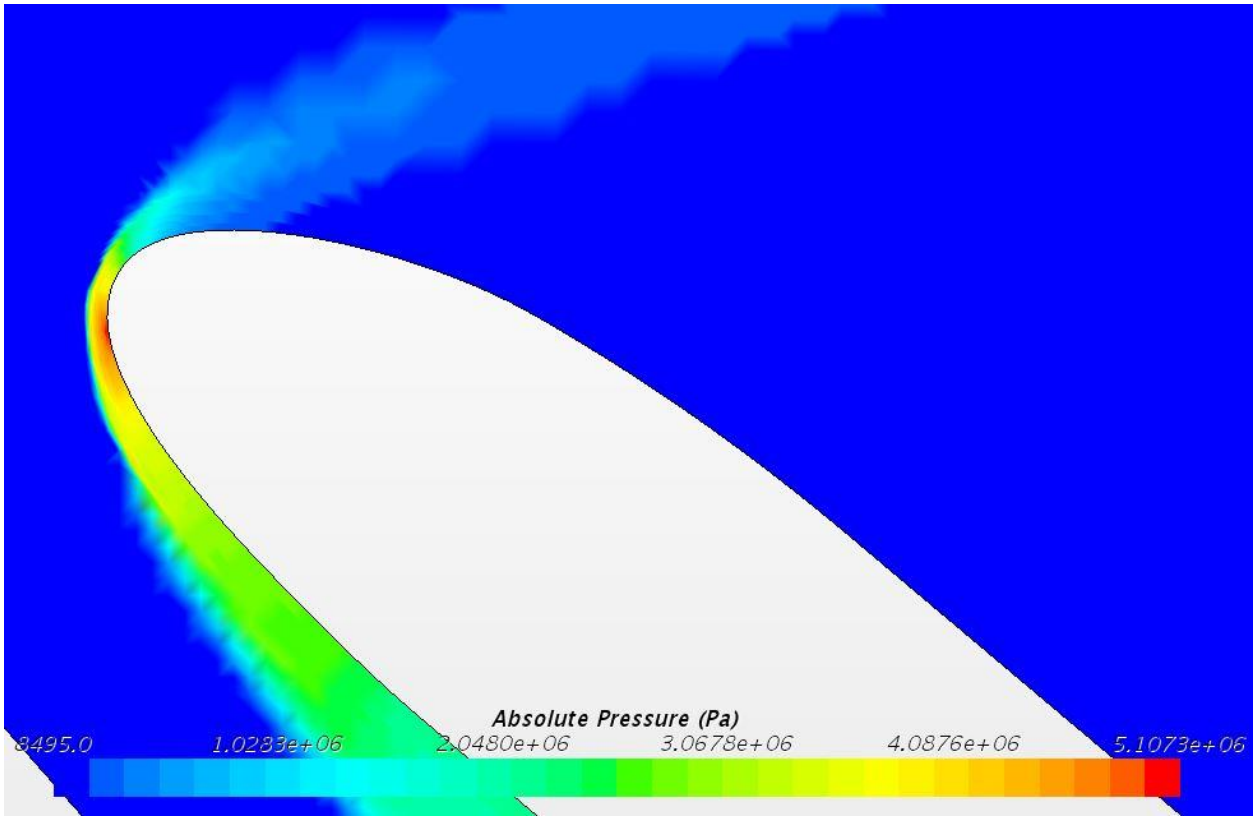

Figure A.17 - Two million cells 100% scale X-37 Absolute Pressure nose

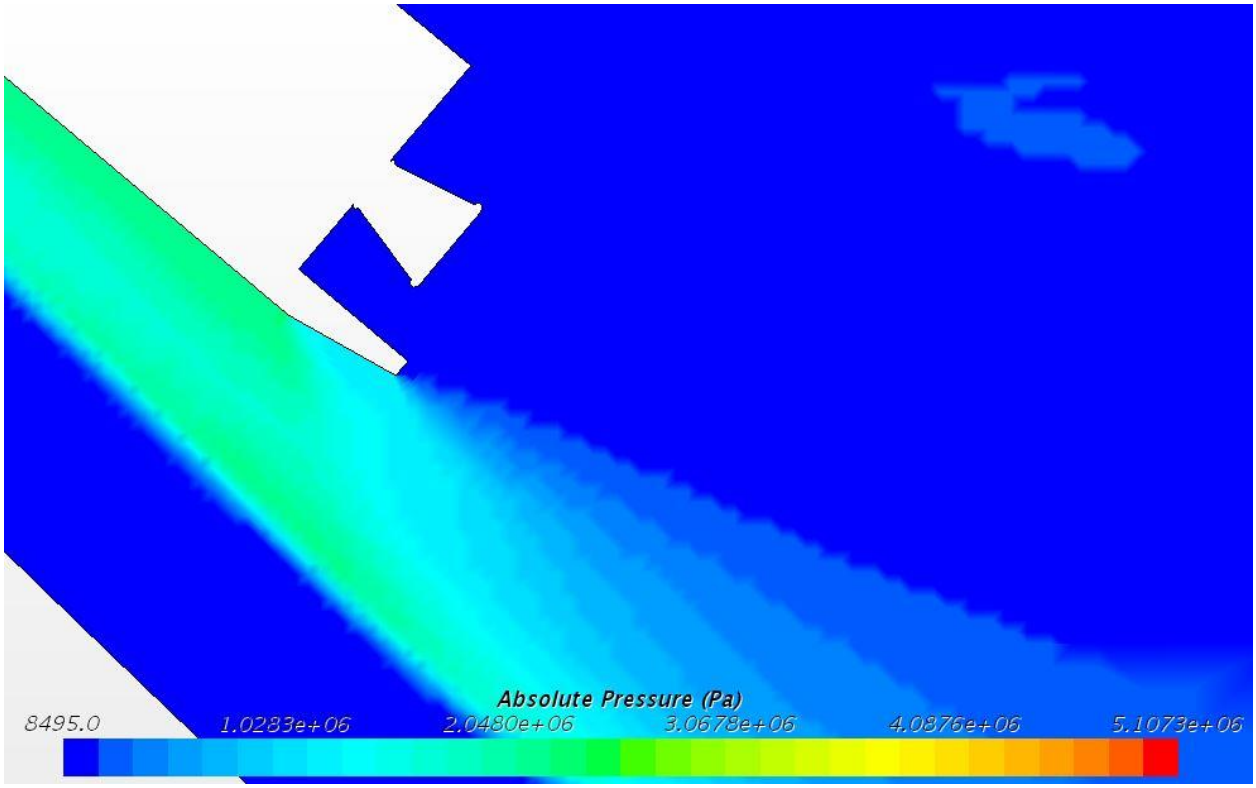

Figure A.18 - Two million cells 100% scale X-37 Absolute Pressure tail

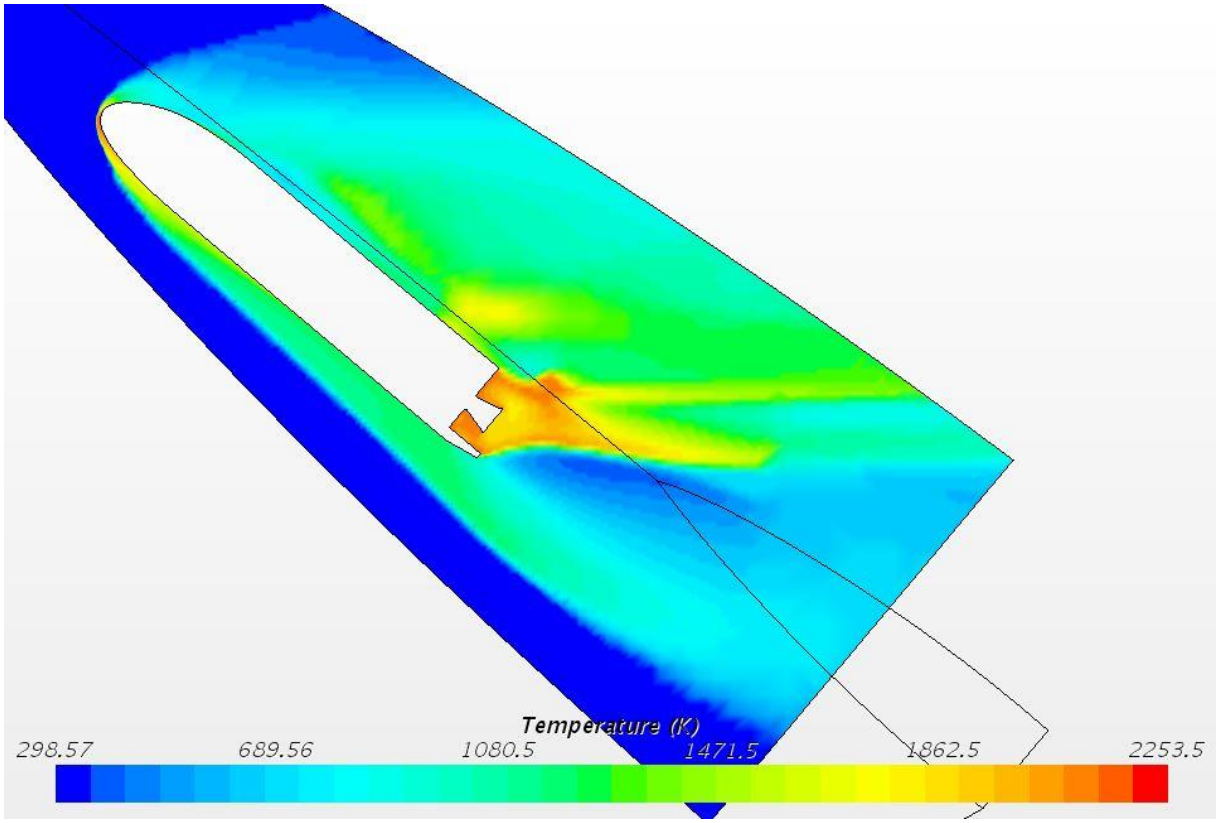

Figure A.19 - One million cells 50% scale X-37 Temperature full body

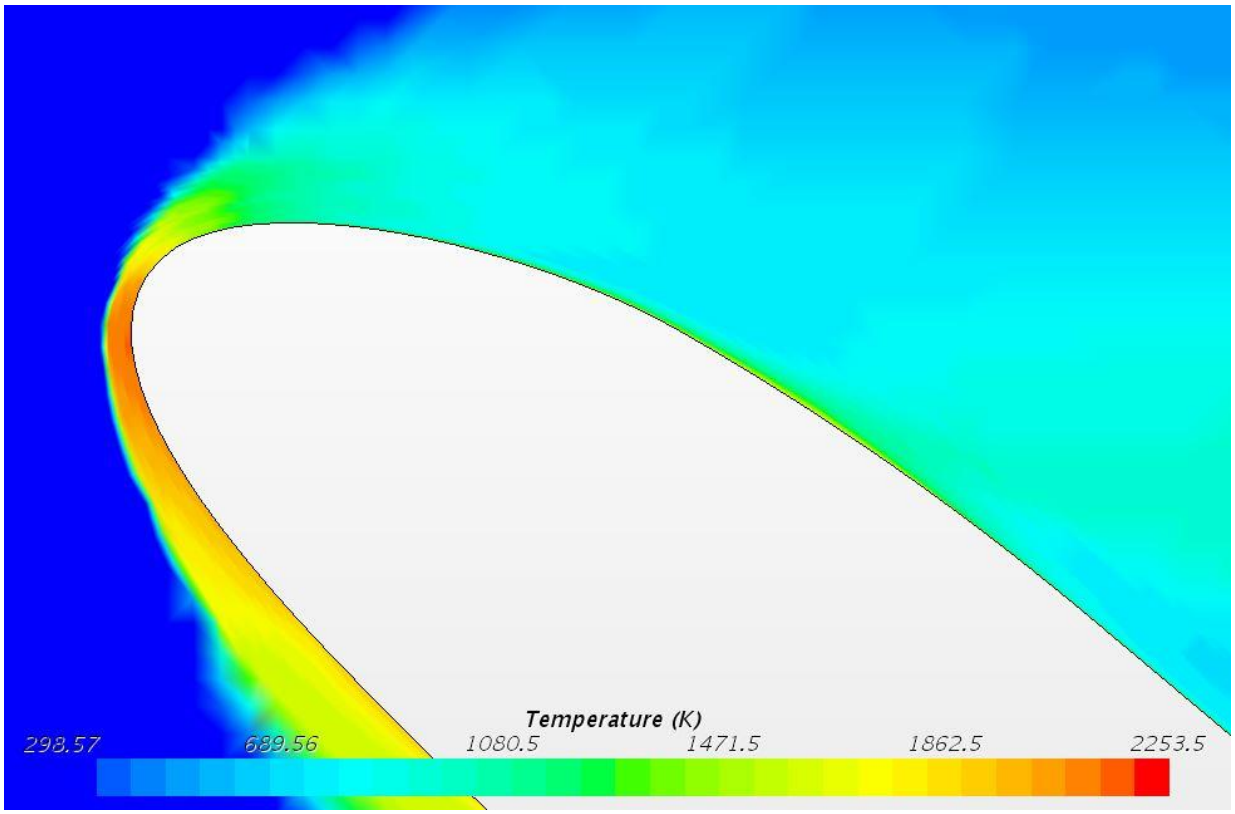

Figure A.20 - One million cells 50% scale X-37 Temperature nose

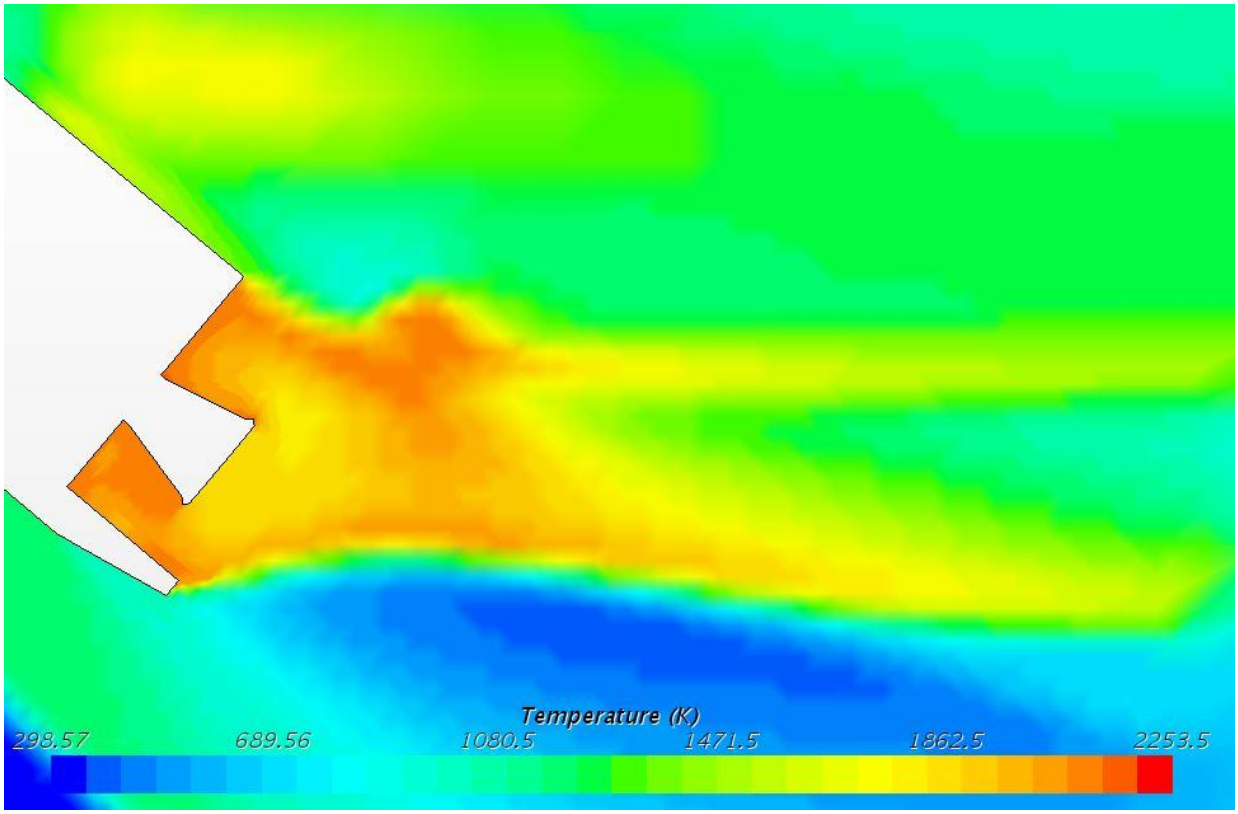

Figure A.21 - One million cells 50% scale X-37 Temperature tail

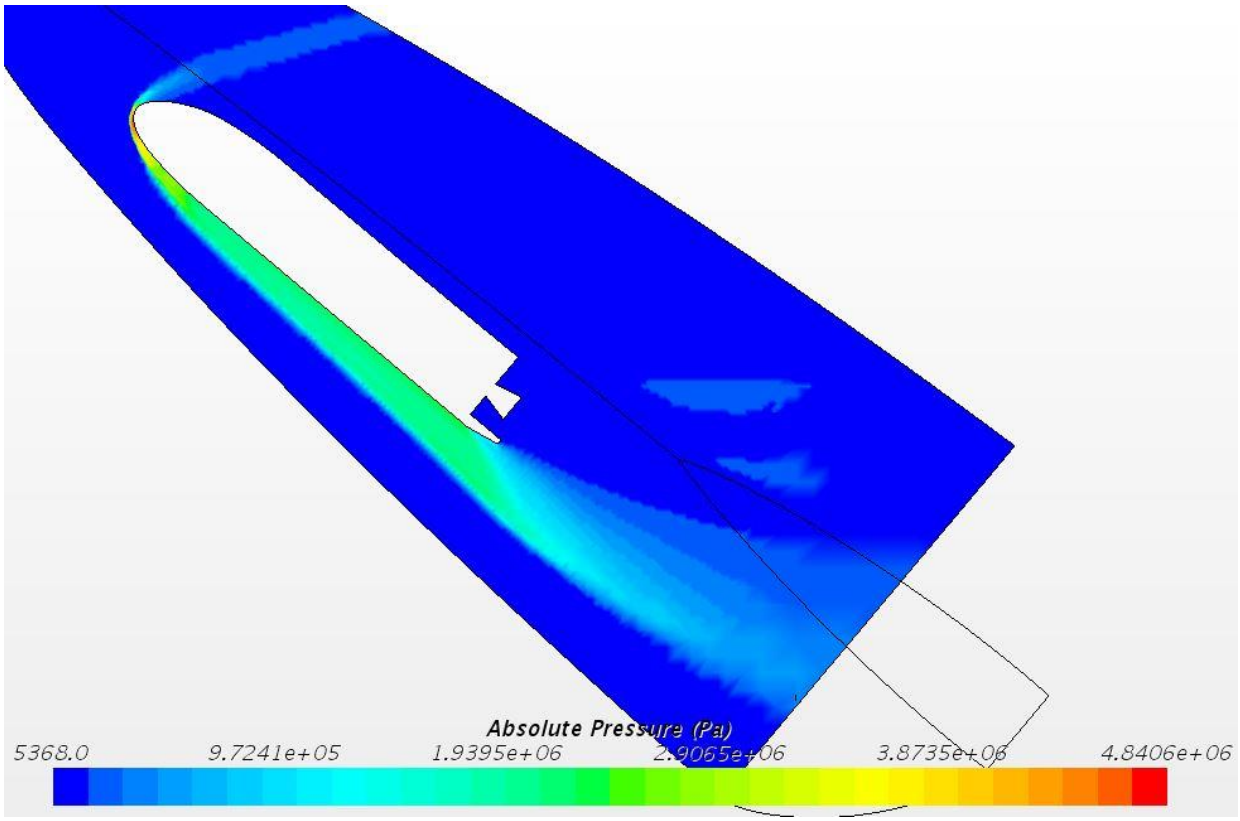

Figure A.22 - One million cells 50% scale X-37 Absolute Pressure full body

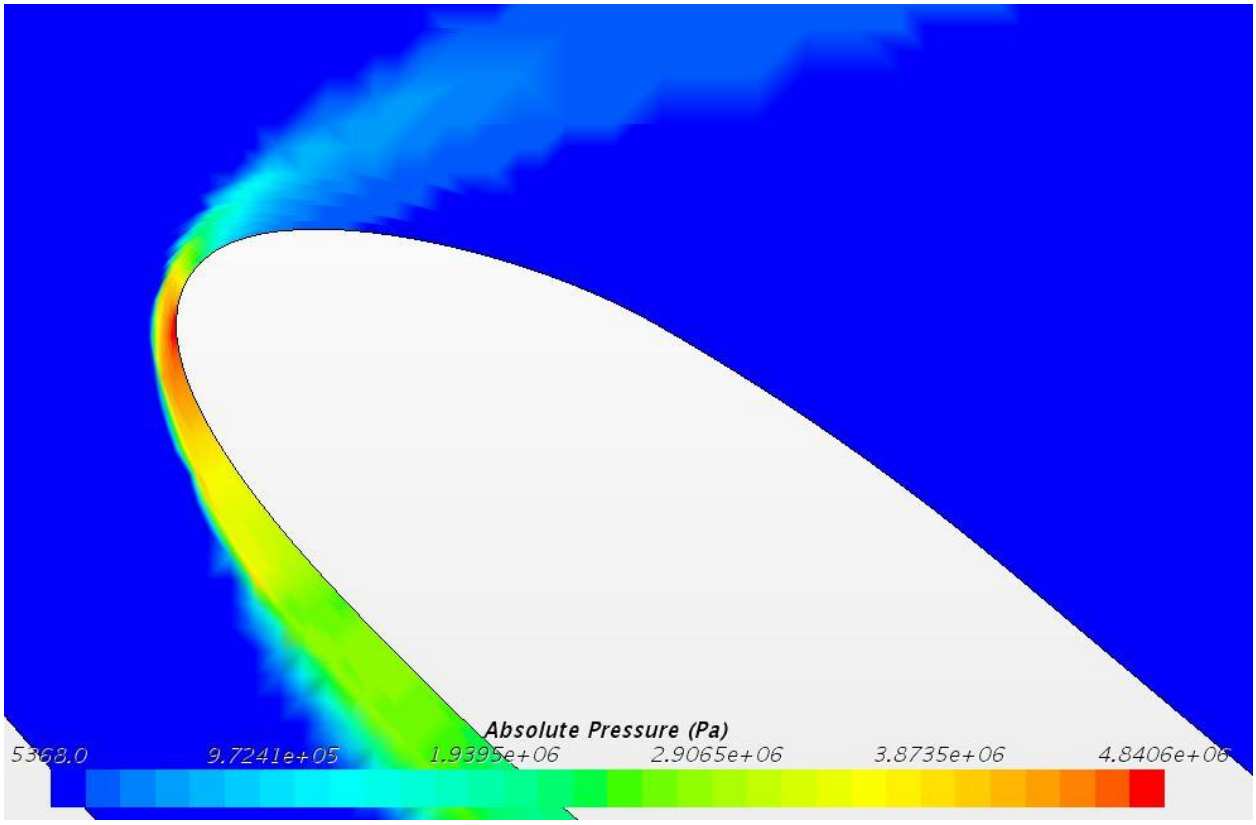

Figure A.23 - One million cells 50% scale X-37 Absolute Pressure nose

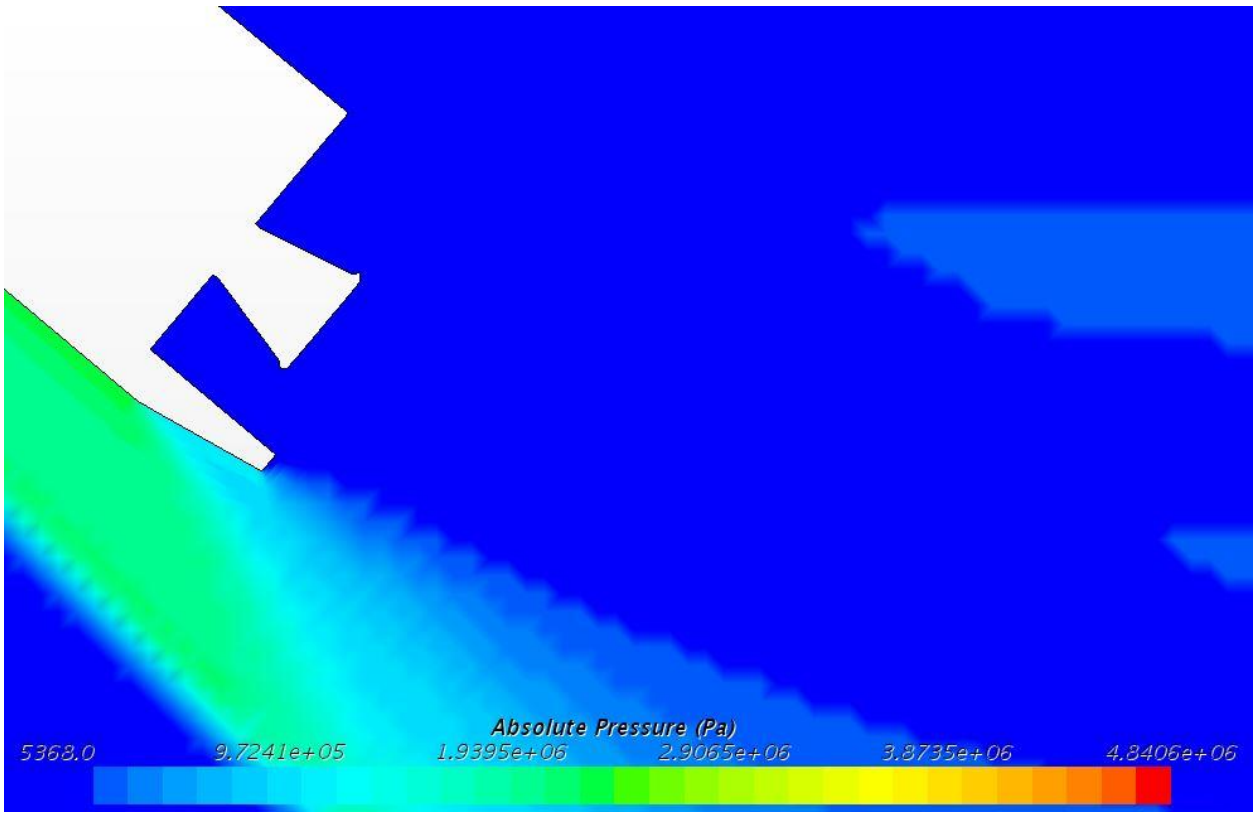

Figure A.24 - One million cells 50% scale X-37 Absolute Pressure tail

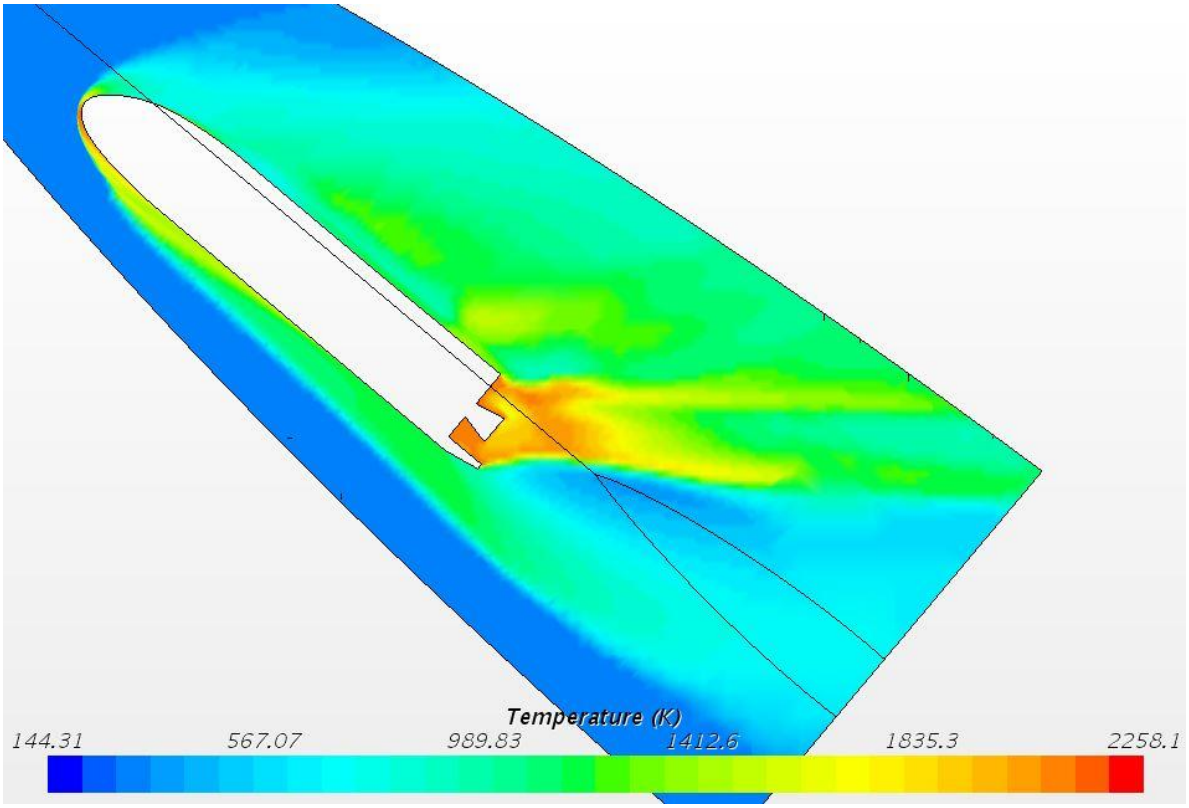

Figure A.25 - 500K cells 25% scale X-37 Temperature full body

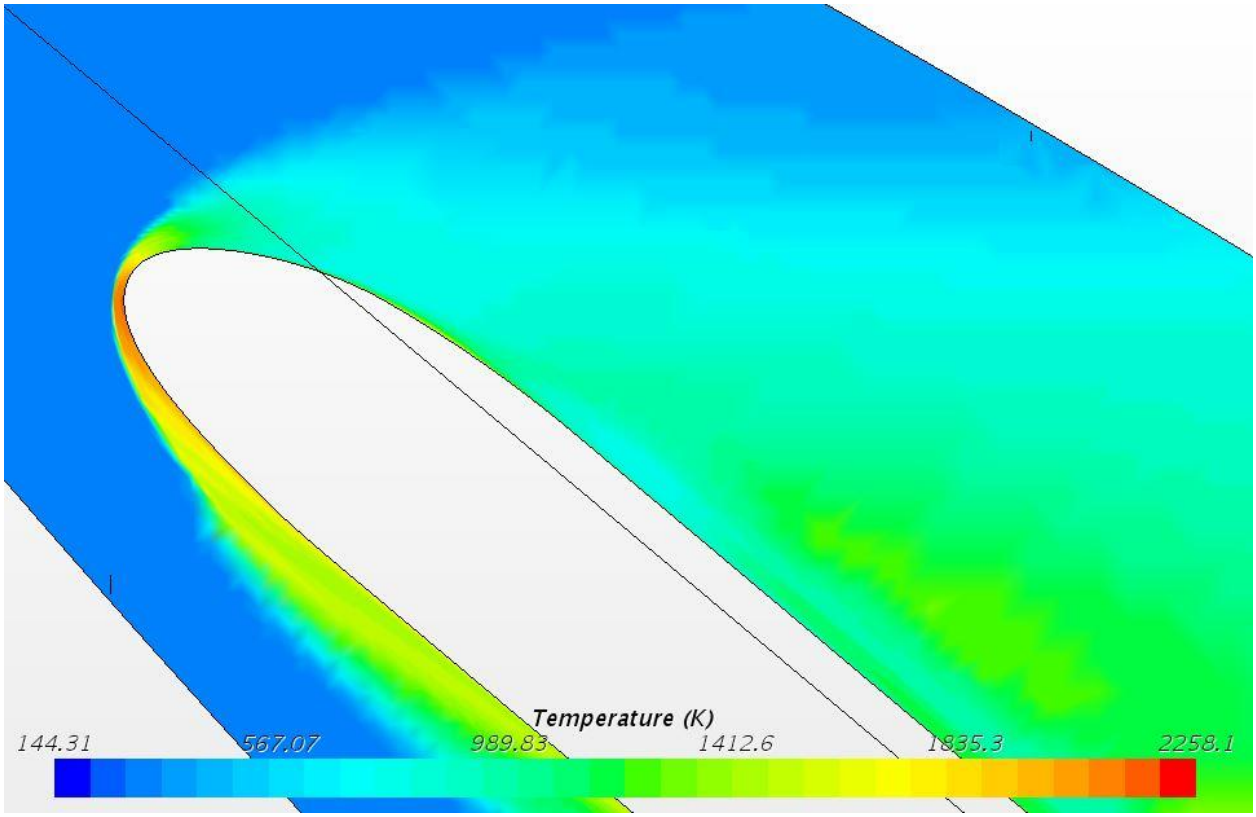

Figure A.26 - 500K cells 25% scale X-37 Temperature nose

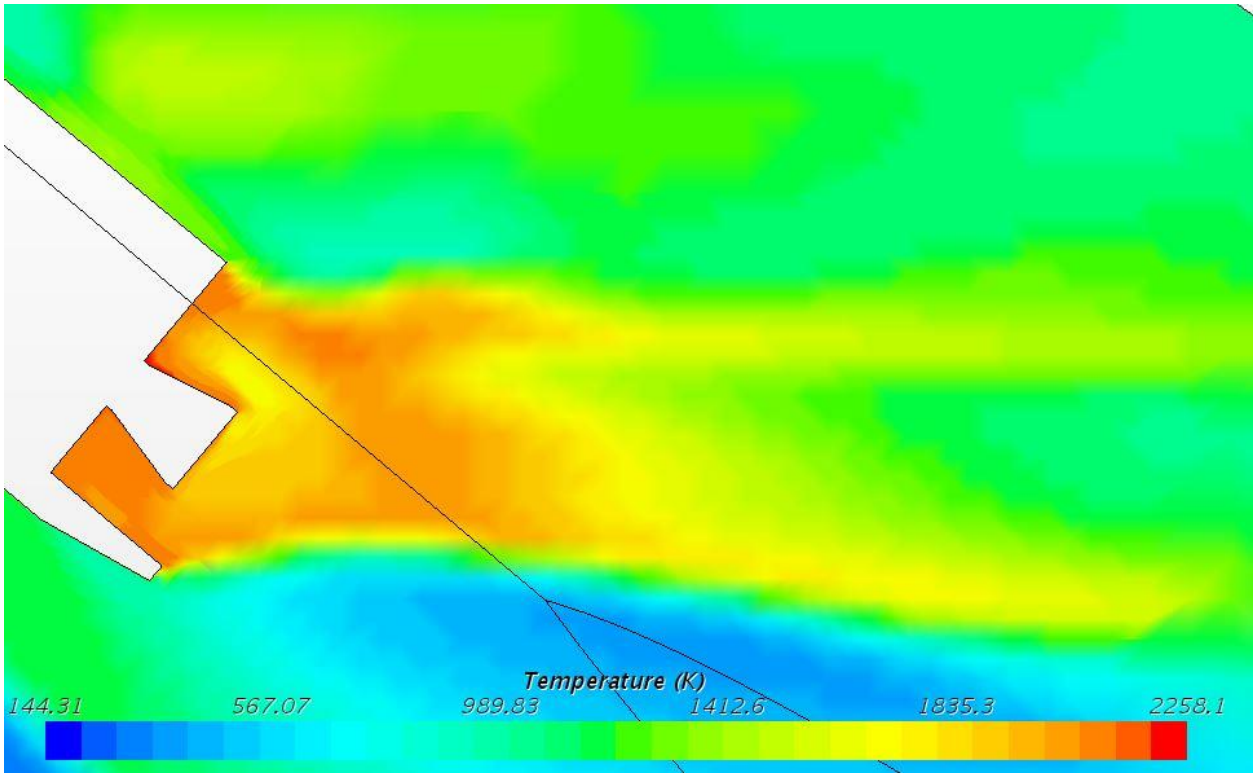

Figure A.27 - 500K cells 25% scale X-37 Temperature tail

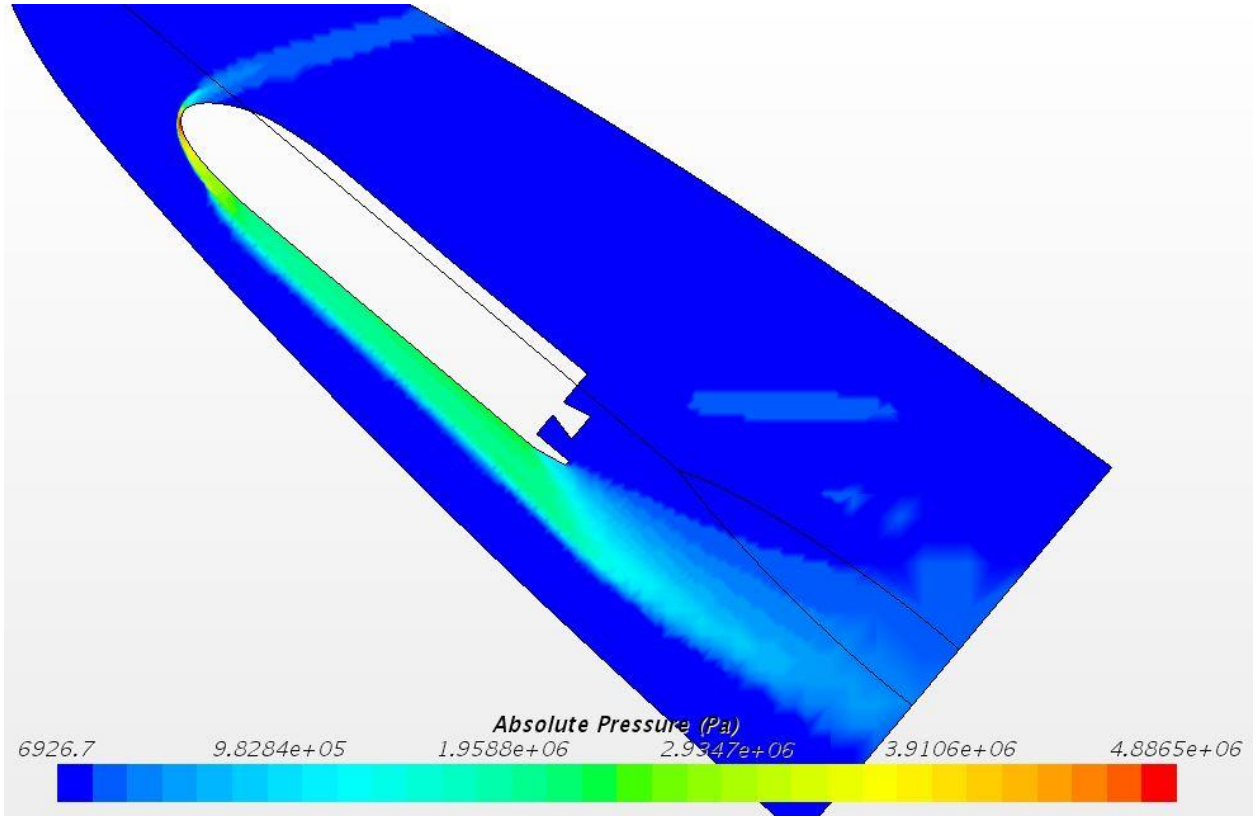

Figure A.28 - 500K cells 25% scale X-37 Absolute Pressure full body

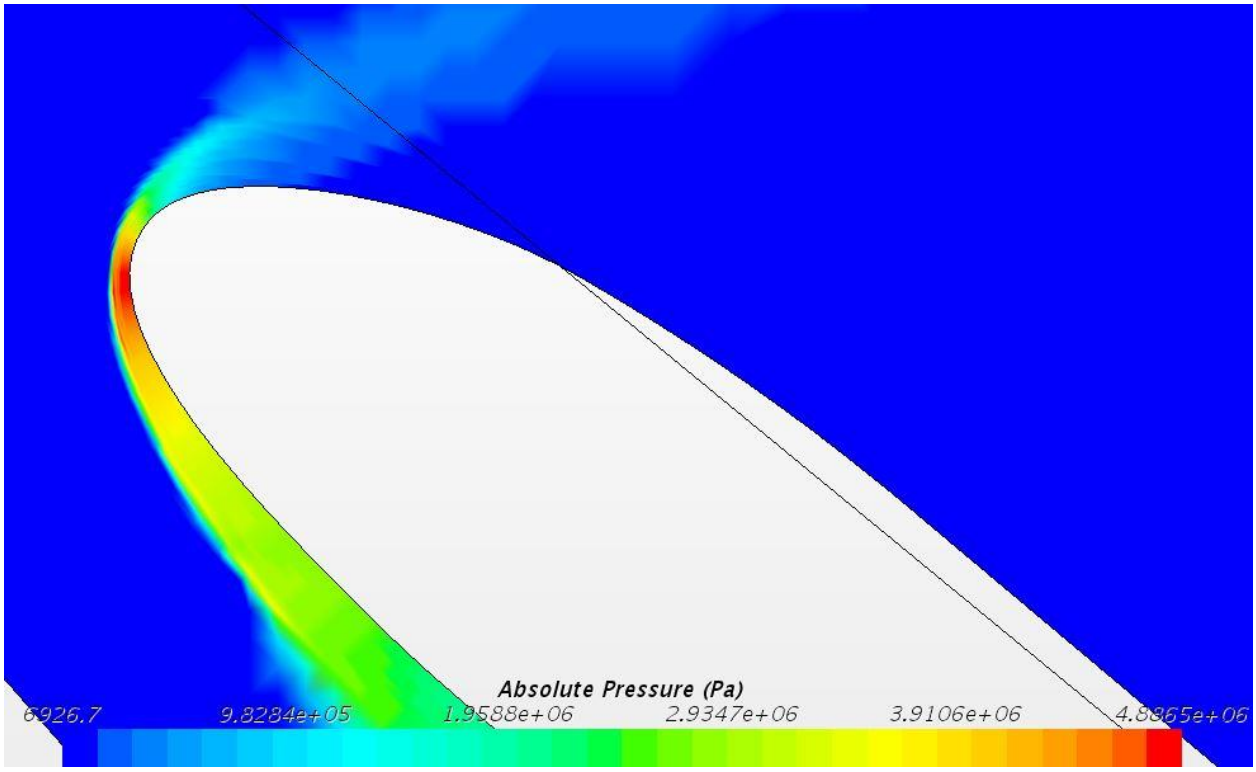

Figure A.29 - 500K cells 25% scale X-37 Absolute Pressure nose

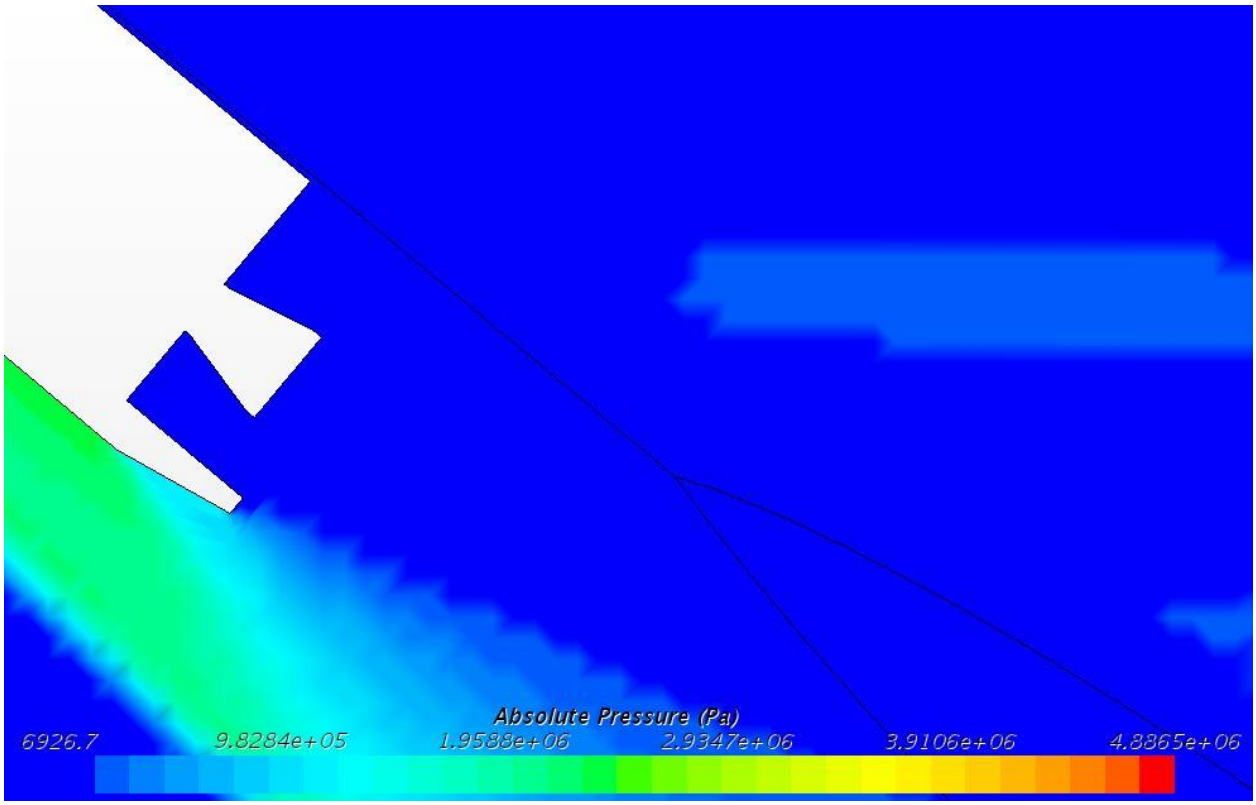

Figure A.30 - 500K cells 25% scale X-37 Absolute Pressure tail

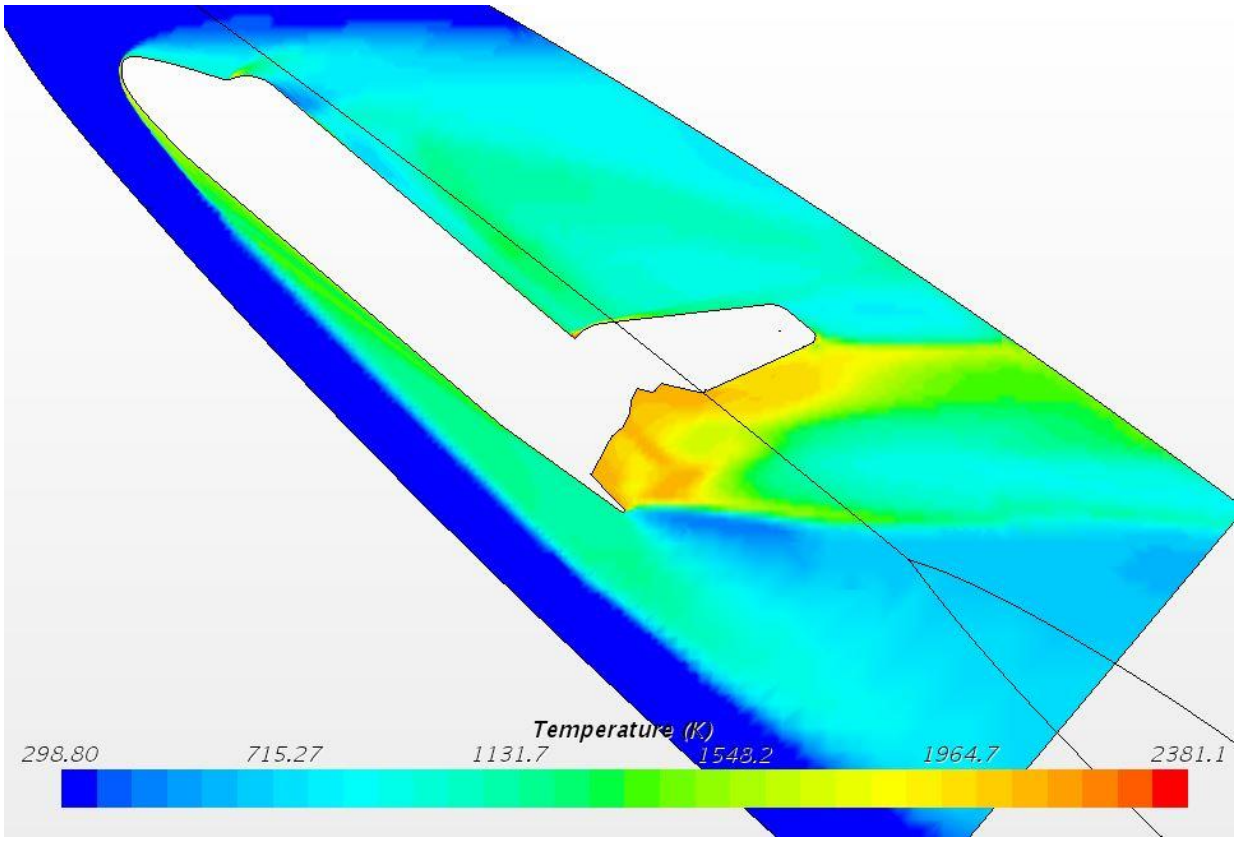

Figure A.31 - One million cells 100% Scale SSO Temperature full body

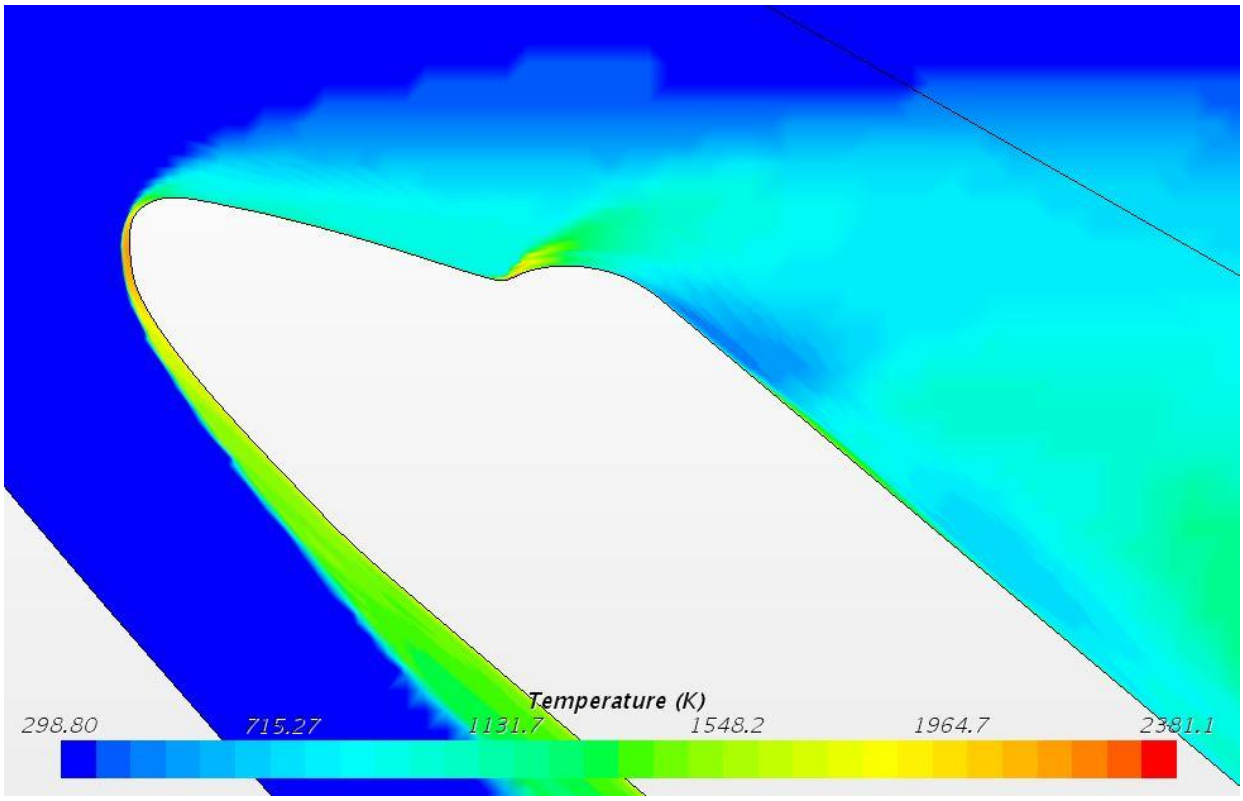

Figure A.32 - One million cells 100% scale SSO Temperature nose

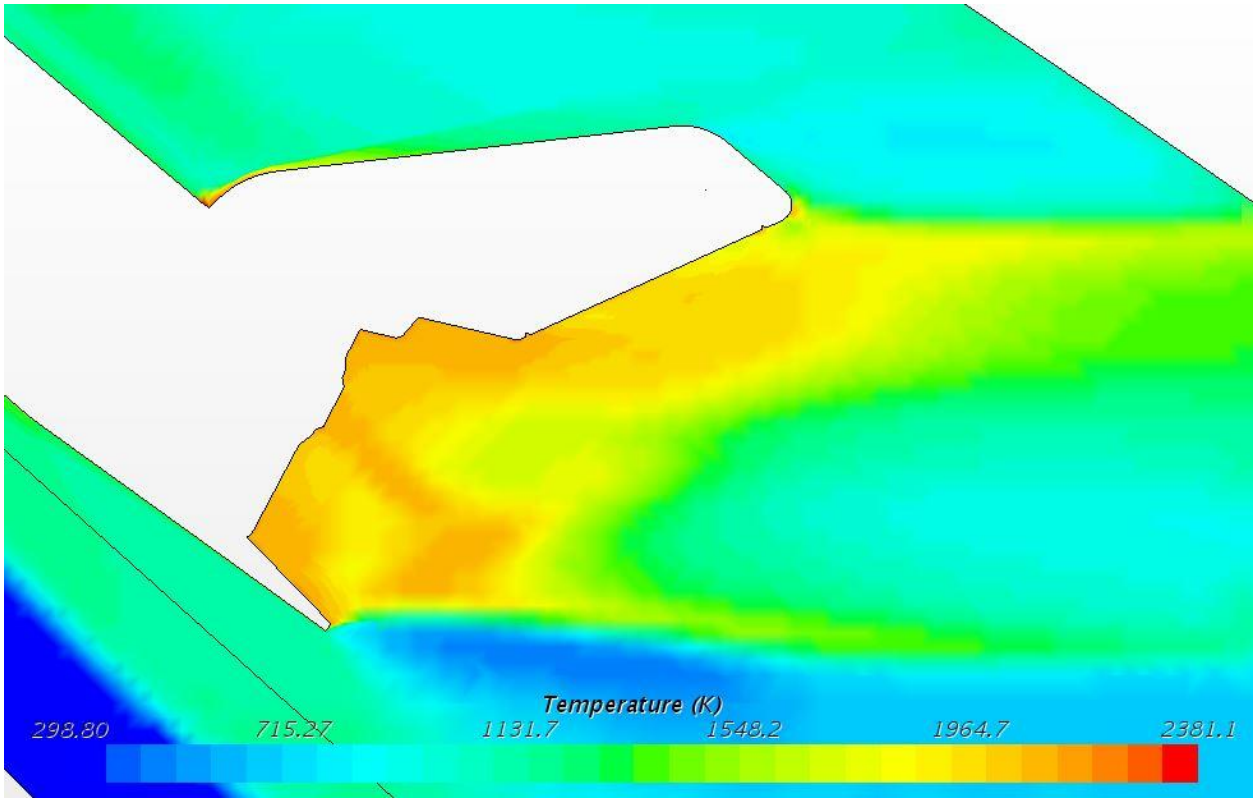

Figure A.33 - One million cells 100% scale SSO Temperature tail

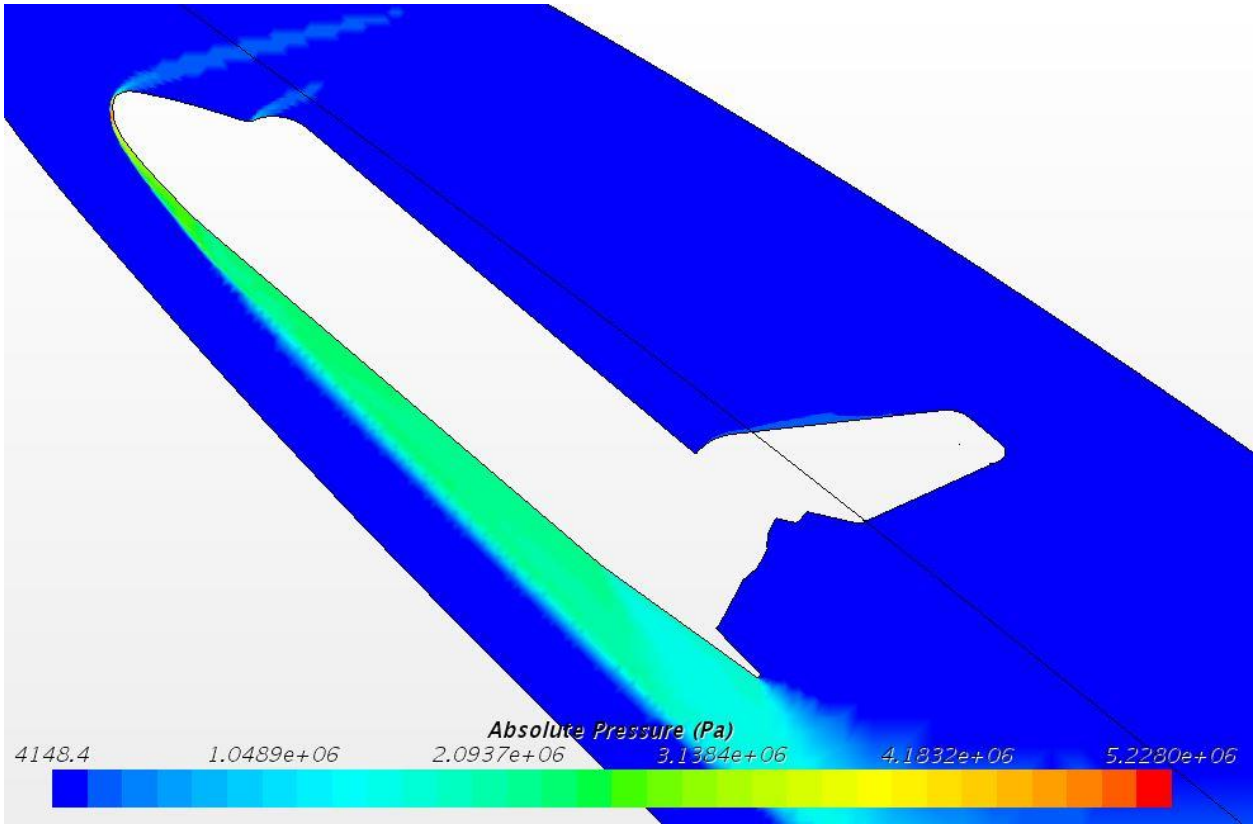

Figure A.34 - One million cells 100% scale SSO Absolute Pressure full body

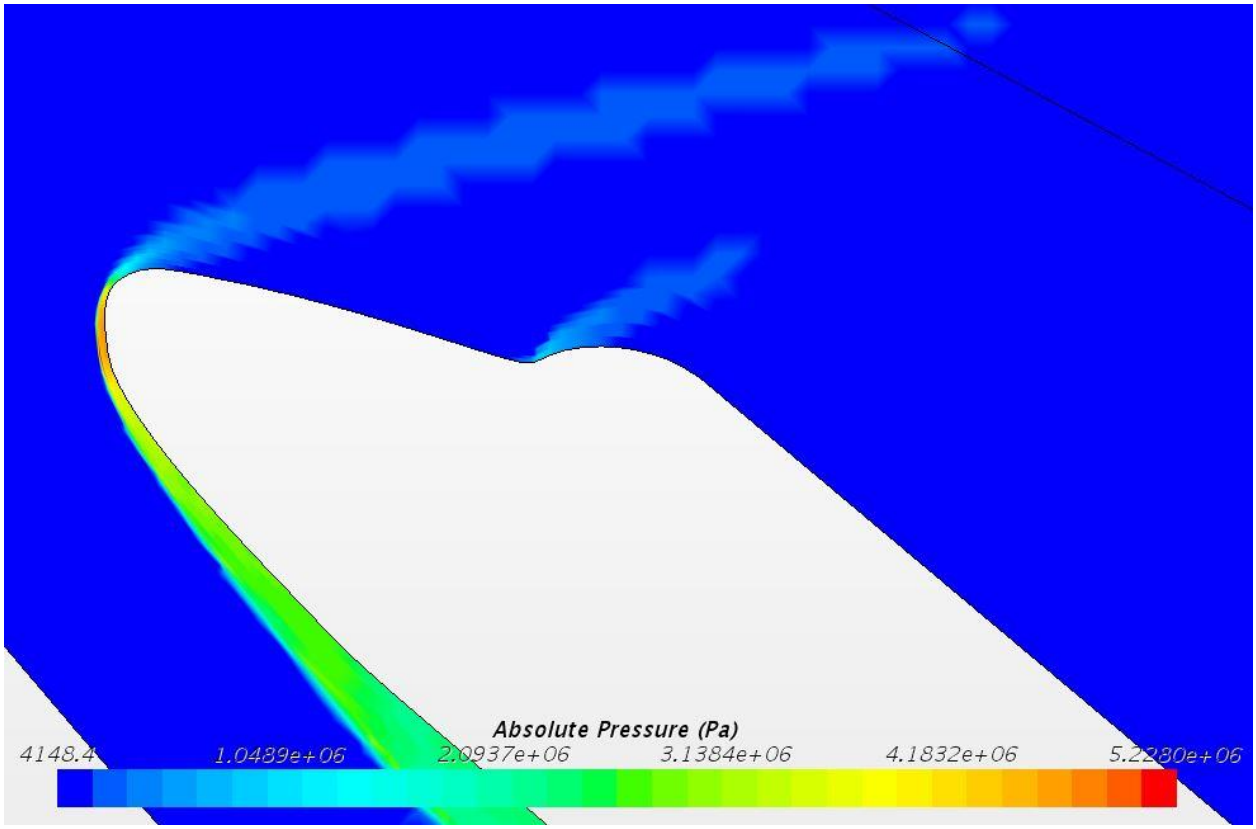

Figure A.35 - One million cells 100% scale SSO Absolute Pressure nose

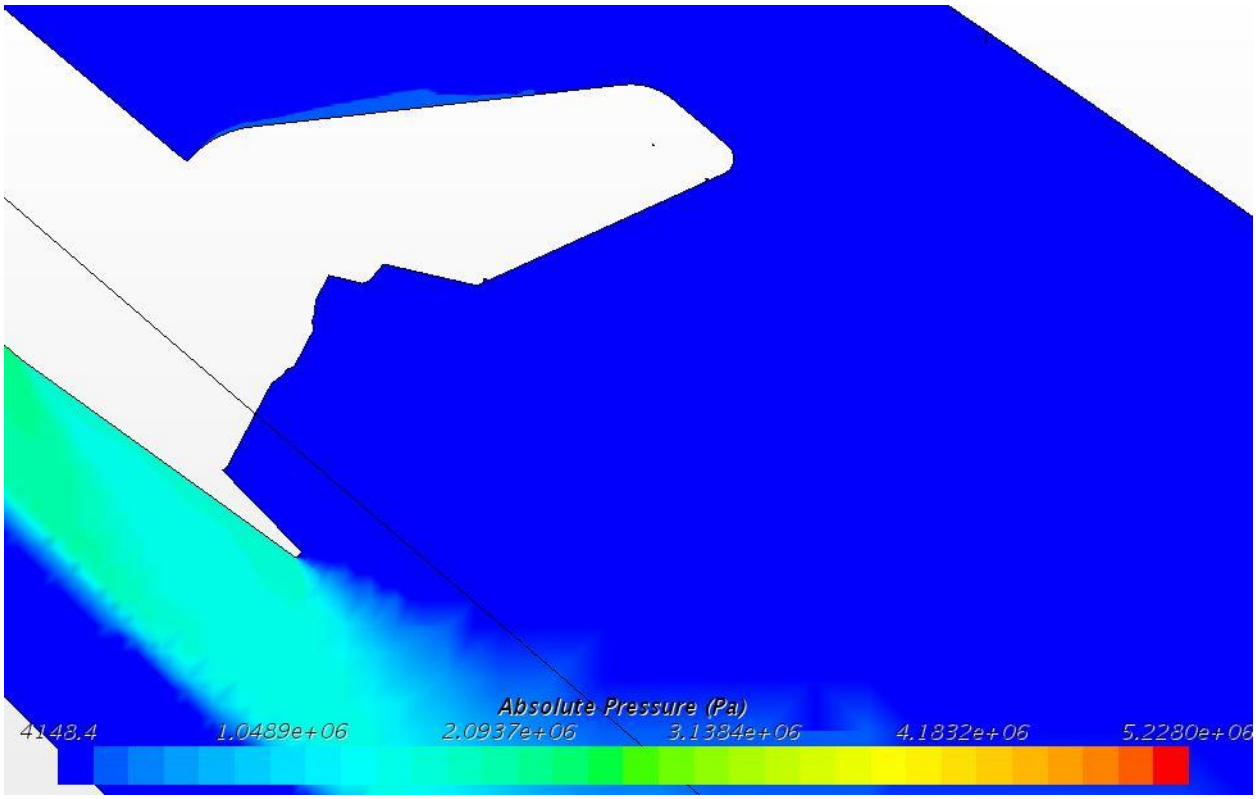

Figure A.36 - One million cells 100% scale SSO Absolute Pressure tail

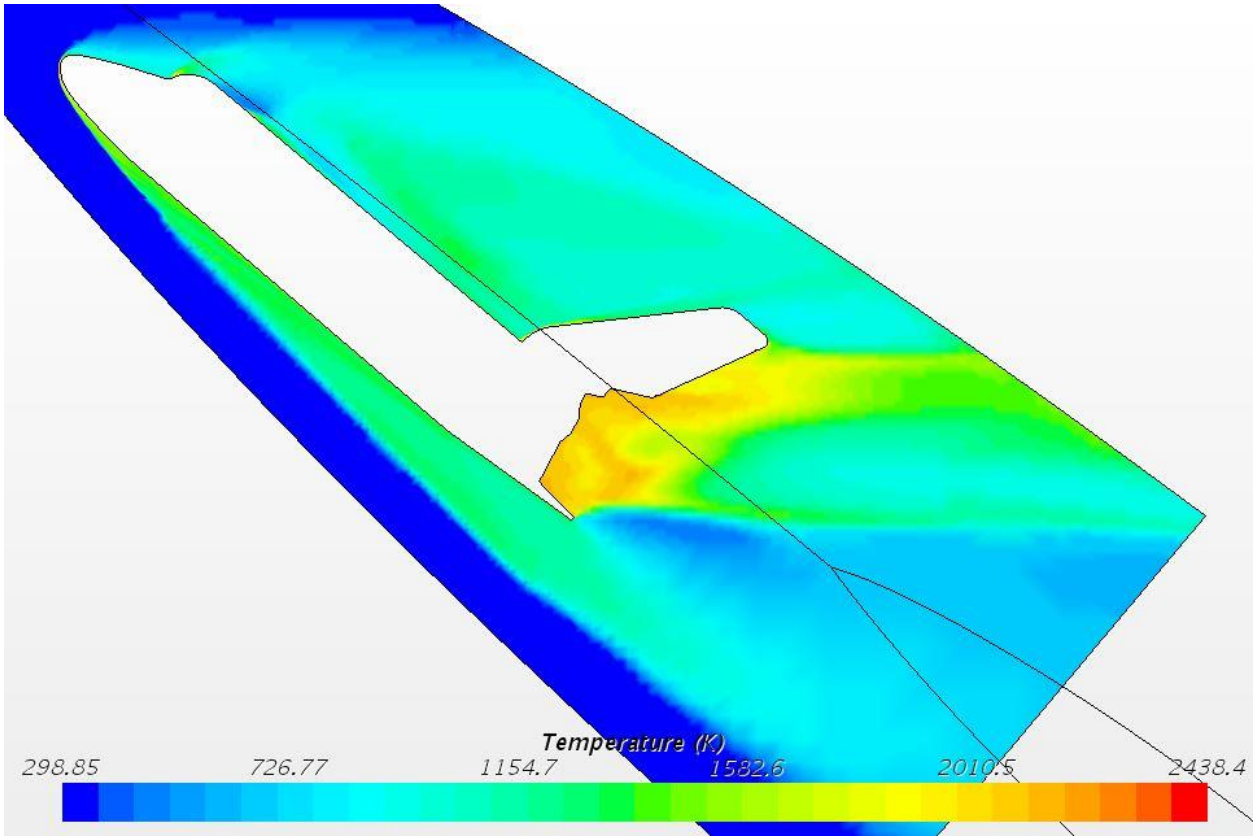

Figure A.37 - One million cells 50% scale SSO Temperature full body

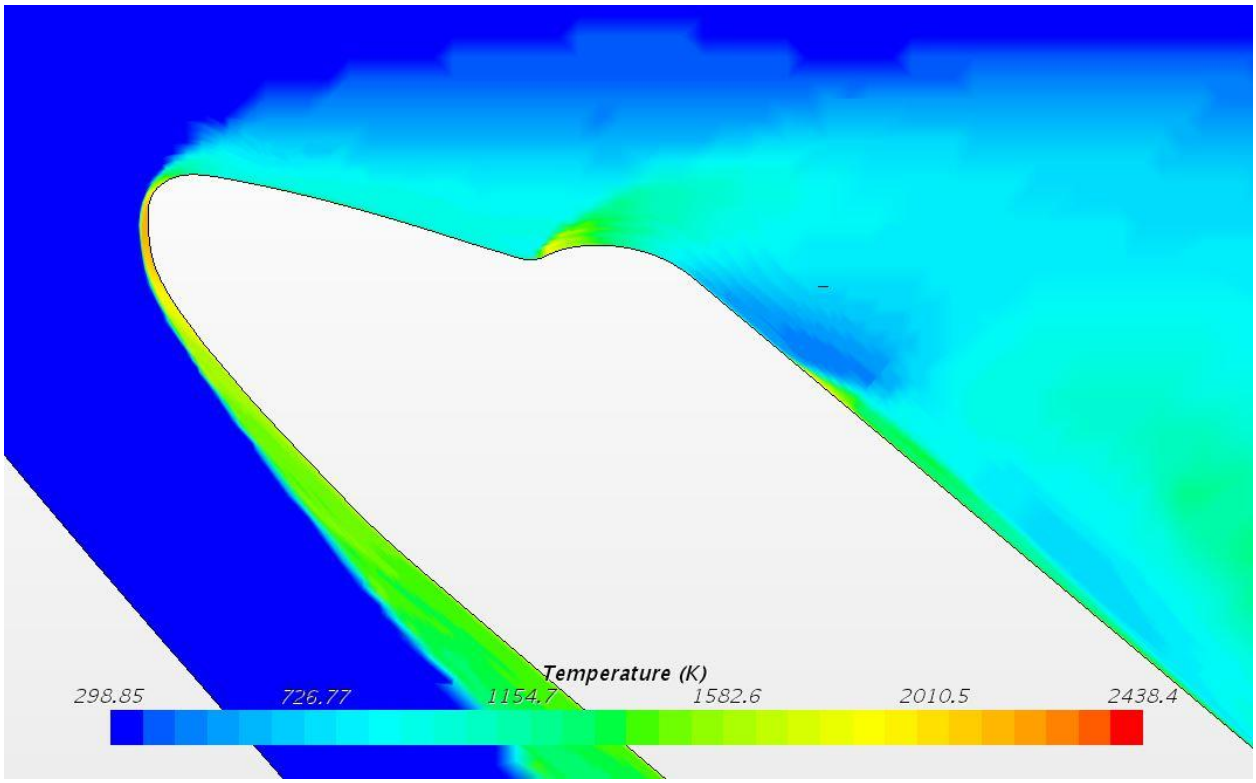

Figure A.38 - One million cells 50% scale SSO Temperature nose

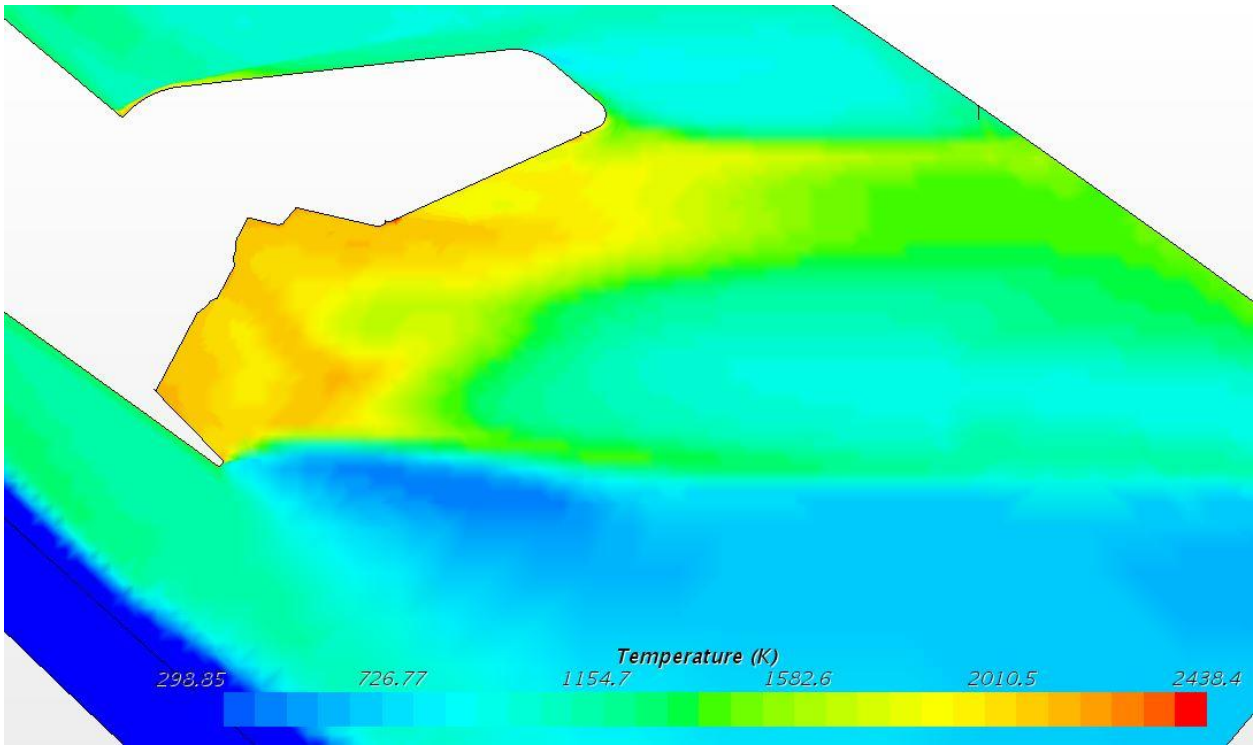

Figure A.39 - One million cells 50% scale SSO Temperature tail

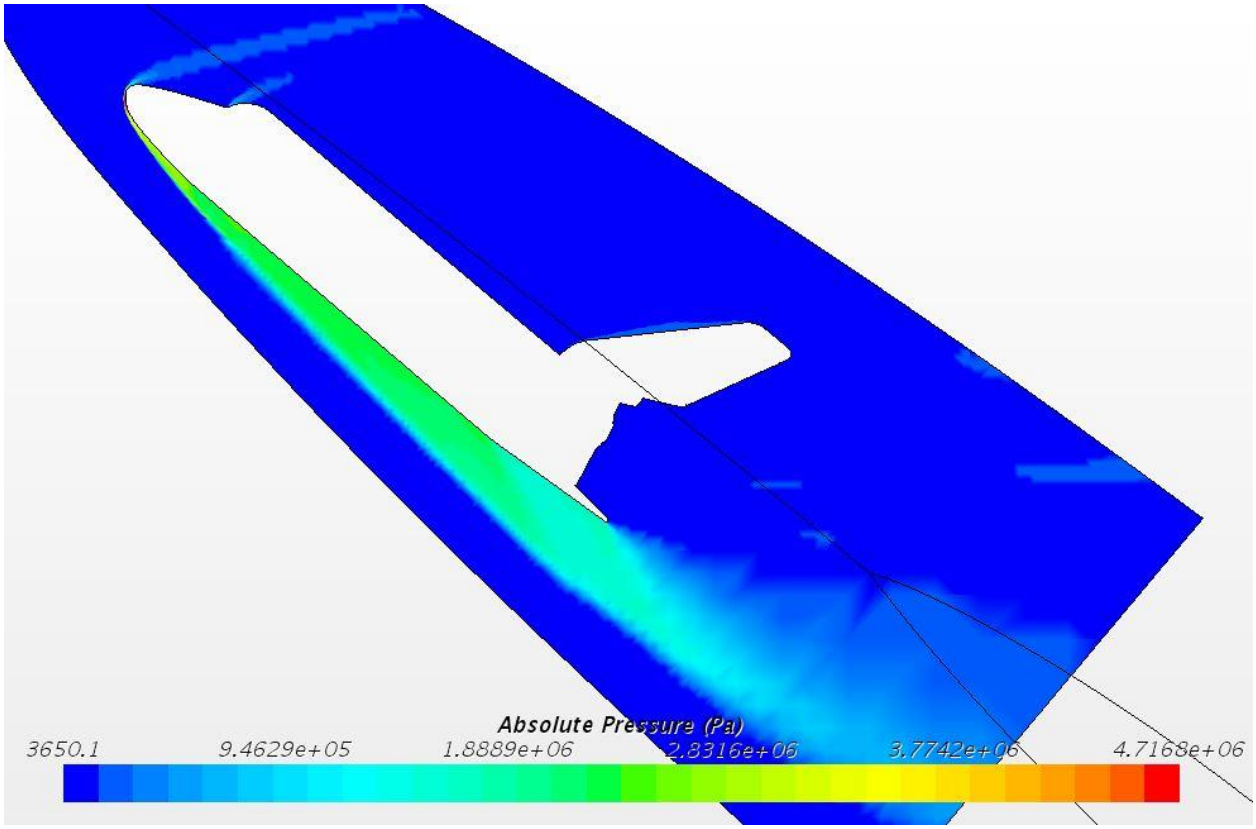

Figure A.40 - One million cells 50% scale SSO Absolute Pressure full body

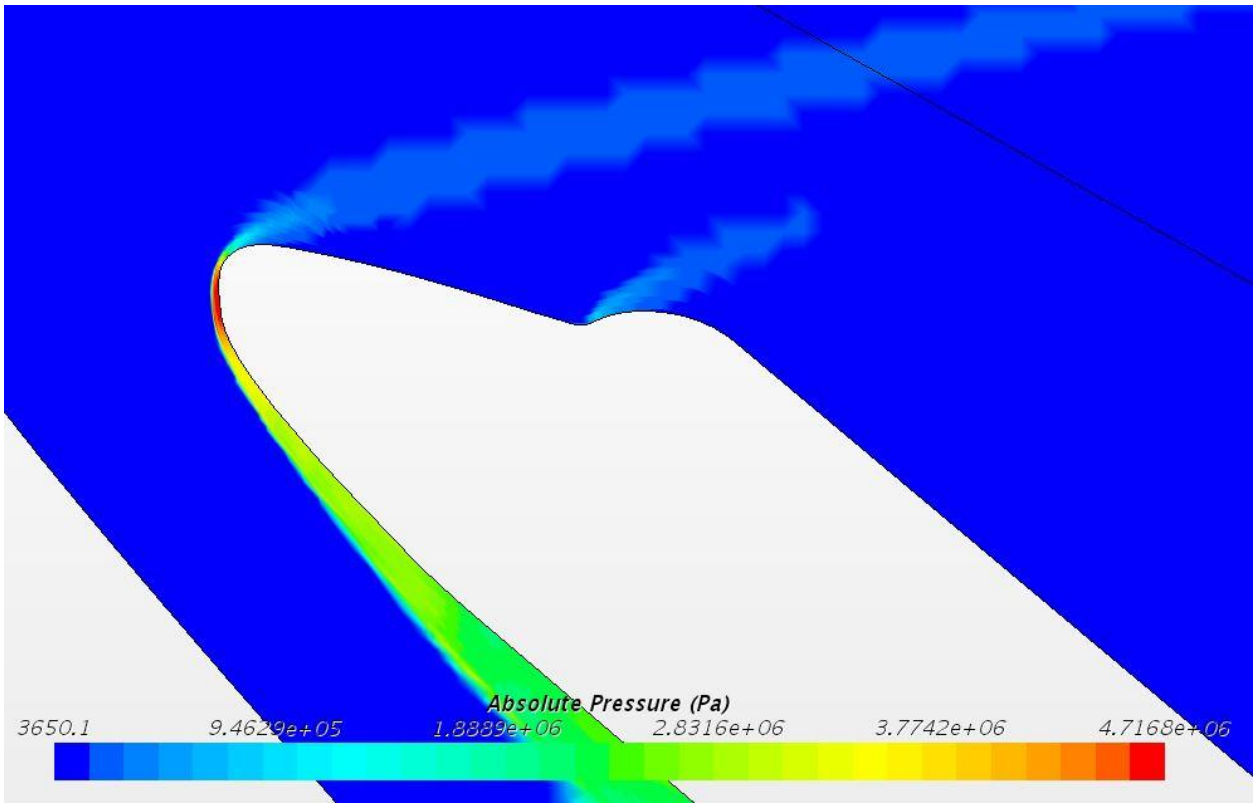

Figure A.41 - One million cells 50% scale SSO Absolute Pressure nose

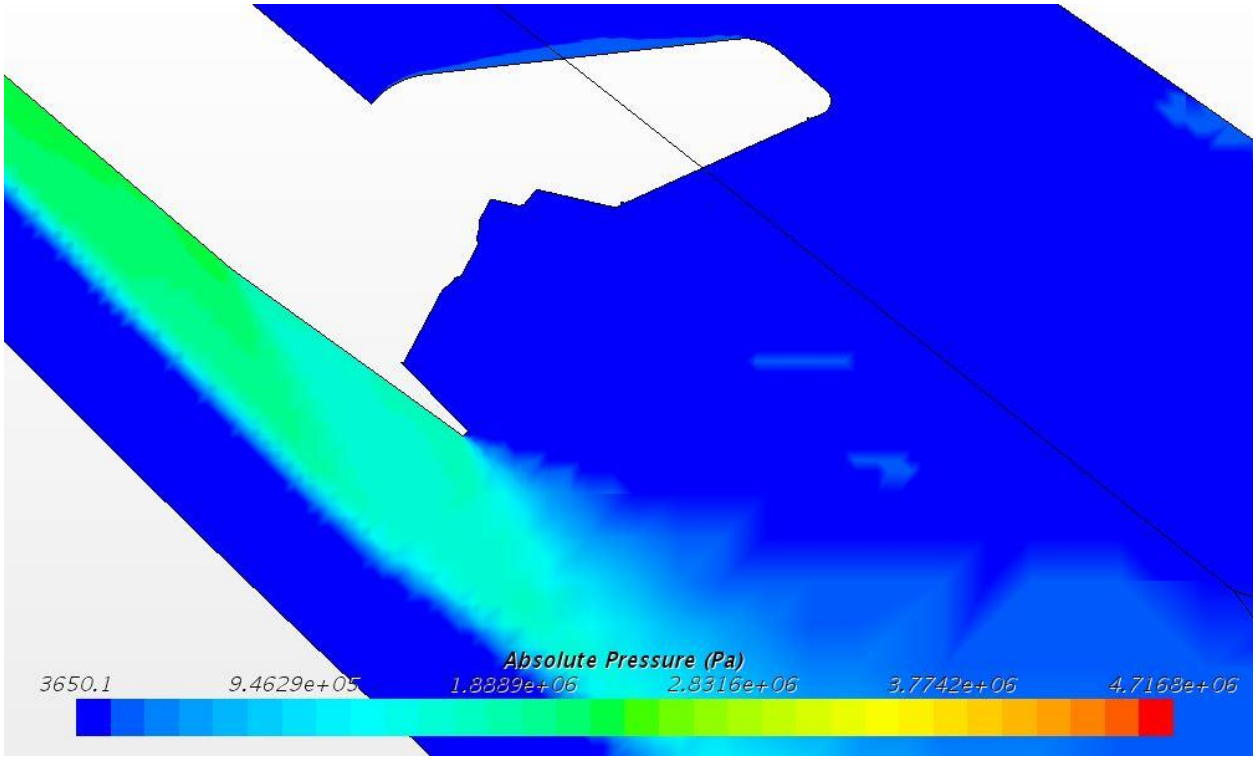

Figure A.42 - One million cells 50% scale SSO Absolute Pressure tail

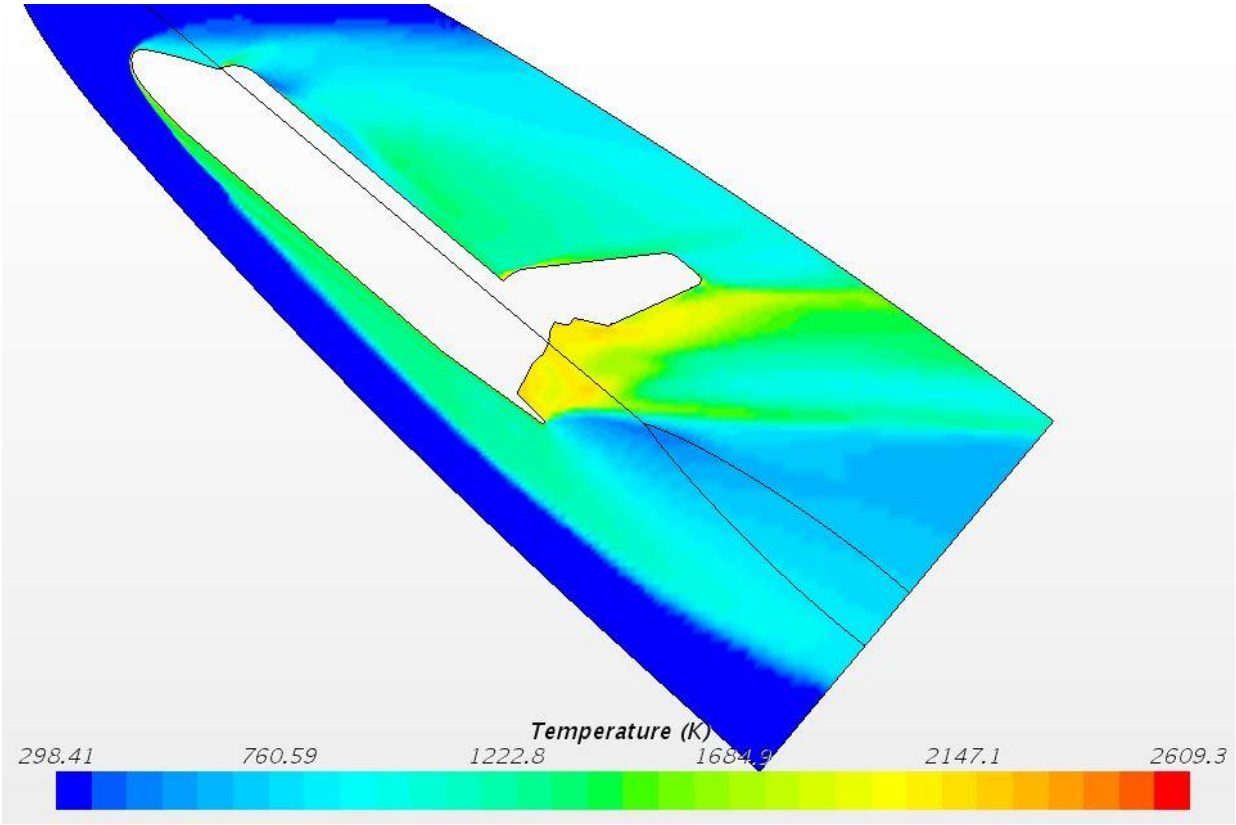

Figure A.43 - One million cells 25% scale SSO Temperature full body

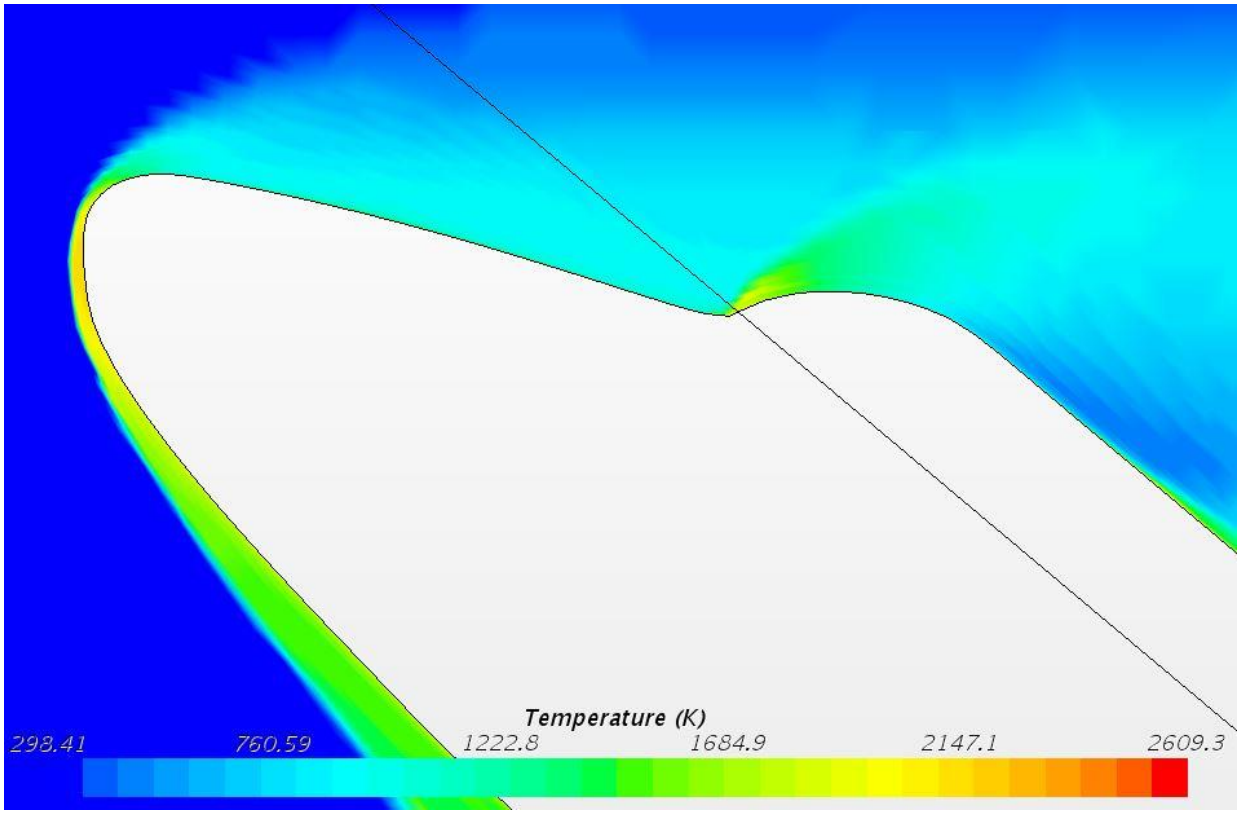

Figure A.44 - One million cells 25% scale SSO Temperature nose

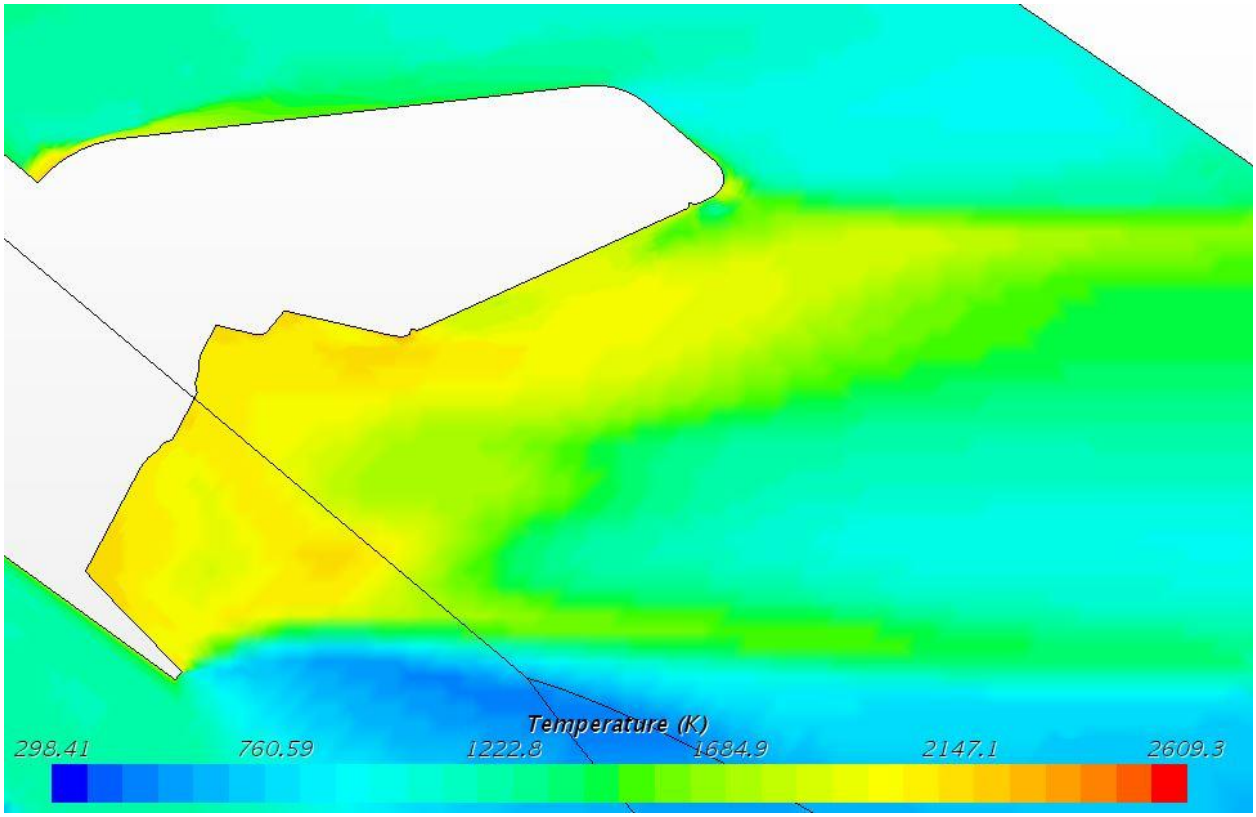

Figure A.45 - One million cells 25% scale SSO Temperature tail

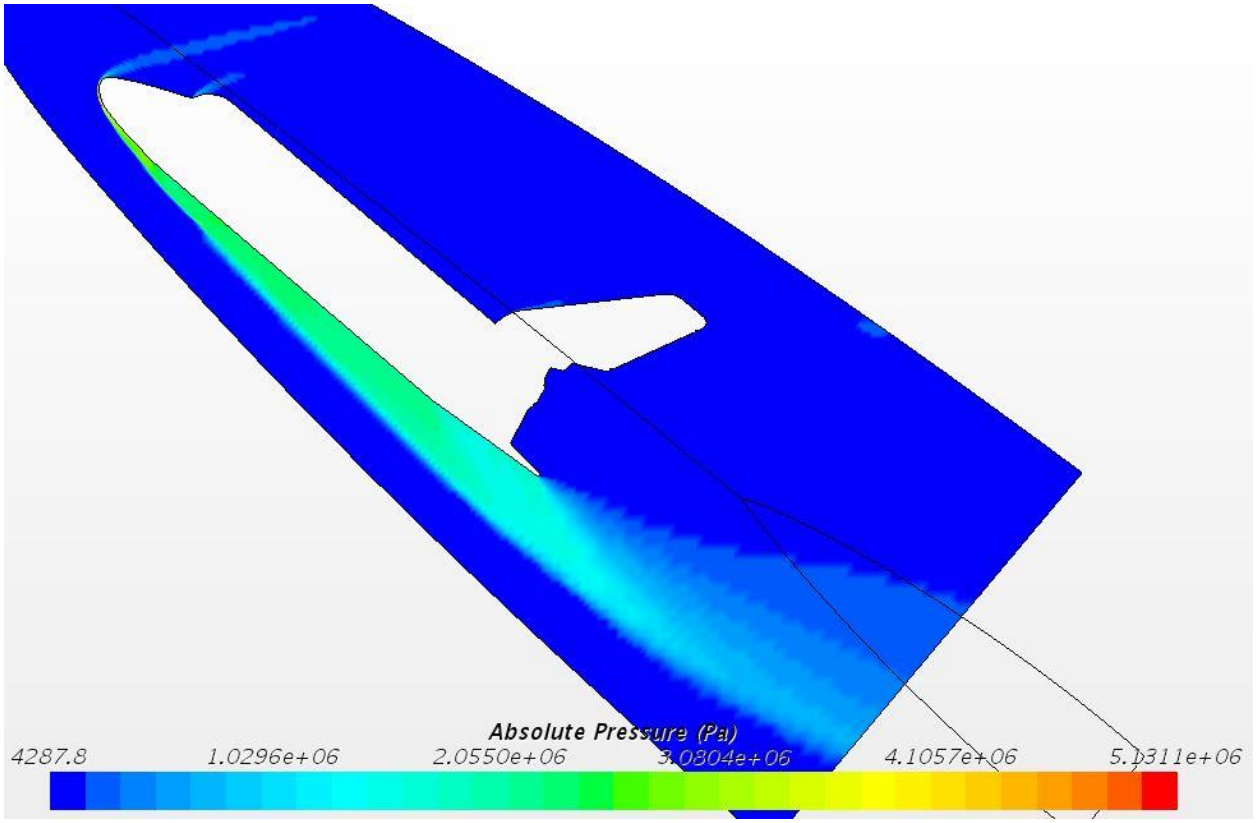

Figure A.46 - One million cells 25% scale SSO Absolute Pressure full body

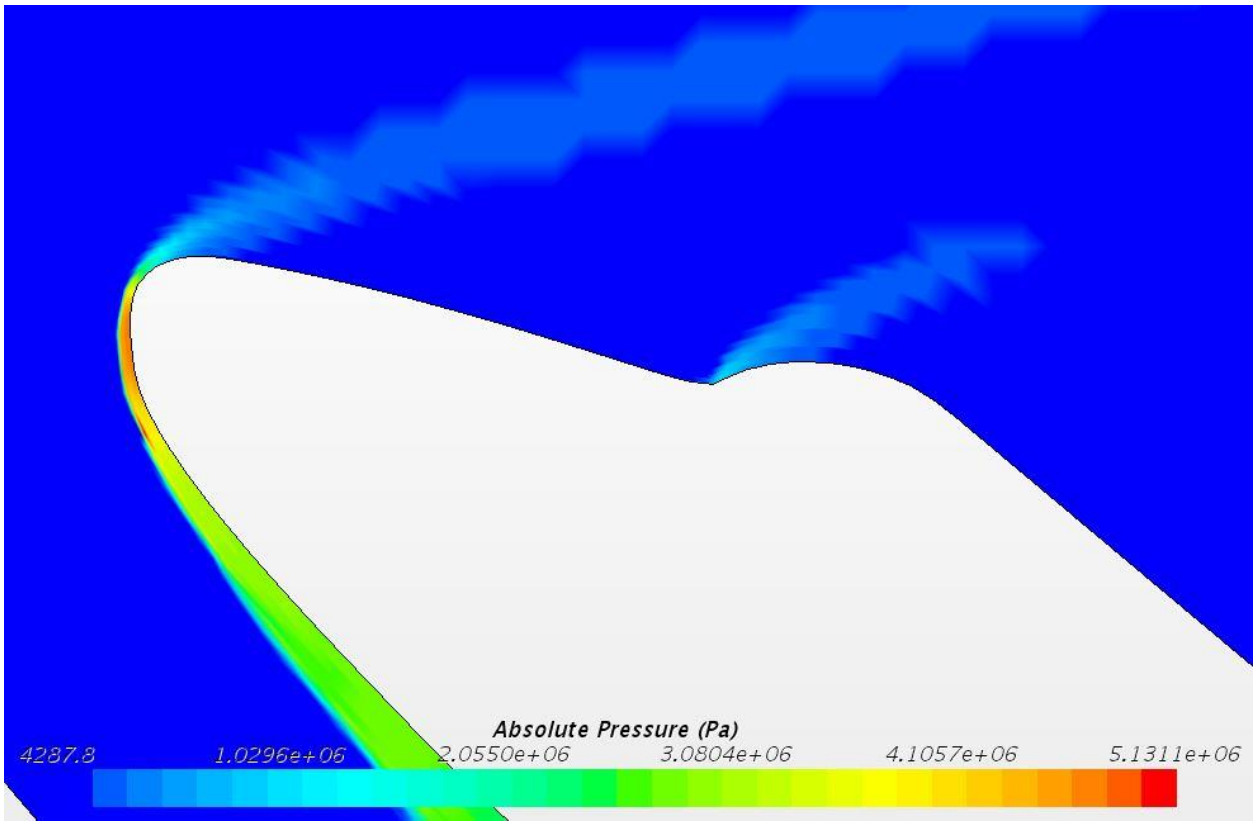

Figure A.47 - One million cells 25% scale SSO Absolute Pressure nose

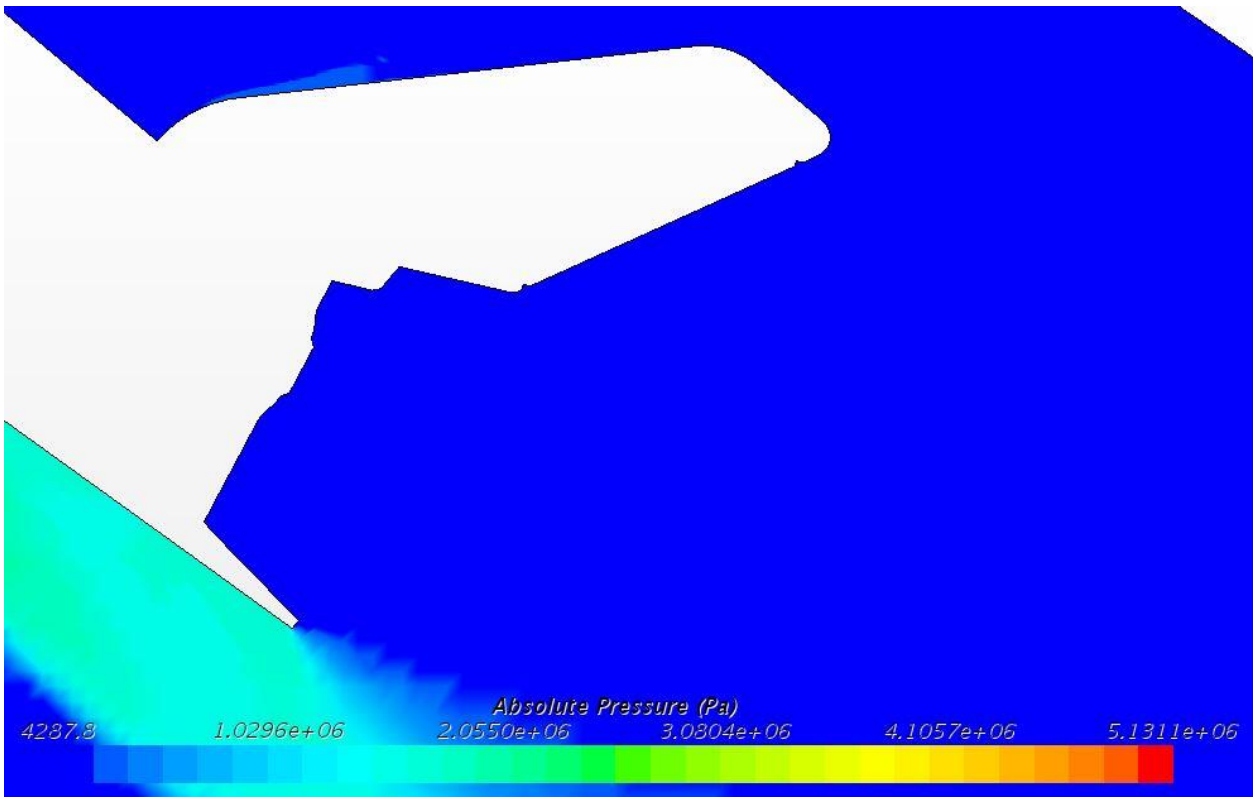

Figure A.48 - One million cells 25% scale SSO Absolute Pressure tail